INTERNATIONAL DOCTORAL
SCHOOL OF THE USC

Juan Alberto
Molina Valero

PhD Thesis

MODELLING FOREST STAND MATURITY FROM NATIONAL FOREST INVENTORY AND TERRESTRIAL LASER SCANNING DATA

Lugo, 2022

Doctoral Programme in Engineering for Rural and Civil Development

DOCTORAL THESIS

MODELLING FOREST STAND MATURITY FROM NATIONAL FOREST INVENTORY AND TERRESTRIAL LASER SCANNING DATA

Juan Alberto Molina Valero

ESCUELA DE DOCTORADO INTERNACIONAL DE LA UNIVERSIDADE DE SANTIAGO DE COMPOSTELA

PROGRAMA DE DOCTORADO EN INGENIERÍA PARA EL DESARROLLO RURAL Y CIVIL

LUGO

2022

DECLARACIÓN DEL AUTOR DE LA TESIS

Modelling forest stand maturity from National Forest Inventory and terrestrial laser scanning data

Yo, **Juan Alberto Molina Valero**, presento mi tesis siguiendo el procedimiento adecuado al Reglamento y declaro que:

1. La tesis abarca los resultados de la elaboración de mi trabajo.
2. De ser el caso, en la tesis se hace referencia a las colaboraciones que tuvo este trabajo.
3. Confirmo que la tesis no incurre en ningún tipo de plagio de otros autores ni de trabajos presentados por mí para la obtención de otros títulos.
4. La tesis es la versión definitiva presentada para su defensa y coincide la versión impresa con la presentada en formato electrónico.

Y me comprometo a presentar el Compromiso Documental de Supervisión en el caso de que el original no esté depositado en la Escuela.

En Lugo, a 5 de septiembre de 2022

AUTORIZACIÓN DEL DIRECTOR / TUTOR DE LA TESIS

Modelling forest stand maturity from National Forest Inventory and terrestrial laser scanning data

D. Juan Gabriel Álvarez González (Director/Tutor)
D. César Pérez Cruzado (Director)

INFORMAN:

Que la presente tesis, se corresponde con el trabajo realizado por **D. Juan Alberto Molina Valero**, bajo nuestra dirección/tutorización, y autorizamos su presentación, considerando que reúne los requisitos exigidos en el Reglamento de Estudios de Doctorado de la USC, y que como directores de esta no incurre en las causas de abstención establecidas en la Ley 40/2015.

De acuerdo con lo indicado en el Reglamento de Estudios de Doctorado, declaramos también que la presente tesis doctoral es idónea para ser defendida en base a la modalidad de **«Monográfica con reproducción total o parcial de publicaciones»**, en la que la participación del doctorando fue decisiva para su elaboración y las publicaciones se ajustan al Plan de Investigación.

En Lugo, a 5 de septiembre de 2022

Funding

This doctoral thesis was supported by the Spanish Ministry of Universities through the University Faculty Training (FPU) fellowship program [FPU16/03057]. The experimental database was supported by the Spanish Ministry of Science and Innovation through the research project "*Modelling the effects of intensity of perturbation on the structure of natural forests and their carbon stocks by using data from the National Forestry Inventory*" [AGL2016-76769-C2-2-R] and the Galician Regional Government through the research project "*Design of forest monitoring systems on a regional scale*" [ED431F 2020/02].

AGRADECIMIENTOS

Con estas líneas quiero expresar mi más sincero y profundo agradecimiento a todas aquellas personas que han hecho posible esta tesis doctoral, la cual ha sido el hilo conductor de una etapa de mi vida profundamente marcada por el aprendizaje, a veces manifestado hasta en sueños lúcidos.

Si en algo no tengo dudas es en ubicar en las primeras líneas de estos agradecimientos a mis padres. Aunque no me han aportado conocimientos técnicos específicos en lo que respecta a este documento, han desbrozado el camino en su totalidad hasta llegar a este punto, siendo mi sustento de vida en el sentido más amplio de la palabra. No menos importante es la presencia de mi hermano y las dos sobrinas que me ha regalado junto con su compañera de vida. Y por supuesto no me olvido del resto de familiares (todos ellos pueden darse por aludidos).

Detrás de un gran trabajo siempre hay unos grandes directores, necesarios para dar pasos más estables en este largo camino andado. En este sentido he sido inmensamente afortunado al haber contado con César Pérez Cruzado y Juan Gabriel Álvarez González como susodichos directores. Del primero de ellos, a parte de la maravillosa combinación de acopio de conocimientos e imaginación para la investigación, regada por la hermosa cualidad de la humildad y un corazón cinco estrellas, quiero destacar su capacidad para despertar en mí el entusiasmo por este sublime trabajo llamado investigación. ¡Ay, la investigación!, con lo poquito que la cuidamos y nos da más alegrías que 10^6 Messis juntos. Sin lugar a duda él ha sido mi MENTOR con mayúsculas en esta etapa profesional. En cuanto al segundo, el enorme prestigio que atesora y del que es pleno merecedor, habla por sí solo. Pero además añadiría su enorme calidad como docente, fruto de su también enorme calidad humana y vasto conocimiento de la materia. Tampoco me olvido del profesor Andres Kiviste, tutor de mi estancia internacional en la Universidad de Ciencias de la Vida de Tartu

(Estonia). Nunca olvidaré el cálido acogimiento que tuve por su parte incluso en los tiempos más duros de la pandemia. En cualquier caso, ¡es MUY difícil tener mejores compañeros de viaje para hacer una tesis!

También agradecer a todos los colaboradores que en algún momento han estado ahí para darme alas diseñadas por sus conocimientos (Adela, Andrea, Antonio, Jesús, Darío, Fernando, María José, Raúl, Ulises, …), porque a todos ellos los considero mentores de mi trabajo en mayor o menor medida. Y por supuesto también ocupan un lugar muy especial mis compañeros de trabajo (Casimiro, Diego, Mario, Joel, Óscar, …) por su gran ayuda y disposición. Y cómo no, de la misma manera valoro la constante y tremenda ayuda de Almudena, plenamente colmada de amabilidad.

De forma más lúdica, mil gracias a los colegas de tesis, con los cuales compartí alegrías y sufrimientos casi siempre aderezados por cafeína (Bea, Cecilia, Diana, Eneli, María, Miguel, Ray, Stefano, …). Y otras mil gracias a los amigos/colegas de toda o parte de la vida, con los que he cerrado bares y con los que he llevado a cabo cientos de aventuras en los entornos más selectos de cada lugar. También tienen un hueco en estas líneas mis antiguas parejas, porque de todas ellas tengo cosas bonitas que recordar.

En un lugar diferenciado del resto, quiero agradecer este trabajo a mis maestros y compañeros de judo del club SENRA por haberme aportado ese equilibrio físico-mental tan necesario para afrontar un proyecto de esta envergadura. "*Mens sana y corpore sano*".

Y como lo mejor se suele dejar para el final, no puedo olvidarme de Isa, mi compañera de vida. Muchas veces mi conciencia. Y a fin de cuentas una de las personas en las que más apoyo encuentro.

Por último, solo me queda agradecer a las personas que haya olvidado para que nadie se me enoje.

Juan Alberto Molina Valero

A mi familia, por educarme en el respeto, la humildad, el esfuerzo y la filantropía

A mis sobrinas Blanca y Julia, por ser la nueva generación en la que debemos depositar nuestros mejores deseos para este mundo

Siendo todo esto así, me pareció conveniente escribir cuál es mi opinión sobre ello. Y si esto que expongo no fuere completo, será principio de algo perfecto. Pido, por tanto, a los hermanos que lean esta obra que pongan por escrito sus dudas, pues quizá mediante ello se encontrará la verdad, si es que yo no la encontré. Y si la he encontrado, como imagino, entonces se manifestará por medio de esas dificultades. La verdad, en efecto, como dice Aristóteles, concuerda consigo misma y se valida por sí sola.

Abū-l-Walīd Ibn Rušd
(Averroes)

PREFACE

This doctoral thesis, submitted under the modality «monograph with total or partial reproduction of publications», summarizes 5 years of research work and includes 3 main articles (partially and/or totally reproduced), all of which are published in journals indexed in the Journal Citation Reports (JCR). The monograph also includes other results, discussions and conclusions derived from the research work and supported by the findings reported in the articles. In addition to the main articles, all other research activities derived from this research (other articles, conference communications and software development, etc.) are listed in this preface.

Main articles included in the thesis

I. Molina-Valero, J. A., Diéguez-Aranda, U., Álvarez-González, J. G., Castedo-Dorado, F., and Pérez-Cruzado, C. (2019). Assessing site form as an indicator of site quality in even-aged *Pinus radiata* D. Don stands in north-western Spain. *Annals of Forest Science*, *76*(4), 1-10. https://doi.org/10.1007/s13595-019-0904-1

   This article has been partially reproduced in the following sections:

   1. Introducction (mainly in 1.2.2 Assessment of site quality using National Forest Inventory data)
   3. Material and methods (mainly in 3.2 Site form as a suitable site quality index for the studied forests)
   4. Results and discussion (mainly in 4.1 Site form: an indicator of site quality in uneven-aged stands)
   5. Conclusions (first)

II. Molina-Valero, J. A., Camarero, J. J., Álvarez-González, J. G., Cerioni, M., Hevia, A., Sánchez-Salguero, R., Martín-Benito, D. and Pérez-Cruzado, C. (2021). Mature forests hold maximum live biomass stocks. *Forest Ecology and Management*, *480*, 118635. https://doi.org/10.1016/j.foreco.2020.118635

This article has been partially reproduced in the following sections:

1. Introducction (mainly in 1.1 Stand maturity as a reference framework in forests and 1.2.1 Biomass stock as a proxy for stand maturity)
3. Material and methods (mainly in 3.3 Estimation of maximum biomass stock based on National Forest Inventory data)
4. Results and discussion (mainly in 4.2 Estimation of degradation intensity in terms of maximum biomass stock based on National Forest Inventory data)
5. Conclusions (second)

III. Molina-Valero, J. A., Martínez-Calvo, A., Ginzo Villamayor, M. J., Novo Pérez, M. A., Álvarez-González, J. G., Montes, F., and Pérez-Cruzado, C. (2022). Operationalizing the use of TLS in forest inventories: The R

package FORTLS. *Environmental Modelling & Software*, *150*, 105337. https://doi.org/10.1016/j.envsoft.2022.105337

This article has been partially reproduced in the following sections:

1. Introducction (mainly in 1.4 Terrestrial laser scanning (TLS) as an emerging approach in forest inventories)
3. Material and methods (mainly in 3.5 Modelling the state of maturity by terrestrial laser scanning (TLS) data)
4. Results and discussion (mainly in 4.4 Modelling relationships between forest maturity and terrestrial laser scanning (TLS))
5. Conclusions (fourth)

Authors contribution

In the above articles, the authors responsibilities were, according to the CRediT (Contributor Roles Taxonomy) framework:

- **Juan Alberto Molina Valero**: Conceptualization, Investigation, Formal Analysis, Methodology, Software, Visualization, Writing - original draft, Writing - review & editing.
- **Juan Gabriel Álvarez González**: Conceptualization, Formal analysis, Methodology, Writing - review & editing, Supervision, Funding acquisition.
- **César Pérez Cruzado**: Conceptualization, Data curation, Methodology, Formal Analysis, Project administration, Writing - review & editing, Supervision, Funding acquisition

- **Ulises Diéguez Aranda (Study I)**: Formal Analysis, Writing - review & editing, Funding acquisition.
- Fernando Castedo Dorado **(Study I)**: Data curation, Writing - review & editing, Funding acquisition.
- **Jesús Julio Camarero (Study II)**: Conceptualization, Data curation, Methodology, Resources, Supervision, Writing - review & editing.
- **Matteo Cerioni (Study II)**: Methodology, Resources, Writing - review & editing.
- **Andrea Hevia (Study II)**: Methodology, Resources, Writing - review & editing.
- **Raúl Sánchez Salguero (Study II)**: Methodology, Resources, Writing - review & editing.
- **Darío Martín Benito (Study II)**: Data curation, Funding acquisition, Resources, Writing - review & editing.
- **Adela Martínez Calvo (Study III)**: Data curation, Methodology, Software, Writing - review & editing.
- **Maria José Ginzo Villamayor (Study III)**: Software, Writing - review & editing.
- **Manuel Antonio Novo Pérez (Study III)**: Software.
- **Fernando Montes (Study III)**: Conceptualization, Methodology, Writing - review & editing.

Journal's performance

Study	Journal	Category	JIF 2020
I	*Annals of Forest Science*	Forestry	2.583 (Q1)
II	*Forest Ecology and Management*	Forestry	3.558 (Q1)

III	*Environmental Modelling & Software*	Computer science, interdisciplinary applications - engineering, environmental - water resources - environmental sciences	5.288 (Q1-Q2-Q1-Q1)

Other articles as first author

Molina-Valero, J. A., Ginzo Villamayor, M. J., Novo Pérez, M. A., Álvarez-González, J. G., & Pérez-Cruzado, C. (2019). Estimación del área basimétrica en masas maduras de *Pinus sylvestris* en base a una única medición del escáner láser terrestre (TLS). *Cuadernos de la Sociedad Española de Ciencias Forestales*, *45*, 97-116. https://doi.org/10.31167/csecfv0i45.19887

Molina-Valero, J. A., Ginzo Villamayor, M. J., Novo Pérez, M. A., Álvarez-González, J. G., Montes, F., Martínez-Calvo, A., and Pérez-Cruzado, C. (2020). FORTLS: An R Package for Processing TLS Data and Estimating Stand Variables in Forest Inventories. *Environmental Sciences Proceedings*, *3*, 38. https://doi.org/10.3390/IECF2020-08066

Other articles as coauthor

Alonso-Rego, C., Arellano-Pérez, S., Guerra-Hernández, J., Molina-Valero, J. A., Martínez-Calvo, A., Pérez-Cruzado, C., ... and Ruiz-González, A. D. (2021). Estimating Stand and Fire-Related Surface and Canopy Fuel Variables in Pine Stands Using Low-Density Airborne and Single-Scan Terrestrial Laser Scanning Data. *Remote Sensing*, *13*(24), 5170. https://doi.org/10.3390/rs13245170

Guerra-Hernández, J., Botequim, B., Bujan, S., Jurado-Varela, A., Molina-Valero, J. A., Martínez-Calvo, A., and Pérez-Cruzado, C. (2022). Interpreting the uncertainty of model-based and design-based estimation in downscaling estimates from NFI data: a case-study in Extremadura (Spain). *GIScience & Remote Sensing*, *59*(1), 686-704. https://doi.org/10.1080/15481603.2022.2051383

Software

Molina-Valero, J. A., Martínez-Calvo, A., Ginzo Villamayor, M. J., Novo Pérez, M. A., Álvarez-González, J. G., Montes, F., and Pérez-Cruzado, C. (2021). Automatic Processing of TLS Point Cloud Data for Forestry Purposes. R package version 1.0.6. https://CRAN.R-project.org/package=FORTLS

Apart from the aforementioned articles, the results generated in this doctoral thesis have been spread in:

Conferences

Molina-Valero, J. A., Diéguez-Aranda, U., Álvarez-González, J. G., Castedo-Dorado, F., and Pérez-Cruzado, C. (2018). Site form as indicator of site productivity for even-aged stands: a case study for *Pinus radiata* D. Don stands in north-western Spain. In *New Frontiers in Forecasting Forests 2018*. Stellenbosch (South Africa). https://www.iufro.org/download/file/29788/6631/40100-40207-40300-40402-50104-stellenbosch18_pdf/

Molina-Valero, J. A., Allikmäe, E., Álvarez-González, J. G., and Pérez-Cruzado, C. (2018). Analysis of spatial forest structure in natural mountainous beech forest of the Cantabrian Range. In *11th International Beech Symposium*. IUFRO - University of Tuscia. Viterbo (Italy). https://exceptionaltrees.files.wordpress.com/2019/03/iufrobeech2018_proof.pdf

Molina-Valero, J. A., Sánchez Salguero, R., Pérez-Cruzado, C., Álvarez-González, J. G., Camarero, J. J., and Hevia, A. (2019). Tree-rings improve forest site productivity estimations in Atlantic Iberian *Pinus pinaster* forests. In *1st Meeting of the Iberian Ecological Society & XIV AEET Meeting*. Asociación Española de Ecología Terrestre (AEET) & Sociedad Ibérica de Ecología (SIBECOL) - University of Barcelona. Barcelona (Spain).

http://www.aeet.org/mm/file/Abstract%20Book%20SIBECOL2019.pdf

Molina-Valero, J. A., Ginzo Villamayor, M. J., Novo Pérez, M. A., Álvarez-González, J. G., and Pérez-Cruzado, C. (2019). Obtención de métricas relacionadas con el área basimétrica en masas maduras de *Pinus sylvestris* a partir de un único muestreo de TLS. In *Jornada científico-técnica del Grupo de Trabajo Ibérico de Inventario y Teledetección Forestal*. Sociedad Española de Ciencias Forestales (SECF) & Sociedad Portuguesa de Ciencias Forestales (SPCF). Madrid (Spain).

Molina-Valero, J. A., Ginzo Villamayor, M. J., Novo Pérez, M. A. Álvarez-González, J. G., and Pérez-Cruzado, C. (2019). Obtención de métricas relacionadas con variables dasométricas de altura en masas maduras de *Pinus sylvestris* a partir de un único escaneo de TLS. In *Modelización forestal en la era de la información. Retos y soluciones en un futuro incierto*. Sociedad Española de Ciencias Forestales (SECF). Solsona (Spain).

Molina-Valero, J. A. (2019). Estimación de la intensidad de perturbación sobre la estructura y el stock de carbono en bosques naturales. In *JIPAS 2019: I congreso de la juventud investigadora en producción primaria sostenible y calidad y seguridad alimentaria*. Red de Inmunogenom & Agrupación Estratégica BioReDes. Lugo (Spain). http://hdl.handle.net/10347/20875

Molina-Valero, J. A., Ginzo Villamayor, M. J., Novo Pérez, M. A., Álvarez-González, J. G., Montes, F., and Pérez-Cruzado, C. (2020). FORTLS: un paquete de R para a estimación de variables dasométricas para o seu uso en inventario forestal. In *VII Xornada de Usuarios de R en Galicia*. Oficina de Software Libre do CIXUG. Santiago de Compostela (Spain). https://www.youtube.com/watch?v=oXTdfl7YM4I

Molina-Valero, J. A., Põldveer, E., Álvarez-González, J. G., Laarmann, D., Korjus, H, and Pérez-Cruzado, C. (2021). The assessment and comparison of structural patterns among Mediterranean, temperate and boreal mature forest of *Pinus sylvestris*. In *Third*

ESP Europe Conference. Ecosystem Services Partnership and Estonian University of Life Sciences. Tartu (Estonia) https://cdn.aanmelderusercontent.nl/i/doc/b331e1d35349762b0f6f0bec74956fce?forcedownload=True

Molina-Valero, J. A., López Álvarez, O., Martínez-Calvo, A., and Pérez-Cruzado, C. (2021). Evaluación del uso del Escáner Láser Terrestre en inventario forestal a escala de monte. Un caso de estudio en base a la estimación de la biomasa arbórea. In *Workshop sobre Teledetección Próxima Terrestre para Aplicaciones Forestales*. University of Santiago de Compostela. Lugo (Spain). http://hdl.handle.net/10347/27511

Molina-Valero, J. A., Aulló-Maestro, I., Parras, A., Pérez Cruzado, C., and Montes, F. (2021). Assessing the ForeStereo sensor and the FORTLS R package for estimating stand variables in mature forests. In *SilviLaser2021*. TU Wien & Umweltdata. Viena (Austria). https://repositum.tuwien.at/handle/20.500.12708/19082

Molina-Valero, J. A., Sánchez-Salguero, R., Pérez-Cruzado, C., Álvarez-González, J. G., and Hevia, A. (2022). Escáner Láser Terrestre TLS para aplicaciones forestales en pinares. In *Selvicultura y Gestión de Pinares de Pino Piñonero y otros Pinares Mediterráneos*. University of Huelva, Asociación Forestal Andaluza & Junta de Andalucía. Huelva (Spain).

Molina-Valero, J. A., Ginzo Villamayor, M. J., Novo Pérez, M. A., Álvarez-González, J. G., Montes, F., and Pérez-Cruzado, C. (2022). FORTLS: un paquete de R para el uso operativo de dispositivos terrestres de tecnología LiDAR en inventario forestal. In *8º Congreso Forestal Español. Sociedad Española de Ciencias Forestales*. Lleida (Spain). https://8cfe.congresoforestal.es/sites/default/files/actas/8CFE-171.pdf

Participation in research projects

National

Conservation *vs.* management. Definition of management intensity indicators and provision of ecosystem services: monitoring and optimization (PID2020-119204RB-C22).

Modelling the effects of intensity of perturbation on the structure of natural forests and their carbon stocks by using data from the National Forestry Inventory (AGL2016-76769-C2-2-R).

Regional

Design of forest monitoring systems on a regional scale (ED431F 2020/02).

Los Pinares Andaluces como sumideros de carbono: Cuantificación, modelización y gestión forestal desde una perspectiva histórica (UHU-1266324).

Organizing and scientific committee

Molina-Valero, J. A., Rodríguez-Ruiz, J., Pérez-Cruzado, C., and Martínez-Calvo, A. (2021). Actas del Workshop sobre Teledetección Próxima Terrestre para Aplicaciones Forestales. University of Santiago de Compostela. Lugo (Spain). http://hdl.handle.net/10347/27511

Courses

Molina-Valero, J. A., and Martínez-Clavo, A. (2022). Curso práctico de procesado y análisis de datos tomados con dispositivos terrestres de tecnología LiDAR mediante el paquete de R FORTLS. Aplicaciones al Inventario Forestal (25 h). University of León. Ponferrada (Spain).

Seminars

Molina-Valero, J. A. (2021). FORTLS: An R Package for Processing TLS Data and Estimating Stand Variables in Forest Inventories. Ciclo de seminarios de actividades formativas de Máster oficial Universitario en Geomática, Teledetección y modelos espaciales aplicados a la Gestión Forestal. Grupo de Investigación de la Universidad de Córdoba de evaluación y restauración de sistemas agrícolas y forestales (ERSAF). Córdoba (Spain). https://www.youtube.com/watch?v=8CtRnIG6tpk

Worshops

Molina-Valero, J. A., Martínez-Clavo, A., and López-Álvarez, O. (2021). Taller para el procesado y análisis de los datos tomados con el Escáner Láser Terrestre (TLS) mediante el paquete de R FORTLS (3.5 h). Workshop sobre Teledetección Próxima Terrestre para Aplicaciones Forestales. University of Santiago de Compostela. Lugo (Spain).

CONTENTS

ABSTRACT

Estimation of forest maturity linked to the biomass (or carbon) stock capacity is considered one of the most important issues regarding forest management and planning in the most recent forest strategies and policies. This doctoral thesis explores such relationships and considers the use of stand level maximum biomass stock (MBS) as a proxy for forest maturity through site quality gradient, as a measure that can feasibly be estimated from National Forest Inventory (NFI) data. The research study was conducted in Spain using NFI data and a non-probabilistic collection of mature plots. Both data sources correspond to maritime pine (*Pinus pinaster* ssp. *atlantica* H. de Vill.), Scots pine (*Pinus sylvestris* L.), beech (*Fagus sylvatica* L.), beech-fir and silver fir (*Abies alba* Mill.) forests.

The field data were used to test the hypothesis that mature forests not affected by recent large disturbances hold the MBS potential for their respective site qualities, even for degrees of naturalness (or maturity) prior to old-growth. This was possible by using the site form (SF), an age-independent reliable site quality index. SF is suitable for both even-aged and uneven-aged stands, as it is defined as the dominant height at a reference dominant diameter. The performance of SF for characterizing site quality was evaluated by comparison with the well-known site index (SI) in even-aged *Pinus radiata* D. Don stands. After confirming the aforementioned hypothesis and approaches, the relative biomass stock (BS, %) was estimated at national scale by using the NFI data for the forests under study. For this purpose, a logarithmic quantile regression was fitted to the highest values of the scatter plot $biomass \sim SF$, hence parametrizing an equation representative of the MBS with which to compare $BS(\%)$ for each NFI plot.

The relationship between forest structure and forest maturity was also examined in this thesis. Both variables are directly related to forest complexity and consequently to many ecosystem services. The

structure of mature forest stands was characterized, as this stage of growth represents the reference conditions for emerging forestry practices aimed at optimizing ecosystem services. This variable was also assessed for mature stages of the different types of forest under study: in different biogeographical regions (Boreal, in Estonia; Atlantic and Mediterranean, in Spain) in the case of Scots pine forests, and for the highest degrees of naturalness (long untouched and old-growth forest) in the case of beech-fir forests (in the Spanish Pyrenees). While some features such as size differentiation mingling were greater at higher degrees of naturalness (reaching the highest values in old-growth forest), others showed the opposite trend (e.g. tree species biodiversity) or remained stable from lower to higher degrees of naturalness (e.g. horizontal tree distribution). Regarding the different biogeographical regions, a generalized gradient of structural complexity (Boreal > Atlantic > Mediterranean) was observed for some of the features, with no differences between Atlantic and Boreal regions in relation to species richness or mingling. Regarding the forest types, beech forests were significantly poorer in tree species richness and mingling, and beech-fir and silver fir were structurally the most heterogeneous, mainly due to the shade-tolerant nature of silver fir.

Finally, the potential of terrestrial laser scanning (TLS) (or terrestrial LiDAR) technology for estimating forest features in mature stands was explored. For this purpose, the R package FORTLS was developed for processing and analyzing TLS data and obtaining metrics and variables related to important forest attributes. The accuracy of estimation was similar to that obtained with the state-of-the-art technologies for conventional stand level variables. It was also demonstrated that is possible to fit predictive models with the set of metrics and variables generated by FORTLS. In this sense, MARS models usually performed better for predicting variables such as the absolute (Mg ha^{-1}) and relative ($BS(\%)$) biomass stock and also the degree of naturalness assessed by the naturalness score index (NS). The findings reported in this thesis all suggest that high biomass values can be reached at lower degrees of naturalness than the old-growth stage. However, highly complex forest structural features may only be observed at more mature stages. In addition, further research should

include technologies like TLS as auxiliary tools for forest management and planning to improve the accuracy, precision, temporal frequency and spatial scale of forest monitoring.

Keywords: close-range remote sensing; carbon sequestration; forest growing stock; forest monitoring; open-source software; natural forests; site productivity; terrestrial-based-technologies

RESUMEN

1 Introducción

La evaluación de la madurez de los bosques (o grado de naturalidad) es cada vez más un requerimiento exigido por las políticas de conservación y gestión forestal sostenible a nivel global. Al margen de controversias terminológicas, "old-growth" es el término por antonomasia para referirse a los grados de madurez más altos, haciendo alusión a bosques que han llegado a los últimos estadios de la sucesión ecológica bajo una dinámica natural y en ausencia de perturbaciones antrópicas. Estos bosques tienen un alto potencial para proveer servicios ecosistémicos, por lo que se consideran un marco referencial en la gestión y conservación, haciéndose cada vez más necesaria su caracterización mediante indicadores asequibles. Estos indicadores en la mayoría de los casos se centran en las características estructurales, que son las más fáciles estimar a partir de inventarios forestales (IF) convencionales. Sin embargo, estudios recientes ponen de manifiesto que indicadores crono-funcionales obtenidos a partir de datos dendrocronológicos pueden ser más precisos debido a que aportan información sobre toda la dinámica histórica del bosque.

Un aspecto fundamental de los bosques es su papel como sumidero de carbono. Es por esto por lo que las acciones de conservación, restauración y gestión forestal sostenible han sido incorporadas como líneas estratégicas en los grandes acuerdos de las conferencias de las Naciones Unidas sobre el cambio climático (protocolo de Kyoto, proyectos REDD+ y Acuerdo de París) para el secuestro de gases de efecto invernadero. Tanto los mecanismos que estos acuerdos contemplan para el secuestro carbono, como la nueva estrategia forestal europea, han puesto a los bosques *old-growth* en el centro de miras debido a su capacidad para generar servicios ecosistémicos. No obstante, el rol de estos bosques como sumideros de carbono no está tan

claro y existe gran controversia al respecto. Hay trabajos que demuestran que se puede llegar al máximo stock de carbono en estados de madurez previos al de *old-growth*, y otros que aseguran que incluso en estados de madurez tan altos aún existe potencial para incrementar la cantidad de carbono almacenado. En cualquier caso, la fracción de biomasa más importante, tanto por su dinamismo como por representar el principal sumidero de carbono en los inventarios de gases de efecto invernadero, pertenece a los árboles vivos (biomasa aérea y subterránea). En esta tesis doctoral se estudia a nivel nacional (España) en base al Inventario Forestal Nacional (IFN) y una red de parcelas en bosques maduros: (i) si estos bosques maduros tienen la capacidad de seguir almacenando carbono, y (ii) la posibilidad de definir una expresión matemática característica del máximo stock de biomasa (MBS) para las tipologías de bosques estudiados.

Todo lo comentado anteriormente juega especial relevancia en los mecanismos de compensación de las emisiones de CO_2, donde se necesitan metodologías para la estimación del carbono almacenado en los bosques lo más exactas y operativas posibles. En este sentido, no está muy claro como estimar el stock de carbono almacenado en un bosque con respecto al potencial máximo que este podría alcanzar. Esto es debido a que las estimaciones se hacen en base a dos o más mediciones en el tiempo, lo cual puede dar lugar a las siguientes incongruencias: (i) ¿qué pasa si solo hay un IF?; (ii) se puede dar el caso de que el stock de carbono se mantenga igual (p. ej. si dos mediciones consecutivas ocurren en un mismo punto de la gestión); (iii) aunque el stock de carbono aumente, cómo sabemos si este aún podría seguir aumentando, o ya ha llegado a su potencial máximo; y (iv) ¿cómo comparamos valores de calidades de estación diferentes? Para eso es necesario definir una línea base, que en bosques con cobertura arbórea continua no es tan evidente como en plantaciones donde hay una corta final. Es en este punto donde la capacidad que tiene un bosque para almacenar carbono a lo largo de su vida juega un papel relevante, pudiéndose establecer un máximo determinado por su madurez y para un gradiente de calidad de estación. Demostrando que los bosques maduros en ausencia de grandes perturbaciones son capaces de alcanzar el MBS, y sabiendo que todos los grados de madurez deben estar

representados en un IF de base probabilística, sería posible estimar el porcentaje aproximado de carbono almacenado con respecto al máximo potencial (p. ej. a escala nacional utilizando el IFN). Para esto es necesario utilizar un índice de calidad de estación factible cuando la edad de los árboles es desconocida y la estructura no necesariamente regular, como es el caso del índice de forma (SF) que es definido como la altura dominante para un diámetro dominante de referencia.

Por otro lado, se sabe que muchas de las propiedades estructurales de los bosques están directamente relacionadas con su madurez y por ende con la provisión de servicios ecosistémicos. Estas propiedades están descritas principalmente por los patrones en la distribución espacial horizontal y vertical de los árboles. Además, son los atributos más utilizados para caracterizar los bosques con grados de madurez altos, pudiendo ser fácilmente alteradas mediante prácticas selvícolas y así hacer una gestión orientada a la obtención de atributos característicos de la madurez, lo cual es cada vez más demandado tanto por la sociedad como por las estrategias y políticas forestales. En este sentido, se vuelve necesaria la caracterización de los atributos estructurales de bosques maduros, a poder ser mediante variables fácilmente registrables en IFs. En esta tesis se caracteriza la estructura en condiciones de madurez para los tipos de bosques estudiados, diferentes regiones biogeográficas y distintos grados de madurez.

Las metodologías empleadas en la evaluación y monitoreo de los bosques están en continua mejora, especialmente en las últimas décadas gracias a la aparición de tecnologías como los sensores remotos. En este sentido la tecnología LiDAR (*Light Detection and Ranging*) es muy interesante por su capacidad para generar información tridimensional de gran utilidad para la estimación de variables utilizadas en aplicaciones forestales. Por un lado, los dispositivos LiDAR aerotransportados ya son operativos en muchas aplicaciones. Por otro lado, los dispositivos terrestres como el escáner láser terrestre (TLS) están mostrando un gran potencial para su implementación en los IFs gracias, entre otras cosas, a su alta precisión. De hecho, existen decenas de algoritmos capaces de procesar estos datos. Sin embargo, aún hace falta desarrollar las metodologías adecuadas para hacer operativo su uso en aplicaciones prácticas de IF. Con este objetivo, en esta tesis doctoral

se ha desarrollado el paquete de R FORTLS, capaz de automatizar el procesado de datos pertenecientes a dispositivos terrestres de tecnología LiDAR. Este permite (i) estimar variables a nivel de árbol individual, (ii) estimar variables de masa, (iii) generar métricas relacionas con atributos de masa, y (iv) optimizar el diseño de parcela mediante la calibración con datos de campo. Además, incluye metodologías que permiten la corrección de oclusiones cuando se trabaja con escaneos únicos de TLS, los cuales tienen una mayor eficiencia en el muestreo.

Aunque el TLS ha sido principalmente utilizado en la estimación de variables forestales convencionales, existen algunos trabajos donde se ha explorado su potencial para evaluar las características estructurales y por lo tanto de madurez del bosque. En este sentido puede desempeñar un papel relevante debido a la posibilidad de medir de forma rápida y muy precisa los atributos tridimensionales del bosque. A pesar de que muchos estudios se basan en escaneos múltiples, otros han demostrado su utilidad mediante escaneos únicos, distinguiendo propiedades estructurales complejas entre diferentes grados de madurez y/o gestión. Siguiendo esta línea, en la presente tesis se explora el potencial de los escaneos únicos de TLS para la estimación del grado de naturalidad (o madurez) y stock de biomasa relativo (en base al MBS) mediante modelos predictivos utilizando las métricas y variables generadas con FORTLS como información auxiliar.

2 Objetivos

Esta tesis doctoral constituye un trabajo de investigación original que tiene como principal objetivo la evaluación y modelización de la madurez forestal con datos de IFNs y una muestra no probabilística de parcelas pertenecientes a bosques maduros, necesaria para probar las hipótesis planteadas. Para ello también se caracteriza la estructura de estos bosques maduros y se explora el potencial del TLS como dispositivo de medición y predicción de los atributos de madurez planteados.

3 Materiales y métodos

Los principales bosques estudiados en esta tesis doctoral se corresponden con las tipologías pertenecientes a hayedos (*Fagus sylvatica* L.), abetales (*Abies alba* Mill.), sus formaciones mixtas de hayedo-abetales, pinares de pino pinaster de la zona atlántica (*Pinus pinaster* ssp. *atlantica* H. de Vill.) y pino silvestre (*Pinus sylvestris* L.).

Datos

Los datos utilizados provienen de varias bases de datos que pueden ser clasificadas en función de su escala de menor a mayor: a escala regional se cuenta con (i) 158 parcelas permanentes, con entre 2 y 5 mediciones, de pino radiata (*Pinus radiata* D. Don) del noroeste de España establecidas por el grupo de investigación UXAFORES de la Universidad de Santiago de Compostela (USC); y (ii) 27 parcelas maduras (incluyendo estados de *old-growth*) de abetales, hayedos y hayedo-abetales localizadas en el Pirineo español. Estas 27 parcelas pertenecen al proyecto de investigación FORESCHANGE (AGL2016-76769-C2-2-R). A escala nacional se dispone de (iii) una red de 143 parcelas pertenecientes a bosques maduros establecidas en el proyecto FORESCHANGE; y (iv) 7249 parcelas del IFN. Las parcelas de las bases de datos iii y iv corresponden a abetales, hayedos, hayedo-abetales, pinares de pino pinaster y pino silvestre. La última base de datos (v) asciende a escala europea conteniendo parcelas maduras de pino silvestre pertenecientes a zonas mediterráneas y atlánticas (España) y boreales (Estonia), correspondientes al proyecto FORESCHANGE y a la red estonia de parcelas de investigación (Estonian University of Life Sciences), respectivamente.

Índice de forma

En primer lugar, para la red de parcelas permanentes de pino radiata, se han ajustado curvas de calidad de estación para el índice de sitio (SI) -altura dominante a una edad de referencia-, y el índice de forma (SF) -altura dominante para un diámetro dominante de referencia-. Para ello

se ha utilizado el método de diferencias algebraicas generalizadas (GADA) con dos parámetros específicos del sitio mediante el modelo base Hossfeld IV. Con el objetivo de comprobar la idoneidad del SF, se han evaluado las siguientes propiedades consideradas como deseables para cualquier índice de calidad de estación: (i) reproducibilidad y consistencia; (ii) representatividad del sitio; (iii) correlación con la productividad potencial; (iv) comportamiento al menos tan bueno como otros índices utilizados; y (v) decrecimiento de la ratio diámetro/altura a medida que se incrementa la calidad de estación. Una vez validado el SF, este se ha ajustado para los bosques de estudio en los casos en los que no existían modelos previos (abetales y hayedo-abetales). Para ello se ha utilizado la metodología de la curva guía, ya que se trataba de parcelas temporales en la mayoría de los casos. En este caso los modelos base considerados han sido Hossfeld-II y Bertalanfy-Richards. Al igual que antes se han validado las asunciones de los residuos de los modelos y se han comprobado las propiedades que debe satisfacer un índice de calidad de estación.

Estimación del máximo stock de biomasa

Para validar la hipótesis de que el máximo stock de biomasa se alcanza con grados de madurez anteriores a los más altos (p. ej. *old-growth*), se ha trabajado con la base de datos ii que contiene el mayor rango de grados de madurez (incluyendo *old-growth*). En primer lugar, se ha estimado el grado de madurez (conocido como *naturalness score -NS-*) de cada parcela mediante indicadores crono-funcionales obtenidos a partir de datos dendrocronológicos. Después, se ha contrastado el stock de biomasa (aérea y subterránea) perteneciente a los árboles vivos de estas parcelas maduras con todas las parcelas del IFN correspondientes a las mismas tipologías de bosques. Para esto se han tenido en cuenta sus calidades de estación, estimadas mediante el SF previamente validado. Posteriormente, se ha establecido el MBS para cada tipo de bosque en base a la curva logarítmica $MBS \sim SF$ ajustada mediante regresión cuantílica (percentil 95.7) en el gráfico de dispersión de biomasa frente a SF. Finalmente, esta curva ha permitido obtener el stock de biomasa relativo ($BS(\%)$) con respecto al máximo posible, y

evaluar si hay relación entre el $BS(\%)$ y el NS, para probar la hipótesis de que bosques maduros alcanzan el MBS antes de llegar a condiciones de *old-growth*.

Caracterización de la estructura

La estructura ha sido caracterizada en base a índices basados en los 4 árboles más cercanos a cada árbol focal. Estos se han calculado para cada individuo y de esta manera obtener los valores medios a nivel de parcela. Los índices utilizados han sido los siguientes: (i) riqueza de especies, (ii) mezcla de especies, (iii) distribución de madera muerta en pie, (iv) diferenciación diamétrica, y (v) patrón de distribución horizontal de los árboles. Los respectivos valores medios a nivel de parcela han sido comparados entre las parcelas maduras de los bosques de estudio, diferentes regiones biogeográficas (Mediterránea, Atlántica y Boreal) en el caso de pino silvestre, y entre distintos grados de madurez en hayedo-abetales (bosques maduros, *long untouched* y *old-growth*).

Modelización del estado de madurez mediante el TLS

Este apartado consta en primer lugar del desarrollo del paquete de R FORTLS, que tiene el principal objetivo de automatizar el procesado y análisis de datos pertenecientes a dispositivos terrestres de tecnología LiDAR con un propósito forestal. Esta herramienta contiene los principales pasos comunes a otras aplicaciones similares como son la normalización de las nubes de puntos, la detección de árboles y estimación de variables de árbol individual y variables de masa. Asimismo, incluye metodologías para corregir el efecto de las oclusiones en el caso de escaneos únicos de TLS, así como la optimización del diseño de parcela mediante la calibración con datos de campos. Además, genera una serie de métricas con alto potencial para ser relacionadas con variables de masa y poder ajustar modelos predictivos de utilidad para la estimación de variables de interés. Una vez desarrollado FORTLS, algunas de las principales variables de masa estimadas en base a los datos de campo para las parcelas maduras

(densidad -árboles ha^{-1}, N-, área basimétrica – m^2 ha^{-1}, G-, diámetro medio aritmético -cm, $\bar{d}$- y altura media aritmética -m, $\bar{h}$-) han sido comparadas con las estimaciones de FORTLS pertenecientes a escaneos únicos. También, se ha explorado el potencial de las variables y métricas de FORTLS para ajustar modelos predictivos con los que estimar la biomasa absoluta (Mg ha^{-1}) y relativa ($BS(\%)$), así como el grado de naturalidad (NS). Para ello se han ajustado modelos lineales múltiples, MARS y random Forest para diferentes diseños de parcela (área fija, k-tree y de muestreo angular o relascópica). Finalmente se han evaluado qué grupos de métricas han sido más relevantes en los modelos ajustados.

4 Resultados y discusión

Índice de forma

La bondad del ajuste del SF fue similar a la del SI, mostrando estadísticos significativos y familias de curvas de calidad de estación que describían de forma adecuada la tendencia de los datos en ambos casos. Los resultados del ajuste del SF además fueron similares a los que pueden encontrarse en trabajos previos. Por otro lado, se cumplieron las propiedades deseables que cualquier índice de calidad de estación debe cumplir, demostrando así la utilidad del SF frente al SI como el índice de referencia en plantaciones de *P. radiata*. La validación del buen funcionamiento del SF en una situación conocida, sirvió como paso previo para ajustar el SF en dos de las tipologías de bosque utilizadas en esta tesis, como fueron los abetales y hayedo-abetales. Estos nuevamente mostraron estadísticos significativos en la bondad del ajuste, cumpliéndose las asunciones de los residuos del modelo y las propiedades deseables de cualquier índice de calidad de estación. No obstante, cabe destacar que la escasez de datos de estas formaciones en el IFN (solo presentes en Pirineos), la metodología utilizada en el ajuste (curva guía) derivada del uso de parcelas temporales, y la estructura irregular de estas masas; hacen que el ajuste de los modelos sea presumiblemente peor que en condiciones más simplificadas como es el caso de las plantaciones de *P. radiata*.

Estimación de la madurez forestal en términos del stock de biomasa

En primer lugar, y para el caso aquí estudiado de abetales, hayedos y hayedo-abetales pirenaicos, se demostró la hipótesis de que los bosques maduros pueden alcanzar el MBS de árboles vivos con grados de madurez inferiores a los más altos como podría ser el caso de los *old-growth*. En este sentido, los indicadores crono-funcionales obtenidos a partir de datos dendrocronológicos, sirvieron para estimar el grado de naturalidad (NS), demostrando que las masas consideradas como *old-growth* (bosque de Aztaparreta) alcanzaban los valores máximos. Luego se contrastó en base al IFN que estas parcelas alcanzaban los valores máximos de biomasa arbórea viva para sus respectivos valores de SF. Por último, el ajuste de los modelos de MBS sirvió para hacer la comparación del $BS(\%)$ con el NS indistintamente de la calidad de estación, sin observarse relación entre ambos, siendo a veces el $BS(\%)$ mayor para valores de NS menores. Esto demostró la hipótesis de partida de que el MBS puede alcanzarse con grados de madurez anteriores al de *old-growth*.

Este análisis se extendió al resto de los bosques evaluados, observándose nuevamente que las parcelas maduras alcanzaban los máximos valores de biomasa frente a los datos del IFN y para valores similares de SF. De tal modo, pudo obtenerse el $BS(\%)$ para todas las parcelas del IFN mediante el ajuste de las curvas de MBS y hacer una evaluación a nivel nacional. Este alcanza valores medios próximos al 40% en todos los bosques excepto en hayedos donde el $BS(\%)$ es algo superior (~50%). Cuando el $BS(\%)$ se representa en el mapa, en rasgos generales se puede observar una mezcla de valores (0-100%) más o menos homogénea por todo el territorio. Sin embargo, se puede destacar como para las masas de pino pinaster, las zonas con valores más bajos son más frecuentes en zonas donde la recurrencia de incendios es más alta. Por otro lado, también destaca en el caso del pino silvestre como hay una mayor concentración de parcelas con valores altos de $BS(\%)$ en las zonas donde ha habido una gestión más continuada en tiempo (Sierra de Guadarrama y Sierra de la Demanda). También resalta como en el caso de los hayedos, precisamente en la región donde más gestión se hace (Navarra) no se encuentran los valores más bajos de $BS(\%)$.

Caracterización de la estructura

Algunas de las características estructurales han mostrado diferencias en función del tipo de bosque y región biogeográfica, como es el caso de la riqueza de especies arbóreas, claramente menor en los hayedos y pinares de silvestre de la región mediterránea. En cuanto a la mezcla de especies, el hayedo-abetal por su condición de boque mixto con especies tolerantes a la sombra, mostró los valores más altos. La distribución de madera muerta en pie estuvo directamente relacionada con la densidad, encontrándose los valores más altos en los bosques con mayores densidades, tanto entre regiones biogeográficas como entre tipos de bosque. La diferenciación diamétrica mostró un gradiente intraespecífico latitudinal (Boreal > Atlántico > Mediterráneo), posiblemente condicionado por una mayor densidad y episodios de mortalidad natural. También se observó un gradiente interespecífico (hayedo-abetal > abetal > hayedo), posiblemente condicionado por el temperamento del abeto como especie de sombra, lo cual permite la coexistencia de un subpiso de abeto. Este además fue claramente más alto en parcelas con altos grados de madurez como es el caso de los *old-growth* (Aztaparreta). En cuanto al patrón de distribución horizontal, fue muy similar en todos los casos, con una distribución aleatoria que es lo más común en la mayoría de los bosques.

Modelización del estado de madurez mediante el TLS

En primer lugar, el paquete de R FORTLS desarrollado en esta tesis para el procesado y análisis de datos de TLS, ha resultado ser una herramienta satisfactoria para la estimación de variables de masa comunes en IF (N, G, $\bar{d}$, $\bar{h}$) en base a escaneos únicos. La exactitud de los resultados se encuentra próxima a muchas de las referencias bibliográficas. De todas formas, se han encontrado diferencias entre los distintos tipos de bosques, siendo los hayedos los que han mostrado mejores resultados en general. Además, las correcciones de oclusiones no siempre han mejorado los resultados, siendo irrelevantes en la estimación de $\bar{d}$ y $\bar{h}$. Por otro lado, las métricas y variables generadas por FORTLS han resultado ser útiles para la modelización de variables

más complejas como la biomasa arbórea viva, el stock de biomasa relativo ($BS(\%)$) y el grado de madurez (NS). Concretamente los modelos MARS han mostrado los mejores resultados en casi todas las ocasiones. Sin embargo, esto no ha sido tan claro en cuanto al diseño de parcela, siendo la parcela de muestreo angular la que ha presentado mejores resultados en más ocasiones.

5 Conclusiones

El índice de forma (SF) ha demostrado ser un índice de calidad de estación fiable con resultados similares al usual índice de sitio (SI) utilizado en masas regulares, como son las plantaciones de *P. radiata* analizadas en este caso de estudio. Al contrario que el SI, que solo tiene sentido en masas regulares, el SF funciona también en masas irregulares. Esto ha permitido utilizar el SF en los bosques estudiados en esta tesis doctoral, con edad desconocida y estructuras irregulares en muchos casos. Con respecto a la hipótesis de si las masas maduras alcanzan el máximo stock de biomasa (MBS), se demostró para una submuestra de parcelas maduras del Pirineo como grados de madurez previos a los más altos (*old-growth*) pueden alcanzar los valores máximos de biomasa. Estas parcelas maduras también alcanzaron los valores máximos con respecto a los datos del IFN para calidades de estación similares, demostrando por lo tanto que los bosques maduros sin perturbaciones graves recientes definen la línea base del MBS. Estos hallazgos permitieron estimar el stock de biomasa arbórea viva (aérea y subterránea) con respecto al MBS utilizando los datos del IFN; y evaluando así el stock relativo de biomasa ($BS(\%)$) almacenada a nivel nacional, que resultó ser de media algo mayor en hayedos (~50%) que en el resto de formaciones (~40%). Los índices estructurales demostraron su utilidad para discernir algunas características entre diferentes tipos de bosques, estados de madurez y regiones biogeográficas. En cuanto a regiones biogeográfias, los pinares de silvestre de la zona mediterránea mostraron claramente los valores más bajos en riqueza y mezcla de especies, distribución de madera muerta en pie y diferenciación diamétrica, lo cual puede ser en parte debido a su origen como plantaciones (no demasiado viejas) en muchas

ocasiones. Entre tipos de bosques, se puede destacar una mayor complejidad estructural definida por la diferenciación diamétrica en los hayedos-abetales frente al resto, posiblemente debida al temperamento del abeto como especie de sombra. En cuanto a grados de madurez, la diferenciación diamétrica demostró ser el atributo estructural más útil para discernir entre estados de madurez, mostrando claramente los valores más altos en masas clasificadas como *old-growth* (Aztaparreta) y *long untouch* (bosque de Lizardoia). Por último, el paquete de R FORTLS ha demostrado su utilidad en el procesado y análisis de datos pertenecientes a escaneos únicos del escáner láser terrestre (TLS). Aun tratándose de bosques complejos de escanear debido al grado de madurez (árboles grandes que generan muchas sombras, presencia de matorral, etc.), se han alcanzado valores similares a los de referencia en variables de masa habituales en IFs. Además, las métricas y variables generadas por FORTLS han sido útiles para modelizar variables más complejas como el $BS(\%)$ y el grado de madurez (NS). Estos resultados, aún preliminares, indican que la incorporación del TLS a los IFNs podría aumentar las posibilidades de estimación de variables más complejas necesarias para las nuevas estrategias forestales europeas, como por ejemplo aquellas relacionadas con la madurez del bosque.

RESUMO

1 Introdución

A avaliación da madurez dos bosques (ou grao de naturalidade) é cada vez máis un requirimento esixido polas políticas de conservación e xestión forestal sostible a nivel global. Á marxe de controversias terminolóxicas, "old-growth" é o termo por antonomasia para referirse aos graos de madurez máis altos, facendo alusión a bosques que chegaron ás últimas etapas da sucesión ecolóxica baixo unha dinámica natural e en ausencia de perturbacións antrópicas. Estes bosques teñen un alto potencial para prover servizos ecosistémicos, polo que se consideran un marco referencial na xestión e conservación, facéndose cada vez máis necesaria a súa caracterización mediante indicadores alcanzables. Estes indicadores na maioría dos casos céntranse nas características estruturais, que son as máis fáciles de estimar a partir de inventarios forestais (IF) convencionais. Con todo, estudos recentes poñen de manifesto que indicadores crono-funcionais obtidos a partir de datos dendrocronológicos poden ser máis precisos debido a que achegan información sobre toda a dinámica histórica do bosque.

Un aspecto fundamental dos bosques é o seu papel como sumidoiro de carbono. É por isto polo que as accións de conservación, restauración e xestión forestal sostible foron incorporadas como liñas estratéxicas nos grandes acordos das conferencias das Nacións Unidas sobre o cambio climático (protocolo de Kyoto, proxectos REDD+ e Acordo de París) para o secuestro de gases de efecto invernadoiro. Tanto os mecanismos que estes acordos contemplan para o secuestro de carbono, como a nova estratexia forestal europea, puxeron aos bosques *old-growth* no centro de miras debido á súa capacidade para xerar servizos ecosistémicos. Non entanto, o rol destes bosques como sumidoiros de carbono non está tan claro e existe gran controversia ao seu respecto.

Hai traballos que demostran que se pode chegar ao máximo stock de carbono en estados de madurez previos ao de *old-growth*, e outros que aseguran que mesmo en estados de madurez tan altos aínda existe potencial para aumentar a cantidade de carbono almacenado. En calquera caso, a fracción de biomasa máis importante, tanto polo seu dinamismo como por representar o principal sumidoiro de carbono nos inventarios de gases de efecto invernadoiro, pertence ás árbores vivas (biomasa aérea e subterránea). Nesta tese doutoral estúdase a nivel nacional (España) en base ao Inventario Forestal Nacional (IFN) e unha rede de parcelas en bosques maduros: (i) se estes bosques maduros teñen a capacidade de seguir almacenando carbono, e (ii) a posibilidade de definir unha expresión matemática característica do máximo stock de biomasa (MBS) para as tipoloxías de bosques estudados.

Todo o comentado anteriormente xoga especial relevancia nos mecanismos de compensación das emisións de CO_2, onde se necesitan metodoloxías para a estimación do carbono almacenado nos bosques o máis exactas e operativas posibles. Neste sentido, non está moi claro como estimar o stock de carbono almacenado nun bosque con respecto ao potencial máximo que este podería alcanzar. Isto é debido a que as estimacións se fan en base a dúas ou máis medicións no tempo, o cal pode dar lugar ás seguintes incongruencias: (i) ¿qué pasa se só hai un IF?; (ii) pódese dar o caso de que o stock de carbono se manteña igual (p. ex. se dúas medicións consecutivas ocorren nun mesmo punto da xestión); (iii) aínda que o stock de carbono aumente, como sabemos se este aínda podería seguir aumentando, ou xa chegou ao seu potencial máximo; e (iv) ¿cómo comparamos valores de calidades de estación diferentes? Para iso é necesario definir unha liña base, que en bosques con cobertura arbórea continua non é tan evidente como en plantacións onde hai unha curta final. É neste punto onde a capacidade que ten un bosque para almacenar carbono ao longo da súa vida xoga un papel relevante, podéndose establecer un máximo determinado pola súa madurez e para un gradiente de calidade de estación. Demostrando que os bosques maduros en ausencia de grandes perturbacións son capaces de alcanzar o MBS, e sabendo que todos os graos de madurez deben estar representados nun IF de base probabilística, sería posible estimar a porcentaxe aproximada de carbono almacenado con respecto ao

máximo potencial (p. ex. a escala nacional utilizando o IFN). Para isto é necesario utilizar un índice de calidade de estación factible cando a idade das árbores é descoñecida e a estrutura non necesariamente regular, como é o caso do índice de forma (SF) que é definido como a altura dominante para un diámetro dominante de referencia.

Por outra banda, coñécese que moitas das propiedades estruturais dos bosques están directamente relacionadas coa súa madurez e polo tanto coa provisión de servizos ecosistémicos. Estas propiedades están descritas principalmente polos patróns na distribución espacial horizontal e vertical das árbores. Ademais, son os atributos máis utilizados para caracterizar os bosques con graos de madurez altos, podendo ser facilmente alteradas mediante prácticas selvícolas e así facer unha xestión orientada á obtención de atributos característicos da madurez, o cal é cada vez máis demandado tanto pola sociedade como polas estratexias políticas e forestais. Neste sentido, vólvese necesaria a caracterización dos atributos estruturais de bosques maduros, a poder ser mediante variables facilmente rexistrables en IFs. Nesta tese caracterízase a estrutura en condicións de madurez para os tipos de bosques estudados, diferentes rexións biogeográficas e distintos graos de madurez.

As metodoloxías empregadas na avaliación e monitoreo dos bosques están en continua mellora, especialmente nas últimas décadas grazas á aparición de tecnoloxías como os sensores remotos. Neste sentido a tecnoloxía LiDAR (*Light Detection and Ranging*) é moi interesante pola súa capacidade para xerar información tridimensional de gran utilidade para a estimación de variables utilizadas en aplicacións forestais. Por unha banda, os dispositivos LiDAR aerotransportados xa son operativos en moitas aplicacións; por outra parte, os dispositivos terrestres como o escáner láser terrestre (TLS) están a mostrar un gran potencial para a súa implementación nos IFs grazas, entre outras cousas, á súa alta precisión. De feito, existen decenas de algoritmos capaces de procesar estes datos. Con todo, aínda fai falta desenvolver as metodoloxías axeitadas para facer operativo o seu uso en aplicacións prácticas de IF. Con este obxectivo, nesta tese doutoral desenvolveuse o paquete de R FORTLS, capaz de automatizar o procesado de datos pertencentes a dispositivos terrestres de tecnoloxía

LiDAR. Este permite (i) estimar variables a nivel de árbore individual, (ii) estimar variables de masa, (iii) xerar métricas relacionas con atributos de masa, e (iv) optimizar o deseño de parcela mediante a calibración con datos de campo. Ademais, inclúe metodoloxías que permiten a corrección de oclusións cando se traballa con escaneos únicos de TLS, os cales teñen unha maior eficiencia na mostraxe.
Aínda que o TLS foi principalmente utilizado na estimación de variables forestais convencionais, existen algúns traballos onde se explorou o seu potencial para avaliar as características estruturais e polo tanto de madurez do bosque. Neste sentido pode desempeñar un papel relevante debido á posibilidade de medir de forma rápida e moi precisa os atributos tridimensionais do bosque. A pesar de que moitos estudos se basean en escaneos múltiples, outros demostraron a súa utilidade mediante escaneos únicos, distinguindo propiedades estruturais complexas entre diferentes graos de madurez e/ou xestión. Seguindo esta liña, na presente tese explórase o potencial dos escaneos únicos de TLS para a estimación do grao de naturalidade (ou madurez) e stock de biomasa relativo (en base ao MBS) mediante modelos predictivos utilizando as métricas e variables xeradas con FORTLS como información auxiliar.

2 Obxectivos

Esta tese doutoral constitúe un traballo de investigación orixinal que ten como principal obxectivo a avaliación e modelización da madurez forestal con datos de IFNs e unha mostra non probabilística de parcelas pertencentes a bosques maduros, necesaria para probar as hipóteses expostas. Para iso tamén se caracteriza a estrutura destes bosques maduros e explórase o potencial do TLS como dispositivo de medición e predición dos atributos de madurez expostos.

3 Materiais e métodos

Os principais bosques estudados nesta tese doutoral correspóndense coas tipoloxías pertencentes a faiedos (*Fagus sylvatica* L.), abetais (*Abies alba* Mill.), as súas formacións mixtas de faiedo-abetais,

piñeirais de piñeiro pinaster da zona atlántica (*Pinus pinaster* ssp. *atlantica* H. de Vill.) e piñeiro silvestre (*Pinus sylvestris* L.).

Datos

Os datos utilizados proceden de varias bases de datos que poden ser clasificadas en función da súa escala de menor a maior: a escala rexional conta con (i) 158 parcelas permanentes, que teñen entre 2 e 5 medicións, de piñeiro radiata (*Pinus radiata* D. Don) do noroeste de España establecidas polo grupo de investigación UXAFORES da Universidade de Santiago de Compostela (USC); e (ii) 27 parcelas maduras (incluíndo estados de *old-growth*) de abetais, faiedos e faiedo-abetais localizadas no Pirineo español. Estas 27 parcelas pertencen ao proxecto de investigación FORESCHANGE (AGL2016-76769-C2-2-R). A escala nacional disponse de (iii) unha rede de 143 parcelas que pertencen a bosques maduros establecidas no proxecto FORESCHANGE; e (iv) 7249 parcelas do IFN. As parcelas das bases de datos iii e iv corresponden a abetais, faiedos, faiedo-abetais, piñeirais de piñeiro pinaster e piñeiro silvestre. A última base de datos (v) ascende a escala europea contendo parcelas maduras de piñeiro silvestre pertencentes a zonas mediterráneas e atlánticas (España) e boreais (Estonia), correspondentes ao proxecto FORESCHANGE e á rede estoniana de parcelas de investigación (Estonian University of Life Sciences), respectivamente.

Índice de forma

En primeiro lugar, para a rede de parcelas permanentes de piñeiro radiata, axustáronse curvas de calidade de estación para o índice de sitio (SI) -altura dominante a unha idade de referencia-, e o índice de forma (SF) -altura dominante para un diámetro dominante de referencia-. Para iso utilizouse o método de diferenzas alxébricas xeneralizadas (GADA) con dous parámetros específicos do sitio mediante o modelo base Hossfeld IV. Co obxectivo de comprobar a idoneidade do SF, avaliáronse as seguintes propiedades consideradas como desexables para calquera índice de calidade de estación: (i) reproducibilidad e

consistencia; (ii) representatividade do sitio; (iii) correlación coa produtividade potencial; (iv) comportamento polo menos tan bo como outros índices utilizados; e (v) decrecemento do cociente diámetro/altura a medida que se incrementa a calidade de estación. Unha vez validado o SF, este axustouse para os bosques de estudo nos casos nos que non existían modelos previos (abetais e faiedo-abetais). Para iso utilizouse a metodoloxía da curva guía, xa que se trataba de parcelas temporais na maioría dos casos. Neste caso os modelos base considerados foron Hossfeld-II e Bertalanfy-Richards. Do mesmo xeito que antes, validáronse as asuncións dos residuos dos modelos e comprobáronse as propiedades que debe satisfacer un índice de calidade de estación.

Estimación do máximo stock de biomasa

Para validar a hipótese de que o máximo stock de biomasa se alcanza con graos de madurez anteriores aos máis altos (p. ex. *old-growth*), traballouse coa base de datos ii que contén o maior rango de graos de madurez (incluíndo *old-growth*). En primeiro lugar, estimouse o grao de madurez (coñecido como naturalness score -NS-) de cada parcela mediante indicadores crono-funcionais obtidos a partir de datos dendrocronolóxicos. Despois, contrastouse o stock de biomasa (aérea e subterránea) pertencente ás árbores vivas destas parcelas maduras con todas as parcelas do IFN correspondentes ás mesmas tipoloxías de bosques. Para isto tivéronse en conta as súas calidades de estación, estimadas mediante o SF previamente validado. Posteriormente, estableceuse o MBS para cada tipo de bosque en base á curva logarítmica $MBS{\sim}SF$ axustada mediante regresión cuantílica (percentil 95.7) no gráfico de dispersión de biomasa fronte a SF. Finalmente, esta curva permitiu obter o stock de biomasa relativo ($BS(\%)$) con respecto ao máximo posible, e avaliar a posible relación entre o $BS(\%)$ e o NS, para probar a hipótese de que bosques maduros alcanzan o MBS antes de chegar a condicións de old-growth.

Caracterización da estrutura

A estrutura foi caracterizada en base a índices baseados nas 4 árbores máis próximas a cada árbore focal. Estes calculáronse para cada individuo e desta maneira obtivéronse os valores medios a nivel de parcela. Os índices empregados foron os seguintes: (i) riqueza de especies, (ii) mestura de especies, (iii) distribución de madeira morta en pé, (iv) diferenciación diamétrica, e (v) patrón de distribución horizontal das árbores. Os respectivos valores medios a nivel de parcela foron comparados entre as parcelas maduras dos bosques de estudo, diferentes rexións bioxeográficas (Mediterránea, Atlántica e Boreal) no caso de piñeiro silvestre, e entre distintos graos de madurez en faiedo-abetais (bosques maduros, *long untouched* e *old-growth*).

Modelización do estado de madurez mediante o TLS

Este parágrafo consta en primeiro lugar do desenvolvemento do paquete de R FORTLS, que ten o principal obxectivo de automatizar o procesado e análise de datos pertencentes a dispositivos terrestres de tecnoloxía LiDAR cun propósito forestal. Esta ferramenta contén os principais pasos comúns a outras aplicacións similares como son a normalización das nubes de puntos, a detección de árbores e estimación de variables de árbore individual e variables de masa. Igualmente, inclúe metodoloxías para corrixir o efecto das oclusións no caso de escaneos únicos de TLS, así como a optimización do deseño de parcela mediante a calibración con datos de campos. Ademais, xera unha serie de métricas con alto potencial para ser relacionadas con variables de masa e poder axustar modelos predictivos de utilidade para a estimación de variables de interese. Unha vez desenvolvido FORTLS, algunhas das principais variables de masa estimadas en base aos datos de campo para as parcelas maduras (densidade -árbores ha^{-1}, N-, área basimétrica -m^2 ha^{-1}, G-, diámetro medio aritmético -cm, $\bar{d}$- e altura media aritmética -m, $\bar{h}$-) foron comparadas coas estimacións de FORTLS pertencentes a escaneos únicos. Tamén, explorouse o potencial das variables e métricas de FORTLS para axustar modelos predictivos cos que estimar a biomasa absoluta (Mg ha^{-1}) e relativa ($BS(\%)$), así como o grao de

naturalidade (NS). Para iso axustáronse modelos lineais múltiples, MARS e random Forest para diferentes deseños de parcela (área fixa, k-tree e de mostraxe angular ou relascópica). Finalmente, avaliouse qué grupos de métricas foron máis relevantes nos modelos axustados.

4 Resultados e discusión

Índice de forma

A bondade do axuste do SF foi similar á do SI, mostrando estadísticos significativos e familias de curvas de calidade de estación que describen de forma axeitada a tendencia dos datos en ambos os casos. Ademais, os resultados do axuste do SF foron similares aos que se poden atopar en traballos previos. Por outra banda, cumpríronse as propiedades desexables que calquera índice de calidade de estación debe cumprir, demostrando así a utilidade do SF fronte ao SI como índice de referencia en plantacións de *P. radiata*. A validación do bo funcionamento do SF nunha situación coñecida serviu como paso previo para axustar o SF en dúas das tipoloxías de bosque utilizadas nesta tese, como foron os abetais e faiedo-abetais. Estes novamente mostraron estadísticos significativos na bondade do axuste, cumpríndose as asuncións dos residuos do modelo e as propiedades desexables de calquera índice de calidade de estación. Non entanto, cabe destacar que a escaseza de datos destas formacións no IFN (só presentes en Pireneos), a metodoloxía utilizada no axuste (curva guía) derivada do uso de parcelas temporais, e a estrutura irregular destas masas; fan que o axuste dos modelos sexa presumiblemente peor que en condicións máis simplificadas como é o caso das plantacións de *P. radiata*.

Estimación da madurez forestal en termos do stock de biomasa

En primeiro lugar, e para o caso aquí estudado de abetais, faiedos e faiedo-abetais pirenaicos, demostrouse a hipótese de que os bosques maduros poden alcanzar o MBS de árbores vivas con graos de madurez inferiores aos máis altos como podería ser o caso dos *old-growth*. Neste

sentido, os indicadores crono-funcionais obtidos a partir de datos dendrocronolóxicos, serviron para estimar o grao de naturalidade (NS), demostrando que as masas consideradas como *old-growth* (bosque de Aztaparreta) alcanzaban os valores máximos. Logo contrastouse, en base ao IFN, que estas parcelas alcanzaban os valores máximos de biomasa arbórea viva para os seus respectivos valores de SF. Por último, o axuste dos modelos de MBS serviu para facer a comparación do $BS(\%)$ co NS indistintamente da calidade de estación, sen observarse relación entre ambos, sendo ás veces o $BS(\%)$ maior para valores de NS menores. Isto demostrou a hipótese de partida de que o MBS pode alcanzarse con graos de madurez anteriores ao de *old-growth*.

Esta análise estendeuse ao resto dos bosques avaliados, observándose novamente que as parcelas maduras alcanzaban os máximos valores de biomasa fronte aos datos do IFN e para valores similares de SF. Deste xeito puido obterse o $BS(\%)$ para todas as parcelas do IFN mediante o axuste das curvas de MBS e facer unha avaliación a nivel nacional. Este alcanza valores medios próximos ao 40% en todos os bosques excepto en faiedos onde o $BS(\%)$ é algo superior (~50%). Cando o $BS(\%)$ se representa no mapa, en trazos xerais pódese observar unha mestura de valores (0-100%) máis ou menos homoxénea por todo o territorio. Con todo, pódese destacar como para as masas de piñeiro pinaster, as zonas con valores máis baixos son máis frecuentes en zonas onde a recurrencia de incendios é máis alta. Por outra parte, tamén destaca no caso do piñeiro silvestre unha maior concentración de parcelas con valores altos de $BS(\%)$ nas zonas onde houbo unha xestión máis continuada no tempo (Serra de Guadarrama e Serra da Demanda). Tamén resalta como no caso dos faiedos que precisamente na rexión onde máis xestión se fai (Navarra) non se atopan os valores máis baixos de $BS(\%)$.

Caracterización da estrutura

Algunhas das características estruturais mostraron diferenzas en función do tipo de bosque e rexión bioxeográfica, como é o caso da riqueza de especies arbóreas, claramente menor nos faiedos e piñeirais

de silvestre da rexión mediterránea. En canto á mestura de especies, o faiedo-abetal pola súa condición de boque mixto con especies tolerantes á sombra, mostrou os valores máis altos. A distribución de madeira morta en pé estivo directamente relacionada coa densidade, atopándose os valores máis altos nos bosques con maiores densidades, tanto entre rexións bioxeográficas como entre tipos de bosque. A diferenciación diamétrica mostrou un gradiente intraespecífico latitudinal (Boreal > Atlántico > Mediterráneo), posiblemente condicionado por unha maior densidade e episodios de mortalidade natural. Tamén se observou un gradiente interespecífico (faiedo-abetal > abetal > faiedo), posiblemente condicionado polo temperamento do abeto como especie de sombra, o cal permite a coexistencia dun subpiso de abeto. Este ademais foi claramente máis alto en parcelas con altos graos de madurez como é o caso dos *old-growth* (Aztaparreta). En canto ao patrón de distribución horizontal, foi moi similar en todos os casos, cunha distribución aleatoria que é o máis común na maioría dos bosques.

Modelización do estado de madurez mediante o TLS

En primeiro lugar, o paquete de R FORTLS xerado nesta tese para o procesado e análise de datos de TLS, resultou ser unha ferramenta satisfactoria para a estimación de variables de masa comúns en IF (N, G, $\bar{d}$, $\bar{h}$) en base a escaneos únicos. A exactitude dos resultados atópase próxima a moitas das referencias bibliográficas. En calquera caso, atopáronse diferenzas entre os distintos tipos de bosques, sendo os faiedos os que mostraron mellores resultados en xeral. Ademais, as correccións de oclusións non sempre melloraron os resultados, sendo irrelevantes na estimación de $\bar{d}$ e $\bar{h}$. Por outra banda, as métricas e variables xeradas por FORTLS resultaron ser útiles para a modelización de variables máis complexas como a biomasa arbórea viva, o stock de biomasa relativo ($BS(\%)$) e o grao de madurez (NS). Concretamente os modelos MARS mostraron os mellores resultados en case todas as ocasións. Con todo, isto non foi tan claro en canto ao deseño de parcela, sendo a parcela de mostraxe angular a que presentou mellores resultados en máis ocasións.

5 Conclusións

O índice de forma (SF) demostrou ser un índice de calidade de estación fiable con resultados similares ao usual índice de sitio (SI) utilizado en masas regulares, como son as plantacións de *P. radiata* analizadas neste caso de estudo. Ao contrario que o SI, que só ten sentido en masas regulares, o SF funciona tamén en masas irregulares. Isto permitiu utilizar o SF nos bosques estudados nesta tese doutoral, con idade descoñecida e estruturas irregulares en moitos casos. Con respecto á hipótese de se as masas maduras alcanzan o máximo stock de biomasa (MBS), demostrouse para unha submostra de parcelas maduras do Pirineo que graos de madurez previos aos máis altos (*old-growth*) poden alcanzar os valores máximos de biomasa. Estas parcelas maduras tamén alcanzaron os valores máximos con respecto aos datos do IFN para calidades de estación similares, demostrando polo tanto que os bosques maduros sen perturbacións graves recentes definen a liña base do MBS. Estes achados permitiron estimar o stock de biomasa arbórea viva (aérea e subterránea) con respecto ao MBS utilizando os datos do IFN; e avaliando así o stock relativo de biomasa ($BS(\%)$) almacenada a nivel nacional, que resultou ser de media algo maior en faiedos (~50%) que no resto de formacións (~40%). Os índices estruturais demostraron a súa utilidade para distinguir algunhas características entre diferentes tipos de bosques, estados de madurez e rexións bioxeográficas. En canto a rexións bioxeográfias, os piñeirais de silvestre da zona mediterránea mostraron claramente os valores máis baixos en riqueza e mestura de especies, distribución de madeira morta en pé e diferenciación diamétrica, o cal pode ser en parte debido á súa orixe como plantacións (non demasiado vellas) en moitas ocasións. Entre tipos de bosques, pódese destacar unha maior complexidade estrutural definida pola diferenciación diamétrica nos faiedos-abetais fronte ao resto, posiblemente debida ao temperamento do abeto como especie de sombra. En canto a graos de madurez, a diferenciación diamétrica demostrou ser o atributo estrutural máis útil para diferenciar entre etapas de madurez, mostrando claramente os valores máis altos en masas clasificadas como *old-growth* (Aztaparreta) e *long untouch* (bosque de Lizardoia). Por último, o paquete de R FORTLS demostrou

a súa utilidade no procesado e análise de datos pertencentes a escaneos únicos do escáner láser terrestre (TLS). Aínda tratándose de bosques complexos de escanear debido ao grao de madurez (árbores grandes que xeran moitas sombras, presenza de matogueira, etc.), alcanzáronse valores similares aos de referencia en variables de masa habituais en IFs. Ademais, as métricas e variables xeradas por FORTLS foron útiles para modelizar variables máis complexas como o $BS(\%)$ e o grao de madurez (NS). Estes resultados, aínda preliminares, indican que a incorporación do TLS aos IFNs podería aumentar as posibilidades de estimación de variables máis complexas necesarias para as novas estratexias forestais europeas, como por exemplo aquelas relacionadas coa madurez do bosque.

1. INTRODUCTION

1 INTRODUCTION

1.1 STAND MATURITY AS A REFERENCE FRAMEWORK IN FORESTS

Assessing forest maturity (or degree of naturalness) is a global requirement for sustainable forest management and restoration (Brumelis et al., 2011; Chiarucci and Piovesan, 2020; Winter, 2012). When talking about maturity, "old-growth" is the term most widely used to refer to relatively old forests that have reached late successional states, as far as possible in the absence of allogenic processes (Wirth et al., 2009). Therefore, old-growth or any of the interchangeable terms used in the literature (e.g. natural, primary, pristine and overmature, among others) are used to represent the reference conditions of maturity due to the potential for these forests to provide valuable ecosystem services other than carbon uptake and storage (Krieger, 2001; Watson et al., 2018), such as biodiversity (e.g. Lindenmayer and Franklin, 2002, p. 351) and numerous benefits and habitats that may not be supplied by some managed forests schemes, including clear cutting operations (Lindenmayer and McCarthy, 2002). This has driven an increasingly global effort to identify, monitor and conserve old-growth forests (Spies et al., 2006) as well as to develop silvicultural approaches for restoring and maintaining some old-growth characteristics in currently managed forests (Bauhus et al., 2009; Ford and Keeton, 2017). To implement these conservation and silvicultural practices, functional aspects of ecosystems must be measured in some way. In this regard, naturalness, defined as the degree to which forests are shaped by natural processes in the absence of anthropogenic influences (McRoberts et al., 2012), represents one of the most important criteria (Schultze et al., 2014). It is therefore essential to assess the degree of naturalness of old-growth forests (Bauhus et al., 2009; Frelich and Reich, 2003) and to compare their characteristics with those of previous successional stages (Ford and Keeton, 2017) in order to establish reference conditions and aid the

development of forest conservation and management strategies (Brumelis et al., 2011).

In this thesis we use the definition of old-growth forest proposed by Buchwald (2005), which is mainly based on the attributes of large trees, wide variation in tree sizes, accumulation of dead woody material, multiple canopy layers and gap dynamics. Nevertheless, a precise, single definition of old-growth forests is neither possible nor practical (Wells et al., 1998), as forests can be considered mature in relation to many different environmental services, and correct characterization requires the availability of long-term information on forest stands. Most definitions refer to the duration of development or advanced successional stage (e.g. dominance by mid- to late-successional species, presence of old trees close to the maximum longevity of species), complex structure (e.g. large trees, numerous large logs and snags) and biogeochemical criteria (e.g. biomass equilibrium, closed nutrient cycles) (Spies, 2004; Wirth et al., 2009). In addition, assessing the degree of naturalness of these forests is challenging from a practical perspective, as most European forests have been used by humans for centuries (Peterken, 1996; Winter, 2012). As a result, recent studies have considered chrono-functional indicators based on tree-ring metrics and involving disturbance dynamics (Di Filippo et al., 2017) as these may be more precise than other approaches (Schultze et al., 2014).

Some of the many definitions of old-growth forests (Wirth et al., 2009) have been validated on a very limited types of forest, mainly in temperate regions, because of the relatively large amount research activity in these areas (Spies et al., 2004). Furthermore, very strict definitions of old-growth forests are more difficult to implement from forest inventory (FI) data (McRoberts et al., 2012) and are therefore useless for regionalization processes. This indicates the need to use pragmatic definitions and converge towards common terms (Wirth et al., 2009). In this sense, very strict definitions of old-growth forests decrease their applicability in most situations and cannot be applied to all cases, where other very common states are sufficiently mature to provide valuable goods and services (Felipe-Lucia et al., 2018), and in any event, many ecosystem services can change over short timescales (Snäll et al., 2021). Regarding earlier degrees of naturalness than old-

growth, Wirth et al. (2009) used the term overmature. However, in this thesis we have used the term mature to represent a wider range of naturalness and therefore, more appropriate to the states of maturity considered here. A degree of naturalness prior to old-growth, defined by Buchwald (2005) as long untouched, is used to classify one of the stands included in the thesis data set. The terms referring to forest maturity used throughout this doctoral thesis will be applied as indicated in Figure 1.1.

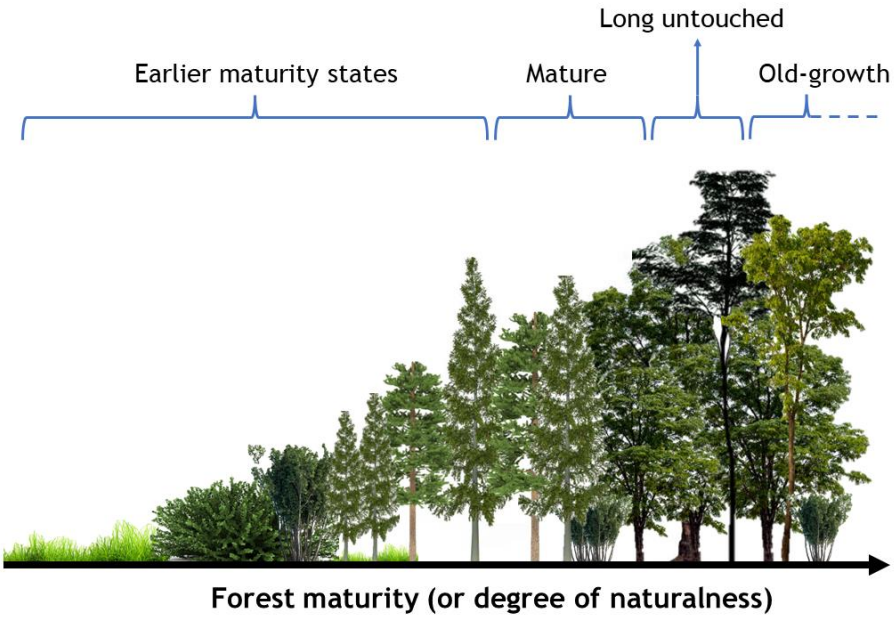

Figure 1.1. Terms used in this doctoral thesis for different levels of forest maturity (or degree of naturalness). Long untouched: Relatively intact forest (stand level) that has been essentially unmodified by human activity for the past sixty to eighty years or for an unknown, but relatively long time (Buchwald, 2005).

1.2 THE ROLE OF CARBON STOCK ACCORDING TO FOREST MATURITY

Forests are considered one of the main global carbon stocks. They harbour ~45% of terrestrial carbon, take up almost one third of human CO_2 emissions and influence climate by exchanging energy, water and chemical compounds with the atmosphere (Bonan, 2008). Implementing restoration plans and sustainable forest management

practices, among other actions, would reduce greenhouse gas (GHG) emissions caused by deforestation and forest degradation (UNFCCC, 2009). However, only land use change, afforestation and reforestation were previously considered the main mechanisms for sequestering carbon (UNFCCC, 1998), while reducing deforestation and forest degradation and promoting sustainable forest management (REDD+ projects) have more recently being incorporated as alternate mechanisms (Angelsen et al., 2012). This bias towards such adaptive measures has coincided with the occurrence of high rates of deforestation, particularly in the tropics (Santilli et al., 2005), affecting both primary and secondary tropical forests (Wang et al., 2020). More recently, temperate old-growth forests have also been the subject of debate due to their importance as carbon sinks and their long history of use and deforestation (Michalak, 2016). The controversy surrounding the effects of past logging episodes has led to an ongoing debate about the importance of old-growth forests as long-term carbon sinks (Carey et al., 2001; Lewis et al., 2009; Luyssaert et al., 2008; Ngo et al., 2013; Soloway et al., 2017) and whether these forests are carbon neutral (Odum, 1969; Hoover et al., 2012; Ķēniņa et al., 2019; Nord-Larsen et al., 2019) or have a limited capacity to grow and mitigate the greenhouse effect (Bugmann and Bigler, 2011; Büntgen et al., 2019; Hubau et al., 2020; Jiang et al., 2020). Nevertheless, the possible ways that disturbance could trigger sudden release of carbon in old-growth forests during successional dynamics must also be considered (Oliver and Larson, 1996; Luyssaert et al., 2008; Wirth et al., 2009). In fact, the frequency of some types of disturbance has increased in recent years due to multiple factors, some of which are related to global change (Seidl et al., 2017).

Although forest carbon management generally considers carbon sequestered in forests and harvested wood products, as well as emissions avoided due to a substitutive effect (IPCC, 2019; Pérez-Cruzado, 2011), carbon sequestration and storage in mature and old-growth forests mainly focuses on living and dead biomass and soil organic carbon (e.g. Ford and Keeton, 2017). Therefore, monitoring carbon in old-growth forests requires measurement of changing live biomass stocks through successional dynamics (Fahey et al., 2010). In

this context, the aboveground biomass of live trees represents the most dynamic carbon pool in forests and can be accurately estimated from data available from National Forest Inventories (NFIs) (Tomppo et al., 2010), by using allometric equations (Jenkins et al., 2003) and carbon concentration values per tree fraction (Pérez-Cruzado, 2011; Pérez-Cruzado et al., 2011; 2012). Although other carbon pools such as soil organic matter, coarse woody debris and understory vegetation can harbour large quantities of biomass in temperate forests (Landuyt et al., 2019; Pan et al., 2011), measurement of these pools is more difficult and expensive (Fahey et al., 2010; Pérez-Cruzado et al., 2012), and the first two pools are also less dynamic than aboveground biomass of live trees. In addition, according to CO_2 fluxes due to Land Use, Land-Use Change and Forestry (LULUCF), as reported in the National Greenhouse Gas Inventories (NGHGIs), the first CO_2 removals occur in the forest land carbon pool, which includes (apart from harvested wood products) above- and below-ground biomass (excluding soil carbon); the remaining forest land is the main carbon sink, with 87% of the total assigned to forest land pool (Grassi et al., 2022).

It has long been observed that above a certain limit of density, even-aged stands converge towards a similar basal area at stand level, determined by the site capacity (Piennar and Tumbull, 1973). According to the premise that undisturbed forests should reach a state of equilibrium (Dawkins, 1958), the basal area reached in this state may represent the maximum site productivity (Adlar, 1980; Assman, 1970; MacLean and Bolsinger, 1973) and therefore also the maximum volume and biomass capacity. More recently, carbon storage has been assumed to be maximal in old-growth forests that have not suffered any natural and/or human-induced disturbance, because the dynamics of these forests reach an almost steady state (Smithwick et al., 2002). However, it has also been suggested that biomass storage reaches maximum values in forests characterized by lower degrees of naturalness (e.g. mature forests) than in old-growth forests, in which live biomass represents the largest carbon pool (Fisk et al., 2002; Hoover et al., 2012; Ķēniņa et al., 2019; Nord-Larsen et al., 2019). The aim of this doctoral research was to study the usefulness of stand stocking in terms of biomass as a proxy of forest maturity. Hence, characterizing the upper

limit or threshold of carbon storage through a site quality gradient (because biomass productivity is site quality dependent: Burkhart and Tomé, 2012; Skovsgaard and Vanclay, 2008) may be helpful for estimating the relative biomass storage potential. Nevertheless, although NFIs provide large national-scale data, they are not suitable for assessing the degree of naturalness due to the lack of long-term data sets (McRoberts et al., 2012) and the scarce number of indicators (Alberdi et al., 2019). Therefore, a better understanding of the capacity of mature and old-growth forests to hold maximum biomass stock must be based on the use of appropriate reference plots (Hubau et al., 2020; Phillips and Brienen, 2017; Pregitzer and Euskirchen, 2004).

1.2.1 Biomass stock as a proxy for stand maturity

In recent years, greater importance has been attached to carbon stocks in forest biomass and also to forest maturity, with old-growth often considered reference conditions (e.g. Watson et al., 2018) in forest policies (New EU Forest Strategy for 2030) and the scientific literature (Keith et al., 2021; Mackey et al., 2020). Accordingly, in an international context, and in the wake of the Kyoto Protocol (UNFCCC, 1998), deforestation and forest degradation have become the two most important factors for reducing carbon emissions and preventing biodiversity loss, desertification and other types of environmental damage. Under the UN-REDD+ program (www.un-redd.org), annex I countries could compensate their carbon emissions by means of actions in developing countries that lead to reductions in deforestation, forest degradation and the promotion of sustainable forest management, while earlier forestry-related mechanisms have focused on afforestation, reforestation and LULUCF under the clean development mechanisms framework (Angelsen et al., 2012). More recently, the Paris Agreement (COP21, 2015) forced signatory countries to report their progress towards achieving individual targets (known as the Nationally Determined Contributions, NCDs) to mitigate climate change (e.g. creating CO_2 sinks like forests). These NCDs form the mitigation mechanism required to reach the global "stocktake" necessary to fulfil the long-term goals of the agreement (COP21, 2015). In addition, it has

been stressed that these objectives must be achieved according to the best available science (COP21, 2015, Article 14). At the EU scale, the new EU forest strategy (European Commission, 2021), which includes the objective of improving the quantity and quality of EU forests, represents one of the flagship initiatives of the European Green Deal, which intends to reach the EU climate target of reducing at least 55% net GHG emissions by 2030. This strategy is based on guidelines such as strategic monitoring, reporting and forest data collection, among others. At the national scale, the Spanish voluntary carbon market (Real Decreto 163, 2014) contemplates actions such as reforestation or forest restoration after wildfires. As an example of regional scale plans, the Andalusian emission trading system contemplates (apart from afforestation/reforestation) reducing forest degradation by means of restoration, preservation or sustainable management of existing forests to compensate GHG emissions (Ley 8, 2018).

In most cases, the aforementioned carbon emission compensation mechanisms consider a fixed value of carbon stock per unit area and forest type, independently of forest maturity (IPCC, 2019). Total carbon accumulation or uptake is estimated by multiplying the activity data (area of interest) by the emission factor (carbon per unit area). Carbon accounting in these projects consists of comparing the carbon uptake due to the planned action (either a land use change or change in land management) relative to the "business as usual" approach, i.e. not implementing the project. Although the approach used to establish the baseline is straightforward and robust in projects based on land use change (Schelhaas et al., 2004), projects aiming to improve forest management or reduce forest degradation (e.g. REDD+) are far more complex and subject to being affected by previous forest conditions. Forest maturity plays a key role here, and the trade-offs and relationship between carbon stocks and forest maturity warrant detailed study.

Furthermore, the quantification of emissions associated with forest degradation is more uncertain than in LULUCF-like projects, beginning with the lack of a widely agreed and operational definition of forest degradation (Morales-Barquero et al., 2014). With that in mind, among the several groups of goods and ecosystem services that can be degraded in forests (Thompson et al., 2013), carbon storage represents

one of the most important due to its role in mitigating climate change (Friedlingstein et al., 2022) and, aboveground biomass stock may be a suitable indicator (Thompson et al., 2013). However, defining a baseline for comparing the value of this indicator is controversial, as changes in carbon stock are usually assessed by comparing the value at a given time with a reference value determined in the past. Hence, defining the baseline is desirable in order to have reference values available for when the occurrence and extent of forest carbon stock need to be assessed in a single inventory, and thus to avoid that changes in carbon stock cannot be evaluated due to due to the lack of previous reference values.

According to some authors, the carbon stock change approach does not allow evaluation of either the occurrence or extent of carbon stock reached as an indicator of ecosystem services (Pérez-Cruzado et al., 2015), because this approach overlooks the fact that the maximum amount of carbon that can be stored in a given site (evaluated in terms of maximum biomass stock -MBS- in this doctoral thesis) depends on the specific site conditions. An example of the hypothesized relationship between MBS and site productivity for unperturbed mature forests is shown in Figure 1.2. The extent of forest biomass stock level cannot be assessed by ignoring the extent to which the MBS for the specific site conditions departs from the hypothetical actual biomass stock. This is illustrated in Figure 1.2, which also shows that, for the same absolute change in the indicator (live tree biomass) between t_1 and t_2, the forest biomass storage at t_2 depends on the specific site conditions. Therefore, the forest carbon storage cannot be evaluated exclusively by the carbon stock change approach, which only provides information about the absolute change in the value of the indicator between t_1 and t_2. Because many initiatives related to carbon sequestration change over the years, especially in the Paris Agreement (COP21, 2015), there is an urgent need to clearly assess and monitor climate progress in carbon flux reporting in different countries (Grassi et al., 2018; 2021; 2022).

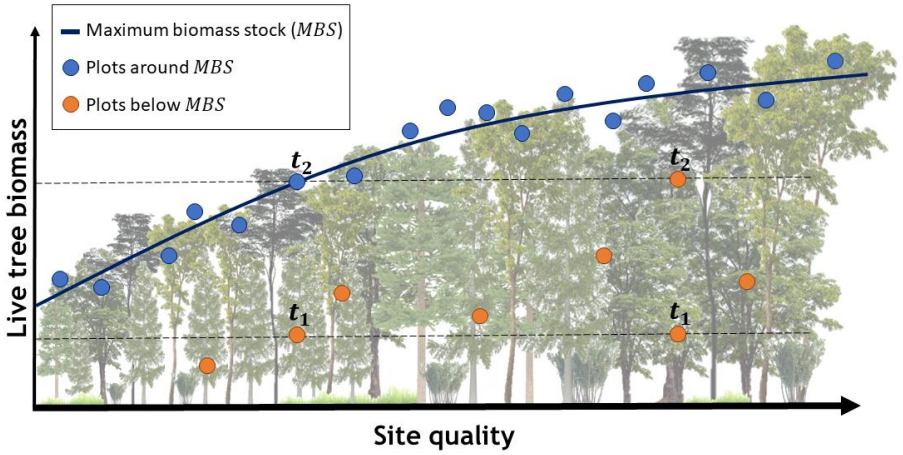

Figure 1.2. Graphic representation of live tree biomass stock in a hypothetical forest type through a site quality gradient including plots harbouring around maximum biomass stock (*MBS*) and lower quantities of *MBS*.

In order to demonstrate the utility of estimating forest carbon storage according to *MBS*, one of the first objectives of this doctoral thesis was to study the relationship between the degree of naturalness of forests and the maximum accumulation of live tree stand biomass (above- and below-ground trees biomass, hereinafter *LTB*) in a range of degrees of naturalness where old-growth forest is considered the highest possible. This is important to ensure that maximum *LTB* stock values can be reached at lower degrees of naturalness than old-growth, therefore enabling estimation of *MBS* in countries such as Spain where old-growth forests are almost non-existent. Another objective consisted of establishing an upper threshold (or baseline) representative of *MBS* through a practical site quality index. The justification for assessing biomass instead of carbon relies on the availability of biomass equations that are suitable and practical for the study area. Nevertheless, carbon is directly related to biomass as its main component.

1.2.2 Assessment of site quality using National Forest Inventory data

Assessing and monitoring forest resources require reliable, accurate estimates of site quality, which are essential for predicting plant biomass growth and yield under different management regimes in both even-aged (Skovsgaard and Vanclay, 2008) and uneven-aged stands (Peng, 2000). Site quality is also important in studies addressing forest disturbances (Wei et al., 2003), forest structure (Larson et al., 2008) and ecological diversity (Franklin et al., 1989), among others. Site quality may be defined as the physical and biological factors that characterize the capacity of a site to support tree growth (Skovsgaard and Vanclay, 2008). According to Vanclay and Henry (1988) and Weiskittel et al. (2011, p. 38), a site quality index should (i) be reproducible and consistent over long periods of time, (ii) be indicative of the site, independent of management and/or stands conditions, (iii) be correlated with the productive potential of the site as a cause-effect relationship, consistent with current knowledge of tree physiology (e.g. Coops et al., 1998) and (iv) perform at least as well as other site quality estimators. Regarding the latter characteristic, less precise site quality estimators may be useful, as long as they are based on widely available sources of information and can therefore be reliably applied at larger scales.

Site index (SI), defined as the average total height of the dominant trees of the stand at a given reference age, is one of the most commonly used indicators of site quality for even-aged stands (Weiskittel et al., 2011, p. 38). This stems from the fact that total tree height (h) growth is correlated with stand volume productivity, and dominant h (H_0) is not greatly affected by stand density or thinning treatments (assuming thinning from below) (Burkhart and Tomé, 2012, p. 131). Nevertheless, SI has several drawbacks: (i) its use is questionable for uneven-aged stands because of the initial suppression of advanced regeneration, especially for shade tolerant species, and also because SI is an age-dependent approach, and age has nebulous meaning in the context of uneven-aged forests (Burkhart and Tomé, 2012, p. 339); (ii) identifying tree ages is a costly task; and (iii) stand age is often not known/available

or is of dubious reliability, e.g. in NFIs (Tomppo et al., 2010), which limits the use of SI for large-scale monitoring purposes. Although age-independent methods have been developed to overcome the latest problem, thus enabling modelling of the H_0 growth and estimation of SI in the absence of age data (e.g. Tome et al., 2006; Arias-Rodil et al., 2015), the reliability of these methods has not been widely tested. Assessment of more age-independent methods is therefore desirable.

Site form (SF), defined as the H_0 of the stand at a reference dominant diameter (defined as the average dbh -diameter at breast height measured at 1.3 m from the ground- of the dominant trees of the stand, D_0) (Vanclay and Henry, 1988), is an alternative method of estimating site quality for different stand structures (even- and uneven-aged) because it does not require information about stand age. In this regard, SF may be useful for estimating site quality in most NFIs, in which age is usually unknown (Tomppo et al., 2010). Historically, Trorey (1932) first reported the use of the $h{\sim}dbh$ relationship as a site quality estimator. However, it was not until 1957 that McLintock and Bickford (1957) proposed a site quality index based on Meyer's mathematical expression (Meyer, 1940). The method was further established by Stout and Shumway (1982) and Reinhardt (1982). The term "site form" was proposed by Vanclay (1983) to distinguish it from "site index", and other researchers subsequently used SF in different studies in the 1980s and 1990s (Lamson, 1987; Nicholas and Zedaker, 1992; Reinhardt, 1983; Vanclay, 1992; 1994; 1995). However, reports of its use are scarce in scientific paper published in the last two decades (Adeyemi, 2016; Aguiree et al., 2022; Ahmadi et al., 2017; Moreno-Fernández et al., 2018).

For many species, dominant trees and therefore D_0 and H_0 are scarcely influenced by stand density or intermediate cutting, relative to small natural disturbances (Burkhart and Tomé, 2012, p. 131; Clutter et al., 1983, pp. 65-66). It is therefore possible to propose the hypothesis that under natural dynamics, dbh and h growth of dominant trees are not strongly affected, with the $H_0{\sim}D_0$ relationship being appropriate for estimating site quality (Bakuzis, 1969; Vanclay and Henry, 1988). Mean dbh is known to be influenced by stand density, with wide spacing being more beneficial than close spacing for higher average

stand dbh. However, at any given development stage, there is a lower limit below which no further increase in dbh growth will take place (Clutter et al., 1983). Nonetheless, older and dominant trees respond less strongly than younger trees to increases in dbh because they have not been greatly affected during their lives. Thus, D_0 and H_0 are more appropriate for estimating site quality.

To prove the suitability of SF, some studies have analyzed the relationship between SI and SF for a given species and between these indices and variables traditionally used as measures of site quality (Buda and Wang, 2006; Beltran et al., 2016; Duan et al., 2018; Fu et al., 2018a; Huang and Titus, 1993; Wang, 1998). However, only Wang (1998) and Beltran et al. (2016) considered species growing in even-aged stands, showing that the overall accuracy of both methods was similar. It must also be noted that the comparative performance of SI and SF can only be correctly determined in even-aged stands because SI, as previously defined, has no meaning in uneven-aged stands. Therefore, based on the results and given that SF does not require information on stand age, further research considering this less commonly used approach seems worthwhile (Drew, 2021).

For all of the aforementioned reasons, and considering the uneven-aged structure in most of the experimental plots and/or unknown age of these plots, the SF index was considered an indicator of site quality in the present research. Thus, one of the research objectives was to compare the performance of SF and SI as site quality indicators. The overall aim was broken down into the following specific objectives: (i) to develop dynamic equations for estimating SI and SF, (ii) to compare the correlation between SI and SF predictions at plot level, (iii) to analyse the consistency of both indices when applied to data obtained by remeasuring the same plot, and (iv) to evaluate the correlation between both indices and a direct measure of site quality.

1.3 THE ROLE OF FOREST STRUCTURE ACCORDING TO MATURITY

Forest structure refers to the three-dimensional arrangement of individual trees and other plants. It plays an important role in ecological process because it is linked to forest dynamics, growth and yield

(Pretzsch, 2009) and is an indicator of biodiversity (Ishii et al., 2004), resilience against disturbance (Dobbertin, 2002) and provision of many ecosystem services (Felipe-Lucia et al., 2018; Shugart et al., 2010). Forest structure can be interpreted by the horizontal tree distribution patterns, as the spatial arrangement of the trees or the spatial distribution of the different tree species (species intermingling), and the tree size distribution (Aguirre et al., 2003), as well as by other characteristics such as density, vertical tree distribution patterns and age composition (del Río et al., 2016). The arrangement of the horizontal tree distribution can be aggregated, random or regular (Figure 1.3 a); being the random arrangement the most common in forests (Pommerening, 2002). The different species and tree sizes can be found close to each other, thus displaying a high degree of mingling, or they can be spatially segregated (Figure 1.3 b). Heterogeneity in these structural features, which can be assessed by different measures and indices (del Río et al., 2016; McElhinny et al., 2005), is related to forest ecological quality (Pommerening, 2002; Seidel et al., 2019). Structure

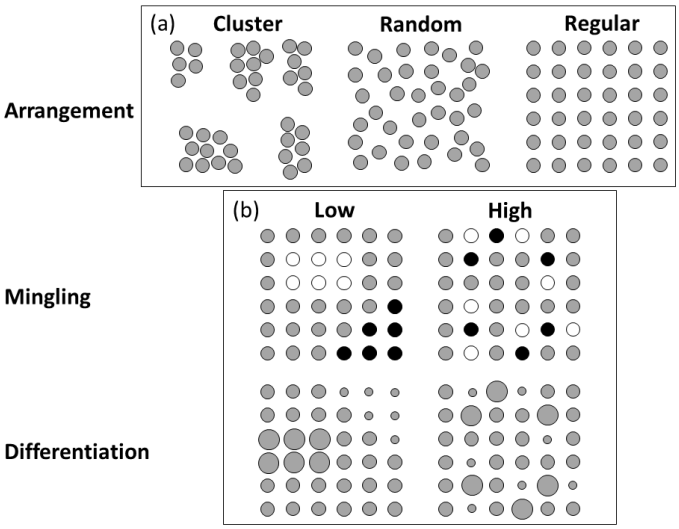

Figure 1.3. Some of the main features of spatial forest structure: tree arrangement (top); species mingling (middle), from low (left) to high degree (right) of mingling (different colours represent different species); and size differentiation (bottom), from low (left) to high degree (right) of differentiation. (Adapted with permission from Aguirre et al., (2003). Copyright 2003, Elsevier Science B. V.).

is therefore considered an important aspect in managing forests as complex systems (Messier et al., 2013), as a higher degree of naturalness is associated with greater structural heterogeneity (Põldveer et al., 2020). Besides, structure is the most common attribute evaluated in characterizing old-growth forests (Wirth et al., 2009). In this respect, mingling of different sizes of tree, considered one of the key structural variables providing spatial heterogeneity (Pommerening and Särkkä, 2013), can be altered through silviculture practices (Seidel et al., 2019), e.g. enhancing carbon storage through management of old-growth attributes (Ford and Keeton, 2017). Nevertheless, not all ecosystem services can be improved at the same time in the management unit (Snäll et al., 2021), and prioritization of forest uses (e.g. timber harvesting, protection, etc.) for the most suitable stands is therefore recommendable at landscape management level in multi-purpose forestry (de Assis Barros et al., 2022; Simons et al., 2021). Regarding forest management, it has been demonstrated in a case study in the Chinook Community Forest in Canada that the use of old-growth attributes as management criteria is better in terms of ecosystem service provision than the use of age-based criteria (de Assis Barros et al., 2022). Hence, characterizing old-growth structural features that are easy to assess, if possible, would be desirable for these new approaches in forest management.

Apart from determining the relationships between forest structure and ecosystem service provision (Felipe-Lucia et al., 2018; Penone et al., 2019), characterization of the structure among different types of forests, the degree of naturalness, forest management schemes and intensities, as well as understanding how structural attributes change over time, have become important topics in forest science (Dieler et al., 2017; Felipe-Lucia et al., 2020; Schall et al., 2018; Stiers et al., 2018). In this regard, the structure of mature stands may remain rather constant, unlike earlier stages (Schall et al., 2018), although the changes do not necessarily occur at a similar rate to changes in biomass stock (Figure 1.4). Recent studies in the Estonian hemiboreal forests (e.g. Põldveer et al., 2021) have shown that plots with higher structural heterogeneity, evaluated with the structural complexity index (SCI) (Zenner, 1998), do not always yield higher volumes (based on living

trees). Thus, higher biomass stocks can be reached at earlier stages than those corresponding to old conservation forest. In addition, forests growing on poor sites showed notably lower structural heterogeneity for the same types of forests (Põldveer et al., 2020), indicating different structural behaviour according to site quality. Meyer et al. (2021a) reported significant differences in "old-growth" characters in European beech forests between different stages of old-growth and earlier degrees of naturalness according to most structural indicators used. However,

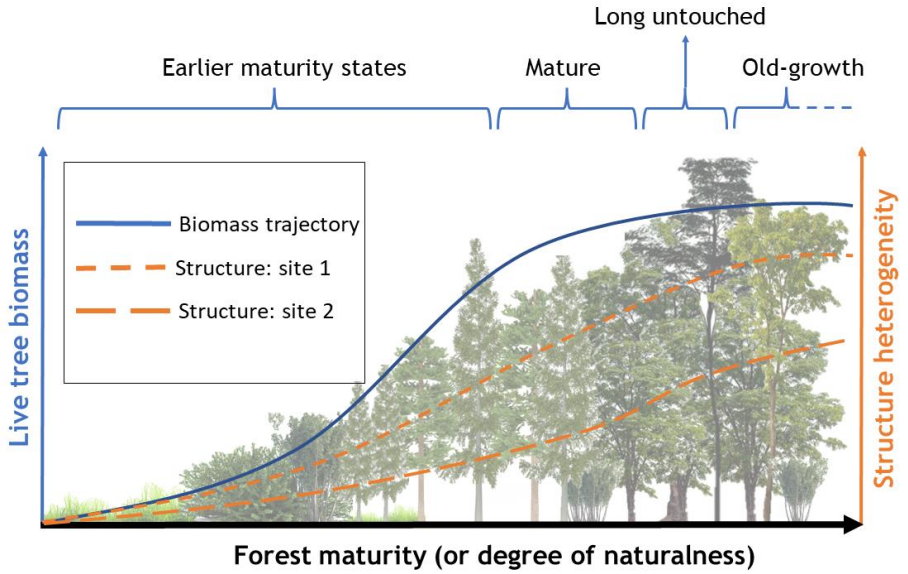

Figure 1.4. Hypothetical trends in live tree biomass (*LTB*) stock (left-hand side y axis and blue line), and structural heterogeneity (right-hand side y axis) for site 1 (upper dashed orange line) and site 2 (lower dashed orange line), according to forest maturity. Structural heterogeneity curves show several hypothetical trends, which can be influenced by structural patterns and also by site quality.

some indicators such as number of tree species or volume of living trees reached similar or even higher values at earlier degrees of naturalness, and thus old-growth stages do not necessarily promote higher spatial structure heterogeneity. For example, according to species richness and mingling, earlier stages (e.g. mid-successional) tend to harbour higher species heterogeneity because they often include both early and later-successional species (Connell, 1978). Nevertheless, owing to gap

dynamics and multiple layers of vegetation, other structural features such as horizontal and vertical canopy distribution tend to be more heterogeneous in old-growth forests (Messier et al., 2009). In the same way, size differentiation also tends to indicate higher degrees of mingling in old-growth forests, especially in the presence of shade-tolerant species, with more complex structures thus being reached (Messier et al., 2009). In any case, no structural features are exactly the same for all forest types and site conditions.

Assessing forest structural features according to maturity was one of the overall objectives of the research reported in this doctoral thesis. For this purpose, very common patterns of forest structure were first characterized in mature conditions. Secondly, the following comparisons of structural features were evaluated among dissimilar forest types (inter specific), different biogeographical regions (intra-specific), and between the highest degrees of naturalness (long untouched and old-growth) and mature forests.

1.4 TERRESTRIAL LASER SCANNING (TLS) AS AN EMERGING APPROACH IN FOREST INVENTORIES

Forest inventories (FIs) have improved since they were first introduced, owing to the continuous appearance of new technologies, especially in the last few decades since the emergence of remote and proximal sensing. In this technological context, light detection and ranging (LiDAR) systems provide 3-dimensional point clouds, which are suitable for estimating tree attributes and are very useful for many forestry applications (Dubayah and Drake, 2000). This technology has proved operationally viable for estimating essential FI variables at stand level, such as arithmetic mean h ($\bar{h}$, m), basal area (G, m^2 ha^{-1}) and volume (V, m^3 ha^{-1}), with airborne laser scanning (ALS) devices (White et al., 2016; Wulder et al., 2012). Terrestrial laser scanning (TLS) devices, such as LiDAR devices with millimetric precision, show great potential for enhancing FIs (Dassot et al., 2011; White et al., 2016) and also forest ecology research (Calders et al., 2020; Danson et al., 2018). Apart from yielding much higher spatial resolution under the canopy, the main advantages of using TLS data are that they provide better

observations of near-ground vegetation than ALS data (White et al., 2016) and thus better trunk coverage for estimating the woody component, one of the most important components in FIs. In fact, TLS-based approaches can provide very accurate estimates of the dbh and stem curve, with the single-scan approach yielding values of 1-4 and 1.3-6 cm respectively, depending on the stand conditions (Liang et al., 2018a). These values are close to those required in practical applications such as FIs. However, TLS devices have not been yet adopted in FIs, for several reasons: (i) difficulties in the automation of data processing to provide reliable measurements of important forest variables, (ii) high acquisition costs; (iii) limited software; and (iv) lack of trained personnel (Liang et al., 2016). Many researchers agree that affordability is the main key challenge to overcome, emphasizing that automation of point cloud processing with attainable and easy-to-use software capable of extracting information related to important forest attributes is essential (Dassot et al., 2011; Liang et al., 2016; 2018a; Newnham et al., 2015; White et al., 2016).

As TLS data sets comprise millions of points, sophisticated methods for automatic processing are required. Many algorithms with a high level of automation and that are able to extract tree attributes, such as dbh, h and stem volume (v, m^3), have been developed in the last two decades (Cabo et al., 2018; Liang et al., 2011; 2018b; Olofsson et al., 2014; Olofsson and Holmgren, 2016; Zhang et al., 2019). Although most algorithms yield acceptable dbh and stem curve estimates according to FI requirements, stem detection and estimation of h cause bottlenecks in the process, especially with single-scan approaches (Krok et al., 2020; Liang et al., 2018a). Some of the algorithms developed have also been included in software applications, such as SimpleForest (Hackenberg et al., 2015), 3D Forest (Trochta et al., 2017) and AutoStem^{TM} (Bienert et al., 2007), among others (Krok et al., 2020). However, these programs have some drawbacks for use in FIs: (i) they focus on single-tree rather than stand level approaches (SimpleForest); (ii) they involve semi-automatic processing (3D Forest); and (iii) the software is only available commercially (AutoStem^{TM}) (i.e. it is not free or open source). Furthermore, the previous studies have mainly focused on replicating plot-based

measurements, which does not extend conventional inventory approaches from a sampling perspective and thus limits the utility of TLS in FIs, the main purpose of which is to estimate important forest variables at larger scales (e.g. stand and regional) than tree and plot levels (Newnham et al., 2015; White et al., 2016). Methods that enable TLS to be used for FI purposes must therefore contemplate the use of different approaches (Newnham et al., 2015) and other procedures, in which measurement of all trees in the sample plots should not necessary be feasible (Liang et al., 2018a). Because of this, further research is required to address the challenges in the operational use of TLS (Liang et al., 2018a).

In this research, the R package FORTLS (Molina-Valero et al., 2022) was developed with the objective of automating the processing of terrestrial-based devices point cloud data and estimating variables for forestry purposes. To fulfil this objective, FORTLS enables (i) detection of trees and estimation of dbh and other tree attributes, (ii) estimation of some stand variables (e.g. $\bar{h}, G, V$), (iii) computation of metrics related to important tree attributes estimated in FIs at stand level, and (iv) optimization of plot design for combining TLS and field measured data. The package also includes several features for correcting occlusion problems to improve the estimation of stand variables. The first versions of FORTLS were based on single-scan TLS data, with the aim of facilitating operational use, and the package has been designed as relatively easy-to-use open-source software aimed at use by both scientists and technical users. Relative to multi-scan and multi-single-scan approaches, the single-scan approach improves data acquisition, shortens the processing time and increases the sample size in a cost-efficient manner, mainly because it does not require pre-scanning tasks involving location of artificial reference objects (Holopainen et al., 2014) or automated post-processing matching methods (Liu et al., 2017). These features of the FORTLS package may enable the operational use of TLS in FIs, in combination with model-assisted inference approaches.

1.4.1 Approaches for estimating forest maturity by TLS

Although TLS has displayed high accuracy in estimating some of the most important variables in FIs (Liang et al., 2018a), its use in assessing structural complexity, and thus the degree of naturalness, has also been evaluated (Ehbrecht et al., 2017, Seidel et al., 2016). As heterogenous forest structures are correlated with the provision of many ecosystem services (Felipe-Lucia et al., 2018), such as biodiversity (Lindenmayer et at., 2000) and forest scenic beauty (Ribe, 2009), silvicultural practices increasingly focus on generating heterogeneous structures (Puettmann et al., 2012; 2015). Although there is no precise, widely accepted definition of stand structure, the most important characteristics are related to the three-dimensional arrangement of the tree components (Pretzsch, 2009; Wirth et al., 2009). Furthermore, measures used to estimate structural indices are very laborious to carry out, especially in large areas, as measurement of distances between trees and tree attributes are usually required. TLS is therefore a promising method for these purposes due to the high performance of LiDAR technology in providing 3-dimensional point clouds (Malhi et al., 2018). In this respect, some studies have focused on multi-scan approaches to yield the best possible representation of forests, demonstrating that TLS can be used to quantify canopy space filling, e.g. in a temperate broad-leaf mixed forest (Seidel et al., 2013). Other studies have quantified the structural variability by measuring the "rugosity", defined as the standard deviation projected on the horizontal axis of the vegetation density along the vertical axis (Hardiman et al., 2011; 2013). In this case, because of the need to sample by transect design, a ground-based portable canopy LiDAR system was used. Finally, TLS single-scan approaches have also yielded useful results in relation to distinguishing structural complexity features among different degrees of forest management (Ehbrecht et al., 2017), including old-growth states (Seidel et al., 2016). The single-scan approach has the advantages of enabling faster field work and post-processing as it is used as independent data source, in which each scanner represents a unit sample, although at the expense of problems due to occlusions. However, in the previous cases (Ehbrecht et al.,

2017; Seidel et al., 2016), metrics related to coordinates of point clouds were used satisfactorily. Apart from the measurement approach, another great advantage of TLS is the possibility of easily increasing the time scale in high frequency and long-term time series, thus improving monitoring. This can be useful for example to study phenological dynamics, as done by Campos et al. (2021) who demonstrated that TLS time-series can capture sprouting and leaves growing during the spring period in a boreal mixed forest dominated by conifer trees of Finland, and consequently monitoring the forest phenology. This information may be very important for detecting phenological changes caused by climate change (Calders et al., 2015).

Beyond more conventional applications for forest mensuration, tree architectural information at different scales may be key to obtaining new insights (Disney, 2019). Apart from high accuracy and precision in predicting tree structure, very detailed measurements of branch architecture can help to understand how tree structure and metabolism vary with size (known as Metabolic Scaling Theory, MST -West et al., 1997-). Such information is useful e.g. for understanding how trees fill space by the vascular system along with trade-offs between hydraulic safety and efficiency (Savage et al., 2010). To this effect, e.g. Lau et al. (2019) proved the utility of TLS for estimating branch scaling predictions of MST in tropical trees in Guyana, although fine branches represent the main bottleneck. Crown structure, which is also difficult to measure by conventional methods, has been found to be one of the most important attributes explaining stem growth thanks to the advantages of TLS (Yrttimaa et al., 2022). All of these recent findings may represent new paradigms in understanding the physiological implications (e.g. growth) of forest structure at a greater level of detail than ever before. As a result, many aspects of more mature forest, with a high degree of naturalness and supposedly more complex structure (Messier et al., 2009), will be understood much better in terms of the relationships between structure and LTB stock. Regarding the objectives proposed here, the potential of the TLS single-scan approach was evaluated by means of FORTLS to estimate conventional stand level variables and absolute (Mg ha^{-1}) and relative LTB stock (BS, %) in mature conditions with the aim of developing a new approach for

estimating the ecosystem service carbon stock. Although most previous studies involving assessment of forest maturity are based on measuring/estimating specific variables or structural indices, in the present study, the degree of naturalness was evaluated for states ranging from mature to old-growth conditions. For this purpose, both direct estimates and also several modelling approaches using all of the TLS auxiliary information generated with FORTLS were explored.

2. OBJECTIVES

2 OBJECTIVES

This doctoral thesis reports original research carried out with the main objective of assessing and modelling forest stand maturity by using data obtained in National Forest Inventories (NFIs) and non-probability sampling of field plots. Other main aims included characterizing structure of mature forests and exploring the potential of terrestrial laser scanning (TLS) data as a proxy for forest mensuration data. Data from the Spanish NFI and from experimental plots located in mature forests were used to test new methods potentially applicable to other situations.

The specific scientific objectives are as follows:

1. To test a site quality index suitable for data obtained in NFIs.
2. To study the relationship between forest maturity and maximum accumulation of live tree stand biomass.
3. To establish an upper threshold representative of maximum live tree biomass stock through a site quality gradient.
4. To characterize the structure of the mature forests under study and also differences between biogeographical zones.
5. To develop open-source software able to process TLS point clouds to produce variables and metrics useful for assessing forest attributes, including forest maturity.
6. To assess the potential of single-scan TLS data for estimating stand level variables, biomass stock and maturity.

3. MATERIAL AND METHODS

3 MATERIAL AND METHODS

3.1 TYPES OF FOREST STUDIED

Forests dominated by the following species were considered in this doctoral thesis: beech (*Fagus sylvatica* L.), maritime pine (*Pinus pinaster* ssp. *atlantica* H. de Vill.), Scots pine (*Pinus sylvestris* L.) and silver fir (*Abies alba* Mill.). Most of these are widespread across forested areas in Spain (Table 3.1) and are mainly located in mountainous regions. Regarding stand composition, the study focused on pure (i.e. with at least 90% of the basal area [G , m^2 ha^{-1}] corresponding to the main species) and mixed stands (only beech-fir forests, with at least 90% of G corresponding to beech and silver fir species). These forest types can be classified as *South western European mountainous beech forests* for both beech and beech-fir dominated communities; *Atlantic Maritime pine forests of the Atlantic biogeographical region*; *Nemoral and Mediterranean Scots pine forests*; and *Mountainous Silver fir forests* (Barbati et al., 2006; 2010). Finally, even-aged stands of radiata pine (*P. radiata* D. Don), described by Barbati et al. (2016) as "*plantations of not-site-native species*", were also included for the purpose of testing some of the research hypotheses proposed in this thesis.

Table 3.1. Area covered in Spain by the types of forest studied

Main species	Surface area covered (ha)	Forest type (EFT – Type level)
Beech	395,413	South western European mountainous beech forest (7.1)
Beech-fir	*	
Maritime pine	242,062	Atlantic Maritime pine forest (2.7)
Radiata pine	263,534	Plantations of not-site-native species (14.2)

Scots pine	1,030,916	Nemoral (2.2) and Mediterranean Scots pine forests (10.4)
Silver fir	<184,671	Mountainous Silver fir forest (7.9)
Forested area	**18,343,530**	

Source: Spanish forest statistical yearbook of 2019 (MITERD, 2021). Forest types correspond to the European forest types described by Barbati et al. (2006; 2010).

* Surface area was not calculated for beech-fir dominated communities because these were not included as a specific forest type.

South western European mountainous beech forest

These forests comprise a wide range of beech- or beech-fir-dominated communities, with part of their distribution included in the Cantabrian and Pyrenees ranges (Barbati et al., 2006). The forests are widely distributed in the Cantabrian range where they dominate the mountainous landscape in many areas, forming pure beech stands (Figure 3.1), but becoming rare towards southern locations (even reaching the Iberian range) due to the Mediterranean influence. The peak presence of pure stands occurs in the westernmost Pyrenees, becoming scarcer towards the eastern Pyrenees. Mixed beech-fir communities appear in shaded areas in the western and central Pyrenees (Costa Tenorio et al., 1997). The existence in the study area of an old-growth beech-fir forest (Aztaparreta) is remarkable (Costa Tenorio et al., 1997, pp. 140-141; Gil Pelegrin et al., 1989) (Figure 3.2).

Figure 3.1. Panoramic view of a pure beech forest in the Cantabrian range corresponding to a selected beech stand (Natural Park of Redes, Asturias). The

image, consisting of multiple photographs taken by TLS FARO Laser Scanner Focus^{3D} X 130, covers the full horizontal range (0-360º).

Figure 3.2. Panoramic view of a mixed beech-fir forest in the west Pyrenees (Integral Natural Reserve of Aztaparreta, Navarra). The image, consisting of multiple photographs taken with a TLS FARO Laser Scanner Focus^{3D} X 130, covers the full horizontal range (0-360º).

Atlantic Maritime pine forest

Many of these forests are distributed along the Atlantic coast and were originally established by reforestation on sandy coastal dunes (Barbati et al., 2010), which in our study area are mainly located in the northwest (NW) Iberian Peninsula (Figure 3.3). Although there is no clear consensus regarding the taxonomic status of Atlantic maritime pine as a subspecies (Alía et al., 1996; Franco, 1997), there is evidence for higher productivity and different phenology relative to the Mediterranean populations (Alía et al., 1997; Bravo-Oviedo et al., 2011). From a biogeographical point of view, Atlantic maritime pine populations probably expanded from Portugal throughout NW Spain in the seventeenth century (Ruíz Zorrilla, 1980), and they are now widely distributed in this area.

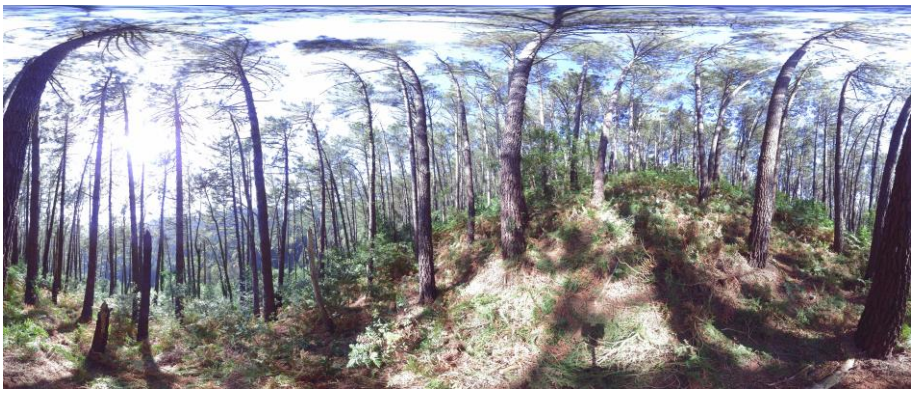

Figure 3.3. Panoramic view of an Atlantic maritime pine forest reforestation from 1941 (Rodoiros, Asturias). The image, consisting of multiple photographs taken with a TLS FARO Laser Scanner Focus^{3D} X 130, covers the full horizontal range (0-360º).

Nemoral Scots pine forest

Barbati et al. (2006) describes this forest type as follows: "Forests dominated by *Pinus sylvestris* ssp. *sylvestris* distributed mainly in the nemoral Europe and further east in the wooded steppe belt of western Eurasia. These forests may be originated from both natural regeneration and artificial planting." In the southern Atlantic region, they have usually been established by afforestation or reforestation. They include Scots pine forest plantations that are no longer intensively managed and/or mature plantations with low intensity of management, showing somewhat natural features: e.g. mixed tree canopy composition, significant ingrowth of self-sown trees and uneven-aged diameter distribution. In Spain they are mainly located in the Pyrenees range, although some redoubt stands can be found in the Cantabrian range, e.g. "Pinar de Lillo" (Figure 3.4) and "Velilla del Río Carrión" (Costa et al., 1997).

Figure 3.4. Panoramic view of Pinar de Lillo (Montaña de Riaño y Mampodre Regional Park, León). The image, consisting of multiple photographs taken with a TLS FARO Laser Scanner Focus^{3D} X 130, covers the full horizontal range (0-360º).

Mediterranean Scots pine forest

According to Barbati et al. (2006), these correspond to pure Scots pine forests in the Mediterranean region, including mountainous and oro-Mediterranean distributions, and they are mainly located in the Iberian, Cordillera Central and Baetic ranges. Populations of the Baetic ranges (Sierra Nevada and Sierra de Baza), which represent the southernmost location for this species, are considered a specific subspecies (*Pinus sylvestris* subsp. *nevadensis* H. Christ) (Franco, 1997) (Figure 3.5). About 35% of the distribution area of this species in Spain is thought to correspond to artificial planting (Costa et al., 1997).

Figure 3.5. Panoramic view of a Mediterranean Scots pine forest corresponding to subsp. *nevadensis* (Sierra Nevada National Park, Granada). The image, consisting of multiple photographs taken with a TLS FARO Laser Scanner Focus^{3D} X 130, covers the full horizontal range (0-360º).

Mountainous Silver fir forest

This type of forest is formed by pure silver fir communities, distributed at the montane level of the major European mountains (almost exclusively located in the central and central-eastern Pyrenees in the study area, Figure 3.6). It is mainly found in association with mountainous beech forest, which can often form mixed beech-fir forests (Barbati et al., 2010). The mountainous silver fir forests are located in drier soils in areas where beech disappears (mainly north aspect between 1200 and 1600 meters above sea level -m.a.s.l.-) and also in subalpine areas (shady aspect up to 2000 m.a.s.l.) together with the mountain pine (*Pinus uncinata* Ramond ex DC. in Lam. & DC.) in the highest zones (Costa et al., 1997).

Figure 3.6. Panoramic view of the subalpine mountain silver fir forest "Mata de València", which represents the largest mountain silver fir forest in Spain. It is located in the peripheral zone of the Aigüestortes i Estany de St. Maurici National Park (San Andreu de Valencia d'Aneu, Catalonia). The image, consisting of multiple photographs taken with a TLS FARO Laser Scanner Focus^{3D} X 130, covers the full horizontal range (0-360º).

Plantations of not-site-native species (P. radiata)

These forests correspond to plantations of non-native European forest species, in this case of *P. radiata* (Figure 3.7). They are used in industry as a source of raw material for wood processing (timber) and are managed by short-rotation forestry (Barbati et al., 2006). They are usually characterized by a simplified structure of pure even-aged stands because of the associated silvicultural management. However, despite their biological features, these plantations are an important forest economic resource in northern Spain, being the second most harvested tree species in Spain, with a total of 5,020,460 m^3 in 2018; and reaching the highest value among the conifers (MITERD, 2021).

Figure 3.7. Panoramic view of timber stage *P. radiata* plantation stand located in northwest Spain (Castro de Rei, Galicia). The image, consisting of multiple photographs taken with a TLS FARO Laser Scanner Focus^{3D} X 130, covers the full horizontal range (0-360º).

3.1.1 Data

This doctoral thesis comprises several sources of data according to the goals and hypothesis to be evaluated in the different chapters. The data sources can be grouped by spatial scale and type of forests (see Table 3.2). The largest database in terms of number of sample plots corresponds to the third and second Spanish National Forest Inventory (SNFI, Villaescusa, 1998; Villanueva, 2005). A network of Spanish mature sample plots, specifically measured for this work and supported by the FORESCHANGE (2016) research project, was established for testing the hypotheses proposed in the present thesis. This mature network includes a regional subset of data referred to in Table 3.2 as "Pyrenees mature forests". This subset of data was selected because it is the only region which includes not only mature stands, but also the highest degrees of naturalness represented by long untouched and old-growth stands. Another regional (northwest Spain) data set corresponding to even-aged *P. radiata* plots, established by the Unit for Sustainable Environmental and Forest Management (UXAFORES), University of Santiago de Compostela, was used to demonstrate the good performance of the site form (*SF*) approach for estimating site quality, relative to the site index (*SI*) method. Finally, a network of mature plots of *P. sylvestris*, belonging to the Estonian Network of

Forest Research Plots -together with their Spanish counterparts belonging to mature *P. sylvestris* forests- was used for comparison of structural features in a broader biogeographical context.

Table 3.2. Data scheme with number of plots by data source and forest types

Spatial scale	National		Regional		Regional
Location	Spain		Northwest Spain	Spanish Pyrenees	Spain and Estonia
Data set (maturity) / Forest type (species)	Spanish mature forests[1] (Mature-old-growth)	SNFI[2] (All degrees of maturity)	Even-aged stands[3] (Young – rotation age)	Pyrenees mature forests[4] (Mature-old-growth)	Spanish and Estonian mature forests[5] (Mature)
Beech (*F. sylvatica*)	**40**	**1658**		**4**	
Beech-fir (*F. sylvatica* and *A. alba*)	**11**	**154**		**11**	
Silver fir (*A. alba*)	**12**	**108**		**12**	
Maritime pine *(P. pinaster)*	**40**	**1068**			
Scots pine *(P. sylvestris)*	**40**	**4261**			**95**
Plantations of *P. radiata*			**158**		
Total plots	**143**	**7249**	**158**	**27**	**95**

[1] Composed of 143 mature forests plots established within the FORESCHANGE (2016) project (see 3.1.1.1 Spanish mature forests)

[2] Plots corresponding to the second (only for beech-fir and silver fir forests) and third Spanish National Forest Inventories (SNFI) (see 3.1.1.2 Spanish National Forest Inventory).

[3] Even-aged *P. radiata* plots located in northwest Spain established by the Unit for Sustainable Environmental and Forest Management (UXAFORES), University of Santiago de Compostela (see 3.1.1.3 Permanent plots of even-aged *Pinus radiata* D. Don stands).

[4] Subset of mature forests plots (FORESCHANGE, 2016) located in the Spanish Pyrenees range and covering the highest degree of naturalness (reaching even old-growth conditions) (see 3.1.1.4 Pyrenees mature plots).

[5] Mature forests plots of *P. sylvestris* belonging to the Atlantic, Mediterranean (FORESCHANGE, 2016) and Boreal (Estonian Network of Forest Research Plots) biogeographical regions (see 3.1.1.5 Mature *Pinus sylvestris* forests belonging to Atlantic, Boreal and Mediterranean biogeographical regions).

3.1.1.1 Spanish mature forests

All of the sampled stands were selected according to two major characteristic features of old-growth forests (Buchwald, 2005; Mosseler et al., 2003): (i) the presence of large trees, and (ii) the presence of relatively old trees (mean age of dominant species approaches half of the maximum longevity for the respective species). Apart from the uncertainty in the use of terms associated with old-growth states or similar (Wirth et al., 2009, p. 19), the sampling plots were referred to as mature from a pragmatic point of view. Initially the SNFI data were studied in detail to identify potential areas including mature stands (by detection of large trees). Next, local experts, published papers and/or reports were consulted to find the most suitable stands. Selection criteria considered essential were the absence of severe natural and/or human-derived disturbance (at least over the last few decades) and full stocking of live trees. Both criteria were used with the aim of yielding plots in conditions of maximum occupancy. Finally, the following sources were consulted: (i) historical records, mainly the two oldest photogrammetric flights at national scale (conducted in 1945–46 and 1956–57), and (ii) bibliographic references (scientific literature and forest management plans). A total of 143 plots distributed at national level were identified, and both the latitudinal and altitudinal range of these species (*A. alba*, *F. sylvatica*, *P. pinaster* and *P. sylvestris*) in Spain were widely covered in order to represent the range of site qualities as fully as possible (Figure 3.8, Table 3.3). These plots represent the most exhaustive network of mature forest observation plots in Spain for these forest types (see section 3.1 Forests studied), corresponding to the data set of the Spanish FORESCHANGE (2016) research project, supported by the State Research Agency (Spanish Ministry of Science and Innovation) and co-funded by the European Regional Development Fund (ERDF). The main dasometric variables of the mature forest stands are included in Table 3.3.

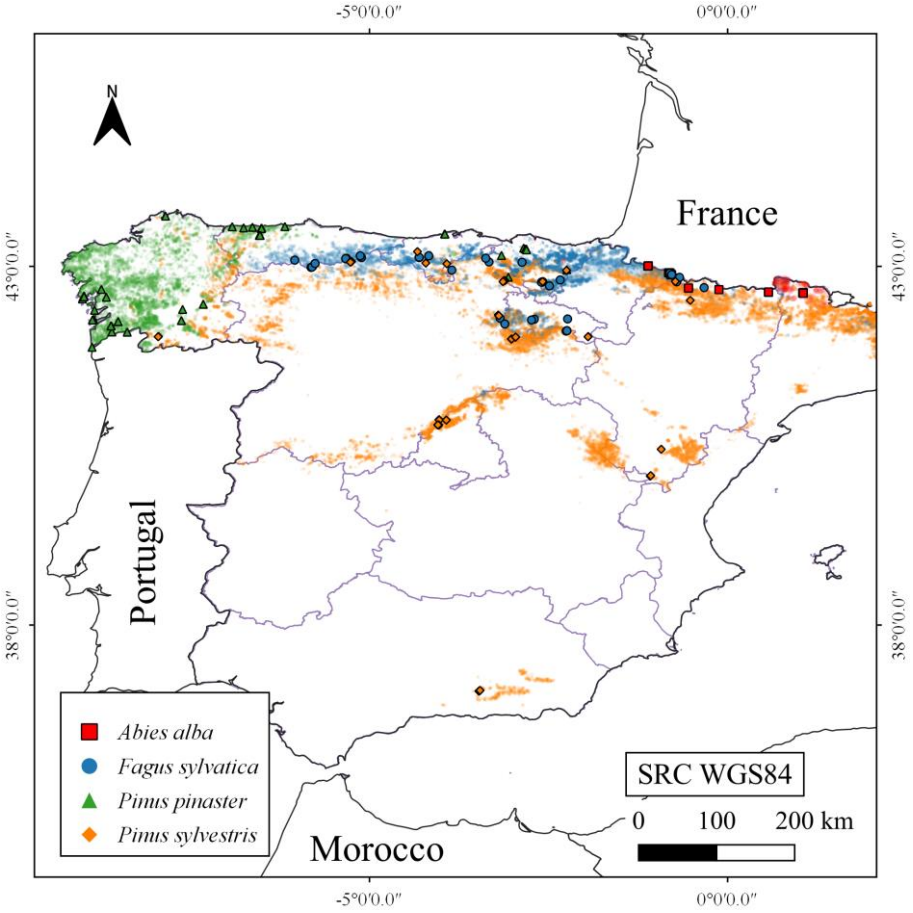

Figure 3.8. Distribution of mature forests plots used in the FORESTCHANGE (2016) project. The shaded areas represent the recent species distribution areas according to the Spanish forest map (Mapa Forestal de España, 2006).

Table 3.3. Statistics of stand variables by forest type. Mean (max – min)

Forest type	N (trees ha^{-1})	G (m2 ha^{-1})	W (Mg ha^{-1})	$\bar{h}$ (m)	$\bar{d}$ (cm)
Beech	333 (111 - 618)	41.94 (24.99 - 59.73)	418.73 (251.09 - 596.17)	55.06 (40.57 - 69.82)	39.39 (22.01 - 54.95)

Beech-fir	774 (297 - 2230)	65.99 (48.46 - 89.57)	607.59 (484.99 - 895.08)	68.35 (53.15 - 76.54)	30.41 (16.14 - 45.22)
Maritime pine	402 (145 - 782)	50.77 (30.06 - 89.89)	289.93 (185.80 - 72.98)	53.82 (40.27 - 63.29)	42.52 (29.81 - 53.81)
Scots pine	348 (55-983)	49.65 (17.49 - 75.26)	342.79 (121.38 - 666.37)	57.19 (39.37 - 82.65)	46.43 (31.06 - 76.94)
Silver fir	579 (283 - 1029)	70.36 (51.78 - 89.31)	613.93 (423.32 - 731.87)	63.98 (52.39 - 76.21)	38.33 (30.03 - 56.09)

N = number of trees per hectare (trees ha^{-1}); G = basal area (m2 ha^{-1}); W = aboveground and belowground live tree biomass (LTB) (Mg ha^{-1}); $\bar{h}$ = arithmetic mean height of live trees (m); $\bar{d}$ = arithmetic mean diameter at breast height (dbh) of live trees (cm).

Field sampling design

All plots were located in fully stocked stands with no evidence of recent disturbance or logging according to all of the previously mentioned features. Sampling was conducted between 2017 and 2019 and was implemented using a circular nested plot design, with 2 levels of nesting (Figure 3.9). All trees with the following characteristics were measured: living and standing dead trees with diameter at breast height (dbh, measured at 1.3 m from the ground level and uphill in the maximum slope line) greater or equal than 7.5 cm in the first level (plot radius 5 m) and greater or equal than 12.5 cm in the second level (plot radius 25 m). The dbh of each tree was measured with a diameter tape to the nearest 0.1 cm, and total tree height (h) was measured with a digital hypsometer (Vertex IV, Haglöf Sweden) to the nearest 0.1 m. In order to map trees position, azimuths (from the north) and horizontal distances from plot centre were measured with a laser measuring device (TruPulse 360°R) to the nearest 0.1° and 0.1 m, respectively. UTM coordinates and elevation of the plot centre were measured with a high accuracy GNSS receiver (Trimble R2). In addition, for the 10-15 tallest trees in each plot, two cores were sampled per tree, as within-tree growth variations are likely to influence the reconstruction of small-

scale disturbances (Copenheaver et al., 2009). The cores were extracted at *dbh*, perpendicular to the maximum slope (on both sides), with a 5 mm increment borer.

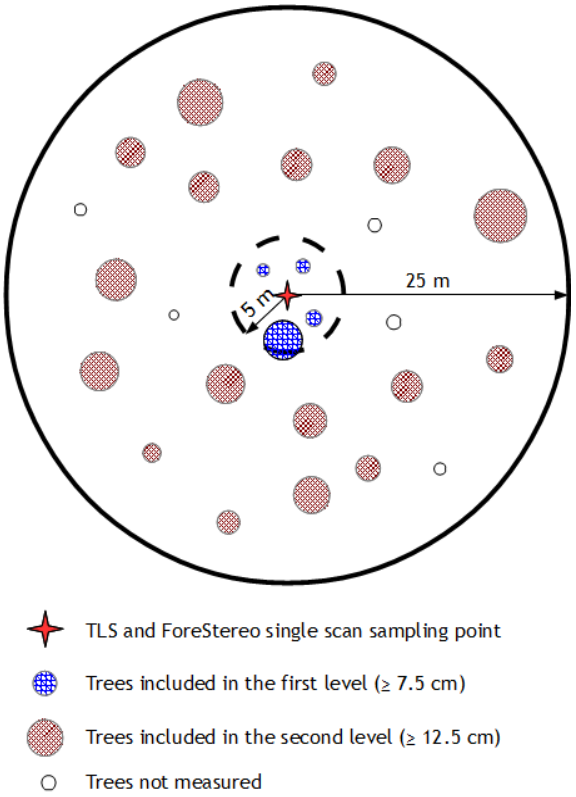

Figure 3.9. The plot design consisted of a circular nested plot with 2 levels. All trees of diameter at breast height (***dbh***, measured at 1.3 m from the ground) greater than 7.5 cm in the first level (plot radius 5 m) and greater than 12.5 cm in the second level (plot radius 25 m) were measured.

Finally, a TLS *FARO Laser Scanner Focus^{3D} X 130* proximal terrestrial laser scanning (TLS) sensing device was used to obtain information from the plot centre, covering the full horizontal range (0-360º) and vertical range (-60-90º) with a resolution of 7.67 mm at 10 m in both, horizontal and vertical angular apertures (see Table 3.4 for technical details).

Table 3.4. Technical specification for *FARO® Laser Scanner Focus^{3D} X 130*

Deflection unit	
Field of view (vertical/horizontal)	300º/360º
Step size (vertical/horizontal)	0.009º (40,960 3D-Pixel on 360º) / 0.009º
Max. vertical scan speed	5.820 rpm or 97 Hz
Laser (optical transmitter)	
Laser class	Laser class 1
Wavelength:	1550 nm
Beam divergence	Typical 0.19 mrad (0.011°) (1/e, half angle)
Beam divergence at exit	Typical 2.25 mm (1/e)

All the technical specifications were extracted from FARO website support information.

3.1.1.2 Spanish National Forest Inventory (SNFI)

The SNFI has the main purpose of providing information about forest resources at national scale approximately every ten years (Alberdi et al., 2010; 2017). So far, 3 SNFIs have been completed, for the periods 1969-75 (SNFI-1), 1986-96 (SNFI-2) and 1997-07 (SNFI-3); the fourth SNFI is still in process. The sampling design consists of a systematic regular squared grid of 1 x 1 km located over the forested areas, which are registered by the Spanish Forest Map (Mapa Forestal de España, 2006). Field measurements are implemented with a circular nested plot design consisting of 4 plots of radius 5, 10, 15 and 25 m, in which trees with $dbh \geq$ 7.5, 12.5, 22.5 and 42.5 cm are measured respectively.

The data used in this doctoral thesis correspond to SNFI-3, and SNFI-2 only for silver fir and beech-fir due to the small number of plots corresponding to these forest types. The entire SNFI data set was filtered, and only those plots including the forest types considered, with at least 90% dominance by the main species in G and a minimum of 10 trees, were treated in the final data set. Number of plots and altitude range for both data sets (Spanish mature forests and SNFI; as in Table 3.2, p. 39) are shown in Table 3.5.

Table 3.5. Number of plots for the forest types considered

Forest type	Number of plots		Altitudinal range (m.a.s.l.)
	Spanish mature forests	SNFI	Spanish mature forests
Beech	40	1658	694 - 1621
Beech-fir	11	154	1083 – 1613
Maritime pine	40	1068	59 - 794
Scots pine	40	4261	718 - 1959
Silver fir	12	108	1207 – 1989
Total	**143**	**7249**	

3.1.1.3 Permanent plots of even-aged *Pinus radiata* stands

This database was used to assess the performance of the *SF* index and corresponds to a network of 158 permanent plots established by the Unit for Sustainable Environmental and Forest Management (UXAFORES), University of Santiago de Compostela. All of the plots were located in pure, even-aged *P. radiata* stands and were measured between two and five times, depending on the plot, during the period 1995-2010. The plots were established throughout the area of distribution of the species in northwest Spain (Figure 3.10). This area is mainly located in the Atlantic Biogeographical Region (European Environment Agency, 2006), where the natural vegetation consists of mesophytic deciduous broadleaved and mixed coniferous-broadleaved forests (Bohn et al., 2000). The climate in the study region is characterized by mild temperatures (annual average temperature 9-14 °C) and a slight water deficit in summer (average annual rainfall 1000-2000 mm; average annual potential evapotranspiration 700-850 mm; water deficit 150-40 mm). Sample stands were established on the most representative soils of the area of distribution of the species in northwest Spain, corresponding with soils developed on granitic rocks (granites and granitic gneisses) and acid schist.

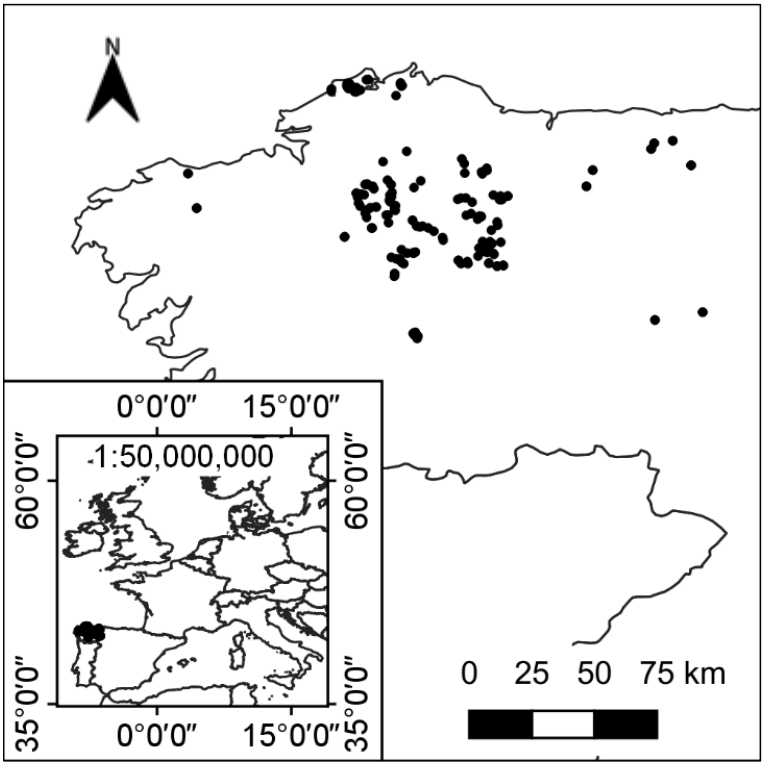

Figure 3.10. Plots location throughout the study area (northwest Spain)

The plots were selected with the aim of representing the existing range of ages, stand densities and site productivities in the study area. The plot size ranged from 625 to 1200 m^2, depending on stand density, to include a minimum number of 30 trees per plot. All trees in each sample plot were labelled with a number, and the dbh was measured with calipers to the nearest 0.1 cm. In the first inventory, h was measured with a Blume Leiss hypsometer to the nearest 0.25 m in a random sample of 30 trees and in an additional sample including the dominant trees (the proportion of the 100 largest dbh trees per hectare, depending on plot size). In the remaining inventories, h was measured with a digital hypsometer (Vertex III, Haglöf Sweden) to the nearest 0.1 m in all trees. Descriptive variables were also recorded for each tree,

e.g. whether they were alive or dead. Summary statistics of the main stand variables for each plot inventory are shown in Table 3.6.

Table 3.6. Summarized data from the sample plots

Variable	1st inventory (158 plots)		2nd inventory (158 plots)		3rd inventory (68 plots)	
	Mean (Max. - Min.)	SD	Mean (Max. - Min.)	SD	Mean (Max. - Min.)	SD
t	21.9 (38 - 5)	8.3	24.7 (41 - 8)	8.0	27.9 (47 - 19)	7.2
N	1083 (4864 - 217)	621.0	989 (4864 - 217)	595.0	829 (1821 - 280)	358.0
G	33.1 (63.1 - 5.3)	11.2	37.6 (69.8 - 10.8)	10.5	41.7 (65.5 - 20.1)	10.6
H_0	19.3 (32.6 - 5.8)	5.6	21.5 (34.0 - 10.9)	5.1	25.3 (35.2 - 17.5)	4.6
D_0	32.5 (61.7 - 10.4)	11.1	35.8 (64.4 - 14.9)	10.4	37.5 (58.9 - 26.2)	7.3
V	271.8 (741.6 – 12.2)	145.5	332.6 (840.1 – 52.3)	148.4	423.9 (769.4 – 158.8)	156.0
W	132.2 (357.2 – 7.1)	62.3	160.8 (406.6 – 27.2)	68.6	204.0 (369.5 – 73.2)	74.6
	4th inventory (32 plots)		5th inventory (10 plots)			
t	30.8 (43 - 19)	5.9	34.3 (44 - 25)	6.8		
N	729 (1824 - 200)	353.0	631 (1136 - 393)	255.0		
G	42.2 (68.1 - 20.1)	10.8	46.7 (68.1 - 34.5)	9.5		
H_0	27.2 (35.1 - 20.4)	4.2	30.3 (35.6 - 20.8)	5.2		
D_0	39.6 (49.0 - 27.4)	5.3	43.0 (49.7 - 35.3)	5.2		
V	453.9 (856.4 – 262.9)	144.9	558.4 (868.7 – 287.0)	166.0		
W	216.4 (416.1 – 115.2)	71.4	264.7 (421.0 – 136.1)	81.3		

t = stand age (yr); N = number of stems per hectare (trees ha^{-1}); G = stand basal area (m^2 ha^{-1}); H_0 = dominant total height of the 100 largest dbh trees per hectare (m); D_0 = dominant dbh of the 100 largest dbh trees per hectare (cm); V = stand aboveground volume (m^3 ha^{-1}); W = stand aboveground biomass (Mg ha^{-1}). V and W were estimated with local stand equations (Diéguez-Aranda et al., 2009). SD = standard deviation.

3.1.1.4 Pyrenees mature forests

To test the hypothesis of whether live tree biomass does not increase after a certain level of naturalness, also referred as maturity in this doctoral thesis, the forest types of European mountainous beech pure (2 stands), beech-fir communities (4 stands) and silver fir (4

stands) located in the Spanish Pyrenees range were considered. This region is where the widest representation of naturalness can be found, reaching even old-growth forest conditions (Sabatini et al., 2018). In total, 27 plots (4 beech, 12 silver fir, and 11 mixed beech-fir stands) were established in the 10 selected stands (Figure 3.11, Table 3.7), covering a wide geographic, climatic and elevational ranges representative of these forest types in the study area. Moreover, these plots are situated close to the southern distribution limit of silver fir in Europe.

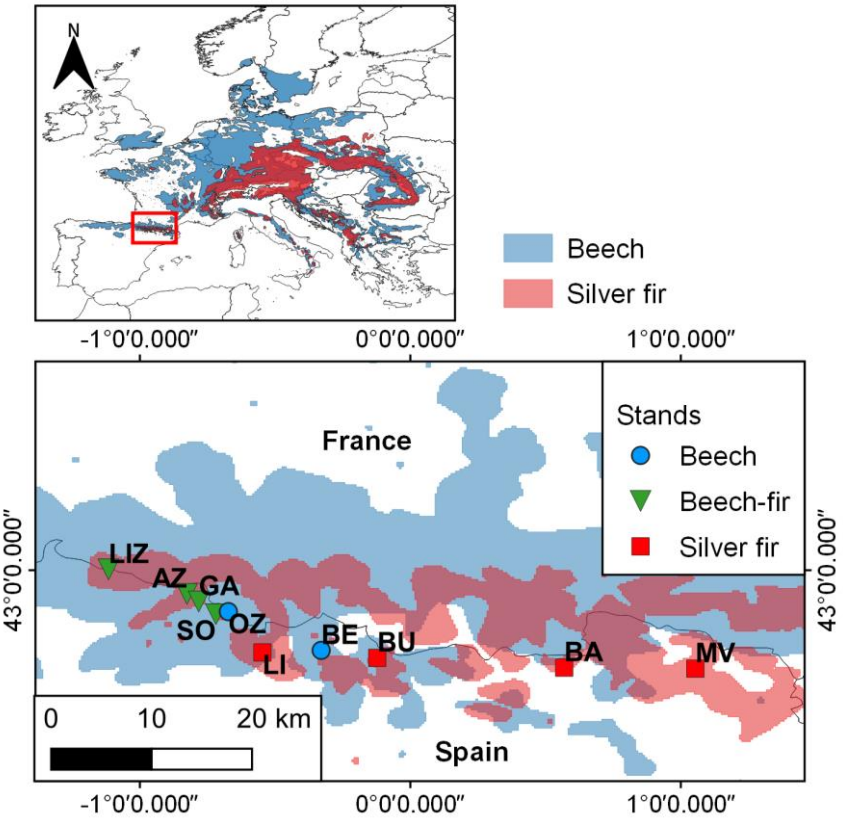

Figure 3.11. Distribution of the Pyrenees mature plots. Top: Distribution of silver fir (*Abies alba*) and European beech (*Fagus sylvatica*) (shapefiles source: EUROFORGEN, www.euforgen.org); bottom: geographical location and stand type in the study sites in the central Spanish Pyrenees. Sites as in Table 3.7, pp. 50-51.

The maturest stands of these forest types in Spain, especially of beech-fir and silver fir, can be found in the study area; in some cases, at ages close to the maximum longevity of both species, around 500 years (e.g. Macias et al., 2006; Di Filippo et al., 2015). These even include some remnant sites considered old-growth (Aztaparreta, 171 ha) and long untouched forests, i.e. the next lower level of naturalness according to Buchwald (2005), (Lizardoia, 64 ha). For more detail about these remnant sites, see Costa et al. (1997); Gil-Pelegrín et al. (1989); Horvat et al. (2018); and Sabatini et al. (2018). This classification forms a gradient of naturalness (old-growth > long untouched > mature) in which the highest degree of naturalness corresponds to stands with large trees, with a wide variation in tree sizes and spacing, large standing and fallen dead trees and abundant canopy gaps. Depending on the time at which human disturbance last occurred, this type of evidence is usually readily visible in mature stands, may still be visible in long untouched stands, but may not be recognizable in old-growth stands (Buchwald, 2005).

Most of the study stands are located on marl and limestone bedrock (basic soils), lutite or slate and sandstone, and moraine deposits (Table 3.7) (Robador Moreno et al., 2020). Climatic data (mean temperatures and total precipitation) were acquired for the period 1950-2018 from the Digital Climatic Atlas of the Iberian Peninsula (Ninyerola et al., 2005), which has a spatial resolution of 200 m and monthly temporal resolution. According to Köppen weather classification, the climate in the western stands is temperate oceanic (Cfb), and in the eastern sites, it is warm-summer humid continental (Dfb). It should be noted also that climate in the study area has become warmer and drier since the 1980s, with several mild droughts occurring during the last four decades (Camarero et al., 2011; Serra-Maluquer et al., 2019).

Table 3.7. Characteristics of the sampling sites. Values are means, and ranges are shown in brackets

Site	Code	Stand type	No. plots	Bedrock	MAT (ºC)	TAP (mm)	Elevation (m.a.s.l.)	*SF*	*N*	*G*	Live tree biomass	Mean age at 1.3 m (years)
Aztaparreta[1]	AZ	BF	1 (B)	Marl Lim	7.0	1510	1573	22.03	555	47.7	498.0	309 (183-386)
			3 (BF)		7.0	1472	1562 (1510-1613)	17.73 (17.27-18.29)	487 (372-581)	59.3 (54.1-64.9)	579.7 (545.5-608.8)	263 (106-434)
Lizardoia[2]	LIZ	BF	3 (BF)	Lut Sand	9.7	1395	1120 (1083-1153)	20.48 (19.30-22.73)	859 (265-1660)	66.6 (53.7-80.9)	673.4 (497.9-851.9)	192 (60-378)
Gamueta[3]	GA	BF	1 (B)	Marl Lim	7.0	1533	1534	20.82	407	46.7	444.7	264 (208-318)
			2 (BF)		7.5	1453	1493 (1483-1503)	18.75 (18.15-19.35)	392 (351-433)	56.2 (48.6-63.9)	564.6 (472.1-567.0)	183 (131-226)
			1 (F)		8.0	1413	1420	18.75	367	30.3	571.4	243 (87-461)
Selva de Oza[3]	SO	BF	3 (BF)	Lut Sand	8.3	1452	1300 (1212-1351)	18.79 (17.59-19.82)	655 (453-927)	59.0 (57.6-60.8)	585.1 (575.7-598.7)	141 (65-222)
			1 (F)		9.0	1390	1207	22.9	560	64.2	544.8	76 (63- 93)
Mata de València[3]	MV	F	4	Slate Sand Mor	5.7	861	1820 (1634-1989)	21.49 (19.97-24.12)	621 (367-779)	66.5 (56.1-82.2)	565.7 (465.0-664.2)	139 (82-200)
Ballibierna[3]	BA	F	3	Lut Mor	8.0	1303	1496 (1491-1502)	23.93 (23.66-24.18)	462 (372-514)	70.3 (65.9-75.7)	565.2 (607.6-728.3)	110 (81-173)

Lierde[3]	LI	F	2	Lut Sand	9.0	1516	1309 (1307-1311)	23.37 (22.69-24.05)	514 (397-632)	71.5 (70.4-72.5)	681.4 (624.9-737.9)	107 (61-155)
Bujaruelo[3]	BU	F	1	Sand Lim	9.0	1611	1285	25.83	402	77.9	814.1	100 (81-136)
Oza[3]	OZ	B	1	Slate Grey	8.0	1479	1432	29.53	362	50.5	554.5	184 (154-217)
Betato[3]	BE	B	1	Mor	9.0	1357	1310	29.64	438	44.4	483.9	106 (80-123)

Stand type: B (beech), BF (beech-fir) and F (silver fir). Bedrock: Grey (greywacke), Lim (limestone), Lut (lutite), Marl, Mor (moraine), Sand (sandstone) and Slate. MAT (mean annual temperature). TAP (total annual precipitation). SF (site form) = dominant height (H_0) of the stand at a reference dominant dbh (D_0). N = stand density (trees ha^{-1}); G = stand basal area (m^2 ha^{-1}).

[1] Small remnant site of old-growth forest (171.06 ha)

[2] Small remnant site of long untouched forest (63.97 ha)

[3] Mature forest

3.1.1.5 Mature *Pinus sylvestris* forests belonging to Atlantic, Boreal and Mediterranean biogeographical regions

This data set corresponds to mature (over 120-year-old) *P. sylvestris*-dominated stands located in the Atlantic, Boreal and Mediterranean biogeographical regions (according to Habitats Directive 92/43/EEC). The Atlantic region is characterized by oceanic climate with mild winters, cool summers, predominantly westerly winds and moderate rainfall throughout the year (Sundseth, 2009a). The Mediterranean region surrounds the homonymous sea, with a climate characterized by hot dry summers and humid, cool winters (Sundseth, 2009b). The Boreal region includes forests and wetlands, spreading from the tundra forests of the Arctic to the west with the Fennoscandian mountains and, to the south, gradually turning to the south into the deciduous forests of the Continental region. The region has relatively flat land, mainly below 500 m.a.s.l. (Sundseth, 2009c). This framework allowed us to cover a wide latitudinal range where this species is distributed in Europe and also represents some of the maturest conditions in Spain and Estonia. The data used for this chapter correspond to the Scots pine plots measured in this doctoral research (12 in Atlantic and 28 in Mediterranean stands) and a data set of 55 well distributed plots in Estonia (Figure 3.12). The Estonian data set belongs to the Estonian Network of Forest Research Plots and was provided by the Estonian University of Life Sciences. Estonian plots were dominated by Scots pine with a circular fixed area plots varying between 20-30 m radius depending on the density and other stand characteristics on site (Kiviste et al., 2015). All trees greater or equal than 4 cm at dbh were measured and their locations recorded (including standing dead trees). To make the data sets more comparable, only trees greater or equal than 7.5 cm at dbh (in accordance with the Spanish plots design) were included in the analysis. Furthermore, those plots with stumps were removed from the Estonian data set as a criterion of maturity and naturalness. Some of the main dasometric variables are summarised in Table 3.8.

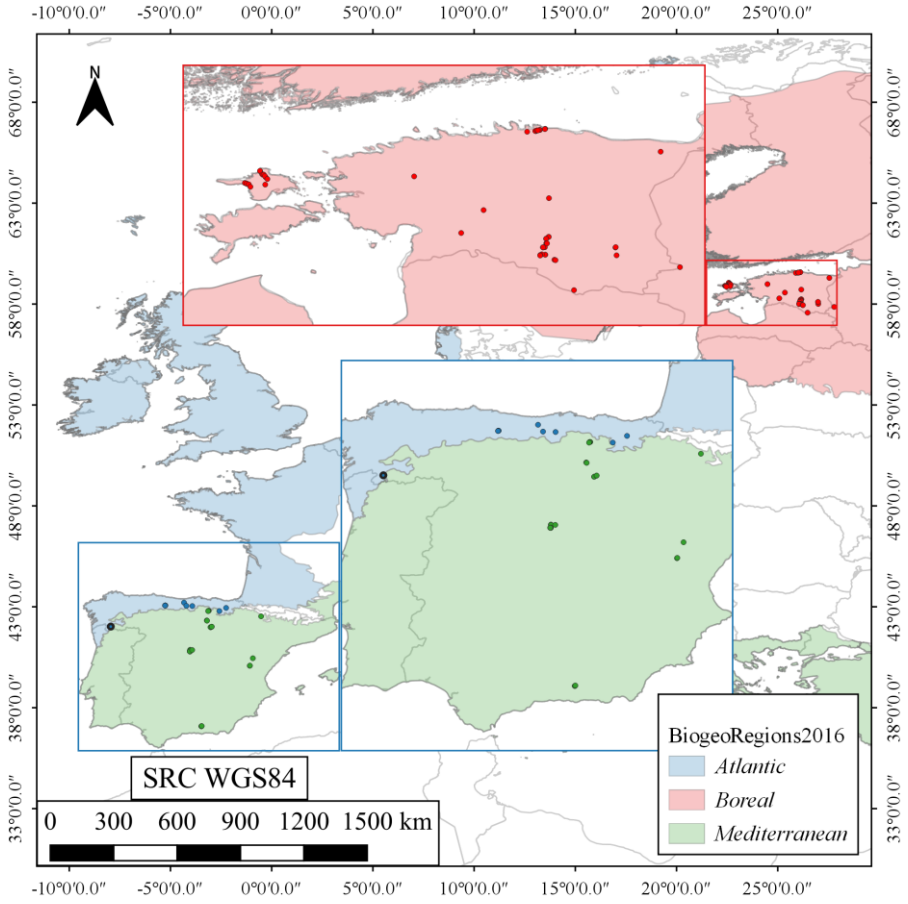

Figure 3.12. Distribution of mature Scots pine plots in the Atlantic, Mediterranean (Spain) and Boreal (Estonia) biogeographical regions according to Habitats Directive (92/43/EEC).

Table 3.8. Statistics of stand variables by biogeographical region. Mean (SD)

Biogeographical region (plots)	N (trees ha^{-1})	G (m^2 ha^{-1})	$\bar{d}$ (cm)	$\bar{h}$ (m)
Boreal (55)	617 (202)	32.93 (7.27)	25.31 (4.21)	22.74 (4.91)
Mediterranean (28)	295 (113)	46.73 (11.83)	44.83 (8.76)	18.05 (5.24)
Atlantic (12)	358 (158)	52.29 (11.99)	43.40 (11.88)	20.84 (4.96)

N = number of stems per hectare (trees ha^{-1}); G = stand basal area (m^2 ha^{-1}); $\bar{d}$ = arithmetic mean dbh (cm); $\bar{h}$ = arithmetic mean h (m). SD (standard deviation).

3.2 SITE FORM AS A SUITABLE SITE QUALITY INDEX FOR THE STUDIED FORESTS

This chapter comprises two sections. The first section reports assessment of the performance of site form (SF), defined as the dominant height of the stand (H_0) at a reference dominant diameter ($D_{0_{ref}}$), as an indicator of site quality. For this purpose, SF was compared to the common site index (SI), defined as the H_0 at a given reference age (t_0), for even-aged *P. radiata* stands in northwest Spain (Molina-Valero et al., 2019a). The second section reports fitting SF models for those species of this work without SF previously available. In both sections, and according to Vanclay and Henry (1988), whenever possible the following important criteria that SF should fulfill to be considered an appropriate site quality index were evaluated: (i) reproducibility and consistency over time; (ii) representativeness of the site, which should not be influenced by stand condition and management; (iii) correlation with site productivity potential; (iv) at least as good as other site quality indices; (v) the ratio dbh/h known as tree taper (likewise stand taper, $d_g/\bar{h}$, where d_g is the quadratic mean dbh and $\bar{h}$ arithmetic mean h), should decrease as site quality increases (Huang and Titus, 1993; Larson, 1963).

3.2.1 Assessing site form performance in even-aged *P. radiata* stands

3.2.1.1 Site index (SI) and site form (SF) dynamic equations

Growth equations of site-dependent forest variables must comply with at least the three following properties (Clutter et al., 1983): (i) biological meaning, they must have a coherent inflexion point and an asymptotic value when the projected stand age approximates infinity; (ii) path invariance, the result of projecting first from t_1 to t_2, and then from t_2 to t_3, must be the same as that of the one-step projection from t_1 to t_3; and (iii) simplicity, models that are too complex and include many interactions between individual variables may be affected by correlations between the variables, making them unstable and with

a low predictive capacity. Most of these properties can be achieved using dynamic equation derivation techniques known in forestry as the Algebraic Difference Approach (ADA) (Bailey and Clutter, 1974) or its Generalization (GADA) (Cieszewski and Bailey, 2000).

In this study, after comparing different base models and ADA and GADA formulations (see Diéguez-Aranda et al., 2005), we focused our attention on GADA-derived dynamic equation with two site-specific parameters and based on the Hossfeld IV model (Hossfeld, 1882), which provided fits for development of SF and SI curves (Table 3.9). In the case of SF, an additional constant of 1.3 (which represent the reference height of dbh measurements) was added to the right-hand side of the equation to force the curves to pass through the point (D_0 = 0, H_0 = 1.3, where D_0 is the dominant dbh). The site-specific local parameters (for each plot, X_0) were simultaneously estimated with the global parameters (for all plots, b_i) using the dummy variable method described in Cieszewski et al. (2000).

Table 3.9. Dynamic equations derived from the base model of Hossfeld IV used for fitting site index (SI) and site form (SF) curves

Model	Site-related parameters	Dynamic equation
$Y = \frac{a_1}{1 + a_2 t^{-a_3}}$	$a_1 = X$ $a_2 = b_2/X$ $a_3 = b_3$	$SI = \frac{X_0}{1 + \frac{b_2}{X_0} t_0^{-b_3}}$ $X_0 = \frac{1}{2}\left[Y_0 + \sqrt{{Y_0}^2 + 4 b_2 Y_0 t_0^{-b_3}}\right]$ $SF = 1.3 + \frac{X_0}{1 + \frac{b_2}{X_0} {D_0}_{ref}^{-b_3}}$ $X_0 = \frac{1}{2}\left[(Y_0 - 1.3) + \sqrt{(Y_0 - 1.3)^2 - 4 b_2 {D_0}_{ref}^{-b_3}(1.3 - Y_0)}\right]$

The t_0 used to predict SI values was 20 years, as established by Diéguez-Aranda et al. (2005) for *P. radiata* plantations in northwest Spain. The $D_{0_{ref}}$ was selected so that it was a reliable predictor of H_0 at other D_0 values (Goelz and Burk, 1992). For this purpose, different base D_0 value and their corresponding observed H_0 values, were used

to estimate $\widehat{H_0}$ at other D_0 values (both forward and backward) for each plot. The results were compared with the values obtained from plot data, after which the relative error ($RE\%$) in predictions was calculated using Eq. 3.1. The number of plot observations (n) used to calculate $RE\%$ at each D_0 was also considered in order to maintain the best possible balance between the lowest possible $RE\%$ and the highest possible n. The proximity to the D_0 for the studied stands at the age of 20 years was also considered, because it is the t_0 in the SI model and therefore, both estimators, SI and SF, may be more comparable.

We fitted the nonlinear models with the `nls` function of the R software environment (R Core Team, 2021). Two goodness-of-fit statistics were calculated: the adjusted coefficient of determination (R^2_{adj}) (Eq. 3.2), which indicates the proportion of the variance of the dependent variable explained by the model; and the root mean square error ($RMSE$) (Eq. 3.3), which assesses the precision of the estimates. In addition, graphical analysis of the residuals and examination of the appearance of the fitted curves overlaid on the trajectories of the H_0 of the plots were also conducted.

$$RE\% = \frac{\sqrt{\sum_{i=1}^{n}(Y_i - \hat{Y}_i)^2 /(n-p)}}{\bar{Y}} \cdot 100 \tag{3.1}$$

$$R^2_{adj} = 1 - \frac{\sum_{i=1}^{n}(Y_i - \hat{Y}_i)^2/(n-p)}{\sum_{i=1}^{n}(Y_i - \bar{Y})^2/(n-1)} \tag{3.2}$$

$$RMSE = \sqrt{\frac{\sum_{i=1}^{n}(Y_i - \hat{Y}_i)^2}{n-p}} \tag{3.3}$$

where Y_i, $\hat{Y}_i$ and $\bar{Y}$ are the observed, predicted and arithmetic mean values of the H_0, respectively; n is the total number of observations; and p is the number of model parameters.

3.2.1.2 Comparative performance of SI and SF as site quality estimators

As previously mentioned, Vanclay and Henry (1988) outlined the characteristics that an index should possess to be accepted as a measure of site quality. In order to assess the consistency of the indices over long periods of time, we first analyzed similarities in the uncertainties in the prediction of SI and SF. This was carried out by visual comparison of the standard deviation of standardized values computed for each plot across different inventories. We standardized the values for each approach from 0 to 1 by using the absolute minimum and maximum values, respectively.

The second criterion of Vanclay and Henry (1988) (i.e. that a site quality index must be indicative of the site and not influenced by the stand conditions or management history) can also be formulated as by Huang and Titus (1993): the $h{\sim}dbh$ relationship of the dominant and codominant trees must not be affected by stand density. We assessed this criterion by means of the Pearson correlation coefficient (r) for comparison between the predicted SI and SF values and Reineke's stand density index (SDI) (Reineke, 1933):

$$SDI = N\,(25/d_g)^{-1.605} \tag{3.4}$$

where N is the stand density (trees ha^{-1}) and d_g is the quadratic mean dbh (cm).

The correlations for the SI and SF values and the direct measure of site quality were determined using the maximum mean annual volume increment (MAI) of each plot as a surrogate for the latter variable. Although other stand variables, such as maximum stand height, basal area, stand basal area increment and periodic annual volume increment, have been used as surrogates (e.g. Vanclay and Henry, 1988; Vanclay, 1994), the maximum MAI is considered the most appropriate direct measure of site quality because it is strongly related to the wood volume that can be obtained in a given site (Skovsgaard and Vanclay, 2008). Soil characteristics and climatic factors are, ultimately, the main drivers of the variation in site quality (Skovsgaard and Vanclay, 2008).

The following sequential steps were carried out to select the data for correlation analysis: (i) prediction of MAI for each plot and inventory by using the stand volume equation for *P. radiata* available in Diéguez-Aranda et al. (2009); (ii) selection of the maximum MAI value observed for each plot; and (iii) comparison of the current age of the plot for the maximum observed MAI with the optimal rotation age (ORA) (the age of the stand for the potential maximum MAI). The ORA was estimated for each plot by using the dynamic whole-stand growth model developed by Castedo-Dorado et al. (2007), with variables corresponding to the inventory closest to the largest observed MAI as input stand variables for each plot. Plots with differences greater than 10 years between the ORA and the current stand age for the maximum observed MAI were excluded. A total of 78 plots out of 158 were finally used for correlation analysis.

In addition to the desirable characteristics suggested by Vanclay and Henry (1988), SF is usually used as a site quality index under the assumption that the ratio $d_g/\overline{h}$ (usually referred in the literature as stand taper) decreases as site quality increases (Huang and Titus, 1993; Duan et al., 2018). This assumption was assessed by computing the correlation (r) between stand taper and predicted SF for each plot-inventory combination. The same analysis was carried out for SI for comparative purposes.

3.2.2 Site form models fitted for the study forests

In the research reported in this doctoral thesis, SF models were developed only for beech-fir and silver fir forests. For the other species, we used the models previously fitted by Moreno-Fernández et al. (2018) (Table 3.10) with significant parameters estimates and good performance of the fitted curves overlaid on the trajectories of the observed H_0 (Moreno-Fernández et al. (2018), Figure 1). All of these SF models were fitted using the Hosffeld-II based model (Eq. 3.6) with different site-specific parameters and guide curve approach.

Table 3.10. Site form (SF) models fitted by Moreno-Fernández et al. (2018)

Forest type	Parameters		Equation
	Estimated	p-value	
Maritime pine	b = 0.13035	$2 \cdot 10^{-16}$	$SF = 1.3 + \frac{D_{0_{ref}}^2}{\left[\frac{D_0}{\sqrt{H_0 - 1.3}} + b \cdot \left(D_{0_{ref}} - D_0\right)\right]^2}$
Beech	a = 2.5473	$2 \cdot 10^{-16}$	$SF = 1.3 + \frac{D_{0_{ref}}^2}{\left[a + \left(\frac{D_0}{\sqrt{H_0 - 1.3}} - a\right) \cdot \left(\frac{D_{0_{ref}}}{D_0}\right)\right]^2}$
Scots pine	b = 0.1386	$2 \cdot 10^{-16}$	$SF = 1.3 + \frac{D_{0\,ref}^2}{\left[\frac{D_0}{\sqrt{H_0 - 1.3}} + b \cdot \left(D_{0_{ref}} - D_0\right)\right]^2}$

D_0 = stand dominant diameter at breast height (dbh) (cm); $D_{0_{ref}}$ = reference stand dominant dbh (cm); H_0 = stand dominant height (m).

As previously mentioned, for these forest types (beech-fir and silver fir forests), all of the data available in the SNFI-2 (Villaescusa, 1998) and SNFI-3 (Villanueva, 2005) were used in addition to the data from the network of plots in mature stands (FORESCHANGE, 2016) specifically measured in this work. This was because of the small number of plots available in the SNFI-3 data set. Although there may be some common plots in both SNFIs, we considered all the plots as temporary, with the objective of generating a methodology capable of dealing with those cases in which only temporary plots corresponding to a single NFI are available. It is important to note that this allowed us to cover the largest possible range of development states and site quality conditions represented in the study area, which contributed to construction of better SF models by preventing bias and representing values in the variable of interest as far as possible (Clutter et al., 1983).

For each plot, H_0 was estimated according to Assman's criteria (Assman, 1970), in which H_0 is obtained from $h \sim dbh$ relationship, where D_0 is computed as the dbh arithmetic mean of the 100 trees per hectare with largest dbh, and H_0 as the estimated h by including D_0 as independent variable in the logarithmic regression:

$$h = a + b \cdot log_{10} \cdot dbh \quad (3.5)$$

where a and b are parameters to be estimated for each sample plot in which the h and dbh of the trees are used as sample data.

The SNFI is based on a systematic sampling design, so that there may be plots in many stands conditions and covering the stand conditions in a probabilistic-based way. The sampling may therefore include some plots with very few trees for which biometrics does not work properly for modelling SF. Thus, in stands that are not sufficiently dense, H_0 may be underestimated due to its lower value in very scarce stands, unlike D_0, for which the same growth usually occurs in widely spaced stands, regardless of the density (Clutter et al., 1983, pp. 65-66). As the H_0/D_0 ratio for different site qualities should be proportional for all D_0 values (Stout and Shumway, 1982), between 1 and 20 trees per plot were assessed for a random subsample of 50 plots for each type of forest, in order to establish a minimum number of trees per plot where H_0/D_0 ratios were stable and the curves did not cross. Finally, SNFI plots were filtered according to this criterion, and those including at least the minimum number of trees necessary to comply with this criterion were selected.

As only one temporary measurement was considered for each plot (i.e. temporary plots), the SF was estimated by the guide curve method (Clutter et al., 1983, pp. 46-50) and either the Hosffeld-II (Eq. 3.6) or Bertalanffy-Richards (Eq. 3.7) growth equations. This was achieved in two steps: (i) base models were fitted to the scatter plot of H_0 against D_0; and (ii) a family of site quality curves was generated with different parameters depending on the SF for a $D_{0_{ref}}$. This allowed development of the same number of family curves as the number of parameters in the models. The base models were modified to yield predictions of H_0 = 1.3 for D_0 = 0 by adding 1.3 to the right-hand side of the equations as shown in Eqs. 3.6 and 3.7.

$$H_0 = 1.3 + \frac{{D_0}^2}{(a + b \cdot D_0)^2} \tag{3.6}$$

$$H_0 = 1.3 + a \cdot \left(1 - e^{(-b \cdot D_0)}\right)^c \tag{3.7}$$

SF models were selected by considering the goodness-of-fit statistics R^2_{adj} and $RMSE$ and, above all, the performance of the site quality curves. Unlike in other works in which $D_{0_{ref}}$ was estimated for a specific base age by means of $D_0 \sim age$ growth models (Duan et al., 2018; Fu et al., 2018a), in this case $D_{0_{ref}}$ values were selected from the models that yielded the lowest $RMSE$ values. Thus, as already mentioned for *P. radiata*, the $D_{0_{ref}}$ was selected so that it was a reliable predictor of H_0 at other D_0 values, in this case, according to Goelz and Burk (1992) considered for different SI and ages. Different base D_0 values were rounded to integers, and the corresponding observed H_0 values, were used to estimate H_0 at other D_0 values (both forward and backward) for each plot, and the estimated hypothetical H_0 values were represented at different $D_{0_{ref}}$ in each interaction. The resulting values were compared with those obtained from plot data, after which the $RE\%$ was calculated using Eq. 3.1. The number of plots used in each interaction (n) to calculate $RE\%$ was used to determine the base D_0 for which $RE\%$ was lower and n was higher, as $D_{0_{ref}}$. Finally, we assessed the assumptions of homoscedasticity and normality in the model residuals by plotting residuals against fitted values, and by means of Q-Q plots and Shapiro-Wilk tests for the standardized residuals.

Once models were fitted, some of the aforementioned desirable criteria that SF index should fulfill were demonstrated. First, it was demonstrated that SF is not influenced by stand conditions. In this respect, according to Beltran et al. (2016), the independence between D_0 and stand density was assessed by means of the correlation (r) between D_0 and SDI (Eq. 3.4) to check that density did not affect D_0. Second, the assumption that stand density should not affect the $H_0 \sim D_0$ relationship in uneven-aged stands, was assessed by the correlation between D_0/H_0 coefficient and SDI (Duan et al., 2018; Fu et al., 2018a). Third, the stand taper ($d_g/\bar{h}$) relationship with SF was checked to determine whether the stand taper decreased as site quality increased (Huang and Titus, 1993; Larson, 1963).

3.3 ESTIMATION OF MAXIMUM BIOMASS STOCK BASED ON NATIONAL FOREST INVENTORY DATA

3.3.1 Assessing live tree biomass stocks at different stages of maturity

3.3.1.1 Dendrochronological methods

The tree cores were air-dried and sanded with increasingly fine sandpapers to distinguish the growth rings. The cores were then visually cross-dated and tree rings were measured to the nearest 0.01 mm with a binocular scope and a tree ring measuring stage (LINTAB™, Rinntech, Heidelberg, Germany). The visual cross-dating was checked using COFECHA software (Holmes, 1983). The ring-width of cores from the same trees and species was established to obtain mean series for individuals and species. Basal area increment (BAI, in cm^2 $year^{-1}$; Eq. 3.8) was estimated as an indicator of tree growth, using the dplR package (Bunn, 2008) implemented in R software (R Core Team, 2021).

$$BAI = \pi(R_t^2 - R_{t-1}^2) \quad (3.8)$$

where R is the radius of the tree and t is the year of ring formation.

Tree age was estimated using cores taken at breast height (1.3 m) and that passed through the stem pith. In cases where the stem pith was not reached, but arcing of the innermost rings was visible, the number of missing rings was estimated by a standard graphical method. Specifically, a template of concentric circles was fitted to the curve of the innermost rings, and constant tree-ring widths were assumed in the missing part of the radius (Duncan, 1989).

Studying radial growth increment patterns can provide useful information about stand and disturbance dynamics, including disturbance due to logging. Growth releases, defined as abrupt and sustained increases in tree-ring widths, are indicative of greater amounts of resources (e.g. light, moisture, nutrients) available to the tree, as a result of the death of canopy trees and subsequent gap formation. Synchronous releases from many trees in the same stand

indicate the occurrence of severe, large-scale canopy disturbance, while many asynchronous releases suggest small-scale events (Lorimer, 1985; Lorimer and Frelich, 1989).

Changes in radial growth, i.e. both increases (releases) and decreases (suppressions), were identified by calculating the percentage growth change (GC; Eq. 3.9) as described by Nowacki and Abrams (1997). GC is a moving average calculated over the prior years (M_1) and subsequent (M_2) 10-year periods for each annual ring.

$$GC = [(M_2 - M_1)/M_1] \cdot 100 \quad (3.9)$$

Releases were calculated using the boundary-line approach, as release potential is not constant during the life history of a tree (Black and Abrams, 2004). This approach involves fitting the best exponential function for M_1 against GC scatter plots, for which we used the criteria described by Ziaco et al. (2012) and fitted different boundary-lines subject to biogeoclimatic zones. In this case, we defined biogeoclimatic zones according to SF, as this site quality index depends on soil and climate conditions. We used the median value of the SF distributions based on SNFI data for each forest type as the threshold for assigning the plots to different SF intervals (Table 3.11, Figure 3.13). Mata de València was the only site with plots in both SF intervals defined for silver fir. After fitting several exponential functions included in the TRADER package for R (Altman et al., 2014), we selected those with the highest coefficients of determination (R^2) (Figure 3.14). The GC values were then scaled as a fraction of the boundary line, which is the maximum potential release. All values higher than 50% of the threshold value were considered major releases, and those between 25-50% of the threshold value were considered minor releases (Figure 3.14). These intervals were established by Ziaco et al. (2012), as most studies using the boundary line approach set a lower limit for minor releases of 20%. Only releases with values above the boundary line during at least 5 consecutive years were considered, as Camarero et al. (2011) described this as a characteristic threshold for detecting logging disturbance in Pyrenean silver fir forests.

Table 3.11. Growth change (GC) models and estimated boundary line parameters for each site form (SF) interval

Forest type	SF	Function	Parameters				R^2
			a	*b*	*c*	*d*	
F	< 21.84	$GC = a + b \cdot M_1 + c \cdot \log M_1 + d \cdot M_1 \cdot \log M_1$	7.84	-6.79	1.85	3.37	0.46
F	≥ 21.84	$GC = a \cdot e^{b \cdot M_1} + c \cdot e^{d \cdot M_1}$	3.35	-0.48	6.04	-3.41	0.99
BF	< 18.41	$GC = a + b \cdot M_1 + c \cdot \log M_1 + d \cdot M_1 \cdot \log M_1$	6.74	-3.99	1.59	1.35	0.85
BF	≥ 18.41	$GC = a \cdot e^{b \cdot M_1} + c \cdot e^{d \cdot M_1}$	5.34	-1.61	2.24	-0.44	0.97
B		$GC = a + b \cdot M_1 + c \cdot \log M_1 + d \cdot M_1 \cdot \log M_1$	10.04	-8.28	3.31	3.49	0.89

Forest type: B (beech), BF (beech-fir) and F (silver fir); Function = best exponential functions fitted for boundary-line approach; M_1 = averaged ring-width of 10-year prior period for each annual ring.

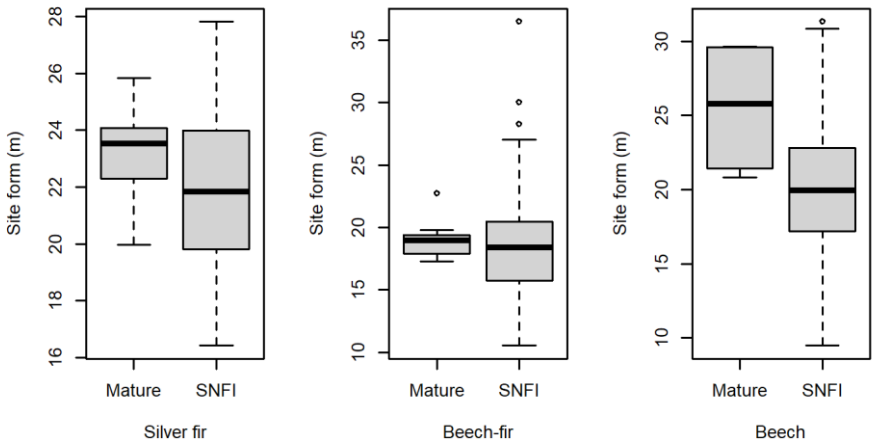

Figure 3.13. Box plots of forest types comparing the ranges of site form (SF) measured in the present study plots (mature forests) and in the Spanish National Forest Inventory (SNFI) plots.

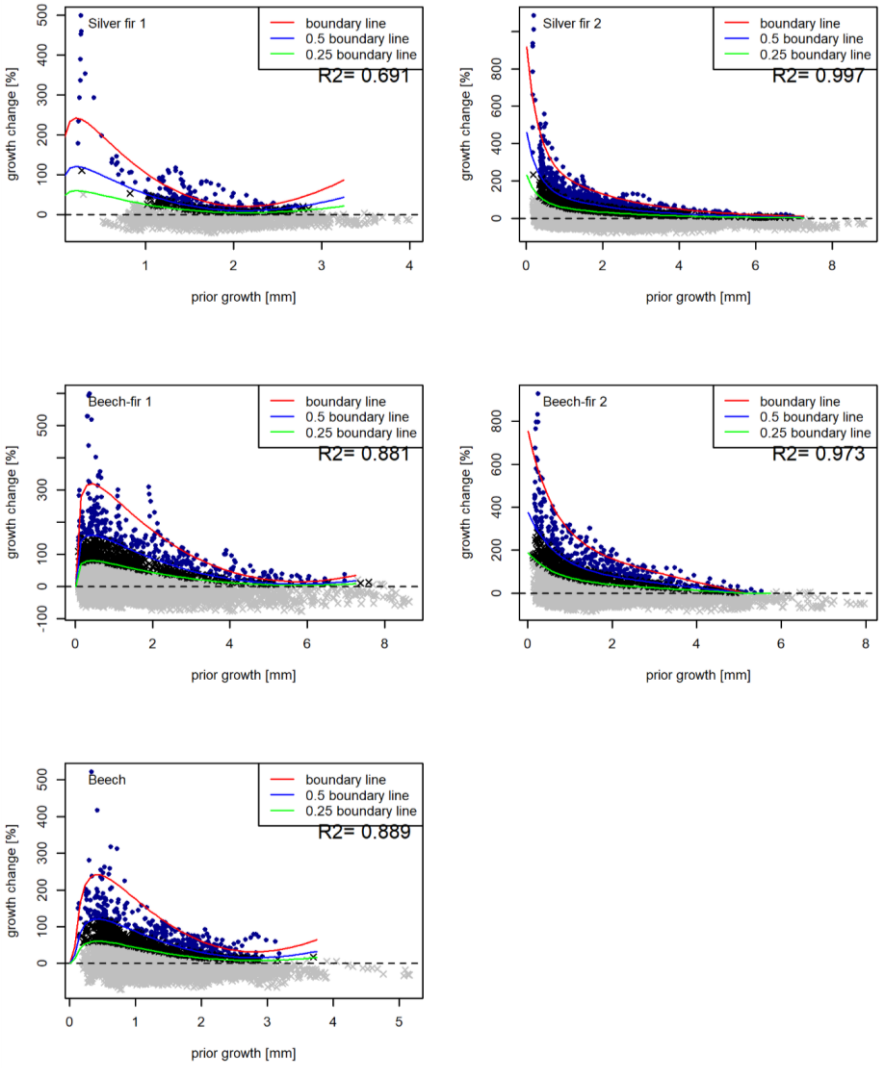

Figure 3.14. Boundary lines fitted in order to calculate growth releases by site form (*SF*) intervals (Table 3.11). Figure generated with the TRADER R package.

3.3.1.2 Establishing the degree of naturalness

The degree of naturalness was assessed at plot level as a naturalness score (*NS*) in order to rank forest functional naturalness on

the basis of the ecological processes experienced by trees. The methodology used was that proposed by Di Filippo et al. (2017).

One plot with fewer than 6 sampled trees was excluded from the analysis as it was not suitable for estimating some metrics proposed by the aforementioned authors (op. cit.) (Table 3.12). Several of the tree ring-based metrics proposed were used, except the mean age of the 10 oldest trees, as 10 dated trees were not available in several of the plots. This yielded 18 tree-ring metrics related to (i) age indicators, (ii) disturbance and suppression indicators, with disturbance events grouped in 20-year intervals, and (iii) growth history indicators. In addition, metrics related to the same naturalness attribute were aggregated into subgroups (Table 3.12). These metrics were explored by means of principal component analysis (PCA) in order to select the variables most strongly related to the degree of naturalness. After checking the significance of the first principal component (PC1) by means of Horn's parallel analysis (Horn, 1965), we selected those metrics with the highest loadings on PC1 per subgroup as the best variables for evaluating NS. Selected metrics were analyzed in a second PCA, and the PC1 scores were assigned to NS.

Table 3.12. Metrics used to assess the naturalness score (NS) according to Di Filippo et al. (2017)

Type	Subgroup	Metric	Description
AI	1	*MEAN* (year)	Mean canopy age
		MEDIAN (year)	Median canopy age
	2	*RANGE3* (year)	Age range between the mean of the 3 youngest and the 3 oldest trees measured
	3	*AGE3* (year)	Mean age of the 3 oldest trees
		AGE5 (year)	Mean age of the 5 oldest trees
		MAX (year)	Age of the oldest tree
GHI	4	*TrajRANGE3* (year)	Range between the mean of the 3 youngest and the 3 oldest ages when growth trajectories reached dbh = 37.5 cm
		TrajSLOW3 (year)	Mean of the 3 oldest ages when growth trajectories reached dbh = 37.5 cm
		TrajSLOW3mean (year)	TrajSLOW3 minus mean age of growth trajectories at dbh = 37.5 cm

		TrajSLOW3median (year)	TrajSLOW3 minus median age of growth trajectories at dbh = 37.5 cm
DSI	5	*SupN.5* (n)	Mean of the 5 highest number of suppressions per tree in each forest
	6	*SupL.5* (year)	Mean length of the 5 longest total suppressions experienced by tree
		SupLmax (year)	Maximum length of total suppression experienced by a tree in the forest
		MaxSupL.5 (year)	Mean length of the 5 longest single suppression phases experienced by trees
		MaxSupL.max (year)	Maximum length of the single suppression phase experienced by a tree in the forest
	7	*Rel1Yr.H*	[1]Shannon index of first release year in each tree
		Rel1Yr.D	[2]Inverse Simpson index of first release year in each tree
		Rel1Yr.Peak (%)	Highest relative frequency of first release year in each tree

Types of chrono-functional indicators: age indicators (AI), growth history indicators (GHI) and disturbance and suppression indicators (DSI); Subgroups: metrics assess similar features within the same type.

[1] Shannon index: popular metric used in ecology to species diversity by the equation $H = -\sum p_i \cdot \ln(p_i)$, where p_i represents the proportion of individuals belonging to the species i (Shannon, 1949). Higher values of this inverse index indicate higher levels of diversity. In this case, i corresponds to the first releases of each tree occurring in the same year.

[2] Inverse Simpson index: measure of diversity, which is often used to quantify the biodiversity of a habitat in ecology by the equation $D = \left[1 - \frac{\sum n_i(n_i-1)}{N(N-1)}\right]^{-1}$, where n_i is the number of individuals belonging to the species i, and N the total number of individuals (Simpson, 1949). Higher values of this inverse index indicate higher levels of diversity. In this case, i corresponds to the first releases of each tree occurring in the same year.

3.3.1.3 Maximum biomass stock (MBS) capacity models

Because stand biomass depends on site quality, development stage and forest type, the maximum biomass stock capacity (referred to here as MBS), the models developed consisted of the ratio between above- and below-ground live tree biomass (LTB) stock and site quality

per forest type. This is consistent with the findings of Kranabetter (2009), who demonstrated that ecological site classification or direct measures of stand productivity can refine estimates of the upper limits in potential carbon storage. The present work therefore aimed to represent, as far as possible, the range of site qualities for the mature plots measured, covering most of the latitudinal, longitudinal and altitudinal distribution at national scale (Figure 3.8, p. 41; Table 3.5, p. 45). This was assessed by using the SNFI data for the forest types studied.

For the model fitting process, site quality was considered the explanatory variable and was obtained from SF models fitted and considered in section 3.2 (pp. 54-61). Thus, according to the previous approach, the H_0/D_0 ratio was assessed by selecting from 1 to 20 trees per plot for a random subsample of 50 plots for each type of forest, in order to establish a minimum number of trees per plot where H_0/D_0 ratios were consistent. SNFI plots were then filtered according to this criterion, and only those plots including at least the minimum number of trees previously evaluated were selected. Regarding the response variable LTB, the dry biomass of live trees was estimated using the biomass models developed by Ruiz-Peinado et al. (2011; 2012) for Spanish softwood and hardwood tree species. These models are applied at tree level and consider h and dbh as predictors. For the other species not included in the aforementioned models (e.g. *Crataegus monogyna* Jacq., *Ilex aquifolium* L., *Betula* spp., *Sorbus* spp., *Salix* spp., etc.**)**, which were rare in the plots sampled, they were used the biomass models developed by Montero et al. (2005), which uses only dbh as the independent variable. Although very large trees, which are present in the database, were not represented in the sample trees used to fit these biomass models (specially for *A. alba* because is the less spread species), they are the most suitable equations as some of the sampling for deriving model fits were obtained in the study area. In all cases, the total LTB including aboveground biomass (stem, branches and leaves) and belowground biomass (roots) were estimated.

The MBS models were fitted by forest type using all the available data together, for mature and SNFI plots in the study area. LTB per ha was estimated for both sources of data (mature plots and SNFI) by

considering the plot design of SNFI (circular nested plot design) in order to make estimates more comparable. The quantile regression fitting methodology was applied using the modified version of the Barrodale and Roberts algorithm for l_1-regression (Koenker and d'Orey, 1987; 1994), implemented in the R package quantreg (Koenker, 2021). The equation used was a logarithmic regression equation (Eq. 3.10), whose form can adapt to scatter plots of LTB against SF for the highest values of biomass for the function domain in the SF range used, which increases constantly for the MBS. The 97.5% quantile was considered. Therefore, these regressions can be considered the upper boundaries of the maximum LTB stock (i.e. MBS) as the maximum values are represented by the SF gradient.

$$MBS = a + b \cdot \log SF \tag{3.10}$$

3.3.1.4 Assessing mature forests holding MBS

The aforementioned models fitted for the case study corresponding to mature and old-growth plots of beech, beech-fir and silver fir stands located in the Spanish Pyrenees range (see 3.1.1.4 Pyrenees mature forests, pp. 47-51) were used to estimate the proximity of each plot to the MBS in relative terms, as percentages. The degree of MBS reached was considered 100% for those plots with LTB values on the fitted curves; otherwise, the percentage of biomass reached (referred to here as relative biomass stock, $BS(\%)$) compared to the MBS was estimated as follows:

$$BS(\%) = \frac{BS_i}{MBS_{SF_i}} \cdot 100 \tag{3.11}$$

where BS_i is the biomass value of the plot i and MBS_{SF_i} the MBS of the curve for the SF corresponding to plot i.

Hence, all of the LTB stocks were comparable in relative terms, independently of the site quality conditions. In addition to the whole data set, and in order to evaluate the hypothesis that LTB does not increase after a certain degree of naturalness, the LTB stock was

specifically assessed using the gradient of the degree of naturalness obtained in the case study. To this end, both absolute (Mg ha^{-1}) and relative ($BS(\%)$) LTB stocks were compared visually to NS in scatter plots.

3.3.1.5 Assessing $BS(\%)$ for the study species at national scale

Once the hypothesis that mature forests hold maximum LTB stocks was assessed in the case study aforementioned, MBS models were fitted for the other species (maritime and Scots pines) following the same methodology. The $BS(\%)$ for all the data was then estimated, and the LTB stock reached according to MBS in mature and SNFI plots per forest type was compared by means of boxplots. Finally, these values of $BS(\%)$ were also represented in a map using colour palettes, with darker tones indicating higher degrees of $BS(\%)$, and light tones otherwise. The SNFI plot coordinates were used to detect possible managed or degraded areas in terms of $BS(\%)$.

3.4 CHARACTERIZATION OF STAND STRUCTURE

The data sets here analyzed corresponds to: (i) mature plots of Scots pine forests belonging to the Atlantic, Mediterranean and Boreal biogeographical regions (see 3.1.1.5 Mature *Pinus sylvestris* forests belonging to Atlantic, Boreal and Mediterranean biogeographical regions, pp. 52-53); and (ii) mature plots belonging to beech, beech-fir, maritime pine, Scots pine and silver fir forests (see 3.1.1.1 Spanish mature forests, pp. 40-44). In addition to species richness, which is the number of different species appearing at plot level, individual tree indices based on the nearest-neighborhood approach were used to characterize the spatial forest structure. These represented the main elements of forest spatial structure as spatial species and deadwood occurrence, spatial size differentiation and regularity of tree locations (Aguirre et al., 2003), by considering attributes related to the arrangement of tree positions, tree species or their dimensions and deadwood. All of the indices were calculated at individual tree level (reference tree),

considering the four closest neighbours, as previously described (Pommerening, 2006). All of the tree level values were then averaged at plot level in order to compare these features among biogeographical regions and forest types. These indices can take five different values at tree reference level according to the neighbourhood attributes (Table 3.13). Although plot edge correction should be applied to those reference trees with at least one of the neighbours having a distance larger than the distance between the reference tree and the plot boundary (Lilleleht et al., 2014; Pommerening and Stoyan, 2006), in this study these reference trees were excluded from the analysis, and therefore plot edge correction was not necessary.

Table 3.13. Indices based on the nearest-neighborhood approach

Index	Formula
Species mingling	$M_i = \frac{1}{k}\sum_{j=1}^{k} v_j$ where, $M_i \in [0,1]$; k is the number of nearest neighbours; i is the live reference tree; j is the neighbouring tree of the reference tree i; $v_j = \begin{cases} 1, when\ species\ j \neq species\ i \\ 0, otherwise \end{cases}$
Deadwood distribution	$D_i = \frac{1}{k}\sum_{j=1}^{k} v_j$ where, $D_i \in [0,1]$; $v_j = \begin{cases} 1, when\ nieghbour\ j\ is\ a\ dead\ tree \\ 0, otherwise \end{cases}$
Diameter differentiation	$T_i = 1 - \frac{1}{k}\sum_{j=1}^{k} \frac{\min(dbh_i, dbh_j)}{\max(dbh_i, dbh_j)}$ where, $T_i \in [0,1]$;

	$T_i = \begin{cases} \leq 0.05\ very\ even \\ 0.05\ < T_i \leq 0.15\ even \\ 0.15\ < T_i \leq 0.30\ moderately\ uneven \\ 0.30\ < T_i \leq 0.60\ uneven \\ T_i > 0.6\ very\ uneven \end{cases}$
Uniform angle	$W_i = \frac{1}{k}\sum_{j=i}^{k} v_j$ where, $W_i \in [0, 1]$; $T_i = \begin{cases} W_i \to 0\ agregated \\ W_i \to 0.5\ random \\ W_i \to 1\ regular \end{cases}$ α_i is the angle between neighbouring trees; α_0 is the standard angle $[360°/(k+1)]$; $v_j = \begin{cases} 1, when\ \alpha_i < \alpha_0 \\ 0, otherwise \end{cases}$

The indices showed in Table 3.13 can be grouped as follows:

- Spatial species mingling: this feature is measured with the homonymous *species mingling index* (M) (Gadow 1993), which can characterize the degree of homogeneity or heterogeneity in species mixture. High values indicate high spatial heterogeneity, and low values indicate the opposite.

- Spatial deadwood mingling: this is measured by means of the *deadwood distribution index* (D) (Põldveer et al., 2020), which characterizes the spatial arrangement of standing dead trees in a group of trees where the reference tree is alive. High values indicate higher degrees of spatial deadwood heterogeneity, and low values indicate the opposite.

- Spatial size differentiation: this is characterized by means of the *diameter differentiation index* (T) (Gadow, 1999), which assesses the size differences within groups of trees. In this case, low values indicate more homogeneous groups (more similar to even-aged stands), and higher values indicate more

heterogeneous groups (more similar to uneven-aged/size stands). To make this index compatible with others, the T values were grouped as in Table 3.13 according to Gadow and Hui (2002).

- Regularity of tree locations: measured with the *uniform angle index* (W) (Gadow and Hui, 2002), which characterizes the arrangement of trees, classified as regular, random and clumped, with high, intermediate and low values respectively (see Table 3.13, pp. 71-72).

In addition to the use of comparative indices, diameter distributions and $h{\sim}dbh$ relationship among biogeographical regions were also assessed for the first data set considered: mature plots of Scots pine forests belonging to the Atlantic, Mediterranean and Boreal biogeographical regions (see 3.1.1.5 Mature *Pinus sylvestris* forests belonging to Atlantic, Boreal and Mediterranean biogeographical regions, pp. 52-53). As the data were not normally distributed, the non-parametric Kruskal-Wallis test (Kruskal and Wallis, 1952) and a post hoc Dunn's multiple comparison test (Dunn, 1961) were used for comparisons, at a significance level of 0.05.

3.5 MODELLING THE STATE OF MATURITY BY TERRESTRIAL LASER SCANNING (TLS) DATA

3.5.1 Development of FORTLS: an R package for processing TLS data and estimating stand variables in forest inventories

FORTLS has been developed as an R package (R Core Team, 2021) as R is free statistical software accessible to any user interested in the tool. The initial stages of development of this package are outlined in Molina-Valero et al. (2020), although the first version of FORTLS was not available until March 2021. Currently, both the most recent stable version of the package and the most up-to-date version can be downloaded free of charge, from respectively the CRAN (https://CRAN.R-project.org/package=FORTLS) and GitHub

development (https://github.com/Molina-Valero/FORTLS/tree/devel) repositories.

The R package FORTLS has been optimized by implementing C++ code in the most demanding computing processes by means of the Rcpp package (Eddelbuettel, 2013; Eddelbuettel and Balamuta, 2018; Eddelbuettel and François, 2011) and the RcppEigen package (Bates and Eddelbuettel, 2013), enabling integration of the Eigen C++ library for specific matrix calculation. For operations with objects in spatial data classes, the raster (Hijmans, 2020), sf (Pebesma, 2018) and sp (Bivand et al., 2013; Pebesma and Bivand, 2005) packages have been used. As TLS point clouds represent large data sets, FORTLS also imports the vroom package (Hester and Wickham, 2020) for accelerating loading and saving .txt files. Other important packages have been used to generate and save interactive graphics, namely plotly (Sievert, 2020) and htmlwidgets (Vaidyanathan et al., 2020). Apart from the packages included in R base distribution and other accessory packages such as progress (Csárdi and FitzJohn, 2019), scales (Wickham and Seidel, 2020) and tidyr (Wickham, 2021), the other external R packages used for more specific functions are mentioned below, with their respective functions.

The software development explained in this doctoral thesis is mainly based on the latest stable version (1.0.6) of the FORTLS package (available in CRAN until 18/04/2022), which was based on single-scan approach. However, some of the new functionalities and metrics/variables incorporated in the most recent versions (beta), have also been included as they were needed to obtain some of the most recent results. In the following sections, all steps involved in TLS point cloud data processing with FORTLS, as well as the most relevant algorithms, are described: (i) normalization; (ii) tree detection; and (iii) estimation of metrics and variables at stand level.

3.5.1.1 Normalization

The normalization process is a necessary first step in processing point cloud data, and it is implemented in the normalize function (Table 3.14), which for some processes uses the functions

`readLAS`, `clip_circle`, `classify_ground`, `grid_terrain` and `normalize_height` included in the lidR package (Roussel et al., 2020; Roussel and Auty, 2020). Normalization involves obtaining the coordinates relative to plot centre for TLS point clouds supplied as .las or .laz files. The process includes the following steps: (i) classification of points as "ground"; (ii) generation of a digital terrain model (DTM); (iii) computation of coordinates (Cartesian, cylindrical and spherical) relative to DTM; and (iv) reduction of point cloud density.

Table 3.14. Functions included in the FORTLS package

Function (arguments)	Description
correlations(variables = c("N","G","V","d","dg","d.0","h","h.0"), method = c("pearson","spearman"), save.result=TRUE, dir.result=NULL)	Correlation between field estimates and TLS metrics
distance.sampling(id.plots=NULL, strata.attributes=NULL)	Distance sampling methods for correcting occlusion effects
estimation.plot.size(plot.parameters=list(radius.max=25, k.tree.max=50, BAF.max=4), average=FALSE, all.plot.designs=FALSE)	Assessment of consistency of metrics for simulated TLS plots
metrics.variables(distance.sampling=NULL, dir.data=NULL, save.result=TRUE, dir.result=NULL)	Computation of metrics and variables for TLS plots
normalize(x.center=NULL, y.center=NULL, max.dist=NULL, min.height=NULL, max.height=NULL, algorithm.dtm="tin", res.dtm=0.2, csf=list(cloth_resolution=0.5), id=NULL, file=NULL, dir.data=NULL, save.result=TRUE, dir.result=NULL)	Production of relative coordinates and density reduction for TLS point clouds

optimize.plot.design(variables=c("N","G","V","d","dg","d.0","h","h.0"), dir.result=NULL)	Optimization of plot design based on optimal correlations
relative.bias(variables=c("N","G","V","d","dg","d.0","h","h.0"), save.result=TRUE, dir.result=NULL)	Measurement of relative bias between field estimates and TLS metrics
simulations(tree.list.tls, distance.sampling=NULL, tree.list.field, plot.parameters=list(radius.max=25, k.tree.max=50, BAF.max=4), dir.data=NULL, save.result=TRUE, dir.result=NULL)	Computation of metrics and variables for simulated TLS and field plots
[1]**tree.detection.multi.scan**(dbh.min=7.5, dbh.max=200, ncr.threshold=0.1, tls.resolution=list()*, breaks=c(1.0,1.3,1.6), plot.attributes=NULL, save.result=TRUE, dir.result=NULL)	Tree level variables estimation from point clouds corresponding to TLS multi-scan approaches and SLAM devices.
[2]**tree.detection.single.scan**(dbh.min=7.5, dbh.max=200, ncr.threshold=0.1, tls.resolution=list()*, breaks=c(1.0,1.3,1.6), plot.attributes=NULL, save.result=TRUE, dir.result=NULL)	Tree level variables estimation from point clouds corresponding to TLS single-scan approaches.
[3]**tree.detection.several.plots**(id=NULL, file=NULL, normalize.arguments = list(max.dist=NULL, min.height=NULL, max.height=NULL, algorithm.dtm="tin", res.dtm=0.2), tree.detection.arguments = list(dbh.min=7.5, dbh.max=200, ncr.threshold=0.1, tls.resolution=list()*, breaks=c(1.0,1.3,1.6), plot.attributes = NULL), dir.data=NULL, save.result=TRUE, dir.result=NULL)	Tree level variables estimation for multiple plots

The functions and arguments are updated to the latest version FORTLS 1.2.0.

* Arguments necessary to define

[1] New function included in the latest version to process multi-scan (or similar) approaches. [2] Update of the earlier version `tree.detection`. [3] Update of the earlier version `tree.detection.multiple`.

In the initial step, points are classified as "ground" or "not ground" with the Cloth Simulation Filter (CSF) algorithm (Zhang et al., 2016). The DTM is then generated by spatial interpolation of "ground" points. Two methods are available for executing this process: (i) spatial interpolation using a k-nearest neighbour approach with inverse-distance weighting (by default); and (ii) spatial interpolation based on Delaunay triangulation. The point cloud is then normalized by subtracting the DTM created. Once the point cloud has been normalized, Cartesian (x, y, z), cylindrical (ρ -axial distance-, φ -azimuthal angle-, z -height-) and spherical (r -radial distance-, θ -polar angle-, φ -azimuthal angle-) coordinates are calculated relative to the sampling point (TLS device establishment point, or anyone defined in the arguments). Finally, the normalize function applies the PCP algorithm developed by Molina-Valero et al. (2019b) to reduce the point density in single-scan approaches (for multi-scan approaches, point density reduction will be based on random points selection) and thus produce a spatially homogeneous point cloud in which the distribution of points is proportional to the object size. During execution of the PCP, a selection probability $prob(\boldsymbol{p})$ is assigned to each cloud point $\boldsymbol{p}$ according to Eq. 3.12 (see Figure 3.15).

$$prob(\boldsymbol{p}) = \frac{r_p}{r_{max}} \tag{3.12}$$

where $r_{\boldsymbol{p}}$ is the radial distance of the point $\boldsymbol{p}$ from the sampling point, and r_{max} is the radial distance of the farthest point from the plot centre. Finally, the point is selected if the selection probability is equal to or higher than a random value generated from the uniform distribution for the interval [0, 1].

3.5.1.2 Tree detection

Tree detection represents a very important and challenging step in estimating variables of interest in TLS-assisted FIs. This is partly due to occlusions, which are much more important when working with single scans. This process of tree detection is implemented in the

`tree.detection.single.scan` function, which has been designed to detect as many trees as possible from point cloud data obtained as `normalize` function output.

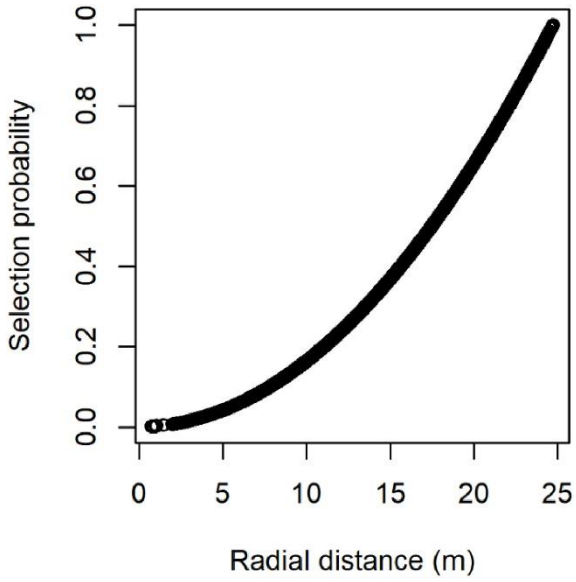

Figure 3.15. Selection probability of points corresponding to a single-scan according to the radial distance from the plot centre, implemented in the normalize function.

In the tree detection process, one or several horizontal slices from the original point cloud are extracted. Slices at heights of 1.0, 1.3 and 1.6 m ± 5 cm over the terrain (all around 1.3 m as reference section to estimate *dbh*) are considered by default in `tree.detection.single.scan`. The probability of detecting trees increases when more than one slice is considered. However, the `tree.detection.single.scan` function can also extract (if specified in the arguments) slices at other heights when trees are not identifiable at these pre-established values. Each horizontal slice is processed by algorithms that are able to (i) remove branches and foliage points, (ii) detect point clusters corresponding to potential tree sections, and (iii) classify detected point clusters as tree sections, or not, according to several tests. The tree sections detected in all horizontal

slices are then merged, and for each tree detected, the `tree.detection.single.scan` function estimates certain attributes by (i) calculating the coordinates corresponding to the centre of the tree section at breast height (1.3 m above ground level) and its horizontal distance from the plot centre; (ii) estimating the dbh, h, stem volume (v), etc.; (iii) classifying the tree as fully visible or partially occluded; and (iv) obtaining the number of points corresponding to normal section slice (1.3 m ± 5 cm) for both original and reduced point clouds. The main steps involved in the previously mentioned algorithms for detecting tree sections for each horizontal slice and for estimating metrics and variables related to the tree attributes detected are described in the following subsections and summarized in Figure 3.16.

Removing branches and foliage points

For each horizontal slice, this first step aims to remove points corresponding to fine branches and foliage (e.g. leaves and shrubs) and mainly to retain points at the stem, for which we considered local surface variation, also known as the normal change rate (NCR). This is a quantitative measure of curvature feature useful for discerning some "noisy" points (Pauly et al., 2002), with higher values representing more curved surfaces (predictably fine branches and foliage). The NCR index is estimated at point level considering a local neighbourhood, as follows. Given a fixed radius r, the set of local neighbours of a point $\boldsymbol{p}$ is denoted by $\{\boldsymbol{p}_i\}_{i\in N_{\boldsymbol{p},r}}$, where $N_{\boldsymbol{p},r}$ is the index set of all cloud points satisfying the condition that $d(\boldsymbol{p},\boldsymbol{p}_i) < r$ (where d is the Euclidean distance). The NCR for point $\boldsymbol{p}$ is then estimated by eigenanalysis of the 3 x 3 covariance matrix $\boldsymbol{C_p}$ of its local neighbourhood (Eq. 3.13).

$$\boldsymbol{C_p} = \frac{1}{N_{\boldsymbol{p},r}} \sum_{i\in N_{\boldsymbol{p},r}} (\boldsymbol{p}_i - \overline{\boldsymbol{p}})(\boldsymbol{p}_i - \overline{\boldsymbol{p}})^T \tag{3.13}$$

where $\overline{\boldsymbol{p}}$ is the centroid of the local neighbourhood of $\boldsymbol{p}$. Obtaining the eigenvalues $\{\lambda_i\}_{i=0}^{2}$ by singular value decomposition of $\boldsymbol{C_p}$ and assuming that $\lambda_0 \leq \lambda_1 \leq \lambda_2$, λ_0 describes the variation along the

normal surface, the extent to which the points deviate from the tangent assuming that $\lambda_0 \leq \lambda_1 \leq \lambda_2$, λ_0 describes the variation along the normal surface, the extent to which the points deviate from the tangent plane is estimated (Pauly et al., 2002). Hence, the NCR index for radius r at point $\boldsymbol{p}$ is defined as follows (Eq. 3.14):

$$NCR_r(\boldsymbol{p}) = \frac{\lambda_0}{\lambda_0 + \lambda_1 + \lambda_2} \tag{3.14}$$

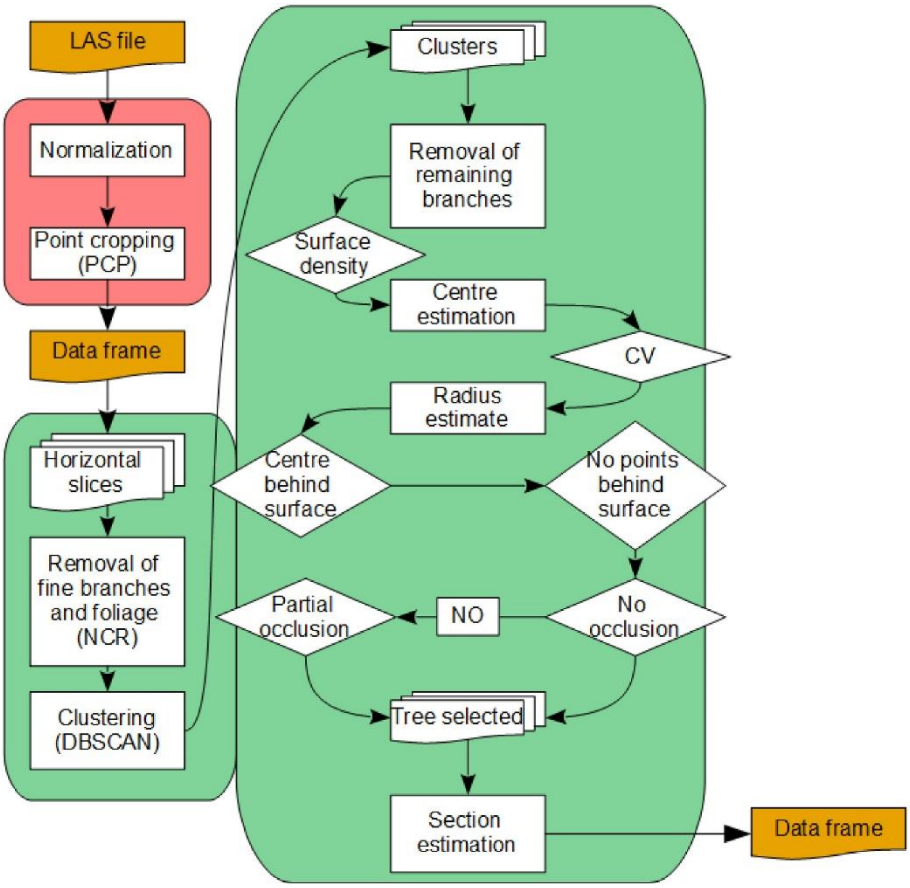

Figure 3.16. FORTLS workflow for normalization (red) and tree detection (green) processes. All of the processes included here are described in sections 3.5.1.1 Normalization and 3.5.1.2 Tree detection.

Once NCR is computed, $\boldsymbol{p}$ is retained as a stem point if the NCR value is lower than a pre-established threshold (Figure 3.17 a). In accordance with other studies, in the tree detection functions, the neighbourhood was established with a radius of 5 cm considered suitable for calculating NCR for the stem separation in forests (Ma et al., 2016; Xia et al., 2015). The threshold value of NCR used to remove branches and foliage points was established as 0.1 by default, also according to other studies in which the index has already been used with the same objective and obtaining good results (e.g. Jin et al., 2016; Zhang et al., 2019). Nevertheless, other NCR thresholds can be specified by users in the corresponding argument of the functions.

Detection of point clusters

Once branches and foliage points have been removed from the horizontal slice, the next step is to detect point clusters corresponding to potential tree sections. This process involves several steps: (i) a clustering process is first applied to the horizontal projection of Cartesian coordinates of points; (ii) points corresponding to possible branches are then removed using surface density approaches; and (iii) clusters with fewer points than expected for a full visible stem are discarded.

As mentioned above, potential tree sections are first detected through a clustering process applied to the horizontal projection of Cartesian coordinates. This clustering process is performed by the Density-Based Spatial Clustering of Applications based on the Noise (DBSCAN) method (Ester et al., 1996) and applied with the `dbscan` function in the homonymous R package dbscan (Hahsler et al., 2019). The size of the epsilon neighbourhood is established as the minimum distance between two consecutive points at the farthest distance from TLS in the respective horizontal slice, and a minimum of 5 points required in that epsilon neighbourhood. This algorithm detects as many as possible sections corresponding to trees (according to occlusion conditions), as well as other possible clusters generated by other items (branches, shrubs, etc.), and has been used in previous studies of TLS

with the same objective (Ferrara et al., 2018; Molina-Valero et al., 2019b).

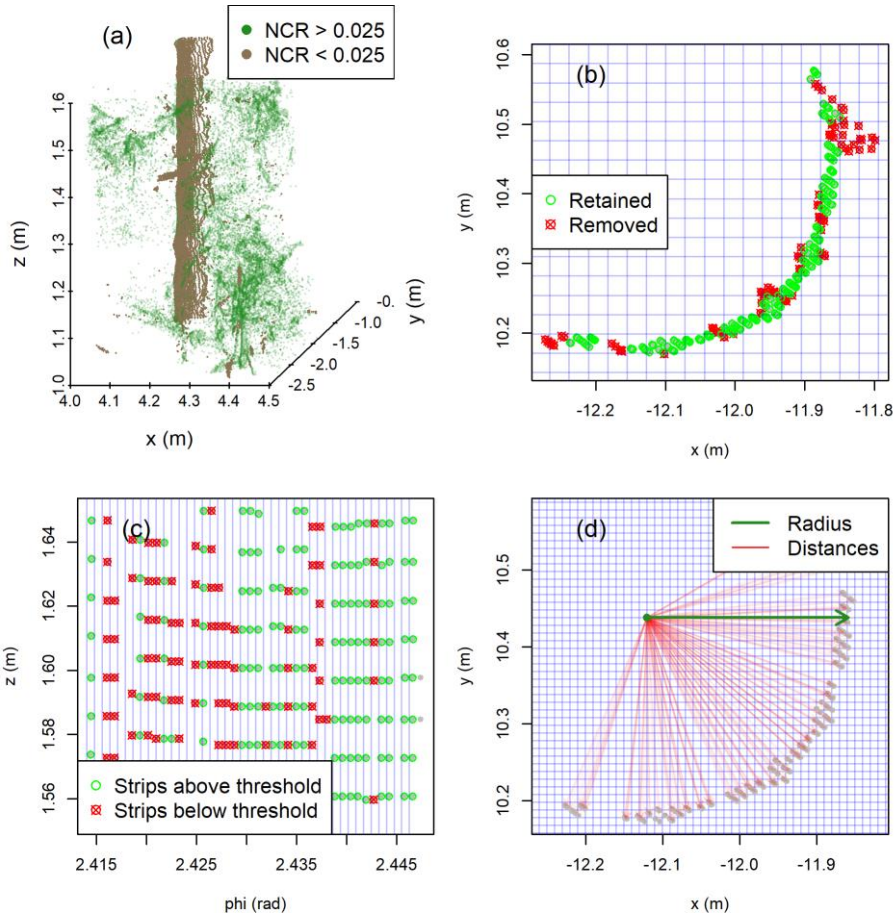

Figure 3.17. Detection of potential tree sections implemented in the `tree.detection.single.scan` function: (a) points corresponding to branches and foliage (green) are removed by applying the NCR index for a threshold of 0.025; (b) refinement of extracted stem points where those points included in grid cells with fewer points than the median (red points) are removed; (c) estimation of the approximate number of points ($\boldsymbol{n}$) that each strip must contain if the section corresponds to a tree fully viewed by TLS, the green points represent those cells containing more or the same number of points as $\boldsymbol{n}$; and (d) estimated location of tree section centre (green point) and radius calculated (green wide arrow) as the average of all distances (red fine arrows) between cluster points and the grid intersection allocated as the tree centre.

For refining extracted stem points, we used a similar approach to that proposed by Zhang et al. (2019) in order to remove any branches remaining in the clusters, based on the principle that stems should generate more points than other parts of the tree (due to the fractal-size distribution according to West et al. (1999)); in addition, these points should have a predominantly vertical distribution. Thus, if the point cloud is vertically projected and rasterized in a grid, cells over stems usually include more points than those located over branches and foliage. Each cluster is thus rasterized on the horizontal plane (x and y Cartesian coordinates) with an adapted grid step size of twice the distance between two consecutive points at mean cluster distance from TLS, and those points included in cells with fewer points than the median value of the number of points per cell will be removed (Figure 3.17 b).

At this point of the process, several tests were used to distinguish those clusters corresponding to tree sections. Each cluster was first projected vertically with cylindrical coordinates (φ, z) and divided into regular strips bound by vertical scan resolution (α_v) (Figure 3.17 c). As stems completely visibly from TLS must generate the maximum possible number of points according to scan resolution and distance from the TLS instrument, we estimated the approximate number of points that each strip must include if the section corresponds to a fully visible tree. As normalized coordinates are projected on a horizontal plane, the slope effect was first corrected to calculate the vertical resolution (Δv) in coordinate z at cluster real distance from TLS (m), as follows (Eq. 3.15):

$$\Delta v = 2 \times \frac{tan\ (\alpha_v/2)}{\bar{r}_{cluster} \Big/ \cos(\overline{slope})} \tag{3.15}$$

where α_v is the vertical scan resolution (rad), $\bar{r}_{cluster}$ is the mean radial distance in spherical coordinates from TLS to cluster (m), and $\overline{slope}$ is the mean slope of cluster according to DTM (rad). The number of points n that each strip must contain in fully visibility conditions is then computed as follows (Eq. 3.16):

$$n = \frac{\Delta z}{\Delta v} \tag{3.16}$$

where Δz is the slice thickness (m), and Δv is the previously defined vertical resolution (Eq. 3.15). Only those clusters with at least one strip including the number of points n that every strip must contain in fully visibility conditions were selected.

Once clusters have fulfilled all of the previous checks, the next step involves obtaining the centre of the potential tree section. With this aim, regular square grids of 1 cm were overlapped on each cluster selected. The tree section centre was then considered as the intersection grid point where the variance of the distances between this intersection and all the cluster points reaches the lowest value (Figure 3.17 d), considered to occur when the coefficient of variation of distances is less than 0.1, otherwise the cluster is disregarded. Finally, the radius of the tree section was computed as the average of all the distances between the estimated centre and remaining cluster points at the moment of algorithm processing.

Cluster classification

This step consists of checking multiple geometric features and indices to verify which clusters finally correspond to tree sections. Most criteria used are based on those determined by Molina-Valero et al. (2019b), and they were applied to each cluster. The first test involves checking whether the centre is located behind the cluster points relative to TLS (on the occluded part). This is considered fulfilled when at least 95% of the cluster points have a lower cylindrical coordinate ρ (hence closer than sampling point) than the tree centre. The second test consists of checking for the absence of points behind the tree surface, which is considered true when at least 95% of the distances between cluster points and the tree centre are greater than half of the estimated radius. This can be visually checked by means of a distance histogram (Figure 3.18 a). The similarity between the cluster shape and the circumference arc is then assessed, checking those extreme points in cylindrical coordinate ρ are farther from TLS than central points (Figure 3.18 b).

This is possible when trees are largely visible from TLS, but otherwise will not be possible due to partial occlusions. In such cases, the clusters were checked to determine whether they form a smaller arc of a circle (Figure 3.18 c). For this purpose, the Pearson coefficient correlation was calculated for φ values in increasing order and with the correlative numbering (Figure 3.18 d). Those clusters with values below 0.975 were removed.

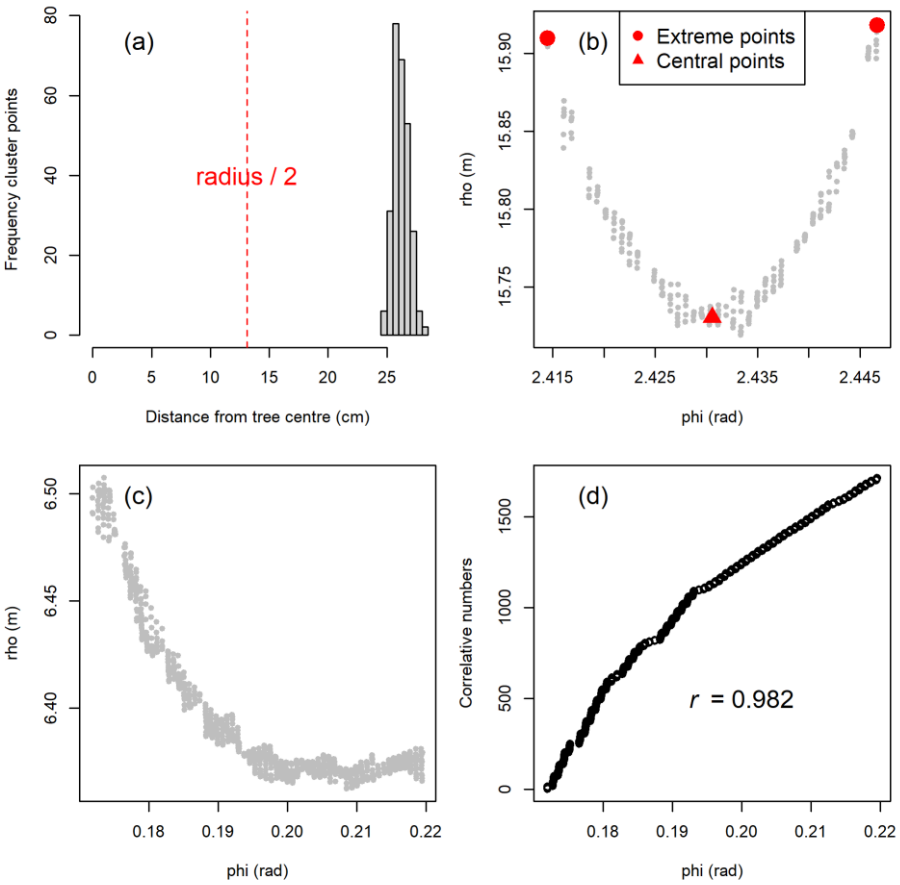

Figure 3.18. Representation of some of the tests implemented in the `tree.detection.single.scan` function to distinguish those clusters corresponding to tree sections: (a) histogram of distances between cluster points and estimated tree centre to check for the absence of points behind the tree surface; (b) mean coordinates of points included in first and last coordinate percentiles (red

points) and in the middle cluster φ ± TLS angle aperture (red triangle); (c) tree partially occluded; and (d) assessment of the Pearson's correlation ($\boldsymbol{r}$) between values in increasing order and their corresponding correlative numbers.

Estimating tree attributes

When several sections are identified at different heights, those corresponding to the same trees are joined using the DBSCAN algorithm on the horizontal projection, and some tree attributes are obtained: coordinates of normal section centre and horizontal distance from plot centre, estimated *dbh*, h, and v, indicator of partial occlusion and number of points corresponding to normal section slice for original and reduced point clouds.

When trees are exclusively detected at 1.3 m, the *dbh* is estimated directly as twice the radius estimated at this height (h_{sec}). Conversely, when trees are detected from other section(s), a linear taper equation is fitted with radius as the response variable and section height as the explanatory variable (Eq. 3.17):

$$radius = \beta_0 + \beta_1 \cdot h_{sec} \tag{3.17}$$

The radius at 1.3 m is then predicted from each different section, as follows (Eq. 18):

$$\widehat{radius}_{1.3} = radius_i + \hat{\beta}_1 \cdot (1.3 - h_{sec_i}) \tag{3.18}$$

where $radius_i$ and h_{sec_i} are the estimated radius and the height corresponding to section i, and $\hat{\beta}_1$ is the slope parameter fitted in the linear regression (Eq. 3.17). Hence, dbh is computed as twice the averaged predicted radius.

Finally, the number of points ($n.pts$) corresponding to a normal section slice (± 5 cm) in the original point cloud is computed and also estimated for each detected tree *j* by using the dbh values previously computed as follows (Eq. 3.19):

$$n.pts.est_j = dbh_j \frac{\sum_{i \in I} \frac{n.pts_i}{dbh_i}}{\#I} \tag{3.19}$$

where the index set I corresponds to all detected trees fully visible at 1.3 m, and $\#I$ is the number of trees fully visible at 1.3 m. The number of points and the estimated number of points for the point cloud reduced are obtained in a similar way.

The most recent versions of FORTLS also include estimation of h, as the 99.9th percentile of z coordinate of points delimited by Voronoi polygons formed by trees detected; and v, by modelling stem profile as a paraboloid (Eq. 3.24).

3.5.1.3 Computing TLS metrics and variables at stand level

Once normalization and tree detection processes for each point cloud are completed, TLS metrics and variables can be estimated at stand level for three different plot designs, all of which are included in the `metrics.variables` function. These plot designs are circular fixed area, k-tree and angle-count (Bitterlich, 1948) plots (Figure 3.19), each of which is defined by a unique design parameter (radius, k and basal area factor, respectively) that must be specified in the function arguments.

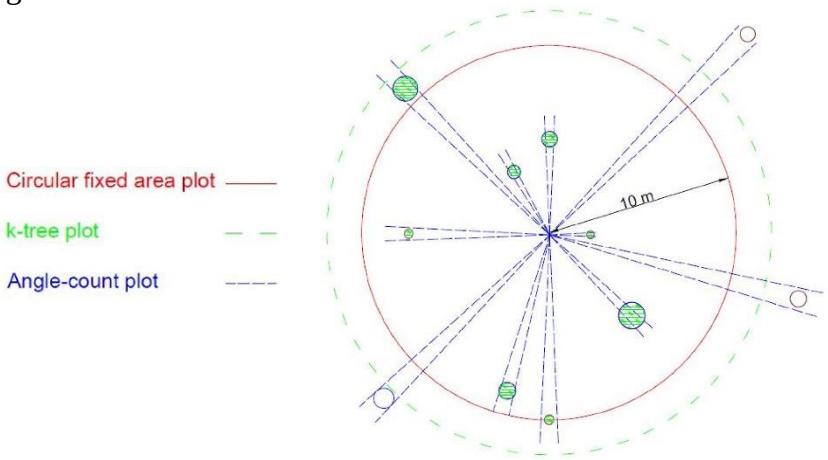

Figure 3.19. Example of the three plot designs considered in FORTLS for the same sampling point. Circular fixed plot of 10 m radius (red) includes 7 trees; k-tree plot for k = 8 (green) yields a larger radius than circular fixed area; and angle-count plot (blue) with a particular basal area factor (BAF) includes 7 trees.

Stand level metrics

Metrics are computed using points directly from normalized point cloud in a similar way as in the FUSION/LDV software for aerial LiDAR data analysis and visualization (McGaughey, 2009). These are mainly descriptive statistics of the points coordinates such as percentiles, means or variance, among others. All of the metrics are listed and described in Table 3.15:

Table 3.15. Metrics included in FORTLS

Metric	Description
`n.pts`, `n.pts.est`, `n.pts.red`, `n.pts.red.est`	Number of points and estimated number of points corresponding to normal sections slices (1.3 ± 0.05 m) of trees in the original point cloud (`n.pts` and `n.pts.est`, respectively); and number of points and estimated number of points corresponding to normal sections slices of trees in the reduced point cloud (`n.pts.red` and `n.pts.red.est`, respectively).
`P01`, …, `P99`	Height percentiles (m) derived from z coordinates of TLS point clouds relative to ground level.
`mean.arit.z/rho/r`, `mean.qua.z/rho/r*`, `mean.geom.z/rho/r*`, `mean.harm.z/rho/r*`, `median.arit.z/rho/r*`, `mode.arit.z/rho/r`	Central tendency statistics of the coordinates z, ρ (rho, horizontal distance) and r (radial distance or distance to TLS): arithmetic, quadratic, geometric and harmonic means; median; and mode, respectively.
`var.z/rho/r`, `sd.z/rho/r`, `cv.z/rho/r*`, `d.z/rho/r*`, `id.z/rho/r*`, `max.z/rho/r`, `min.z/rho/r`,	Dispersion statistics of the coordinates z, ρ and r: variance, standard deviation, coefficient of variation, range, interquartile range, maximum, and minimum, respectively.
`kurt.z/rho/r`, `skw.z/rho/r`	Kurtosis and skewness of the coordinates z, ρ and r, respectively.
`L2.z/rho/r*`, `L3.z/rho/r*`, `L4.z/rho/r*`, `L3.mu.z/rho/r*`, `L4.mu.z/rho/r*`, `L-CV.z/rho/r*`, `median.a.dz/rho/r*`, `mode.a.d.z/rho/r*`	Descriptive statistics of the of the coordinates z, ρ and r: L-moments of order 2, 3 and 4, ratio of L1 and L2 moments, third and fourth central moments, median of the absolute deviations from the overall median; and mode of the absolute deviations from the overall mode, respectively.

`PA.mean.z/rho/r`, `PA.2m`	Percentage of points above arithmetic mean (coordinates z, ρ and r) and 2 m (z).
`weibull.b.z/rho/r`, `weibull.c.z/rho/r`	Scale and shape parameters, respectively, for Weibull distribution fitted for the coordinates z, ρ and r.
`CRR.z/rho/r`*	Canopy relief ratio (arithmetic mean / maximum) for the coordinates z, ρ and r.
`P.max`, `PA.2m.max`, `PB.2m.max`*	Ratios of the number of observed laser returns and the maximum number of laser returns; number of observed laser returns above 2 m in height and the maximum number of laser returns above 2 m in height; number of observed laser returns below 2 m in height and the maximum number of laser returns below 2 m in height, respectively.

* New metrics included in the most recent versions of FORTLS

Stand level variables

The variables represent estimates based on tree attributes detected from TLS point cloud data, further aggregated at stand level, and finally expanded to per unit area (hectare, ha). The following variables are available:

- Apparent stand density (N.tls, trees ha^{-1}), which is estimated for trees detected in a similar procedure to that used in conventional inventories for circular fixed area and k-tree plots (Eq. 3.20) and angle-count plots (Eq. 3.21):

$$N.tls = \frac{10000}{\pi R^2} \cdot n \tag{3.20}$$

$$N.tls = \sum_{i=1}^{n} \frac{\text{BAF}}{g_i} \tag{3.21}$$

where R is the plot radius (m), n is the number of trees detected in the corresponding plot design, BAF is the basal area factor (m^2 ha^{-1}), and g_i is the basal area of the tree i (m^2).

- Apparent stand basal area (G.tls, m^2 ha^{-1}), which is estimated from trees detected in a similar procedure to that used in conventional inventories for circular fixed area and k-tree plots (Eq. 3.22) and angle-count plots (Eq. 3.23):

$$G.tls = \frac{10000}{\pi R^2} \sum_{i=1}^{n} g_i \tag{3.22}$$

$$G.tls = \text{BAF} \cdot n \tag{3.23}$$

with notation as before.

- Apparent stand stem volume (V.tls, m^3 ha^{-1}), which is estimated for trees detected by modelling the stem profile as a paraboloid and calculating the volumes of revolution for fixed area and k-tree plots (Eq. 3.24) and angle-count plots (Eq. 3.25):

$$V.tls = \frac{10000}{\pi R^2} \sum_{i=1}^{n} \pi \cdot \frac{h_{P_{99.9}i}^2}{2} \cdot \frac{\left({dbh_i}/{2}\right)^2}{h_{P_{99.9_i}} - 1.3} \tag{3.24}$$

$$V.tls = \sum_{i=1}^{n} \frac{\text{BAF}}{g_i} \cdot \pi \cdot \frac{h_{P_{99.9}i}^2}{2} \cdot \frac{\left({dbh_i}/{2}\right)^2}{h_{P_{99.9_i}} - 1.3} \tag{3.25}$$

where $h_{P_{99.9}i}$ and dbh_i are the 99.9th percentile of z coordinate of points delimited by Voronoi polygons formed by trees detected (m) (i.e. estimates of h) and dbh (m) for tree i, respectively.

- Mean and dominant dbh (cm), which are estimated for arithmetic, quadratic, geometric and harmonic means. In the case of dominant diameters, only the n largest trees per ha (according to dbh) are considered. Although it can be specified in the arguments, the 100 largest trees per ha are considered by default.

- Mean and dominant h (m), which are estimated for arithmetic, quadratic, geometric and harmonic means. For dominant heights, only the n largest trees per ha (according to dbh) are considered. Although the number of trees can be specified in the arguments, the 100 largest trees per ha are considered by default.

In the previous calculations, for the k-tree design, the plot radius R is defined as the mean of horizontal distances of trees k and k+1 (Kleinn and Vilčko, 2006).

Dealing with occlusions

All FORTLS functions used for estimating stand variables also include correction of occlusions approaches. In the case of angle-count plots, occlusion corrections are based on gap probability attenuation with distance from TLS depending on a Poisson distribution. In the case of circular fixed area and k-tree plots, distance sampling methods and shadowing effect correction are considered. In order to obtain occlusion corrections based on distance sampling methods, the `distance.sampling` function must first be executed and the values obtained must be incorporated as an argument for functions which compute stand variables, whereas the other corrections are computed by default. A brief description of the occlusion corrections implemented is provided below.

1. Poisson attenuation model

This method has been used in measurements with TLS (Strahler et al., 2008; Lovell et al., 2011) and optical (Montes et al., 2019) instruments to reduce the device-related bias in the angle-count-based approach. This is based on geometric gap probability (P_{gap}), which decreases exponentially following a Poisson distribution (Eq. 3.26):

$$P_{gap}(\lambda, D_E, R) = e^{(-\lambda D_E R)} \quad (3.26)$$

where λ is the number of trees per m^2, D_E is the effective dbh and R is the horizontal distance to the farthest tree. The corrected stand density (N.pam, trees ha^{-1}) for angle-count plots is then obtained as follows (Eq. 3.27):

$$N.pam = N.tls/F(\lambda D_E R) \tag{3.27}$$

where F is a function defined as $F(t) = \frac{2}{t^2}\left(1 - e^{-t}(1+t)\right)$, with $t = \frac{\lambda D_E D}{2\sqrt{BAF}}$ and $D_E \approx \overline{dbh}\left(1 + C^2_{v_{dbh}}\right)^2$: see Strahler et al. (2008) and Lovell et al. (2011) for further details. Similarly, corrected stand basal area (G.pam, m^2 ha^{-1}) and volume (V.pam, m^3 ha^{-1}) are computed.

2. Point transect sampling

This approach is based on the point transects method from distance sampling methods (Buckland et al., 2001). These methods use detection functions $g(r, \theta)$ with variable r (distance from sampling point) and parameter θ, which describe how the probability of detection decreases as distance increases. We used Half-Normal (Eq. 3.28) and Hazard-Rate (Eq. 3.29) functions as these have been successfully used in measurements with TLS (Astrup et al., 2014) and optical (Montes et al., 2019) devices:

$$g(r, \theta) = e^{\left(\frac{-r^2}{2\sigma^2}\right)} \tag{3.28}$$

$$g(r, \theta) = 1 - e^{-\left(\frac{r}{\sigma}\right)^{-b}} \tag{3.29}$$

Parameter θ includes the shape (b) (only in the Hazard-Rate function) and the scale (σ), which was also expanded with dbh as a covariate into an exponential function (Eq. 3.30) according to Ducey et al. (2013) and Astrup et al. (2014):

$$\sigma = \alpha_0 e^{(\alpha_1 dbh)} \tag{3.30}$$

Parameter θ is estimated by maximum likelihood (Clark, 2016; Miller and Thomas, 2015; Marques and Buckland, 2003) with data left-truncated at 1 m according to Astrup et al. (2014). The fitting process is carried out by means of the `ds` function included in the R package Distance (Miller et al., 2019). Once the parameters of detection functions are estimated, the probability of tree detection (P_i) is estimated with Eq. 3.31, which is implemented in the expansion factor of circular fixed area and k-tree plots as in Eq. 3.32:

$$P_i = \frac{2}{R^2}\int_0^R rg(r,\hat{\theta}) \tag{3.31}$$

$$EF = \sum_{i=1}^{n} \frac{10000}{(P_i \pi R^2)} \tag{3.32}$$

where R is the plot radius (m), and EF is the expansion factor. Multiplying N.tls by these EFs yields corrected stand densities (N.hn, N.hr, N.hn.cov, N.hr.cov, trees ha^{-1}). Similarly, corrected stand basal area (G.hn, G.hr, G.hn.cov, G.hr.cov, m^2 ha^{-1}) and volume (V.hn, V.hr, V.hn.cov, V.hr.cov, m^3 ha^{-1}) are computed.

All of these estimates are obtained by previously executing the `distance.sampling` function, which returns P_i and also values of parameter estimates of detection functions and the corresponding Akaike information criterion (AIC) of these fits.

3. Correcting the shadowing effect

This approach was developed by Seidel and Ammer (2014) for single-scan mode. These authors used the approach to correct the shadowing effect, which generates shaded unsampled areas (Eq. 3.33), according to the shaded area percentage related to the total area sampled:

$$A_{shadow} = \left[\frac{(\pi R^2) - (\pi r_{tree}^2)}{360°}\left(\frac{dbh}{r_{tree}}\right)\right] - \left[\frac{\pi\left(dbh/2\right)^2}{2}\right] \quad (3.33)$$

where R is the radius of the plot (m), and r_{tree} is the distance between the TLS instrument and the tree centre. This method is implemented for circular fixed area and k-tree plots and yields a plot specific correction factor defined by the unsampled area percentage ($\sum_{i=1}^{n} A_{shadow_i} / (\pi R^2)$; where A_{shadow_i} represent the shadow area for tree i) per plot (e.g. 3%, thus the specific correction factor would be 1.03) was used to compute corrected estimates for stand density (N.sh, trees ha^{-1}), basal area (G.sh, m^2 ha^{-1}) and volume (V.sh, m^3 ha^{-1}). All of the aforementioned variables are summarized in Table 3.16.

Table 3.16. Variables available in FORTLS

Variables	Description
`N*` / `N.tls`	Stand density (N, trees ha^{-1})
`G*` / `G.tls`	Stand basal area (G, m^2 ha^{-1})
`V*` / `V.tls`	Stand volume (V, m^3 ha^{-1})
`N.hn**`, `N.hr**`, `N.hn.cov**`, `N.hr.cov**`, `G.hn**`, `G.hr**`, `G.hn.cov**`, `G.hr.cov**`, `V.hn**`, `V.hr**`, `V.hn.cov**`, `V.hr.cov**`	N, G and V with occlusion corrections based on distance sampling methodologies
`N.sh**`, `G.sh**`, `V.sh**`	N, G and V with correction of the shadowing effect
`N.pam***`, `G.pam***`, `V.pam***`	N, G and V with occlusion correction based on a Poisson attenuation model
`d*`, `dg*`, `dgeom*`, `dharm*` / `d.tls`, `dg.tls`, `dgeom.tls`, `dharm.tls`	Stand mean dbh (cm), using arithmetic ($\bar{d}$), quadratic (d_g), geometric, and harmonic means, respectively.
`h*`, `hg*`, `hgeom*`, `hharm*` / `h.tls`, `hg.tls`, `hgeom.tls`, `hharm.tls`	Stand mean height (h, m), using arithmetic, quadratic, geometric, and harmonic means, respectively.
`d.0*`, `dg.0*`, `dgeom.0*`, `dharm.0*` / `d.0.tls`, `dg.0.tls`, `dgeom.0.tls`, `dharm.0.tls`	Stand dominant mean $dbh(D_0, \text{cm})$, using arithmetic, quadratic, geometric, and harmonic means, respectively.

`h.0*`, `hg.0*`, `hgeom.0*`, `hharm.0*` / `h.0.tls`, `hg.0.tls`, `hgeom.0.tls`, `hharm.0.tls`	Stand dominant mean h (H_0,m), using arithmetic, quadratic, geometric, and harmonic means, respectively.

* Variables estimated from field measurement data

** Variables only estimated for circular fixed area and k-tree plot design

*** Variables only estimated for angle-count plot design

Optimizing the plot design

Two different approaches can be used to find the best possible plot design depending on whether validation field data are available or not. The approaches are represented in the FORTLS workflow (Figure 3.20) and detailed below.

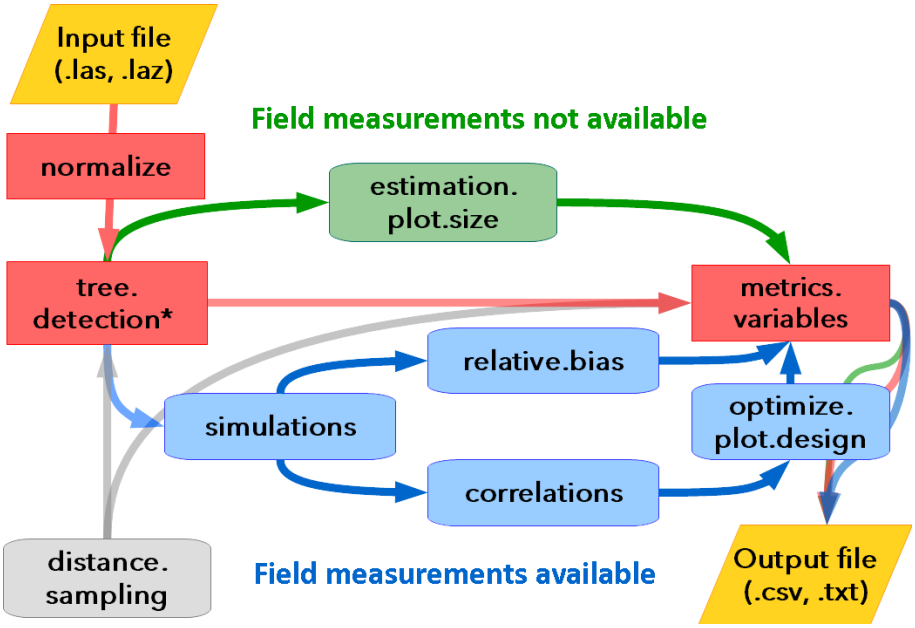

Figure 3.20. Workflow of FORTLS, representing tree detection, estimation of metrics and variables related to forest attributes (red) with no field data available (green) and with field data available (blue); optional functions (grey), and initial input files and final output files (orange).

* This step is composed of several functions (see Table 3.14, pp. 75-76) depending on the origin of the data (single or multiple TLS scans, SLAM devices, etc.).

Analysis of estimation stability

The function `estimation.plot.size` estimates both apparent tree density (N.tls, trees ha^{-1}) and apparent basal area (G.tls, $m^2\ ha^{-1}$) for all of the aforementioned plot designs. In the case of circular fixed area design, concentric plots, in regular increments of 0.1 m radius (by default) to the maximum radius specified in the arguments, are simulated for computing N.tls and G.tls. As a result, line charts of estimates based on plot size are obtained. For k-tree design, all possible plots are defined by $k = \{1, 2, \dots, n\}$, where 1 is the nearest tree and n the farthest tree considered in the argument `k.max` (or the farthest detected/existing tree if the argument is not specified). Finally, for the angle-count design, variables will be estimated for regular BAF increments comprised from 0.1 to the `BAF.max` specified in the arguments. All of these line charts were inspired by Figure 3 in Brunner and Gizachew (2014).

Validation with field measurements

For cases when field data are available, a set of interconnected functions was designed to assess the performance of processed TLS data relative to the corresponding field data: `simulations`, `relative.bias` and `correlations`.

The field data necessary to conduct the analysis described hereinafter are tree dimensions (dbh and h) and horizontal distance relative to the TLS scanner. In the latest versions, other variables, such as v and tree biomass (w), estimated by the users can be included (optional). Analysis of the performance is based on comparisons between these two data sources for the different plot designs and sizes. The first function is `simulations`, which computes (in a similar way as `estimation.plot.size`) all of the previously mentioned metrics and variables for TLS data (see section 3.5.1.3 Computing TLS metrics and variables at stand level, pp. 87-97) and the corresponding variables based on field data (see Table 3.16, pp. 94-95).

The `relative.bias` function was designed for direct comparison of TLS-based and field based (or any other reference source

of data) estimates or measurements, by means of relative bias (Eq. 3.33).

$$Bias(\%) = 100 \cdot \frac{1}{n}\sum_{i=1}^{n}\frac{(\hat{y}_{FORTLS_i} - \hat{y}_{FIELD_i})}{\hat{y}_{FIELD_i}} \quad (3.33)$$

where $\hat{y}_{FIELD_i}$ and $\hat{y}_{FORTLS_i}$ are the values of the field estimate and its TLS counterpart, respectively, corresponding to plot i for $i = 1, \ldots, n$. Relative bias is assessed for all the simulations to find the best possible plot design for each variable of interest.

For possible approaches other than direct estimation of variables, the package has functions that assess the best possible plot designs according to the correlations between variable estimates from field data and metrics/variables derived from TLS. The `correlations` function computes both Pearson and Spearman correlation coefficients for common set of plots and all simulations and plot designs considered. For each variable of interest, this function produces the optimum correlations for all simulations. The `optimize.plot.design` function then produces a graphical representation of the strongest correlations for all variables of interest.

3.5.2 Assessment of FORTLS for estimating stand level variables in mature forests

The data analyzed corresponded to a subset of 135 out 143 plots corresponding to mature forests (see 3.1.1.1. Spanish mature forests). The plots comprised beech (40 plots), beech-fir (11 plots), silver fir (12 plots), maritime pine (32 plots) and Scots pine (40 plots) forests. Beech-fir and silver fir forests were analyzed together (23 plots). All of those plots were measured by TLS single scans located at the plot centre and analyzed with the R package FORTLS (Molina-Valero et al., 2022) mainly based on stand level forest variables. In this respect, the main stand level forest variables N, G, $\bar{d}$ and $\bar{h}$ were estimated following the package workflow (Figure 3.20, p. 95). Plot designs corresponded to circular fixed area (radius = 15 m), k-tree (k = 10) and angle-count (BAF = 1) plots. Variables estimated on the basis of field data and TLS

single scans processed with FORTLS were then compared according to relative bias (Eq. 3.33, p. 97), relative $RMSE$ (Eq. 3.34) and the Pearson's correlation coefficient (r). For those variables expanded by surface unit (N and G), both the direct estimates and the occlusion correction methodologies based on correcting the shadowing effect (Seidel and Ammer, 2014) and Poisson attenuation model (Strahler et al., 2008; Lovell et al., 2011) -in the case of angle-count plots- were used. This corrections were selected instead of other methods implemented in FORTLS for the following reasons: (i) they performs better in most cases (Montes et al., 2019); (ii) they are more suitable because they can be used with only one plot, unlike distance sampling methodologies which may need several plots to fit the detection functions (Astrup et al., 2014); and (iii) mixing plots belonging to different forest structures may be a wrong approach in distance sampling methods as detection probability based on distance depends directly on forest structure.

$$RMSE(\%) = 100 \cdot \frac{1}{n} \sqrt{\sum_{i=1}^{n} \frac{(\hat{y}_{FORTLS_i} - \hat{y}_{FIELD_i})^2}{\hat{y}_{FIELD_i}}} \qquad (3.34)$$

where $\hat{y}_{FIELD_i}$ and $\hat{y}_{FORTLS_i}$ are the values of the field estimate and its TLS counterpart, respectively, corresponding to plot i for $i = 1, \dots, n$.

The point clouds were first obtained as input data, as .las files from .fls files (format generated by FARO devices) corresponding to TLS single scans, by means of the SCENE software, which is specifically designed for FARO laser scanners. Following the FORTLS workflow, and with the aforementioned plot design, only those functions related to tree detection (`tree.detection.several.plots`) and estimation of variables (`metrics.variables`) were applied. Point clouds were supplied as .las files and normalized the in `tree.detection.several.plots` function leaving the default values of the arguments. The outputs were data frames with the list of

trees detected and some of their attributes, and the reduced normalized point clouds were saved in the working directory as .txt files. Finally, the `metrics.variables` function was run using the aforementioned plot parameter designs. This process generated a .csv file with a set of variables and metrics for all the plots at stand level, from which the target variables N, G, $\bar{d}$ and $\bar{h}$ were selected.

3.5.3 Exploring the assessment of biomass and maturity with TLS single-scan approach

The potential of the TLS single-scan approach to assess biomass and maturity was explored by means of predictive models. For this purpose, multiple linear regression (MLR), multivariate adaptive regression splines (MARS) (Friedman, 1991) and classification and regression trees (CART) (Breiman et al., 1984) methods were used. This allowed assessment of the relationship between estimates based on field data (as response variables) and TLS metrics and variables (as explanatory variables). For response variables, the live tree biomass (LTB) was assessed as previously explained, and the degree of maturity was assessed in terms of naturalness and biomass stock according to the naturalness score (NS) (Di Fillipo et al., 2017) and relative biomass stock ($BS(\%)$) indices. As the objective was to explore several options for assessing biomass and maturity from TLS single-scan data, the three plot designs included in FORTLS (circular fixed area, k-tree and angle-count plots) were considered. In addition, for each plot design, several plot sizes were defined according to regular size increments, from radius 7.5 to 25 m, 1 to 25 trees, and 0.1 to 4 BAF, with increments of 0.1 m, 1 k and 0.1 BAF, respectively. For this purpose, the `simulations` function, which yields all of the estimates of the variables (for field and TLS data) and metrics (only for TLS data) across continuous regular increments in plot sizes, was used. This was useful for exploring different plot sizes and thus finding the most suitable plot design for estimating LTB, NS and $BS(\%)$ from TLS data. Previously mentioned models (MLR, MARS and CART) were fitted for all estimates obtained with the simulations function, with LTB, NS and $BS(\%)$ as response variables, and metrics and variables generated

using FORTLS as explanatory variables. In the case of MLR, explanatory variables were selected using stepwise forward regression method and entering predictors based on p values (less than 0.1) until there were no longer any variables to enter. This was executed with the function `ols_step_forward_p` included in the R package olsrr (Aravind, 2020). Regarding the MARS, regression models were built according to techniques described in Friedman (1991; 1993) by using the `earth` function in the homonymous R package earth (Milborrow, 2021). CART models were fitted using the `rpart` function in the homonymous R package rpart (Therneau and Atkinson, 2022). Finally, the R^2 values (Eq. 3.35) obtained for each fit were plotted to explore the behaviour of the different models through different plot designs and sizes, in order to select the best-performing models.

$$R^2 = 1 - \frac{\sum_{i=1}^{n}(Y_i - \hat{Y}_i)^2}{\sum_{i=1}^{n}(Y_i - \bar{Y})^2} \tag{3.35}$$

Finally, the most influential explanatory variables included in the selected models for LTB, NS and $BS(\%)$ were analyzed. This was done by grouping the selected explanatory variables by type (N, G, V, d and h) and grouping metrics based on the coordinates involved (z, rho and r) (Table 3.17). Star plots were constructed to determine the most important groups of explanatory variables included in the models.

Table 3.17. Groups of explanatory variables considered in the analysis

Group	Explanatory variables
N	`N.tls, N.hn, N.hr, N.hn.cov, N.hr.cov, N.sh, N.pam`
G	`G.tls, G.hn, G.hr, G.hn.cov, G.hr.cov, G.sh, G.pam`
V	`V.tls, V.hn, V.hr, V.hn.cov, V.hr.cov, V.sh, V.pam`
d	`d.tls, dg.tls, dgeom.tls, dharm.tls, d.0, dg.0, dgeom.0, dharm.0, d.0.tls, dg.0.tls, dgeom.0.tls, dharm.0.tls`
h	`h.tls, hg.tls, hgeom.tls, hharm.tls, h.0, hg.0, hgeom.0, hharm.0, h.0.tls, hg.0.tls, hgeom.0.tls, hharm.0.tls`

n	n.pts, n.pts.est, n.pts.red, n.pts.red.est
z	P01, …, P99, mean.arit.z, mean.qua.z, mean.geom.z, mean.harm.z, median.arit.z, mode.arit.z, var.z, sd.z, cv.z, d.z, id.z, max.z, min.z, kurt.z, skw.z, L1.z, L2.z, L3.z, L4.z, L-CV.z, median.a.d.z, mode.a.d.z, PA.mean.z, PA.2m, weibull.b.z, weibull.c.z, CRR.z, P.max, PA.2m.max, PB.2m.max
rho	mean.arit.z, mean.qua.rho, mean.geom.rho, mean.harm.rho, median.arit.rho, var.rho, sd.rho, cv.rho, d.rho, id.rho, max.rho, min.rho, kurt.rho, skw.rho, L1.rho, L2.rho, L3.rho, L4.rho, L-CV.rho, median.a.d.rho, mode.a.d.rho, PA.mean.rho, weibull.b.rho, weibull.c.rho, CRR.rho
r	mean.arit.r, mean.qua.r, mean.geom.r, mean.harm.r, median.arit.r, mode.arit.r, var.r, sd.r, cv.r, d.r, id.r, max.r, min.r, kurt.r, skw.r, L1.r, L2.r, L3.r, L4.r, L-CV.r, median.a.d.r, mode.a.d.r, PA.mean.r, weibull.b.r, weibull.c.r, CRR.r

Metrics and variables are described in Table 3.15 (pp. 88-89) and Table 3.16 (pp. 94-95).

4. RESULTS AND DISCUSSION

4 RESULTS AND DISCUSSION

4.1 SITE FORM: AN INDICATOR OF SITE QUALITY IN UNEVEN-AGED STANDS

4.1.1 Assessing site form performance in even-aged *P. radiata* stands

4.1.1.1 SI and SF dynamic equations

A reduced Hossfeld IV model with $b_1 = 0$ was used in this study. The model coincides with M6 in Wang et al. (2007) and model 11 in Cieszewski (2002). The parameter estimates provided by both GADA-derived dynamic equations were significant at the 5% level (Table 4.1). The R^2_{adj} and $RMSE$ values were 0.988 and 0.634 m for SI, and 0.986 and 0.687 m for SF. Visual comparison of the fitted curves overlaid on the trajectories of the observed dominant heights (H_0) (Figure 4.1) confirmed the good performance of both models.

Table 4.1. Parameter estimates and goodness-of-fit statistics for SI and SF dynamic equations.

Modelled variable	Parameter		p-value	R^2_{adj}	$RMSE$ (m)
	b_1	0.00			
SI	b_2	8059.00	$2 \cdot 10^{-16}$	0.988	0.634
	b_3	1.62	$2 \cdot 10^{-16}$		
	b_1	0.00			
SF	b_2	83199.00	$2 \cdot 10^{-16}$	0.986	0.687
	b_3	1.61	$2 \cdot 10^{-16}$		

The changes in H_0 with dominant dbh (D_0) (SF curves) were modelled with similar accuracy as the changes in H_0 over time (SI

curves) in the case study. The goodness-of-fit statistics for the *SF* models were superior to those obtained by Beltran et al. (2016) for even-aged mature stands of *Nothofagus alpine* (Poepp. & Endl.) Oerst. and *Nothofagus obliqua* (Mirb.) Oerst. in temperate forest sites in northwest Patagonia (Argentina). The asymptotic H_0 values for all of the *SF* curves were not within the range of observed D_0. Nevertheless, the H_0 asymptotes for the *SI* curves shown in Figure 4.1 seem realistic (30 to 40 m) according to the observed maximum height growth for *P. radiata* in northwest Spain (Diéguez-Aranda et al., 2005). In both models, higher *SI* and *SF* values produced steeper curves, which is a desirable characteristic of site equations (Cieszewski, 2002).

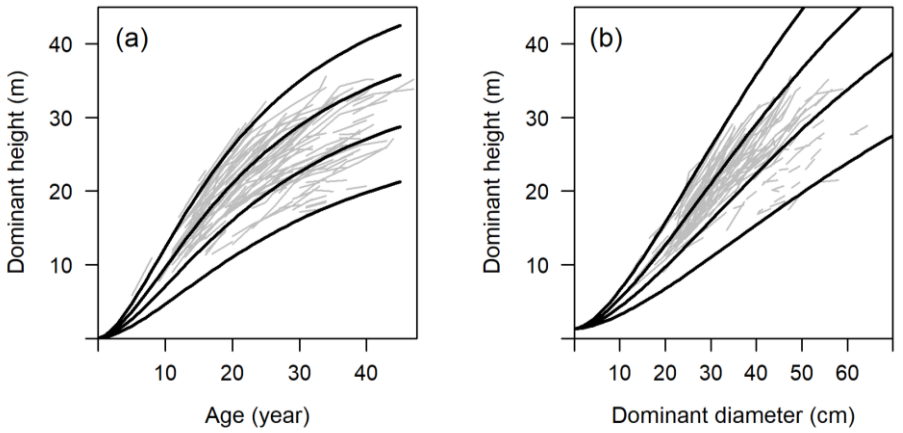

Figure 4.1. (a) *SI* curves and (b) *SF* curves for dominant heights (H_0) of 11, 16, 21 and 26 m at a reference age of 20 years and at a reference dominant *dbh* ($D_{0_{ref}}$) of 30 cm, respectively, overlaid on the observed data.

Although the fitted *SF* model residuals did not display heteroscedasticity, as is required of parametric models, they were not normally distributed (Figure 4.2). In this respect, heavier tails are observed in the Q-Q plot than in normal distributions, which means that more overestimates and underestimates will occur than expected in a normal distribution.

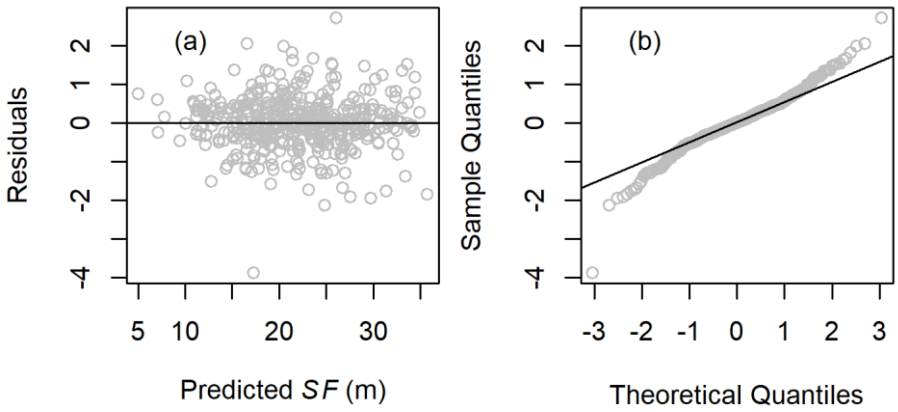

Figure 4.2. (a) Plot of residuals against fitted values for the site form (SF) model and (b) normal Q-Q plot for SF model residuals.

In selecting the base D_0, a value of 30 cm was found to be superior for predicting H_0 at other values of D_0 (Figure 4.3), because it provides a good compromise between the $RE\%$ (about 1%) and the number of observations. Additionally, this value is quite similar to the D_0 for the study stands at age 20 years (t_0, i.e. the reference age of the SI curves). Therefore, a reference D_0 ($D_{0_{ref}}$) of 30 cm was used to obtain the family of SF curves shown in Figure 4.1.

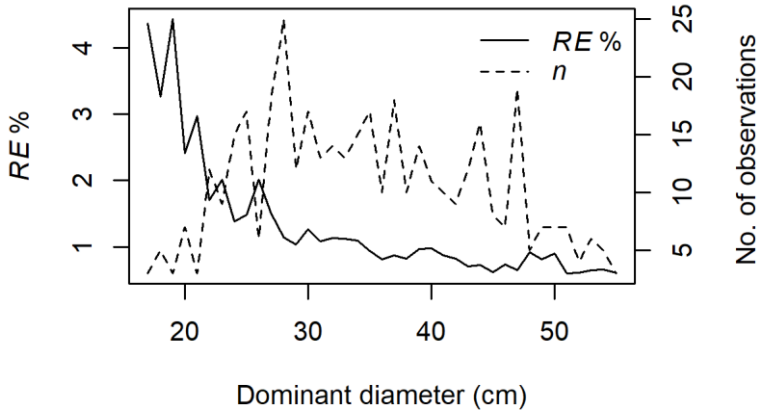

Figure 4.3. Relative error ($RE\%$) in dominant height (H_0) prediction related to choice of reference dominant dbh ($D_{0_{ref}}$).

4.1.1.2 Comparative performance of *SI* and *SF* as site quality estimators

The standardized values of *SI* and *SF* were positively correlated ($r = 0.66$; p-value < 0.05). In addition, the error bars for both variables showed similar uncertainties (Figure 4.4). In very few cases, and mainly for extreme values of *SI* and *SF*, the variability in *SF* prediction was larger than the variability in *SI* prediction. Although *SI* has proven to be more stable than *SF* (a higher proportion of plots with lower estimation errors), *SF* also yielded satisfactory results. Considering that the projection period contemplated (a maximum of 15 years) was almost half the usual rotation age for the species in northwest Spain (Castedo-Dorado et al., 2007), it can be assumed that the first criterion suggested by Vanclay and Henry (1988) (reproducibility and consistency over time) was also achieved by *SF*. Moreover, analysis of the standard deviations in *SI* and *SF* estimations for each plot showed that the uncertainties associated with both methods were usually similar. This indicates alike uncertainty in both indices when predicting site quality for different stand development stages in the same plot.

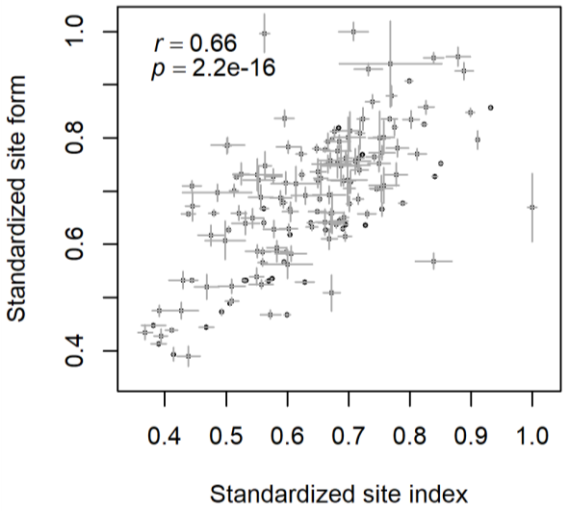

Figure 4.4. Relationship between the standardized *SI* and *SF* predictions for each plot (dots). Error bars (grey) represent the standard deviations of the predictions. ***r*** is the Pearson correlation coefficient and ***p*** is the associated p-value.

Regarding the influence of stand density, as expected, the stand density index (SDI) was not significantly correlated with either SI ($r = 0.13$, $p = 0.08$) or SF ($r = 0.024$, $p = 0.62$; Figure 4.5). This suggests that SF may be a consistent indicator of site quality in *P. radiata* across different management regimes. Thus, the second criterion was fulfilled by both indices (although a weaker correlation with SDI was obtained in the case of SF). This result was not surprising, as it is generally accepted that H_0 is not greatly affected by stand density or thinning treatments, which do not impact dominant trees (Clutter et al., 1983, p. 65), as in the stands under study.

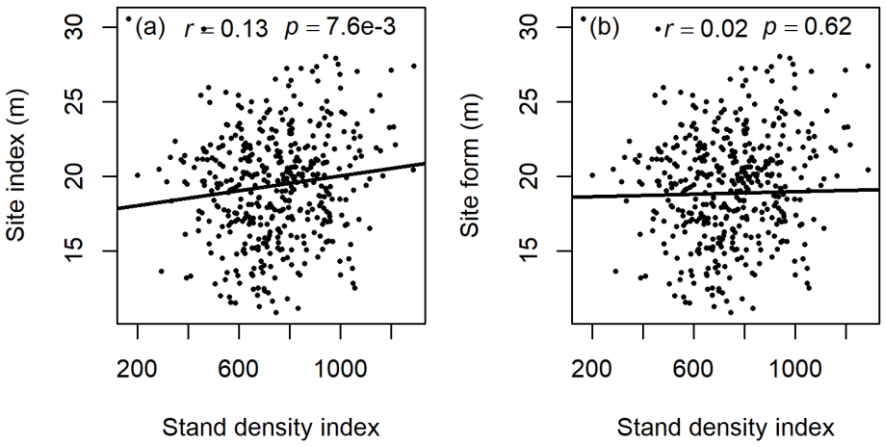

Figure 4.5. Scatter plots of the predicted (a) SI and (b) SF against stand density index (SDI) for each re-measurement of all the plots. The black line illustrates the linear regression between the two variables. r is the Pearson correlation coefficient and p is the associated p-value.

The predicted values of SI and SF were positively and significantly correlated with the maximum mean annual volume increment (MAI) observed for the 78 selected plots (Figure 4.6). SI was more closely correlated with this surrogate of site quality ($r = 0.89$) than SF ($r = 0.70$). The correlation between the maximum observed MAI and SI was slightly higher than for SF, although it was high for both indices, emphasizing that both are related to the productive potential of

the site. Similar results were obtained by Fu et al. (2018a) for the correlations between annual volume increment and *SI* or *SF* in uneven-aged stands of Mongolian oak (*Quercus mongolica* Fisch.) and Korean larch (*Larix olgensis* Henry.).

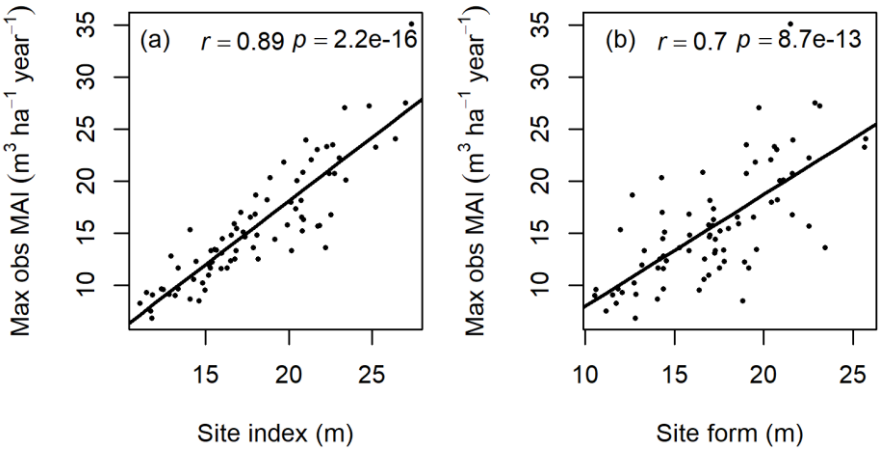

Figure 4.6. Scatter plots of maximum *MAI* (m³ year⁻¹ ha⁻¹) against (a) *SI* and (b) *SF*. The black line illustrates the linear regression between the two variables. ***r*** is the Pearson correlation coefficient and ***p*** is the associated p-value.

The $d_g/\bar{h}$ ratio was negatively and more strongly correlated with *SF* (r = -0.88; p-value < 0.05) than with *SI* (r = -0.62; p-value < 0.05) (Figure 4.7). This result may have been expected *a priori* because like *SF*, stand taper is calculated by an allometric relationship between diameters and height variables. Thus, the assumption that stand taper decreases as site quality increases was fulfilled by both *SI* and *SF*. Therefore, the present findings show that this assumption generally holds true, with increasing site quality leading to increased H_0 for a given D_0. This assumption was more certain for *SF*, which was more strongly correlated with stand taper. This negative correlation may also have been expected *a priori* because for the same reference D_0, higher values of *SF* represent higher values of H_0. It also confirms previous findings for uneven-aged stands (Fu et al., 2018a; Larson, 1963) but

contradicts other findings of no correlation between stand taper and *SI* (Wang, 1998), or a strong positive correlation (Buda and Wang, 2006).

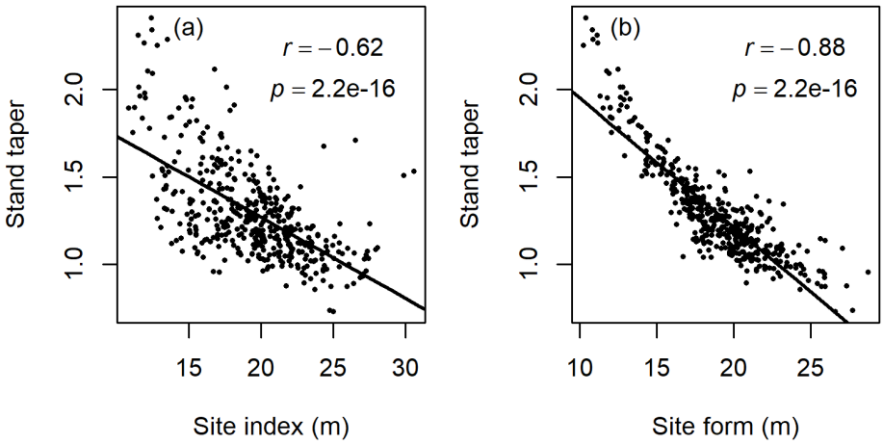

Figure 4.7. Scatter plot of stand taper (d_g/H_0) against (a) SI and (b) SF. The black line represents the linear regression between the two variables. r is the Pearson correlation coefficient and p is the associated p-value.

4.1.2 Site form model fitted for the study species

The Hosffeld-II model with b as fixed parameter, polymorphism and a single asymptote was selected as the best model for predicting SF in silver fir and beech-fir forests, as Moreno-Fernández et al. (2018) found for most of the fitted models. All of the estimated parameters were significant (Table 4.2), and the family of SF curves performed well for both types of forests, as indicated by the scatter plots (Figure 4.8). In this respect, polymorphism has been considered a desirable feature in SF curves, as h and dbh can have different growth trajectories (Fu et al., 2018b). Some references regarding polymorphic SF curves can be found in Reinhart et al. (1982; 1983), for western larch (*Larix occidentalis* Nutt.), including pure, mixed and old-growth forests (especially strong polymorphism in the latter case), and in more recent studies by Duan et al. (2018) and Fu et al. (2018b), for uneven-aged pure forests of spruce (*Picea asperata* Mast.), Korean larch, Mongolian

oak and white birch (*Betula platyphylla* Suk.). Nonetheless, polymorphism also depends on the base model and the curve fitting approach (Clutter et al., 1983).

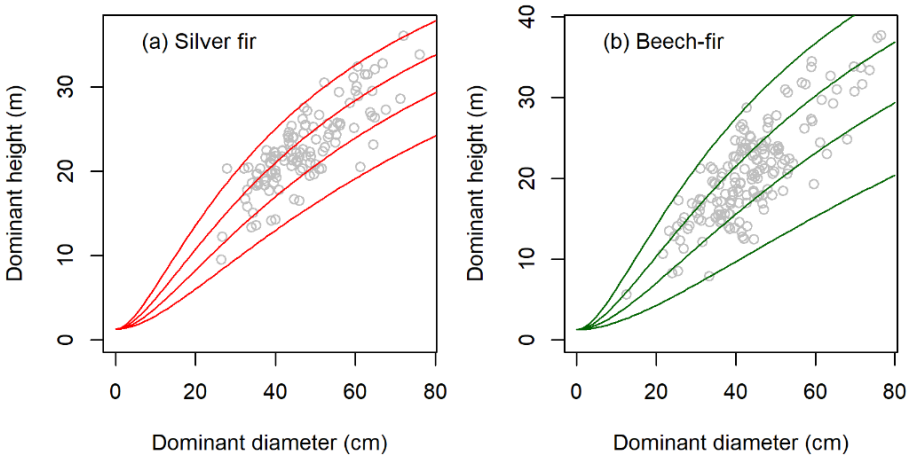

Figure 4.8. Site form (SF) curves for (a) silver fir forests (red lines) and (b) beech-fir forests (green lines). The grey circles represent the plots belonging to the Spanish National Forest Inventory (SNFI) and mature (FORESCHANGE, 2016) stands for these types of forests.

The goodness-of-fit statistics obtained for the SF models indicated similar accuracy, in terms of R^2_{adj} and $RMSE$, to that obtained by Beltran et al. (2016) for even-aged temperate forests of *Nothofagus alpine* and *Nothofagus obliqua* located in mature stands in northwest Patagonia (Argentina). These researchers also used the guide curve method with temporary plots, thus making their study one of the most suitable for comparison regarding the methodology. They observed that the best performance was obtained by fitting a common model for both species, probably due to the higher number of plots involved in the fitting (237 temporary plots) together with similarities in biometric features. In the present study, we did not consider combining both types of forest in the same models because of their different natural dynamics. Comparing our findings with those regarding other methodologies, we obtained similar or even higher accuracy in terms of $RMSE$ compared to the SF model fitted by Ahmadi et al. (2017) for uneven-aged mixed

stands of oriental beech (*Fagus oriental* Lipsky). However, these researchers fitted SF for the $h{\sim}dbh$ relationship, rather than $H_0{\sim}D_0$, obtained from temporary plots and using a modified version of the guide curve methodology developed by Edminster et al. (1991). Conversely, considering studies with permanent plots, our goodness-of-fit statistics indicated lower accuracy than obtained for two natural uneven-aged forests of Korean larch, Mongolian oak, spruce and white birch in northeast China (Duan et al., 2018; Fu et al., 2018a). However, in these studies the best models were fitted by the conventional Algebraic Difference Approach (ADA) (Baley and Clutter, 1974) combined with nonlinear mixed-effects approach and including dummy variables for specific sites. These methods are usually more accurate because the random effects of sample plots are significant (Adame et al., 2008; Calama and Montero, 2004).

Table 4.2. Site form (SF) models, goodness-of-fit statistics and parameters.

Forest type	Goodness-of-fit		Parameters		Equation
	R^2_{adj}	$RMSE$	Estimated	p-value	
Silver fir	0.67	2.70	b = 0.126	2 10^{-16}	$SF = 1.3 + \frac{D_{0\,ref}^2}{\left[\frac{D_0}{\sqrt{H_0 - 1.3}} + b \cdot (D_{0\,ref} - D_0)\right]^2}$
Beech-fir	0.65	3.52	b = 0.113	2 10^{-16}	$SF = 1.3 + \frac{D_{0\,ref}^2}{\left[\frac{D_0}{\sqrt{H_0 - 1.3}} + b \cdot (D_{0\,ref} - D_0)\right]^2}$

R^2_{adj} = adjusted coefficient of determination; $RMSE$ = root mean square error; D_0 = stand dominant dbh; $D_{0_{ref}}$ = reference stand dominant dbh; H_0 = stand dominant height.

The H_0/D_0 ratio, used to select plots that were sufficiently dense for correct estimation of SF, followed approximately parallel and/or proportional trajectories, with few crossing lines from the 10 trees (Figure 4.9). This was more evident for silver fir plots, due to the pure stand composition, than for beech-fir plots, in which the percentage of both dominant species can vary widely among plots, thus particularly affecting H_0/D_0. This analysis was useful for establishing 10 trees as

the reference threshold for selecting the SNFI plots, which is a necessary requirement for fitting *SF* family curves, as D_0 supports an increase in H_0 proportional to site quality (Stout and Shumway, 1982). In these plots, the set of 10 trees also represents a minimum density of 50 trees ha^{-1}, close to the 60 trees ha^{-1} considered in Beltran et al. (2016) as the minimum number of trees required to maintain the H_0 estimates constant.

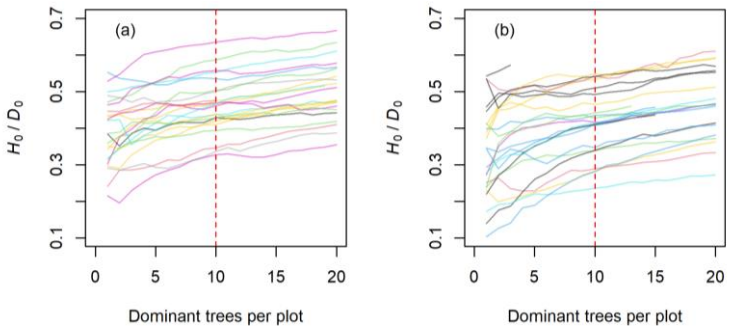

Figure 4.9. H_0/D_0 ratio for 1 to 20 trees considering both mature and Spanish National Inventory (SNFI) plots for (a) silver fir forests and (b) beech-fir forests.

According to base D_0 for estimating *SF*, 40 cm represented the best possible $D_{0\,ref}$ in terms of $RE\%$ and number of observations (Figure 4.10). This method, which was also applied in the previous section to estimate the $D_{0\,ref}$ in *P. radiata SF* models, differed from other methods based on a previously defined base age, which is used in $D_0 \sim age$ models to estimate $D_{0\,ref}$ (Fu et al., 2018a).

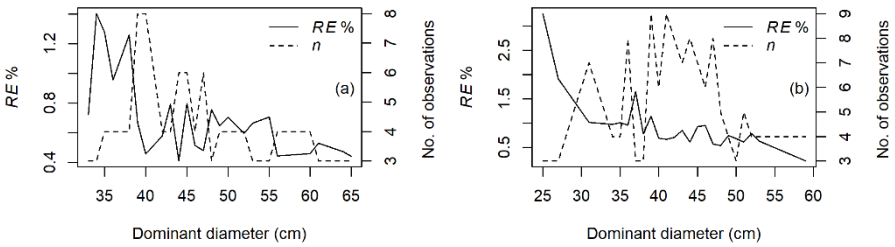

Figure 4.10. Relative error ($RE\%$) in dominant height (H_0) prediction related to choice of reference dominant diameter ($D_{0\,ref}$) for (a) silver fir forests and (b) beech-fir forests.

The fitted model residuals did not exhibit heteroscedasticity (Figure 4.11) and fulfilled the assumption of normal distribution, with p-values of 0.31 and 0.48 in the Shapiro-Wilk test for silver fir and beech-fir models respectively. In addition to the significant results of the Shapiro-Wilk test, the Q-Q plots for beech-fir were slightly skewed to the right, indicating some overestimation in this case. Overall, these results show that there were no significant overestimates or underestimates of *SF* in either case, and therefore both can be considered suitable models. These findings are important as previous studies have also shown no tendency for heteroscedasticity (Duan et al., 2018; Fu et al., 2018a), although different model fit approaches were used.

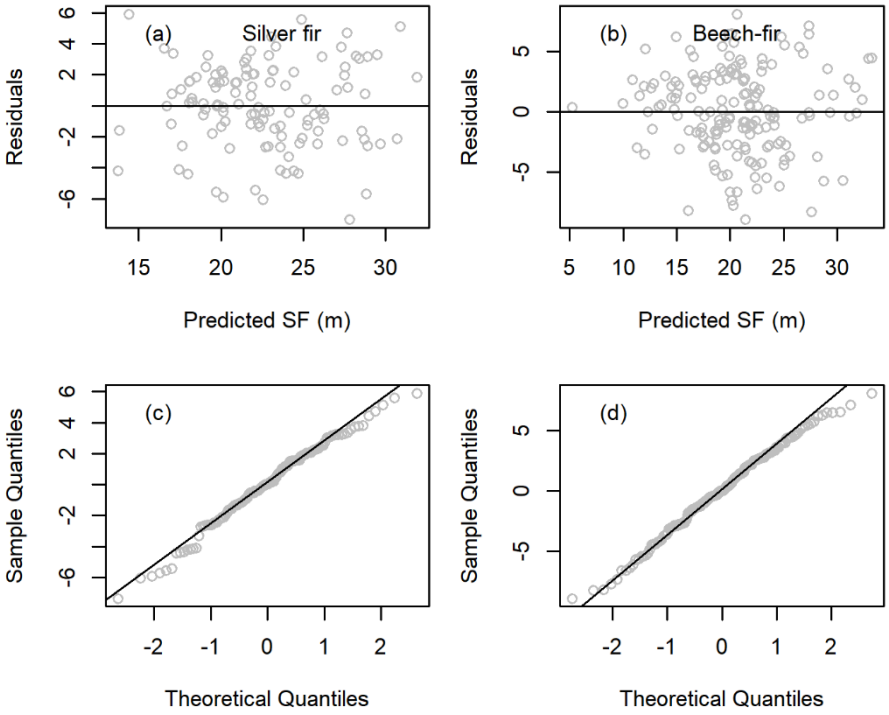

Figure 4.11. Residuals against fitted values for (a) silver fir and (b) beech-fir models; and normal Q-Q plot for residuals for (c) silver fir and (d) beech-fir models.

D_0 was not strongly correlated with SDI (Figure 4.12 a and b), indicating that this variable is not greatly influenced by stand density for the range of conditions considered here. This is a desirable feature for use of D_0 as a reference variable in site quality estimation, as it should be consistent and not dependent on density within a wide range in forests under natural conditions (Bakuzis, 1969; Beltran et al., 2016), thus supporting the hypothesis that diameter growth of dominant trees is not greatly affected by stand density conditions (Huang and Titus, 1993). However, this was more evident for silver fir than beech-fir plots, probably due to the mixed species stand conditions. Another desirable property is the observed independence of stand taper of dominant trees from stand density, which proves the assumption that stand density does not greatly affect the $h{\sim}dbh$ relationship of the dominant and codominant trees in uneven-aged or mixed species stands, above a certain lower density limit (Clutter et al., 1983; Stout and Shumway, 1982). In this respect, stand taper of dominant trees (D_0/H_0) and SDI were not correlated (Figure 4.12 c and d), indicating that the effect of stand density on D_0/H_0 may be negligible for dominant and codominant trees. These findings are consistent with those of previous studies, which reported even lower correlations, but in which the plots were divided into different age classes (Duan et al., 2017; Fu et al., 2018a). Finally, stand taper ($d_g/\bar{h}$) and SDI were negatively correlated (Figure 4.12 e and f), thus fulfilling the assumption that decreasing taper is associated with increasing site productivity (Huang and Titus, 1993; Larson, 1963).

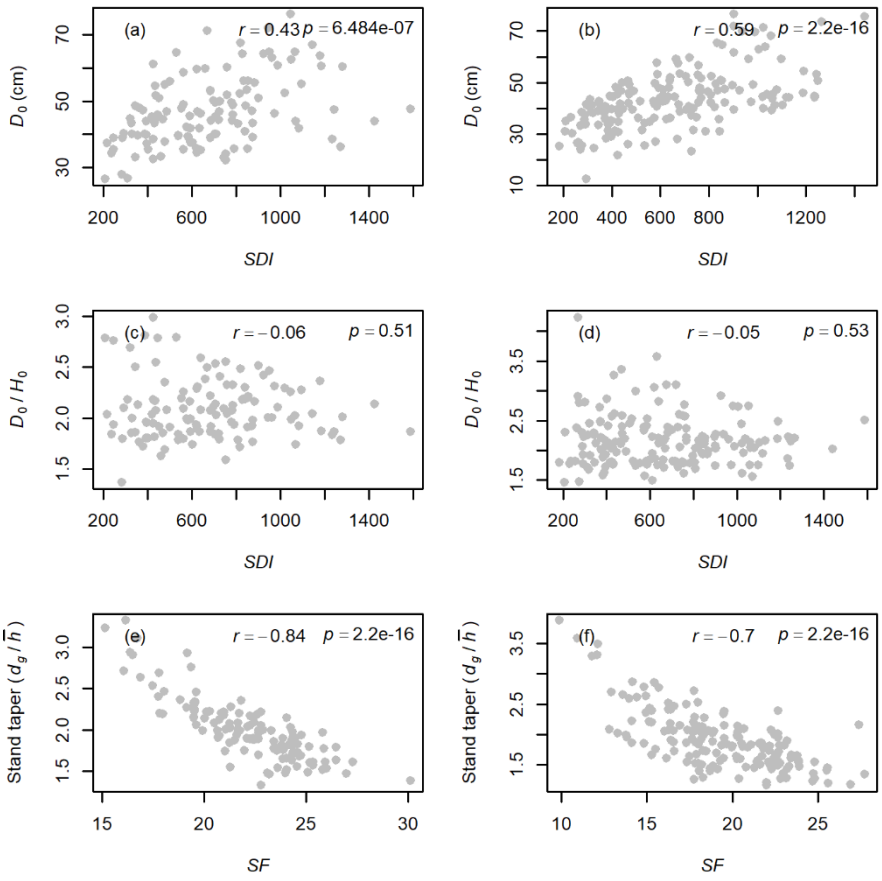

Figure 4.12. Relationships between (i) mean dominant *dbh* (D_0) and stand density index (SDI) for (a) silver fir and (b) beech-fir plots, (ii) stand taper of dominant trees (D_0/H_0) and SDI for (c) silver fir and (d) beech-fir plots, and (iii) stand taper ($d_g/\bar{h}$) and SDI for (e) silver fir and (f) beech-fir plots. All plots correspond to the Spanish National Forest Inventory (SNFI) and mature stands (FORESCHANGE, 2016).

4.1.3 Suitability of site form as an indicator of site quality

Although *SI* has traditionally been considered the reference site quality index for even-aged monocultures in general (Burkhart and Tomé, 2012, p. 131), *SF* also performed well as an estimator of site quality in even-aged *P. radiata* stands according to the findings of this

research (see 4.1.1 Assessing SF performance). Moreover, SF has the main advantage of not requiring age information, but only H_0 and D_0 values, which can be directly derived from field data generally obtained in conventional field inventories. SF is therefore suitable for estimating site quality from existing National Forest Inventory (NFI) data in most countries, where stand age is not generally recorded. In addition, as estimation of forest potential was included in the "Forest Principles" for sustainable forest management in the Earth Summit (UNCED, 1992), SF may be an inexpensive operational estimator, being useful for both designing silvicultural guidelines regarding timber yield at stand level (Pretzsch et al., 2008), and for large scale forest policy decision-making, as in REDD+ projects (Pérez-Cruzado et al., 2015). An example of large-scale use of SF is reported Aguirre et al. (2022) and Moreno-Fernández et al. (2018), who observed that countrywide estimations of SF from NFI were consistent with species autoecology.

However, SF has scarcely been used in the last decades, and recent studies have mainly concerned uneven-aged stands (e.g. Adeyemi, 2016; Ahmadi et al., 2017; Moreno-Fernández et al., 2018). Nevertheless, this may be considered significant as there was just one report of its use between 1995 and 2016 (Herrera-Fernández et al., 2004). Therefore, the most recent findings (Molina-Valero et al., 2019a) contribute to demonstrating the usefulness of SF as a reliable estimator of site quality in pure even-aged stands, which has also been suggested by Beltran et al. (2016). The performance of SF observed in Molina-Valero et al. (2019a) as an indicator of site quality may thus represent a cornerstone for renewed interest in the use of SF for management of even-aged stands on a large scale, where the lack of information on stand age usually leads to the use of more complex methodological solutions (e.g. Arias-Rodil et al., 2015). This was a conclusion of the IUFRO-supported conference "New Frontiers in Forecasting Forests", held in Stellenbosch (South Africa) in September 2018, where Drew (2021) remarked the plausibility of SF as a site quality index, being the inherent potential of a site to support forest growth an essential component of the modelling system. Further research is therefore needed in order to evaluate the effect of past density management on SF predictions.

The research reported in this thesis provides the basis for understanding the performance of SF as a site productivity indicator, as well as new SF models, different from those developed by Moreno-Fernández et al. (2018), for other forest types at national scale. In addition, the forest types for which SF was fitted (*European mountainous beech forests* for beech-fir dominated communities and *Mountainous Silver fir forests*) are similar to the sessile oak-European beech forests and pre-Alpine silver fir-European beech forest types, which were used by Bončina et al. (2021) to fit SF models. This line of research has recently received attention from both the scientific community and end-users, consistent with the recent publication of Aguirre et al. (2022), in which SF models and maps are produced for 24 forest species at national level.

4.2 ESTIMATION OF DEGRADATION INTENSITY IN TERMS OF MAXIMUM BIOMASS STOCK BASED ON NATIONAL FOREST INVENTORY DATA

4.2.1 Assessing live tree biomass stocks at mature stages

4.2.1.1 Growth patterns and disturbance

In both the silver fir and beech-fir stands under study, the basal area increment (BAI, cm^2 time $unit^{-1}$) was highest (ca. 50 cm^2 yr^{-1}) during the 1970-80s, whereas in beech stands the BAI was highest (ca. 25 cm^2 yr^{-1}) in the 1960s (Figure 4.13). Individual tree growth has decreased steadily since the 1970s in some of the silver fir (e.g. Ballibierna -BA-, Lierde -LI- and Bujaruelo -BU-) and beech-fir stands (only Selva de Oza site, SO) and in all of the beech stands (Betato -BE- and Oza, OZ).

Regarding the structural complexity, the structures of both beech-fir and silver fir stands were approximately uneven-aged, as the diameter distribution was a reverse J shape, especially in Aztaparreta (AZ) (Figures 4.14 a and b). By contrast, the structure of the pure beech stands was even-sized, with a normally shaped diameter distribution (Figure 4.14 c).

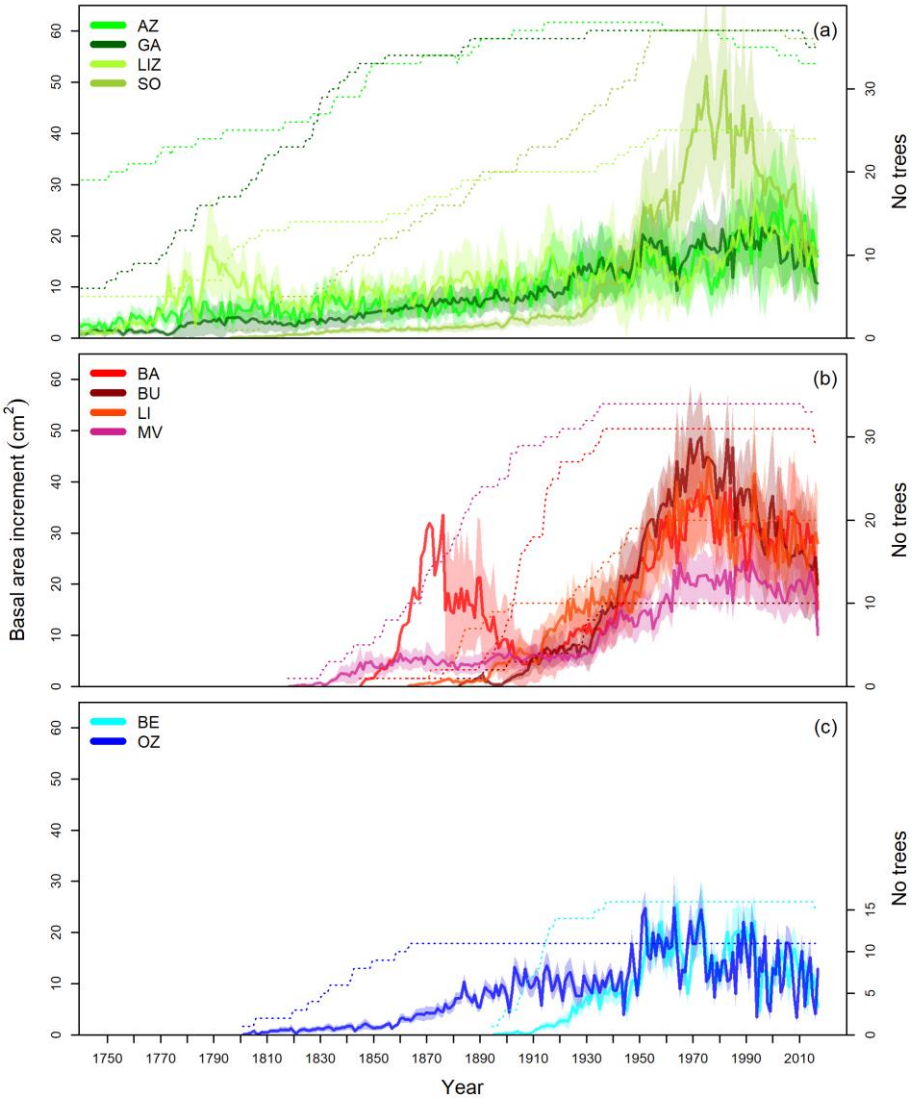

Figure 4.13. Basal area increment (*BAI*) of the 10-15 highest trees per plot for dominant species (silver fir and/or beech) in (a) beech-fir stands, (b) silver fir and (c) beech. The thick solid lines represent mean ***BAI***, and shaded areas represent the confidence intervals (standard errors). The dotted lines show the sample depth for each year and site (right-hand side, y-axis). Sites as in Table 3.7, pp. 50-51.

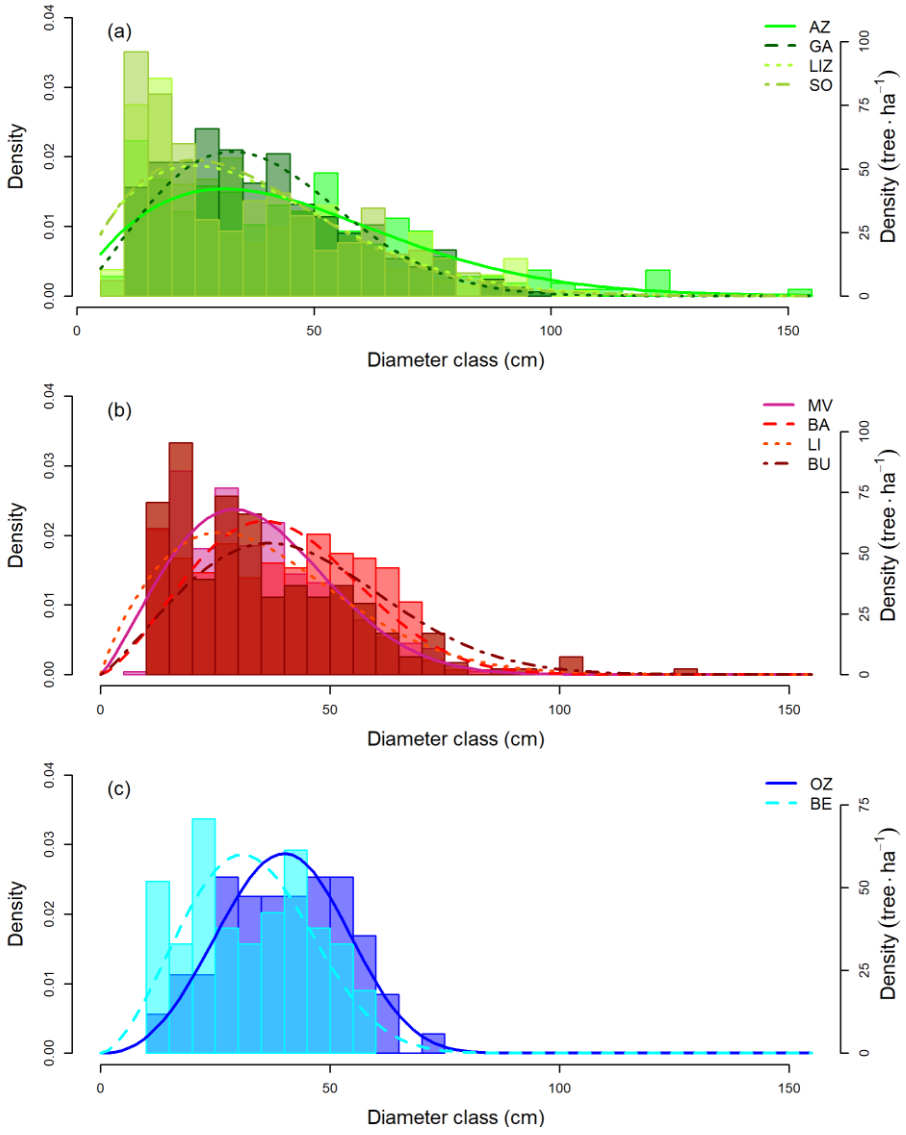

Figure 4.14. Diameter distribution represented by the Weibull density function for (a) beech-fir, (b) silver fir and (c) beech stands. Sites as in Table 3.7, pp. 50-51.

Episodes of severe disturbance occurred in all of the silver fir stands (> 40% of trees affected) (Table 4.3). The main levels of disturbance occurred in the Mata de València (MV) site, with more than 40% of trees affected in two release events (including minor and major) (Table 4.3) and releases peaking at 60% in the 1930s (Figure 4.15 a). The Ballibierna (BA) site has also experienced a long period of disturbance, with more than 30% of trees affected during the 1940s-1950s (Figure 4.15 a). Short, peak releases occurred in the other stands (Lierde -LI- and Bujaruelo -BU-) with around 40% of trees affected in previous years. In all silver fir stands, the intensity and frequency of releases has decreased in the last few decades. Different types of disturbance were observed in the beech-fir stands, which can be differentiated into two main groups. The first group was formed by Aztaparreta (AZ) and Lizardoia (LIZ), which included some of the oldest trees (almost 450 and 400 years, respectively) (Table 4.3), with a disturbance pattern characterized by small but frequent releases (< 20% trees affected), which increased in frequency in the 20th century (Table 4.3, Figure 4.15 b). The second group was formed by the Gamueta (GA) and Selva de Oza (SO) sites, which also included old trees and a similar period of release (> 20% trees affected) in the 1930s-1940s, extending to the 1970s in Selva de Oza, in which the release rate reached the maximum value (Figure 4.15 b). The highest one-off rates of major releases occurred around 1750s-1770s in Lizardoia beech-fir stand (Figure 4.15 b). Beech stands (Oza -OZ- and Betato -BE-) have shown variable release patterns (usually affecting up to 20% of trees), but the frequency of major decreases has been lower in recent decades, particularly in the Oza site. However, there was a common period of two decades (1940-1950s) when the most severe levels of disturbance occurred, especially where most of the releases were major and more than 40% of trees were affected (Figure 4.15 c).

Table 4.3. Tree-ring width data (mean ± SD for the common period 1925-2018) and characteristics of growth releases considering a minimum of 5 trees (for the whole timespan).

Site	Stand type	No. trees	No. radii	*AGE3* (years)	*TrajRANGE3* (years)	*MaxSupL.5* (years)	Timespan	$rbar$	Tree-ring width (mm)	Releases		
										5 – 20% (minor/major)	20 – 40% (minor/major)	> 40% (minor/major)
AZ	BF	26/12	26/12	428	206	232	1632 - 2018	0.12/0.30	1.70 ± 0.83/ 0.89 ± 0.38	18/9	1/0	0/0
LIZ	BF	18/7	20/8	342	205	118	1640 - 2018	0.19/0.20	2.97 ± 0.92/ 0.90 ± 0.37	13/5	8/4	3/0
GA	BF	12/25	23/43	357	205	143	1557 - 2018	0.25/0.44	1.38 ± 0.59/ 1.11 ± 0.35	10/4	3/2	0/0
SO	BF	2/35	2/66	213	57	135	1796 - 2018	*/0.39	2.78 ± 0.89/ 3.22 ±1.11	7/4	5/4	4/4
MV	F	34	64	191	82	44	1818 - 2018	0.30	1.84 ± 0.54	8/5	6/5	2/2
BA	F	31	53	147	119	68	1845 - 2018	0.50	2.53 ± 0.57	8/0	4/2	1/1
LI	F	20	40	146	46	84	1863 - 2018	0.72	2.97 ± 1.27	7/4	4/1	1/1
BU	F	10	20	126	37	38	1882 - 2018	0.52	3.24 ± 0.79	4/2	2/1	1/0
OZ	B	11	21	209	51	52	1801 - 2018	0.64	1.17 ± 0.23	8/0	5/2	1/1
BE	B	15	30	120	35	32	1895 - 2018	0.72	1.93 ± 0.36	6/3	6/5	2/2

Stand type: B (beech), BF (beech-fir) and F (silver fir); No. trees = number of sampled trees analyzed per stand and dominant species (in mixed stands the two numbers correspond to beech and silver fir, respectively); No. radii = number of radii measured (in mixed stands both numbers correspond to beech and silver fir, respectively); *AGE3* = mean age of the three oldest trees; TrajRANGE3 = range between the mean of the 3 youngest and the 3 oldest ages when growth trajectories reach dbh = 37.5 cm; *MaxSupL.5* = average length of the 5 longest single suppression phases experienced by trees; Timespan = complete chronological period; $rbar$ = average pairwise correlation between series obtained with Spearman correlation for dominant species in the case of BF stands; Releases 5 – 20% = disturbance events with 5 – 20% of trees showing releases; Releases 20 – 40% = disturbance events with 20 – 40% of trees showing releases; Releases > 40% = disturbance events with > 40% of trees showing releases. Numbers of trees analyzed to calculate releases over time are shown in Figures. 4.15a, b and c. Sites as in Table 3.7, pp. 50-51.

* In this case there was not enough data to estimate the $rbar$ statistic.

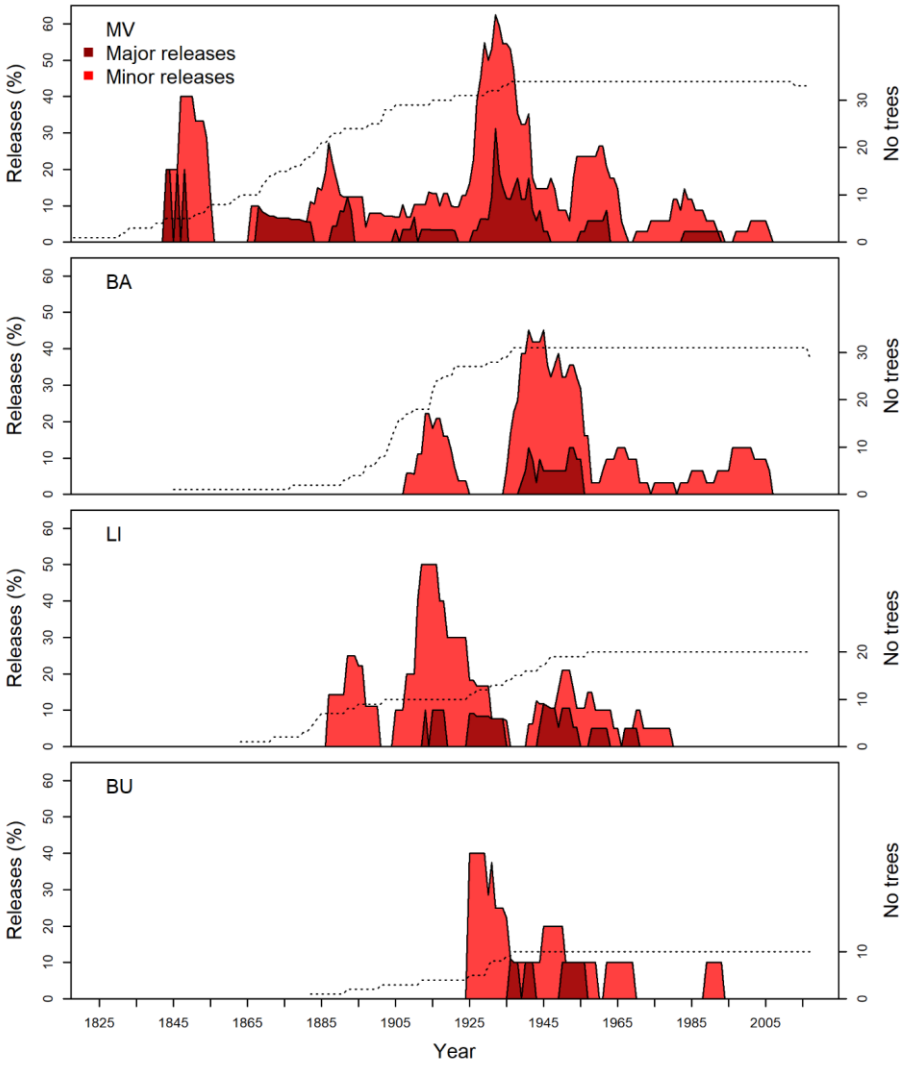

Figure 4.15 a. Major (dark red areas) and minor (light red areas) releases (left y-axis) of silver fir detected in pure stands during the period 1825-2018. The dashed lines indicate the sample depth for each year (right y-axis). Sites as in Table 3.7, pp. 50-51.

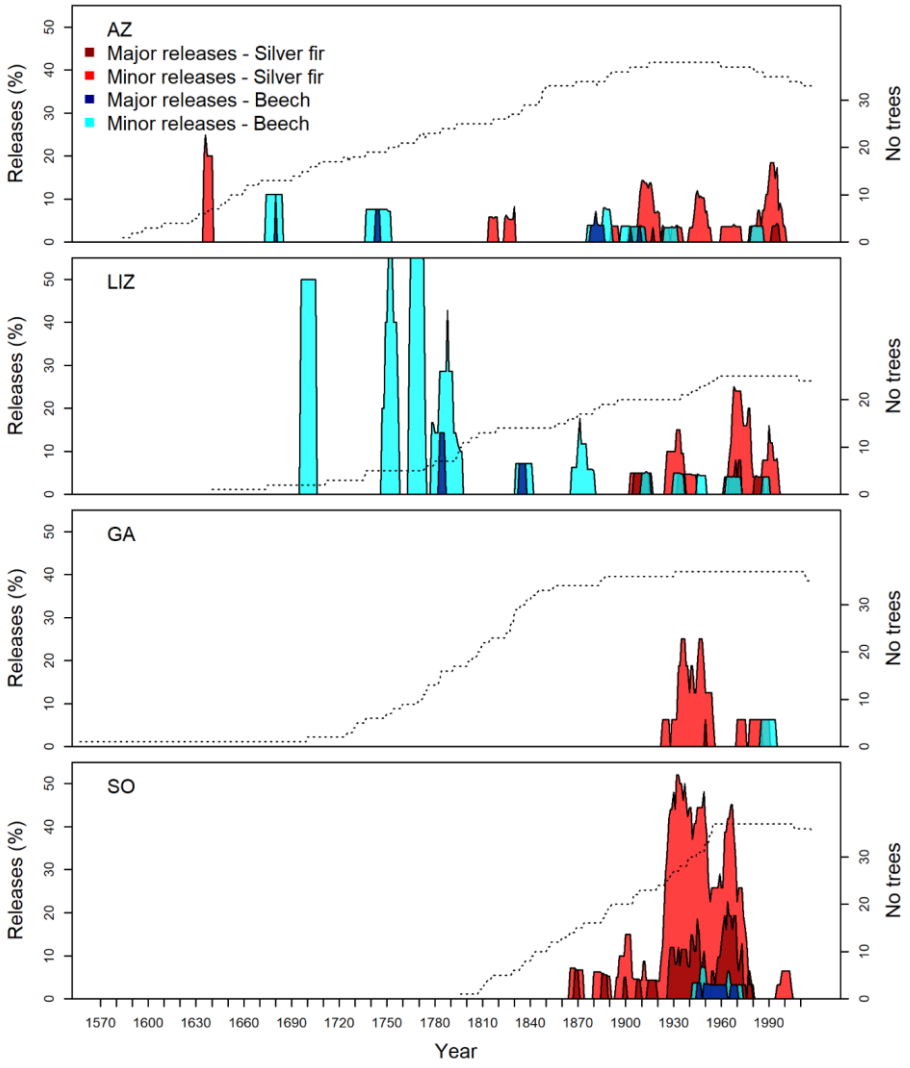

Figure 4.15 b. Major (dark red and blue areas for silver fir and beech respectively) and minor (light red and blue areas for silver fir and beech respectively) releases (left y axes) of silver fir and beech detected in mixed stands during the period 1570-2018. The dotted lines indicate the sample depth for each year (right y-axis). Sites as in Table 3.7, pp. 50-51.

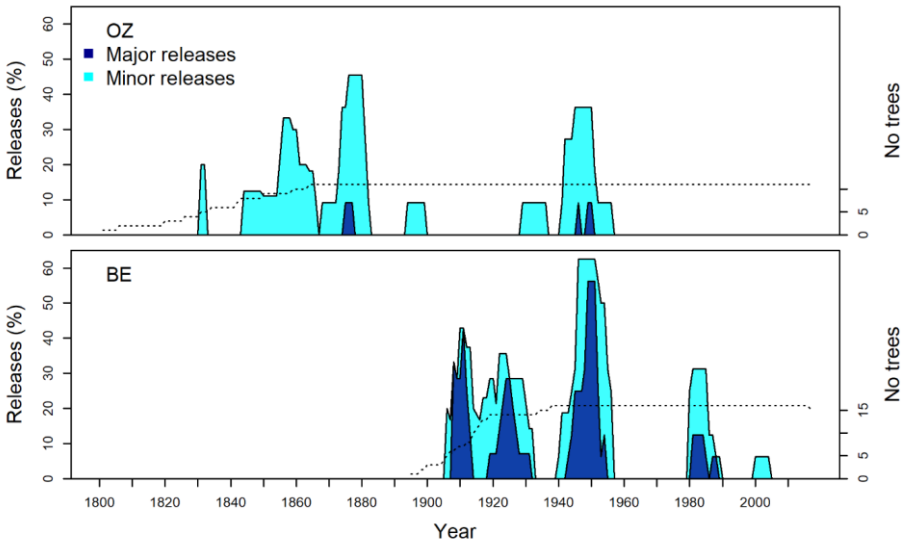

Figure 4.15 c. Major (dark blue areas) and minor (light blue areas) releases (left y-axis) of beech trees detected in pure stands during the period 1800-2018. The dashed lines indicate the sample depth for each year (right y-axis). Sites as in Table 3.7, pp. 50-51.

Overall, the last severe releases occurred synchronously in many stands in the period after the Spanish civil war (1940-1950s) when forest resources were exploited for both pasture and firewood (Gil Pelegrin et al., 1989). In some cases, intensive logging was conducted -as contemplated in the management plan- until 1970s, as in Selva de Oza (Cabrera, 2001). Another famous episode of deforestation in Spanish history, such as the Madoz expropriation (1854-1856), was recorded as anomalous growth in the Mata de València silver fir stand and Oza beech stand. However, natural disturbances, such as synchronous releases, also occurred in the second part of 18th century in Lizardoia, probably due cooling stages of the little ice age in this area (Bourquin-Mingot and Girardclos, 2001). However, in the last few decades, releases have been less important or even non-existent, probably because forest management was abandoned in these areas as a result of conservation policies, and establishment of protected areas such as natural parks were established.

4.2.1.2 Forest maturity

PC1 explained 68.29% of the variability in naturalness considering all metrics, but only five subgroups of metrics had loadings above 0.80 and positive effects (Table 4.4). Five metrics were finally selected as explanatory variables associated with the following indicators:

- Age indicators (AI): mean canopy age (*MEAN*), age range between the mean of the three oldest and the three youngest trees (*RANGE3*) and mean age of the three oldest trees (*AGE3*).
- Growth history indicators (GHI): range between the mean of the 3 youngest and the three oldest trees when growth trajectories reach dbh = 37.5 cm (i.e. slowly growing trees; *TrajRANGE3*).
- Disturbance and suppression indicators (DSI): average length of the 5 longest single suppression phases experienced by trees (*MaxSupL.5*).

PC1 explained 86.97% of the total variability in naturalness when all five of these metrics were considered. This second PCA sorted the plots according to their scores on PC1 (NS), corresponding to old-growth and long untouched forests (e.g. Aztaparreta and Lizardoia sites; see Figure 4.16).

Table 4.4. Metrics used to assess the degree of naturalness according to Di Filippo et al. (2017).

Type	Subgroup	Metric	Loading
AI	1	***MEAN* (year)**	**0.930**
		MEDIAN (year)	0.906
	2	***RANGE3* (year)**	**0.929**
	3	***AGE3* (year)**	**0.976**
		AGE5 (year)	0.970
		MAX (year)	0.963
GHI	4	***TrajRANGE3* (year)**	**0.887**
		TrajSLOW3 (year)	0.845
		TrajSLOW3mean (year)	0.804
		TrajSLOW3median (year)	0.768
DSI	5	*SupN.5* (n)	0.624
	6	*SupL.5* (year)	0.892
		SupLmax (year)	0.854
		***MaxSupL.5* (year)**	**0.899**

	MaxSupL.max (year)	0.860
7	*Rel1Yr.H*	0.539
	Rel1Yr.D	0.502
	Rel1Yr.Peak (%)	-0.424

Types of chrono-functional indicators: age indicators (AI), growth history indicators (GHI) and disturbance and suppression indicators (DSI); Subgroups: metrics assess similar features within the same type; Bold = metrics used to calculate the naturalness score (NS). Metrics description, see Table 3.12, pp. 66-67.

Analysis of the degree of naturalness rendered a reliable classification of plots according to the growth history of the stands (cf. Di Filippo et al., 2017). The highest NS values of these plots correspond to stands considered old-growth (e.g. Aztaparreta -AZ-) (Gil Pelegrín et al., 1989) and long untouched (e.g. Lizardoia -LIZ-) (Sabatini et al., 2018) (Figure 4.16). However, the NS values were low in one of the Lizardoia forest plots, which coincided with a regeneration gap, as indicated by the high stem density (Table 3.7, pp. 50-51). This indicates the difficulty in establishing realistic criteria for old-growth forests at multiple spatial scales ranging from plot to forest scale. High values of NS were also observed for some plots in Gamueta forest (GA), in which the mean canopy age is more than 250 years (Table 3.7, pp. 50-51) and fewer episodes of disturbance were observed than in other beech-fir stands (Figure 4.15 b). The NS values were lower in the other stands, even in those with an uneven-sized diameter distribution characteristic of higher degrees of naturalness (Selva de Oza forest, Figure 4.14 a). Nevertheless, major releases occurred in the mid-20th century (Figures 4.15), probably associated with logging in silver fir stands (Camarero et al., 2011). This highlights the need for chronological and retrospective measurements of tree growth that define naturalness, as argued by Di Filippo et al. (2017). Apart from the degree of naturalness, stands with high values of NS represent a transitional stage that is useful for including in a broader definition of old-growth forest and valuable for assessing carbon dynamics as a function of the degree of naturalness or maturity (Wirth et al., 2009).

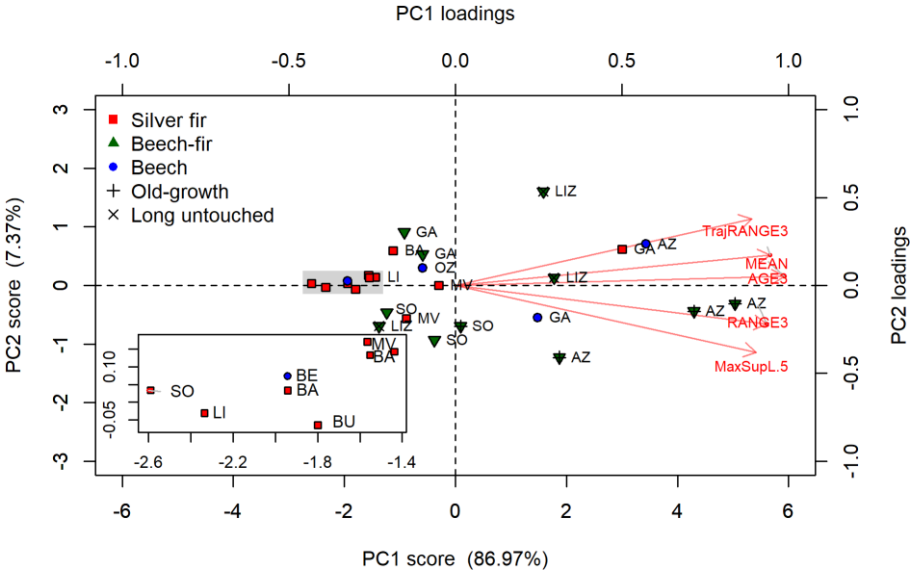

Figure 4.16. Principal component analysis (PCA) with the naturalness metrics most closely correlated with PC1 selected in a previous PCA. Plots are located according to their relative positions based on the first (PC1) and second (PC2) principal components. PC1 scores represent the naturalness score (***NS***) of plots, and loadings represent the correlations between tree-based naturalness metrics and PC1. *AGE3* = mean age of the three oldest trees; *MEAN* = mean canopy age; *RANGE3* = range between the mean of the 3 youngest and the 3 oldest trees measured; *TrajRANGE3* = range between the mean of the 3 youngest and the 3 oldest trees when growth trajectories reach ***dbh*** = 37.5 cm. *MaxSupL.5* (year) = average length of the 5 longest single suppression phases experienced by trees. Inset shows an enlargement of the left side of the figure. Sites as in Table 3.7, pp. 50-51. (One plot of silver fir with fewer than 6 sampled trees was not included in the analysis as it was not suitable for estimating some metrics).

4.2.1.3 Maximum live tree biomass stock models

Before fitting the models, the H_0/D_0 ratio was examined, again showing consistent values from 10 trees (Figure 4.17). Thus, a reference threshold of 10 trees was established for selecting SNFI plots. Although *SF* models of these forests (beech, maritime and Scots pine forests) were previously fitted in Moreno-Fernández et al. (2018), only those plots with more than 10 trees were considered in the processes of this thesis.

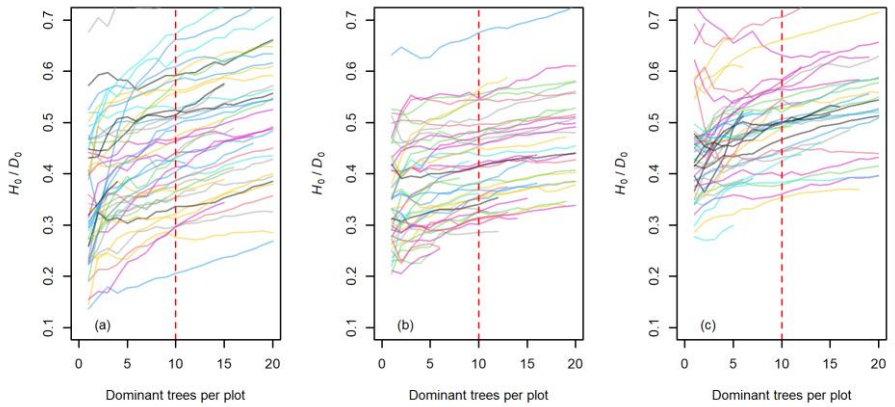

Figure 4.17. H_0/D_0 ratio for 1 to 20 trees considering both mature and SNFI plots for (a) beech, (b) maritime pine and (c) Scots pine forests.

In the first evaluation of live tree biomass (LTB), it was found that most of the study plots yielded the highest extreme values of LTB (including aboveground and belowground), which often exceeded biomass values corresponding to SNFI plots with similar SF values (Figure 4.18). These differences were significant according to Mann-Whitney tests for the three types of forests (p-value < 0.05). Thus, in most mature plots, LTB was maximal at the respective SF values, in contrast to the SNFI plots, which include the whole range of biomass stock (result of being a probabilistic sample). This confirmed that the stands sampled in mature conditions had the highest possible LTB stock at the national scale. Considering that episodes of disturbance had occurred in many of the studied stands, up until 1970s in the most recent cases (Figures 4.15), they can be considered to have recovered high levels of LTB. The capacity for biomass recovery was also reported by Trotsiuk et al. (2016), who concluded that a period of 40-50 years is sufficient for recovery of 90% of aboveground stand biomass after a low degree of disturbance (20 – 40% of canopy removed) in primary *Picea abies* (L.) H. Karst. mountain forests.

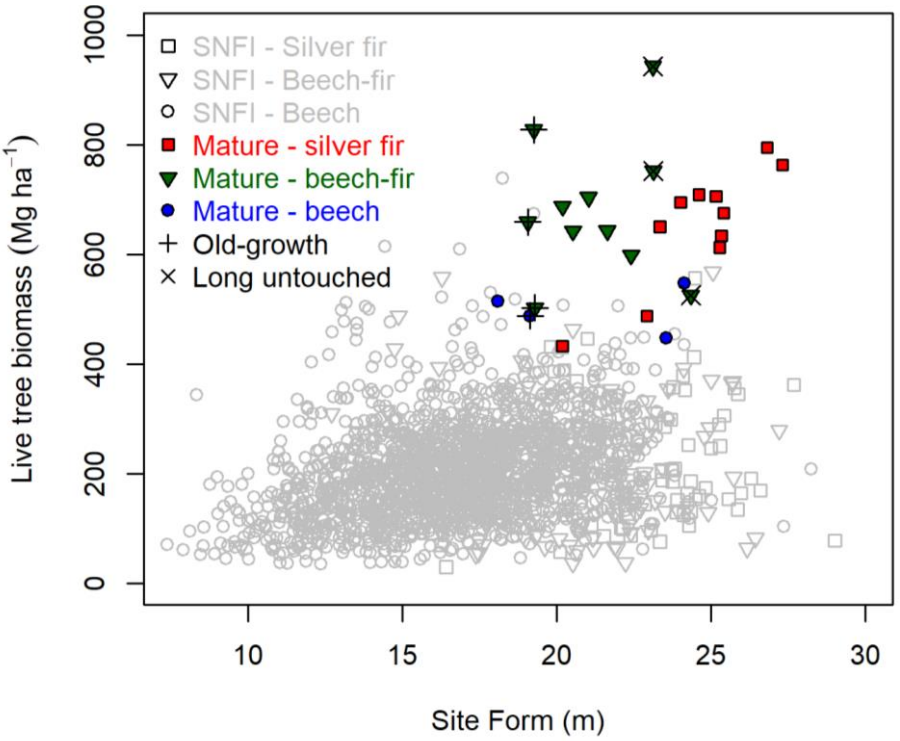

Figure 4.18. Location of the forest plots in a scatter plot of live tree biomass (LTB) against site form (SF). Squares represent silver fir plots, triangles represent beech-fir plots and circles represent beech plots. Empty grey symbols represent the Spanish National Forest Inventory (SNFI) plots, and filled symbols represent the plots sampled in Pyrenean mature forests.

Regarding the maximum biomass stock (MBS) models, the estimated slope parameters were significant in beech, beech-fir and silver fir forests (Table 4.5, p. 137). This means that where the slope parameter is positive and significantly different from 0, LTB increases with SF. For the three types of forests, despite poor fit statistics in some cases, the scatter plots indicated that the MBS curves performed well for the data, with recognizable upper bounds representative of maximum relative biomass stock ($BS(\%)$) (Figures 4.20 a, b and e; p. 138). The mature plots can be found at around these upper boundaries, indicating that undisturbed mature stands represent MBS values, in accordance with Kranabetter et al. (2009).

4.2.1.4 Assessing whether mature forests hold maximum live tree biomass stocks

Total LTB at plot level was not related to the degree of naturalness, and biomass values varied between 400 and 850 Mg ha^{-1} indistinctly across a wide range of NS values (Figure 4.19 a). Total LTB was similar in both silver fir and beech-fir forests, ranging between approximately 500 and 850 Mg ha^{-1}. By contrast, total LTB in beech forests was lower, usually around 400 Mg ha^{-1}. Again, as with the absolute LTB values, $BS(\%)$ and the NS were not significantly related, with most values close to 100% irrespective of NS (Figure 4.19 b). In both LTB and $BS(\%)$, beech stands showed an approximately stable trend, despite differences in the degree of naturalness. By contrast, low NS implied higher biomass in silver fir stands. Interestingly, total LTB in mixed stands peaked in stands of an average degree of naturalness. The fact that silver fir and beech-fir plots always reach higher biomass values than pure beech may be due to the greater structural diversity generated by species diversity and shade tolerant behaviour, confirming that structural diversity can have a stronger effect on productivity than species diversity, because similar values were reached in pure and mixed stands (Dănescu et al., 2016).

Maximum accumulation of LTB was found to be reached at a lower degree of naturalness than old-growth in silver fir, beech and beech-fir Pyrenean stands. This finding is consistent with those of previous studies (Bergamn, 2021; Ķēniņa et al., 2019; Nord-Larsen et al., 2019; Seedre et al., 2015) and contributes to a better understanding of forests capacity to store carbon over time (Hubau et al., 2020; Luyssaert et al., 2008; Pregitzer and Euskirchen, 2004). The network of sites considered in the present study represents the most extensive monitoring system of mature pure and mixed beech-fir stands across the Spanish Pyrenees. Nonetheless, it cannot be ignored there may be some degree of uncertainty due to the limited number of experimental sites considered. Locations were identified by an exhaustive selection process focused on the maximum degree of naturalness which included consulting local experts and historical records. Nevertheless, only two of the sites can be considered old-growth or long untouched stands according to

scientific references (Sabatini et al., 2018). The other ones were mature forests recovering from disturbance at earlier developmental stages and represented the maximum value of LTB, as observed relative to the SNFI plots with similar SF values. This also made it possible to establish thresholds representative of maximum LTB stock through SF values (i.e. MBS models) for the forest types considered.

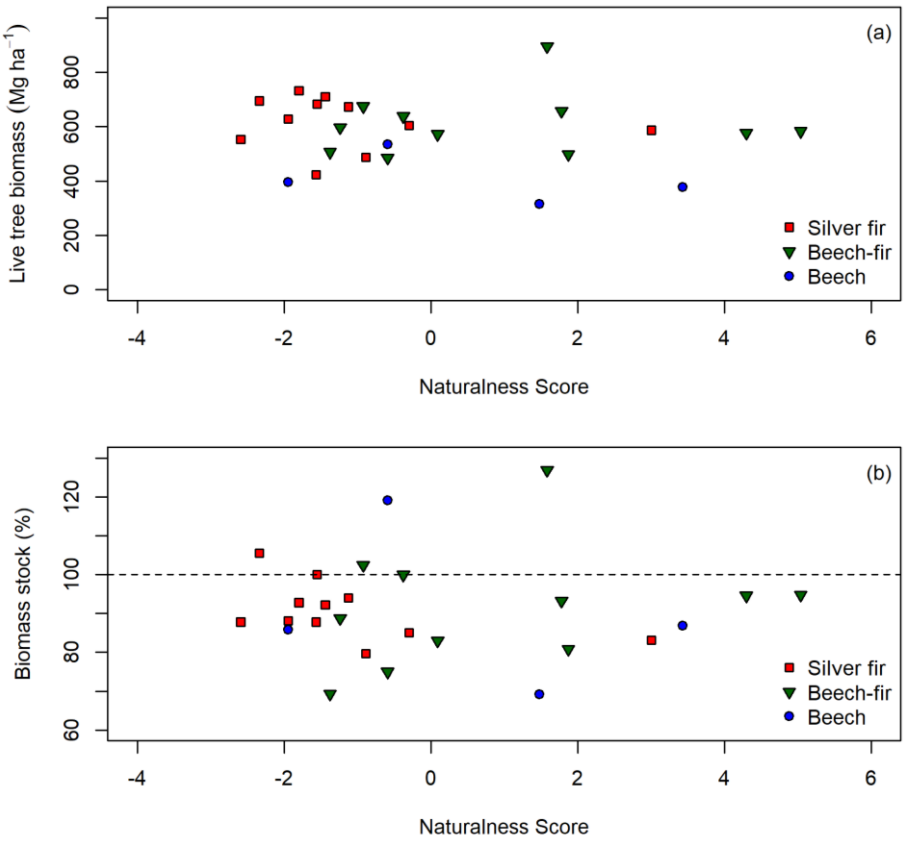

Figure 4.19. Representation of biomass as a function of the naturalness score (NS) of Pyrenean mature forests in (a) absolute (total live tree biomass -LTB-) and (b) relative values (biomass stock -BS(%)-).

The lack of a relationship between LTB and NS demonstrated that in the absence of recent disturbances, biomass stock reaches an approximately constant value after a certain degree of naturalness. This

is consistent with the findings of Nord-Larsen et al. (2019) and Mund (2004), who did not detect any evidence of continuous accumulation of carbon stock in old-growth beech forests. These findings also coincide with those of Idoate et al. (2022), who reported a negative relationship between maturity (assessed by structural features) and biomass increment in Suitland forest reserves monitored since 1955. Nevertheless, biomass trends may differ for NS according to the type of forest, which were more stable in beech stands and reached different peaks in silver fir and beech-fir stands. In particular, an increase in beech-fir biomass, as the best represented forest through NS, was observed in plots representing intermediate levels of naturalness. By contrast, Pregitzer and Euskirchen (2004) concluded that LTB (in terms of carbon stock) increases with age in temperate forests. However, these findings must be considered with caution in light of the huge variability in LTB for the oldest age class, which ranged from close to 0 to approximately 600 Mg Carbon ha^{-1}. Regarding tree level assessments, Stephenson et al. (2014) showed that growth rate increases continuously with tree size, even though stand level productivity declines. Nevertheless, our biomass quantifications are limited because we did not consider all of the trees located in each sampled plot. Further research should also include regenerated, very suppressed and dead trees.

Considering biomass in relative terms, in most plots, $BS(\%)$ was around 100%, and again biomass was not significantly related to NS (Figure 4.19 b). This is also consistent with previous findings (Kranabetter, 2009; Smithwick et al., 2002), though these other studies only considered old-growth forests suitable for storing maximum values of $BS(\%)$, and not earlier stages. Although this result is not conclusive, because of the scarcity of plots in silver fir and beech-fir forests and poor fit statistics, it encourages estimation of the upper reference threshold of LTB stock potential as in Figure 4.20 (p. 138). The stock may reach higher levels if other biomass pools such as standing dead wood and coarse woody debris behave in a similar way, as Ford and Keeton et al. (2017) observed for late-successional biomass in hardwood-conifer forests. Stock estimates can also include soil carbon (litter and mineral soil), which have showed similar behaviour

in Mediterranean soils following afforestation of abandoned crops, tending to a stable state in old forests (Juvinyà et al., 2029). Biomass stock oscillations around MBS may be related to natural gap dynamics, a characteristic feature in mixed conifer-broadleaf forests (Kenderes et al., 2009; Martin-Benito et al., 2020; Nagel et al., 2007; 2014). In this regard, the death of large, senescent trees, which represent huge carbon reservoirs (Büntgen et al., 2019; Stephenson et al., 2014), causes important losses in stand biomass stock, irrespective of the degree of naturalness.

Different biomass trends were observed through NS, depending on the type of forest (Figure 4.19 b). This was the case for beech-fir stands, in which an increase in biomass was observed in plots representing an intermediate degree of naturalness. Despite the limited number of plots considered, the increase may be related to early stages of old-growth, which in temperate forests may yield more live and/or dead trees biomass than at more advanced stages (Bormann and Likens, 1979; Lorimer and Halpin, 2014). In addition, although old-growth beech-fir forest tends to be dominated by beech regeneration (Jaloviar et al., 2017), the increase in biomass may also be due to higher proportions of silver fir being at stages earlier than the old-growth stage, as they represent higher volume than density (Lingua et al., 2011). Beech stands were fairly stable, despite differences in the degree of naturalness. This finding is consistent with those reported by Kucbel et al. (2012) for old-growth beech forests, which are very stable and in which biomass does not necessarily increase with age. Finally, the lack of replicated plots in silver fir and beech-fir stands precludes full discussion of the variability in LTB related to NS.

Despite the lack of replicates of natural silver fir forests, LTB was not higher in the forests characterized by the greatest levels of naturalness. Thus, larger amounts of LTB are not necessarily a good indicator of a higher degree of naturalness, as previously suggested (Burrascano et al., 2013). Although the maximum carbon storage in LTB (as an ecosystem service) may be reached at mature stages rather than at old-growth stages, a complete evaluation of carbon storage in ecosystem services must consider all important carbon pools. Nevertheless, old-growth forests provide valuable ecosystem services

(e.g. biodiversity, landscape values, etc.) other than only biomass storage (hence carbon sequestration) (Wirth et al., 2009). In addition, the cumulative probability of disturbance is higher in old stands (Luyssaert et al., 2008) and may become particularly important in the context of climate change as these stands may face multiple threats (drought, pests, etc.) related to climate warming (Seidl et al., 2017). In some stands in which the degree of naturalness is low, it may be useful to apply carbon-focused silviculture combining structural diversification with enhancement of carbon stocks (Ford and Keeton, 2017). However, further research on biomass and carbon storage in old-growth and mature forests is necessary to clarify these points.

4.2.2 Reference maximum biomass stock models for the study species at national scale

Regarding the MBS curves fitted by quantile regression, some of the forest types, such as beech-fir, Scots pine and silver fir, showed significant coefficients for all of the parameters estimated, and beech forests only for the slope parameter b, according to the null hypothesis of $b = 0$ (Table 4.5). These findings indicate that positive slope parameters, such as those obtained for the aforementioned forest types, can be considered different from 0 and therefore, the LTB increases when SF does, which is biologically consistent. The maritime pine forest did not show significant coefficients in the parameters estimates; which means the slope parameters cannot be considered significantly different from 0, and therefore the maximum LTB increase through SF increase is not statistically significant. In this last case (unlike the others), these results may be explained by the lack of data for the high values of SF. However, regarding visual performance, all species showed logical behaviour, locating the mature plots around MBS curves. This is coincident with Kranabetter (2009), who demonstrated how ecological site classification or direct measures of stand productivity can refine estimates of the upper limits in potential carbon storage. Therefore, quantile regression can be useful when predictions other than the conditional mean are desired (Weiskittel et al., 2011, p.

285) and there is a full range of data covering all of the values of variables.

Table 4.5. Maximum biomass stock (MBS) models, goodness-of-fit statistics and parameters.

Main species	Parameters			Quantile (%)	Logarithmic regression
	Estimates	Std. Error	p-value		
Beech	a = -145.41	200.70	0.469	97.5	
	b = 204.82	70.86	0.004		
Beech-fir	a = -845.35	321.93	0.009	97.5	
	b = 493.65	114.48	0.000		
Maritime pine	a = 44.63	257.66	0.862	97.5	$MSB = a + b \cdot \log(SF)$
	b = 88.18	94.31	0.350		
Scots pine	a = -236.72	25.25	0.000	97.5	
	b = 193.41	10.09	0.000		
Silver fir	a = -2558.81	318.66	0.000	97.5	
	b = 1012.03	105.62	0.000		

The potential biomass stock defined by the MBS curves differed among forest types, for which the major values were found for silver fir and beech-fir forests, with around 700 Mg ha^{-1} for the best site qualities (Figure 4.20). Both forest types show higher structural diversity than the others, due to the shade tolerant behavior of silver fir, confirming that structural diversity can increase stand productivity (Dănescu et al., 2016). By contrast, in both conifer forests the values were minimal, around 300 Mg ha^{-1} for intermediate site qualities. However, Scots pine plots showed a higher site quality gradient due to its wider distribution covering many site qualities; showing also greater biomass values than in hemiboreal old-growth Scots pine stands in Latvia in most cases, where the average value is 171.2 Mg ha^{-1} (Ķēniņa et al., 2019). Finally, mountainous beech forests showed intermediate MBS values, which reached above 400 Mg ha^{-1} in the best site conditions, similarly to those in semi-natural old-growth beech forests in Denmark (Nord-Larsen et al., 2019) and naturally developed beech forests in northwest Germany (Meyer et al., 2021b). However, there are no reliable site quality index estimates available in order to compare the different locations.

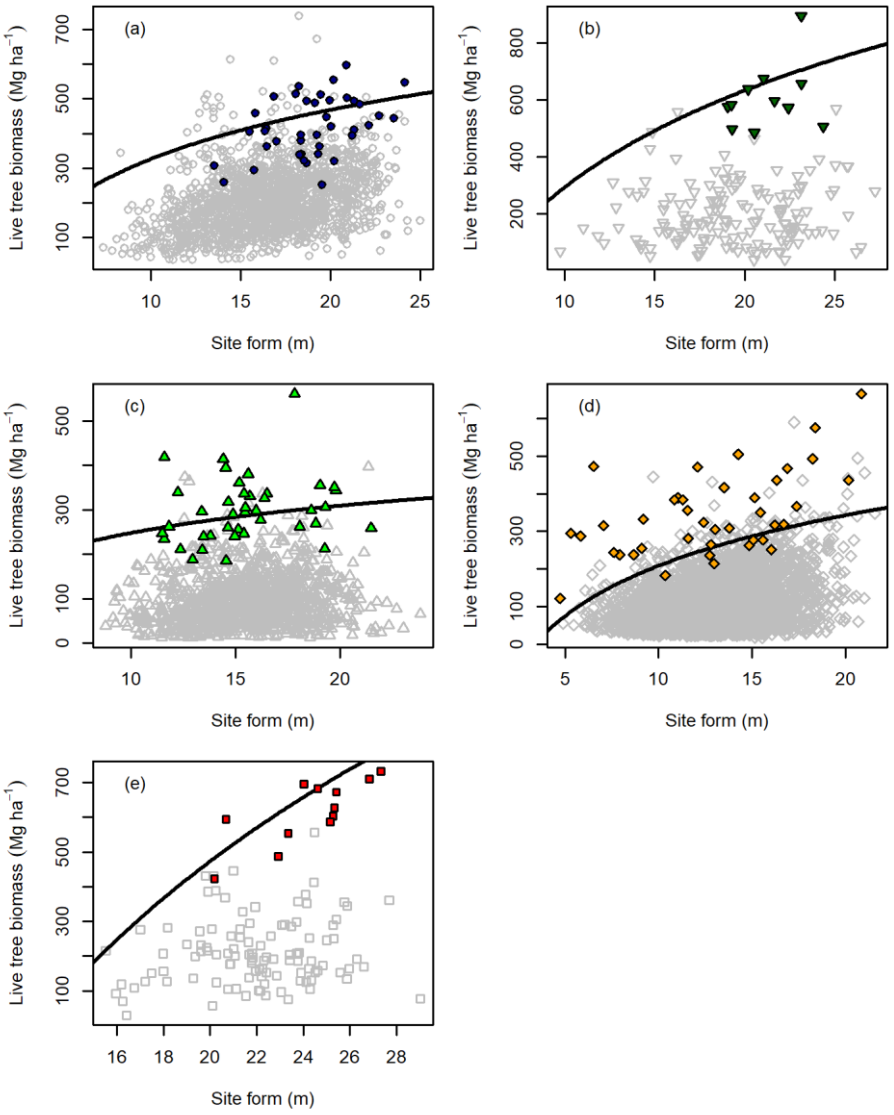

Figure 4.20. Maximum biomass stock (*MBS*) models for (a) beech (circles), (b) beech-fir (inverted triangles), (c) maritime pine (triangles), (d) Scots pine (rhombuses) and (e) silver fir forests (squares). Empty and filled symbols represent the SNFI and mature sampled plots, respectively.

In the case of maritime pine forests, the lack of data for high values of SF may be related to forest management, because *P. pinaster* (both maritime and Mediterranean species) represents one of the main managed species in Spain, reaching 16% of timber cuttings in 2019 (MITERD, 2021). Management is especially intense in northwest Spain, where the top two Spanish provinces (A Coruña and Pontevedra) regarding maritime pine felling, each of them reached between 400,000 and 790,500 m^3 in 2019 (MITERD, 2021). In addition, these provinces represent most of the highest SF values at national scale (Moreno-Fernández et al., 2018, Figures 3 and 4), which partly explains the lack of plots for the high values of SF. Regarding silver fir and beech-fir forests, there are fewer data for the highest values of SF, which may be due to (i) the small number of plots due to the reduced area occupied by these forests, (ii) intense logging during the 20^{th} century in the Pyrenees up to 1970s in some cases (Cabrera, 2001), and (iii) the occurrence of silver fir dieback in the study area (Camarero, 2017; Gazol et al., 2020; Sangüesa-Barreda et al., 2015). For the other species there are sufficient numbers of plots to represent SF and LTB values well enough to fit the MBS models. Furthermore, some of the stands occur in protected areas with no management or severe logging during decades, which means that some of their respective SNFI plots may have reached maximum values of LTB.

4.2.3 Suitability of maximum biomass stock models as indicators of forest maturity in terms of biomass stock

Estimation of growing stock -the total volume of living trees- is very useful as one of the main values reported in the global forest resources assessment conducted by the FAO (FAO, 2020). In this respect, most countries have only one estimate of biomass stock per unit area, which means that biomass and carbon estimates are mainly extrapolated from changes in forest area (FAO, 2020). The methodology developed in this thesis may be useful in these cases, because MBS models have a strong potential to estimate forest maturity

in terms of biomass stock, relating the actual biomass stock to the maximum stock that is potentially achievable. Thus, NFIs in general, and the SNFI in this particular case, are the most valuable data sets due to the high sampling intensity they represent. In this research and according to the methodology developed, 4 out 5 forest types showed similar rates of $BS(\%)$, with average values around 40% (Figure 4.21 b-e). Beech forests included the highest rate of $BS(\%)$ with a mean value of aproximately 50%, and covering the whole range of relative values (Figure 4.21 a). Nevertheless, many of the beech forests occur in protected areas with non-existent or very low levels of management, being one of the least managed species in the study area. These forests also supply approximately 1% of the total cuttings in Spain (mainly used as firewood), providing 6% of the total amount of firewood generated in Spain (MITERD, 2021). The pine forest types (maritime and Scots) represent two of the main species managed in Spain, which increases the probability of finding plots in the SNFI that have been measured just after thinings. Therefore, resulting in lower $BS(\%)$ values compared to the maximum potential for their development stage at the time of collecting data. Maritime pine systematically suffers a high rate of wildfires throughout a large part of the study area, being the second most affected species in 2006-2015, representing 21% (67,374 ha) of the burned area in the region (López-Santalla, 2019, p. 71).

Use of the above methodology is consistent with recent findings, such as those reported by Matuszkiewicz et al. (2021), who estimated the potential carbon stocks in the forest communities in the Białowieża Biosphere Reseve. However, these researchers used a different approach, considering the potential natural vegetation (or climax forest) as the reference for estimating maximum values of carbon stock. They defined the upper limit of carbon stocks by averaging the maximum values obtained from 10,000 replicates of random subsamples from 6 plots (0.04 ha per plot). These plots correspond to the Natural and Cultural Inventory of the Białowieża Forest designed according to a systematic square grid (650 x 650 m). Although this approach can be useful in some contexts, it does not consider the site quality factor and assumes that all locations can reach similar upper threshold of carbon

stocks. However, this may be appropriate for Matuszkiewicz et al. (2021) approach, due to the small latitudinal and altitudinal (135-190 m.a.s.l.) ranges, thus yielding very similar site qualities for the same potential natural vegetation communities. By contrast, the MBS models fitted here have the desirable advantage of contemplating a continuous site quality gradient for application to the forest types assessed at national scale.

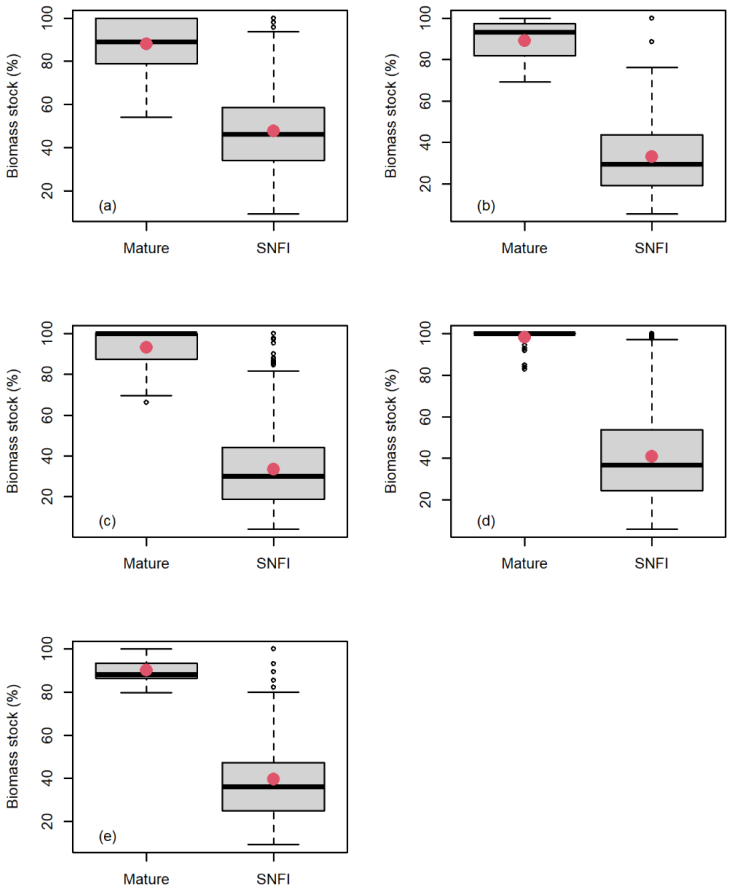

Figure 4.21. Box plots representing the relative biomass stock ($BS(\%)$) estimated for mature and Spanish National Forest Inventory (SNFI) plots for (a) beech, (b) beech-fir, (c) maritime pine, (d) Scots pine and (e) silver fir forests. Red dots indicate arithmetic mean values.

The MBS models were useful for both estimating and representing the biomass stocks relative to the maximum potential at national scale based on SNFI plots, obtaining a similar map to that generated in Matuszkiewicz et al. (2021) in Figure 7. In general, there were no clear trends across Spain for the forest types studied here, and different, randomly interspersed $BS(\%)$ values were obtained (Figure 4.22). Maritime pine yielded slightly lower $BS(\%)$ values in the most northwest part of Spain, which coincide with the provinces (A Coruña and Pontevedra) where management is particularly intense (MITERD, 2021). However, these also coincide with larger areas burned by wildfires (López-Santalla, 2019, p. 41). $BS(\%)$ values were lower for Scots pine plots in the central-east distribution, which may be related to the presence of black pine (*Pinus nigra* Arn. Subsp. *salzmannii* (Dunal) Franco). This species is very common in this part of the Iberian Peninsula (Iberian Mountains), where it sometimes forms mixed conifer stands with Scots and maritime pines. Regarding its southernmost distribution (east Andalucía), very low $BS(\%)$ values can be found, probably partly due to decline processes mainly caused by tree size, competition and climate conditions (Sánchez-Salguero et al., 2012). By contrast, those areas with longer management tradition, as in the central (Sierra de Guadarrama) and central northern areas (Sierra de la Demanda), include the greatest concentration of Scots pine forest plots with high values of $BS(\%)$, probably belonging to the last stages of stand development. Although beech-fir and silver fir forests include few plots and were restricted to the Pyrenees range in northeast Spain (Figure 4.22 b), there is a specific area with the highest $BS(\%)$ values in the northwest of Catalonia region. Many beech forests are part of protected areas with non-existent or very low levels of management. However, although 87% of all the thinnings of this forest type in Spain are conducted in the region of Navarra, (91,229 m^3 in 2019; MITERD, 2019), there were no differences in patterns of $BS(\%)$, but rather slightly higher $BS(\%)$ values relative to other regions (Figure 4.22 a). This proves that sustainable forest management can be compatible with

carbon sequestration policies. Further research is necessary to expand this methodology to estimate $BS(\%)$ for all forested areas in an overall spatial prediction based on remotely sensed data in a similar way to conducted in previous studies for biomass and growing stock volume (Chirici et al., 2020; Nilsson et al., 2017; Nord-Larsen and Schumacher, 2012).

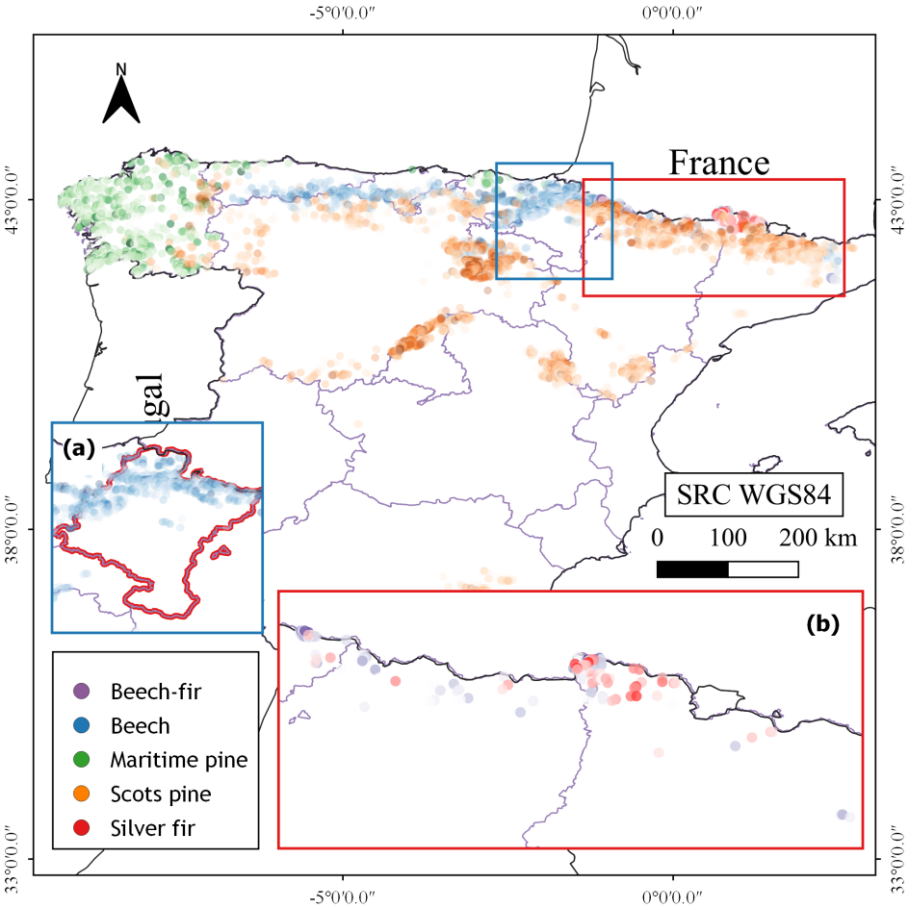

Figure 4.22. Relative live tree biomass stock ($BS(\%)$) represented as a colour gradient, from dark (high $BS(\%)$) to light (low $BS(\%)$) for all of the Spanish National Forest Inventory (SNFI) plots included in this study and belonging to the following forest types: beech (blue), beech-fir (purple), maritime pine (green), Scots pine (orange) and silver fir forests (red). (a) Region of Navarra with beech forest plots; (b) Pyrenees range with beech-fir and silver fir forest plots.

4.3 CHARACTERIZATION OF STRUCTURE IN MATURE FORESTS

4.3.1 Assessment of the spatial structure in mature *P. sylvestris* forests of different biogeographical regions

The data set here analyzed corresponds to mature plots of Scots pine forests belonging to the Atlantic, Mediterranean and Boreal biogeographical regions (see 3.1.1.5 Mature *Pinus sylvestris* forests belonging to Atlantic, Boreal and Mediterranean biogeographical regions, pp. 52-53). According to the diameter distribution, clear differences can be observed among Scots pine forests of the Atlantic, Mediterranean (both from Spain) and Boreal (Estonia) biogeographical regions, especially between the last one and other regions. For the Atlantic and Mediterranean forests, the histogram is skewed to the right, with higher density values for the predominant dbh classes (which are the same in both cases, 30-55 cm) in the case of Atlantic forests, and covering a similar range of dbh classes in both regions. For the Boreal forests, the diameter distribution of Scots pine is slightly skewed to the right, but with a narrower range of dbh classes shifted to lower values (Figure 4.23), indicating more even-size stand conditions as reported by Põldveer et al. (2020) for natural Scots pine plots. However, it must be noted that small trees (4 cm < dbh < 7.5 cm) from Boreal forests were not taken into account, despite they were included in the database. To make the data sets more comparable, as only trees greater or equal than 7.5 cm at dbh were included in the rest of regions. A density gradient with much higher values in Boreal forests, followed by Atlantic and Mediterranean forests (as observed in Table 3.8, p. 53), was observed also in the diameter distributions. The density of other species was superior in Boreal forests, particularly for small dbh classes. These other species are mainly small individuals of *Picea abies*, which due to its shade-tolerant behaviour can regenerate well when canopy gaps are rather small (Metslaid et al., 2007), showing a constant rate of regeneration in relation to stand age in hemiboreal dominated Scots pine (Luguza et al., 2020). On fertile soils, *P. abies* usually forms a second storey under strata dominated by Scots pine, but also including common oak and silver birch (Bušs, 1976). Regarding the Atlantic and

Mediterranean regions, the presence of other species is similar but slightly higher and more widely spread across dbh classes in the Atlantic biogeographical region.

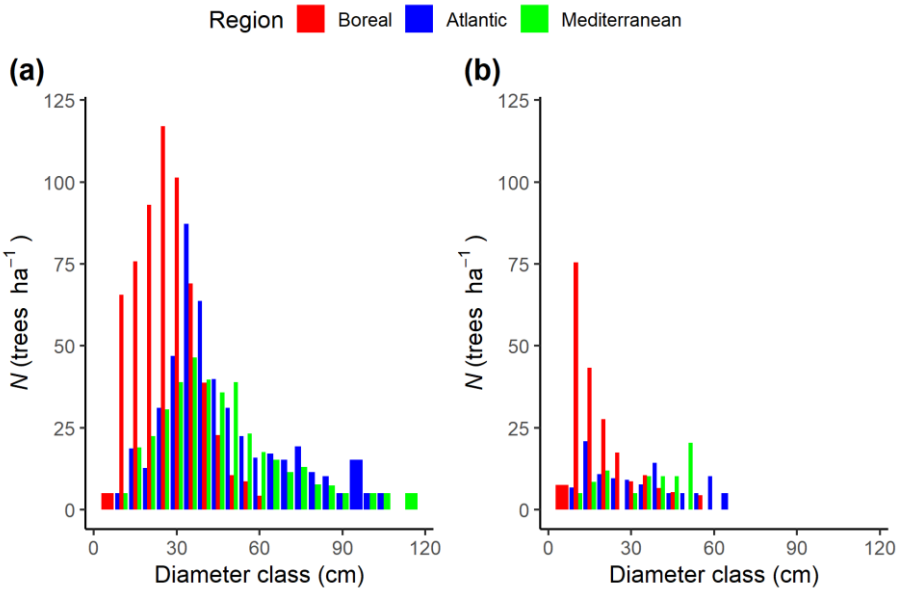

Figure 4.23. Average values of diameter (dbh) distributions for the three biogeographical regions considering (a) only *Pinus sylvestris* species and (b) the other species.

Regarding tree $h{\sim}dbh$ relationship, there is a clear difference between Boreal and the other biogeographical regions (Figure 4.24). Trees in Boreal Scots pine forests are more slender, with smaller dbh at similar h. By contrast, the $h{\sim}dbh$ relationship often overlaps in Mediterranean and Atlantic forests. Hence, there is a transition in the tree $h{\sim}dbh$ relationship between regions with steeper shapes for Boreal, followed by Atlantic and Mediterranean regions. However, in the Atlantic and Mediterranean forests there are shared spaces in the scatter plot, which may be due to the intermediate site conditions and a wider range of site quality conditions. These forests can reach really adverse conditions on the high mountainous areas, especially in the Mediterranean region, characterized by poor soils, hydric stress in

summer and low temperatures in the winter, which cause dormant periods in both summer and winter seasons. In these extreme cases, the forest density is very low, which together with the low site quality, leads to dbh being large relative to h. It is important to note that these results should not be explained by the effects of silvicultural practices since all the plots considered have not been managed at least during the last few decades.

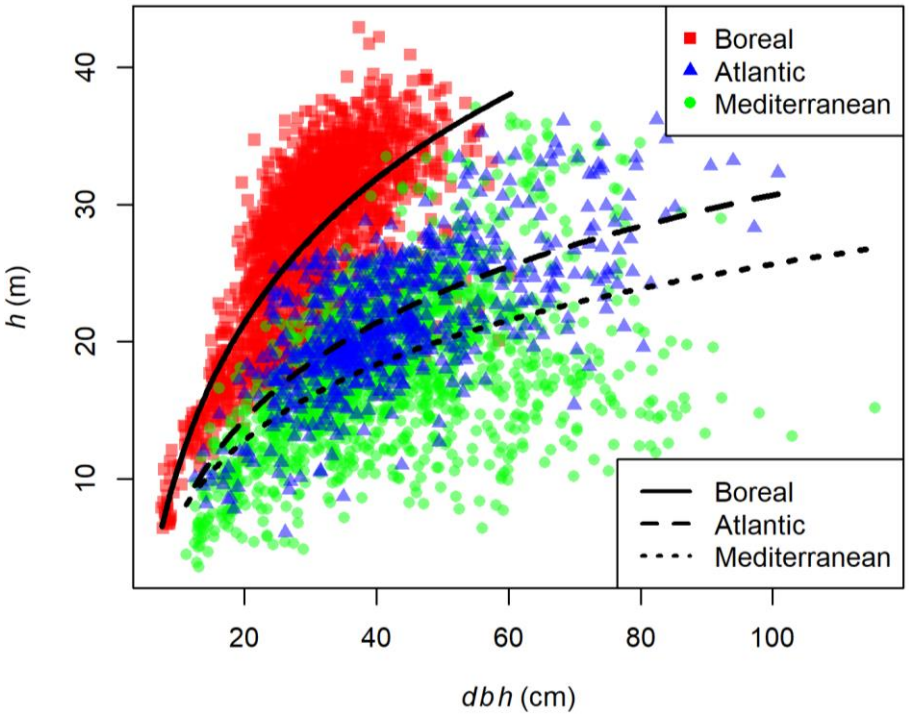

Figure 4.24. $h \sim log(dbh)$ relationship for the three biogeographical regions: Boreal (red squares), Atlantic (blue triangles) and Mediterranean (green points). The lines represent logarithmic regressions for Boreal (solid line), Atlantic (dashed line) and Mediterranean (dotted line) regions.

Among the structural indices, the species richness revealed that Atlantic forests are the most diverse on average, but with no significant differences from Boreal forests (Figure 4.25 a). By contrast, species richness was lowest in Mediterranean Scots pine forests, with most plots corresponding to monospecific stands. In despite of

Mediterranean regions represent some of the most biodiverse ecosystems in the world (Cuttelod et al., 2009), a large proportion of that diversity corresponds to shrub and herbaceous vegetation, which was not surveyed in this work. Moreover, some of the Scots pine forests in this region are plantations located in very poor quality sites (high altitudes and shallow soils) where they form the climax vegetation as monospecific stands. In the same way, Atlantic and Boreal forests are

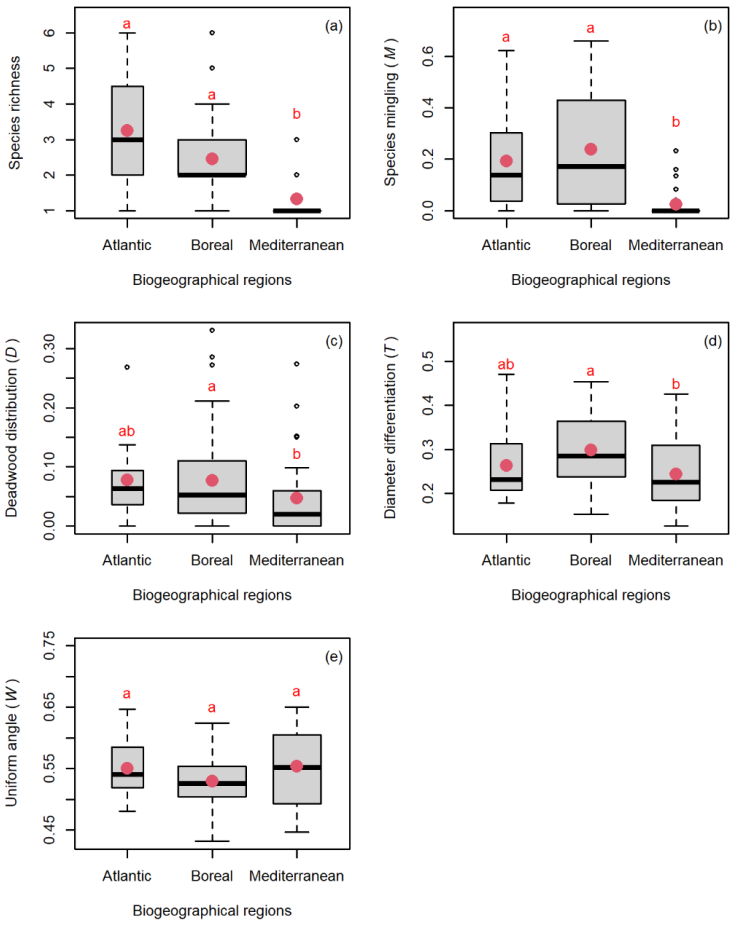

Figure 4.25. Structural indices for the three biogeographical regions (Atlantic, Boreal and Mediterranean): (a) Species richness, (b) Species mingling (*M*), (c) Deadwood distribution (*D*), (d) Diameter differentiation (*T*) and (e) Uniform angle index (*W*). Red dots represent mean values.

much more heterogeneous than Mediterranean forests in terms of mingling of different tree species (Figure 4.25 b). However, although species richness was slightly higher in Atlantic forests than in Boreal forests, the latter were slightly more heterogeneous according to spatial species mingling (M). This may be due to the greater presence of shade tolerant species, especially *P. abies*, as indicated by the diameter distribution (Figure 4.23 b). The values for deadwood distribution (D) were higher in Atlantic and Boreal regions than in Mediterranean regions and therefore, the plots included more snag trees (Figure 4.25 c). In the absence of management, this is probably related to density-dependent tree mortality due to between-tree competition, with higher values of density in the Boreal regions, which was demonstrated as the top cause of mortality in Scots pine forests in Estonia (Laarmann et al., 2009). Diameter differentiation (T) was superior in Boreal than Atlantic and Mediterranean regions, indicating that mature Boreal forests are a bit more uneven-sized (on average) than the others (Figure 4.25 d). The explanation for this may be in part related to stand origin as mature forests studied in Estonia were naturally regenerated, unlike mature forests in Spain, where some of the plots belong to plantations with regular distribution. Nonetheless, all plots are moderately uneven-sized (on average), according to the T index, and thus similar to reference values in Scots pine mature forests (Põldveer et al., 2020). Finally, there were no significant differences between regions in spatial tree distribution (Figure 4.25 e), with average values for the uniform angle index (W), of between 0.5 and 0.6, indicating a random positioning in most cases, which is a very common pattern in most forests in the world (Pommerening, 2002).

4.3.2 Assessment of the spatial structure among different forest in mature conditions

The data set here analyzed corresponds to mature plots belonging to beech, beech-fir, maritime pine, Scots pine and silver fir forests (see 3.1.1.1 Spanish mature forests, pp. 40-44). Among all the forest types, beech forest showed the lowest species richness with only one species (beech) in almost all cases (Figure 4.26 a). Species richness was higher

in the rest of forests, with no significant differences between these; altough Scots pine forests, with a median value of only one species, showed also similarities with beech forests. However, this forest type, together with maritime pine forests, covered the widest range of richness, determined by the inclusion of two biogeografical regions (Atlantic and Mediterranean) in the case of Scots pines, as previously observed (Figure 4.25). The lowest values of species mingling (M) corresponded to beech forests, as expected, and the highest values to beech-fir, due to its mixed forest condition, and there were no significant differences between the other forest types (Figure 4.26 b). In deadwod distribution (D), there were no large differences between forest types, highlighting the slightly lower mean value in beech and slightly higher mean value in silver fir (Figure 4.26 c). The former may be due to very light thinning related to firewood management in many areas, where weak trees are usually felled. In the case of silver fir, the effects of decay are probably reflected in the results (Camarero, 2017). Diameter differentiation (T) indicated differences between beech and silver fir forests, with mixed beech-fir identified as the most uneven-sized (Figure 4.26 d); the lowest values corresponded to pine forests (maritime and Scots pine), which were therefore more evenly sized. In the first case, the presence of shaded tolerant species, such as silver fir, enables the existence of two strata and therefore more differences in dbh size. By contrast, pine forests are more regular in structure due to their behaviour as pioneer species in these locations. However, the values were similar to those obtained for mature Scots pine forests in Estonia (Põldveer et al., 2020), which probably indicates that this is the characteristic structure of mature stands. Finally, the spatial arrangement evaluated by the uniform angle index (W), with mean values of around 0.45 for all forest types (Figure 4.26 e), indicated a characteristic random distribution in most plots (Pommerening, 2002). Regarding maturity, the highest degrees of naturalness, even with very different values of species mingling, were consistent with the highest values of diameter differentiation (old-growth > long untouched > mature, Figure 4.26 d), indicating that this structural feature may be used to distinguish different stage of maturity.

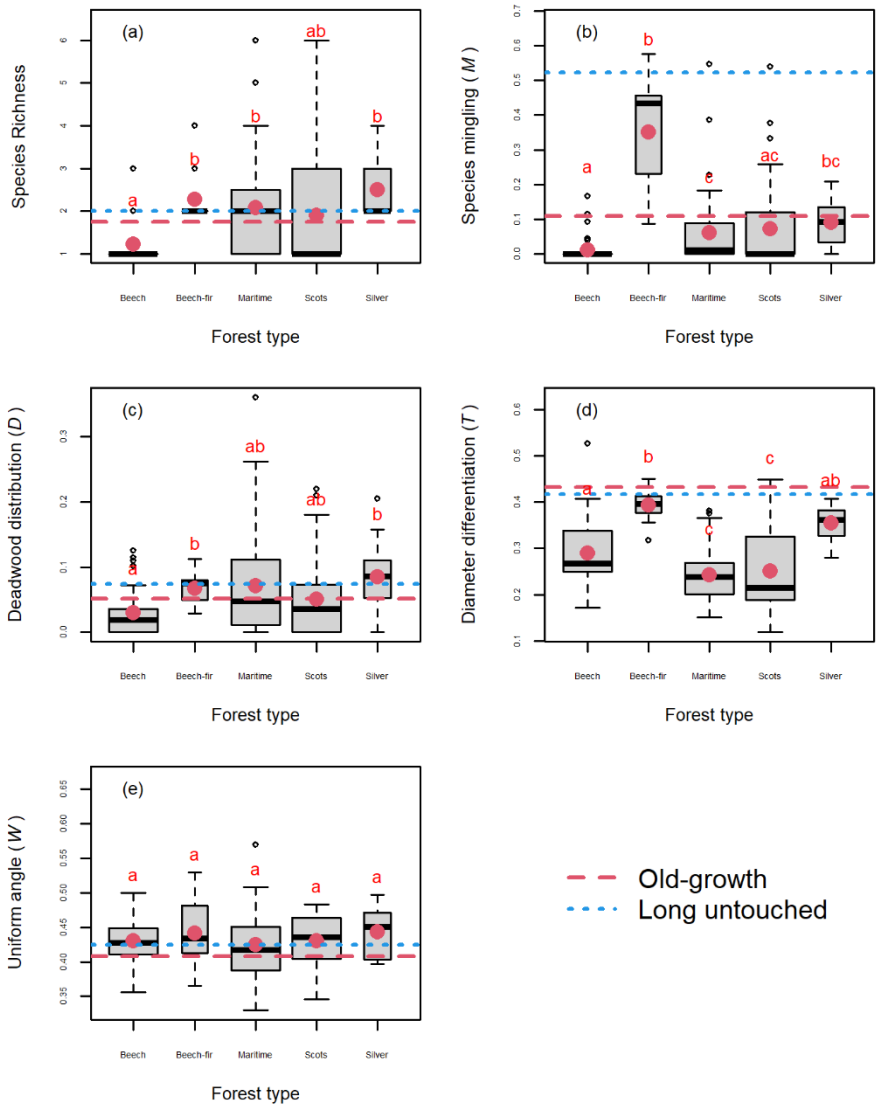

Figure 4.26. Structural indices of the five mature forest types (beech, beech-fir, maritime pine, Scots pine and silver fir). Indices: (a) species richness, (b) species mingling (M), (c) deadwood distribution (D), (d) diameter differentiation (T), and (e) uniform angle index (W). Red dots represent mean values. Dashed red lines represent old-growth forest (Aztaparreta site -AZ-) and dotted blue lines long untouched forest (Lizardoia site -LIZ-).

4.4 MODELLING RELATIONSHIPS BETWEEN FOREST MATURITY AND TERRESTRIAL LASER SCANNING (TLS)

4.4.1 Exploring the potential of FORTLS for assessing stand level variables

Although relative bias can be useful for assessing the accuracy of estimates, the presence of different stands, in some cases with non-identical structures, may compensate for positive and negative values of bias, thus leading to a misinterpretation of the results. However, the mean values may be useful for identifying possible trends in the different forest types. Conversely, relative $RMSE$ does not detect bias but provides information about the mean error and hence the precision of estimates. Overall, plot designs yielded different results according to the variables and forest types (Table 4.6), which may be related to different forest structures. Regarding N, in most cases k-tree plots yielded better results, in terms of bias and $RMSE(\%)$, with the latter showing values around 16% for all forest types, and plots without occlusion correction methods usually yielding more accurate estimates (Figure 4.27 a). Concerning bias, unlike Scots pine, the other forests yielded positive values (Figure 4.28 a). In the case of silver fir/beech-fir, the positive bias may be due to the shade tolerant behaviour of silver fir, which increases the presence of trees below the minimum dbh surveyed (7.5 cm). In that way, FORTLS could have identified trees below 7.5 cm in dbh as corrected due to overestimations of dbh, and therefore of N. On the other hand, the presence of low branches, which is common in silver fir trees, may have generated false tree detection. In maritime pine forests, the presence of shrub vegetation may have led to false detection of trees, being the first source of N overestimation. Beech and Scots pine forests yielded very low bias, which may be due to easier forest structure conditions to detect trees, as they are closer to even-aged/even-sized stands and contain less undergrowth vegetation. Unlike in the other forests, the bias values of 0.13% and -1.32% obtained for beech and Scots pine forests with k-tree plots (k = 10) and occlusion corrections were lower than the negative bias of 2% reported by Strahler et al. (2008), who relied on 8 angle-count plots located in a

Eucalyptus delagatensis and *Eucaluptus dalrympleana* dominated wet sclerophyll forest, with two distinct layers: a sparse upper layer and denser understory of shrubs and small trees. In any case, comparison of N estimates is ambiguous as most studies are based on tree detection rather than N estimation.

Table 4.6. Statistics obtained for all stand level variables estimated with single-scan TLS data processed with FORTLS.

	N			G			$\bar{d}$			$\bar{h}$		
	Bias (%)	*RMSE* (%)	r	*Bias* (%)	*RMSE* (%)	r	*Bias* (%)	*RMSE* (%)	r	*Bias* (%)	*RMSE* (%)	r
Silver fir / beech-fir												
Circular fixed area (n = 23)	7.15	**17.77**	0.84	**3.94**	**25.91**	0.49	-5.44	9.89	0.77	**-2.85**	**8.00**	0.79
	22.17	28.07	0.77	19.70	35.17	0.44						
k-tree (n = 23)	**3.87**	18.36	**0.88**	4.91	31.07	**0.55**	**-2.74**	14.25	0.78	-2.89	11.14	0.75
	9.78	21.68	**0.86**	10.83	32.70	0.52						
Angle count (n = 23)	-9.60	24.68	0.68	-28.78	30.34	0.43	-5.52	**7.49**	**0.83**	-16.60	16.60	**0.81**
	-8.71	24.51	0.68	-28.37	30.08	0.43						
Beech												
Circular fixed area (n = 40)	2.36	19.37	**0.78**	6.29	27.36	0.43	-2.35	10.64	**0.72**	6.12	10.00	0.85
	8.79	21.70	**0.78**	12.81	28.57	0.44						
k-tree (n = 39)	-3.25	**16.36**	0.61	-2.54	27.92	0.21	-2.84	14.47	0.51	7.98	11.52	0.80
	0.13	16.55	0.61	**0.92**	28.72	0.21						
Angle count (n = 40)	-6.24	29.27	0.71	-14.09	19.75	**0.58**	**2.26**	**7.91**	0.69	**-2.66**	**6.18**	**0.89**
	-5.59	29.29	0.71	-13.65	**19.63**	**0.58**						
Maritime pine												
Circular fixed area (n = 32)	-3.97	19.89	0.62	-29.38	29.54	0.62	-15.48	16.78	0.61	2.56	5.26	0.88
	2.82	22.73	0.62	**-24.40**	**25.96**	0.62						
k-tree (n = 30)	-8.72	16.54	**0.71**	-33.57	33.74	**0.65**	-15.89	16.76	0.61	4.29	6.77	0.83
	-5.68	**16.12**	0.70	-31.30	31.80	0.64						
Angle count (n = 31)	-12.21	19.87	0.44	-32.52	32.52	0.47	**-8.70**	**9.32**	**0.77**	**-1.74**	**3.54**	**0.96**
	-11.71	19.85	0.44	-32.20	32.23	0.47						
Scots pine												
Circular fixed area (n = 40)	-12.22	23.12	0.83	-26.74	28.46	0.79	-10.53	12.10	0.82	**1.68**	6.07	0.94
	-3.61	25.27	0.83	-19.56	25.35	0.79						
k-tree (n = 35)	-6.25	**15.73**	0.80	-21.14	25.95	**0.84**	-9.60	12.81	0.81	2.88	7.53	**0.98**
	-1.32	16.72	0.80	**-16.90**	**24.13**	**0.84**						
Angle count (n = 37)	-8.27	21.45	**0.85**	-27.34	28.17	0.78	**-5.61**	**7.72**	**0.89**	-3.87	**4.64**	0.96
	-7.68	21.47	**0.85**	-26.99	27.85	0.78						

Circular fixed area plot corresponds to 15 m radius, k-tree plots to k = 10 trees, and angle-count to BAF = 1.5.

Regarding G, none of the plot designs were consistently superior, although in most cases applying occlusions correction methods improved the estimates. The $RMSE(\%)$ values were around 25% in most cases, decreasing to 20% for beech forests (Figure 4.27 b). Bias was positive, below 5% in silver fir/beech-fir and approximately 1% in beech forests (Figure 4.28 b), probably due to the low bias in N and $\bar{d}$, which are directly involved in G estimation. By contrast, pine forests

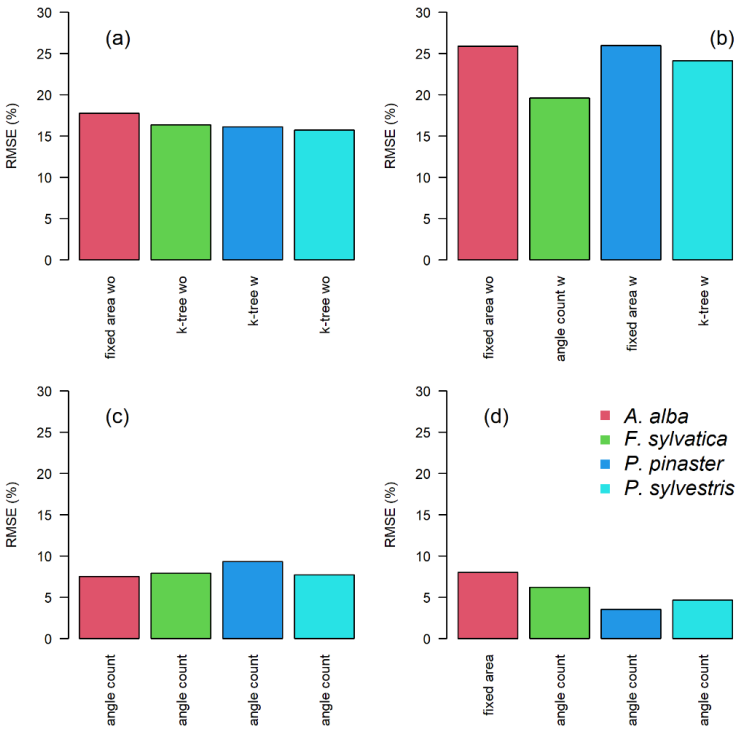

Figure 4.27. Bar plots representing relative $RMSE(\%)$ for the stand level variables according to different plot designs with (w) and without (wo) occlusion corrections: (a) density (N), (b) basal area (G), (c) mean arithmetic dbh ($\bar{d}$), and (d) mean arithmetic height ($\bar{h}$). Bars correspond to silver fir and beech-fir (red), beech (green), maritime pine (blue) and Scots pine (cyan) forests from left to right.

showed large negative biases in accordance with negative biases also in $\bar{d}$, although $RMSE(\%)$ values were not much higher than in other forests. However, it should be noted that all $RMSE(\%)$ values were higher than reported in previous studies based on the single-scan approach, e.g. Seidel and Ammer (2014) reported a relative mean absolute error of 8.4%, obtained by applying the correction of shadowing effect for dense short rotation poplar stands, measured by 15 randomly distributed fixed circular plots of radius 2 m. Other studies, such as that by Lovell et al. (2011), displayed values of 4.41% and 3.13% for plots of 50 and 20 m radius located in a 30-year-old *Pinus ponderosa* plantation and 25-year-old *P. radiata* plantation respectively, and using angle-count plot design with occlusions correction based on Poisson attenuation models. In any case, the forests assessed here represent challenging sampling conditions because of their maturity and lack of management, with twisted trees and the presence of undergrowth vegetation in many cases.

Regarding $\bar{d}$, the $RMSE(\%)$ values were much lower than for previous variables (between 5% and 10%) and slightly higher for maritime pine forests, probably due to the more irregular stem shape (Figure 4.27 c). In this case, angle-count plots always yielded better results. Unlike all conifer species, only beech forests showed positive and low bias probably because of smoother bark and more cylindrical stem shape (Figure 4.28 c). On the other hand, maritime pine, which has a rougher bark than the other species, yielded the highest negative bias and greatest $RMSE(\%)$ for $\bar{d}$. This may be thanks to the algorithm involved in dbh estimation, which considered all points of tree section to estimate dbh, thus also including points corresponding to the bark cavities, which are ignored when measurements are made with tape or calliper in the field. However, the $RMSE(\%)$ values were quite similar for all species, indicating similar accuracy in all cases. Although few studies have assessed variables at stand level and with the single-scan approach, extrapolation of these results to tree level shows that they are consistent with some of the most accurate algorithms, which yield $RMSE(\%)$ values below 10% with conservative algorithms in single-scan mode (Liang et al., 2018a). According to stand level, bias was always lower than the positive bias of 11% reported by Strahler et al.

(2008) for 8 angle-count plots located in a *E. delagatensis* and *E. dalrympleana* dominated wet sclerophyll forest, after using Poisson attenuation model corrections. Finally, and as expected, $\bar{h}$ showed negative bias in most cases due to occlusions in the top parts of the crowns. However, Scots pine plots showed positive bias probably as a result of the occurrence of less dense stands and therefore, a bigger probability of reaching the highest parts of the trees. In any case, the

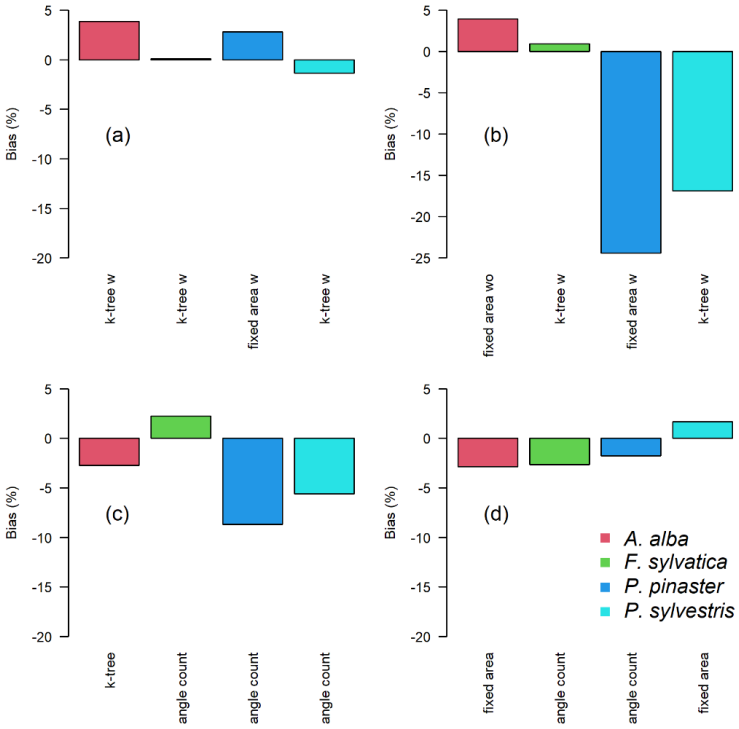

Figure 4.28. Bar plots representing relative bias (%) for the stand level variables according to different plot designs with (w) and without (wo) occlusion corrections: (a) density (N), (b) basal area (G), (c) mean arithmetic dbh ($\bar{d}$) and (d) mean arithmetic height ($\bar{h}$). Bars correspond to silver fir and beech-fir (red), beech (green), maritime pine (blue) and Scots pine (cyan) forests from left to right.

algorithm implemented in FORTLS to estimate h is based on the Voronoi polygons formed by trees detected. So, on the one hand, the accuracy of estimation depends on the success of tree detection, and on

the other hand, multi-layer forests are more susceptible to poor estimates because branches located above supressed trees can be included in h estimation. This applied to silver fir/beech-fir forests, which yielded the highest $RMSE(\%)$ not only because of multi-layer conditions in some cases, but also due to its higher h and denser crown foliage, which hampered the top parts of the crowns being reached with TLS. The best findings recorded in Liang et al. (2018a) yielded $RMSE(\%)$ values of 12-13% with single-scan mode and easy conditions. However, these findings were assessed at tree level rather than at stand level as in this thesis. Even in studies using multi-scan approaches (located systematically at 44 × 44 m in a 2.4 ha) and very high resolution (2 mm aperture at 10 m from TLS) located in a canopy with highly variable openness and dominated by sessile oak (*Quercus petraea* Matt.) with a mixture of other broadleaf species, bias in $\bar{h}$ estimation was negative (-0.8%) (Tochta et al., 2017). Nevertheless, $\bar{h}$ estimates obtained from TLS single-scan approaches are not expected to be used as direct estimates. By contrast, $\bar{h}$ was the variable with highest correlations (Table 4.6), and linear model approaches are thus useful for estimation of this variable. Hence, Scots pine plots showed the highest correlations and may be considered appropriate for model-assisted survey sampling.

From these findings, we can deduce that angle-count plots were generally better for estimating $\bar{d}$ and $\bar{h}$, probably because trees are selected according to their size, and small trees were thus less likely be detected. On the other hand, k-tree plots were better for N estimation, probably because of the high probability of detecting the closest trees. In the case of G, either fixed area or k-tree plots were the best designs, depending on the forest type. Finally, methods with occlusion corrections usually yielded better results for bias, while this was not as clear in terms of $RMSE(\%)$, especially for N estimation. In any case, as most research focuses on individual trees rather than stands, there are few studies available for comparison of stand level variables, especially with single-scan TLS approaches.

4.4.2 Assessing biomass stock with TLS metrics

The model fit including live tree biomass (LTB) as the response variable and FORTLS metrics/variables as auxiliary variables performed well for all species and most plot designs in terms of R^2 (above 0.8), especially with multivariate adaptive regression splines (MARS) and multiple linear models (MLM) (Figure 4.29). However, stable regions with high values of R^2 for wide ranges of plot sizes were not always found, with angle-count and k-tree plots generally yielding better results in this respect. By contrast, circular fixed area plot design showed more irregular behaviour through regular increments in radius.

In most cases the best plot design consisted of angle-count plots with BAF of 0.5. This applied to beech and Scots pine forests, with R^2 values of 0.95 and 0.94 respectively and Pearson correlation coefficients (r) of 0.97 comparing biomass estimates based on field data with fitted values in both cases (Figures 4.30 b and d). For silver fir/beech-fir forests, the R^2 value was 0.92 with a correlation of 0.96 (Figure 4.30 a). Finally, in the only case selected as a k-tree plot, maritime pine forests, yielded a R^2 value of 0.93 with a correlation of 0.96 (Figure 4.30 c).

Although there are few previous studies with which to compare these results, because most studies are based on tree level biomass estimates, our findings can be compared with those reported by Yao et al. (2011), who evaluated estimates of aboveground standing biomass at stand level. The authors estimated the reference value of biomass from field measurements by means of allometric equations (the same methodology as used here) relative to its counterpart estimated from TLS single-scan measurements also by means of allometric equations at stand level (using d_g as explanatory variable). Fitting biomass estimated from field data against fitted values from TLS for 28 plots of conifer and broadleaf species yielded a $RMSE$ of 21.54 Mg ha^{-1} and R^2 of 0.85 (i.e. r = 0.92). However, focusing on site level, the R^2 increased to 0.97 (i.e. r = 0.99).

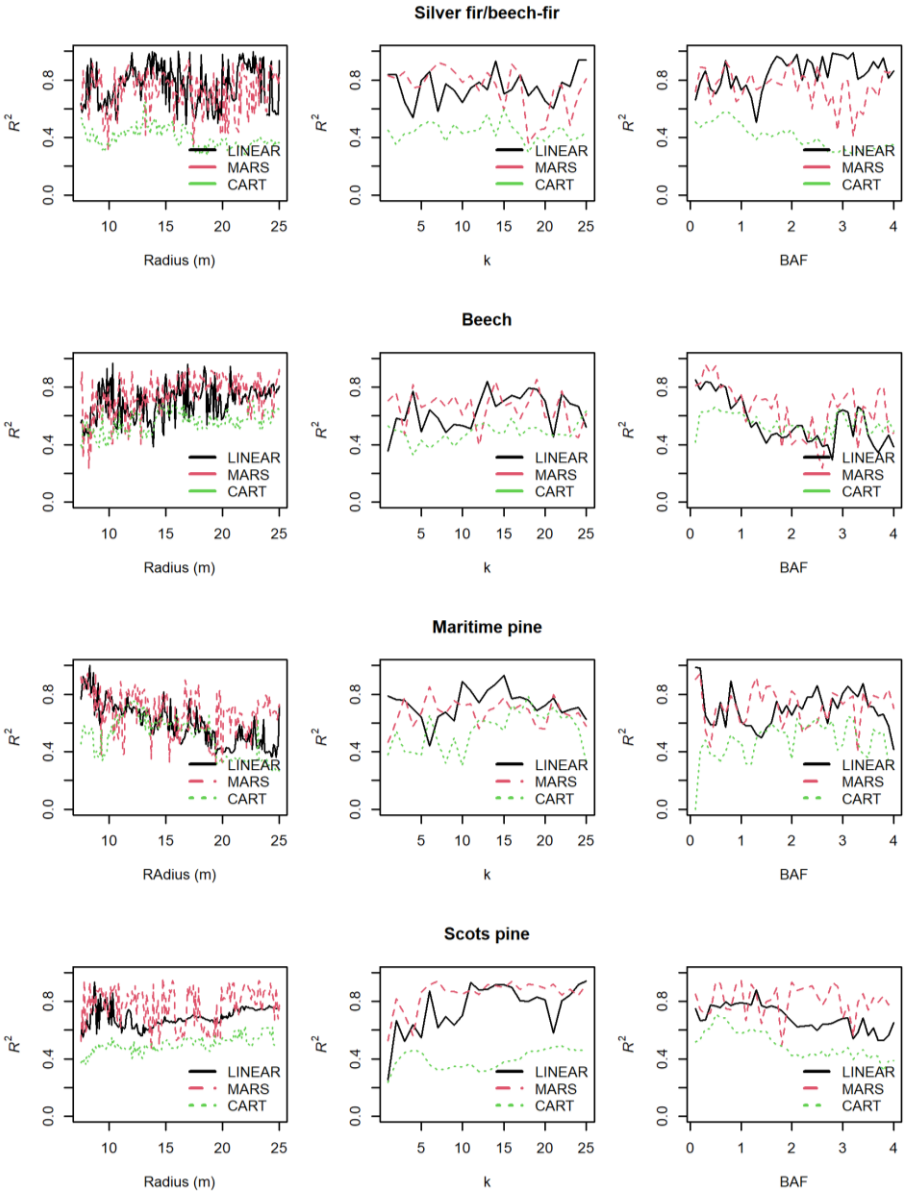

Figure 4.29. Line charts representing R^2 values obtained by fitting live tree biomass (LTB, Mg ha^{-1}) with FORTLS metrics and variables with multiple linear (black lines), MARS (red dashed lines) and CART (green dotted lines) models through regular plot size increments for circular fixed area (first column), k-tree (second column) and angle-count (third column) plots.

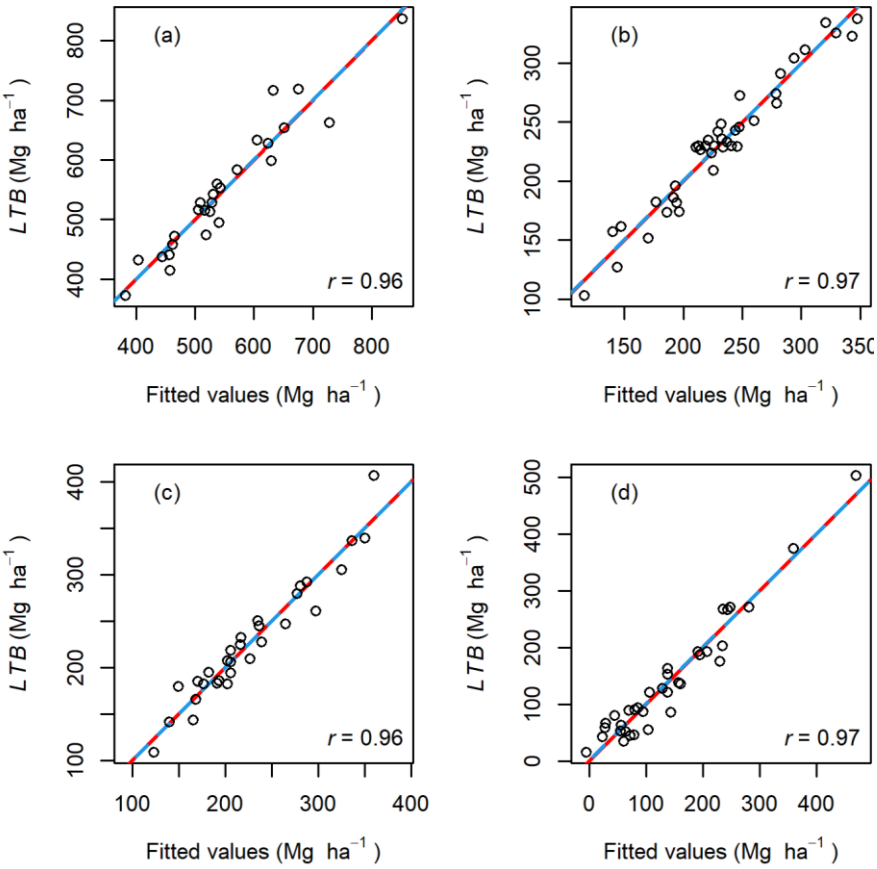

Figure 4.30. Scatter plots of live tree biomass (*LTB*) estimated from field data (Mg ha^{-1}) against *LTB* fitted values for (a) silver fir/beech-fir plots with a multiple linear model (MLM) and angle-count plot design of BAF = 2; (b) beech plots with multivariate adaptive regression splines (MARS) and angle-count plot design of BAF = 0.5; (c) Maritime pine plots with MLM and k-tree plot design of k = 15; and (d) Scots pine plots with MARS and angle-count plot design of BAF = 0.5. Red lines represent the linear model regressions, and blue dashed lines represent a 1:1 relationship. r is the Pearson correlation coefficient.

4.4.3 Assessing the degree of naturalness with FORTLS metrics

Among all plot designs, the angle-count plots again yielded the most stable results in terms of R^2 for values of BAF between 1.5 and 2 approximately (Figure 4.31).

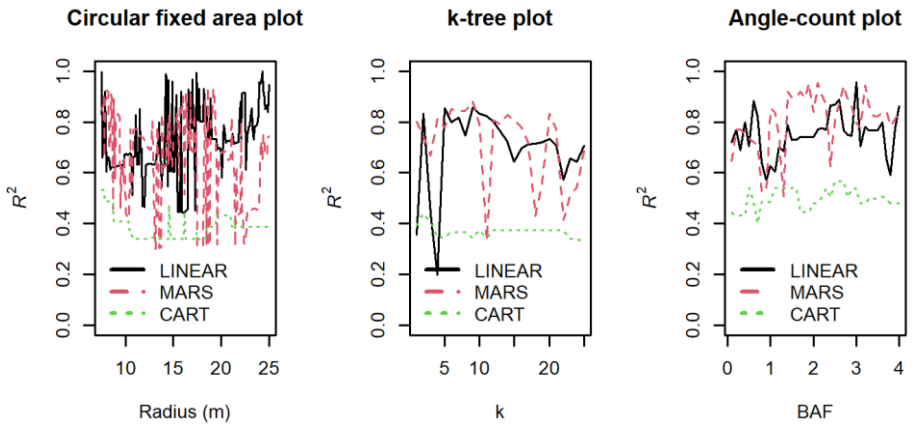

Figure 4.31. Line charts representing R^2 values yielded by fitting naturalness score (NS) with FORTLS metrics and variables with multiple linear (black lines), MARS (dashed red lines) and CART (dotted green lines) models through regular plot size increments for (a) circular fixed area, (b) k-tree and (c) angle-count plots.

One of the highest R^2 values (0.95) was yielded by MARS models and a BAF value of 1.9. For those conditions a correlation of 0.97 between naturalness score (NS) and fitted values (Figure 4.32) was observed. Although high values of R^2 were sometimes reached for the other plot designs (Figure 4.31), the angle-count plots yielded the best performance. This plot design, which applies to every tree included in the survey with its own expansion factor determined by the dbh and distance to plot centre, yielded similar accuracy as fixed area plots, or even higher accuracy in stands of Mediterranean forests with multiple strata and open structures (Piqué et al., 2017). Although this is a preliminary approach, these findings suggest that the degree of naturalness assessed by NS may be estimated using TLS single scans, by means of predictive fitted models. However, additional study cases covering a wider range of degrees of naturalness should be explored in order to determine whether this relationship applies to a wider NS range. Furthermore, other naturalness indices such as the structural complexity index (Zenner, 1998), which is easier to calculate with common forest inventory measurements, can be used to increase the spatial scale for implementation. In any case, estimating naturalness

with TLS, assessed here by the single-scan approach, may facilitate the task, which is difficult to achieve with conventional NFI data (McRoberts et al., 2012).

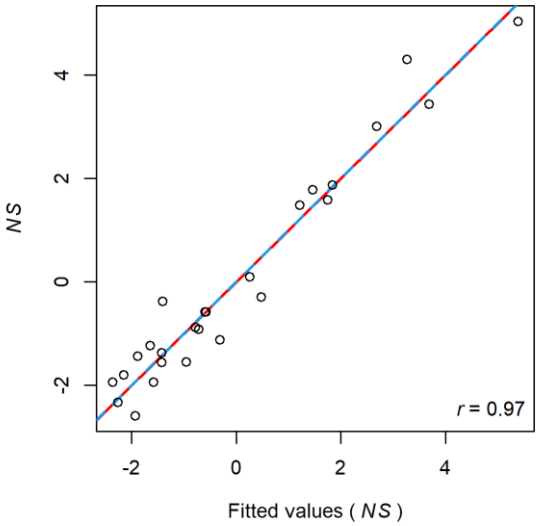

Figure 4.32. Scatter plot of naturalness score (*NS*) estimated from dendrochronology data at plot level, against *NS* fitted values with MARS and angle-count plot of BAF = 1.9. The red line represents the linear model regressions, and the blue dashed line represents the 1:1 relationship.

Other maturity indicators, in terms of biomass stock, such as the $BS(\%)$ developed in this thesis, also showed different behaviour in the fitted models depending on plot design and forest type (Figure 4.33). In general, MARS models performed better in most cases, showing smoother behavior in R^2. As before, stable regions with high values of R^2 for wide ranges of plot sizes were not always found, with angle-count and k-tree plots generally yielding better results in this respect. By contrast, circular fixed area plot design showed more irregular behaviour through regular increments in radius.

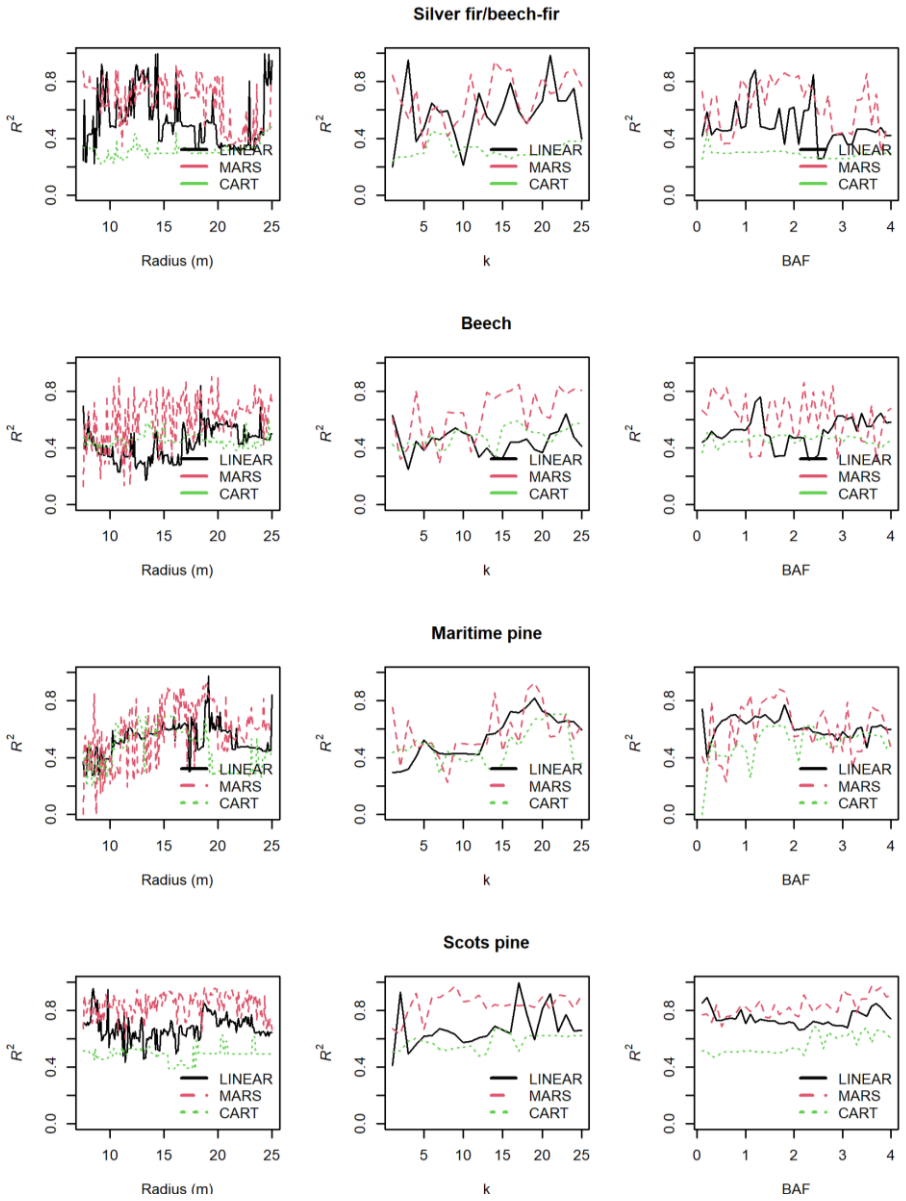

Figure 4.33. Line charts representing R^2 values yielded by fitting maximum biomass Stock (MBS) with FORTLS metrics and variables with multiple linear (black lines), MARS (dashed red lines) and CART (dotted green lines) models through regular plot size increments for circular fixed area (first column), k-tree (second column) and angle-count (third column) plots.

One of the best results was achieved for a k-tree plot design of k = 14, with the correlation between $BS(\%)$ and the fitted values reached 0.97 (Figure 4.34 a). The k-tree plots with around 15 trees yielded the most stable estimation for beech forests in terms of R^2, with correlation correlation of 0.91 (Figure 4.34 b). In the case of maritime pine, angle-count plots with values of BAF between 1 and 2 yielded the best performance, reaching a correlation of 0.96 for BAF = 1.8 (Figure 4.34 c). Finally, k-tree plots and angle-count also yielded the best performance for Scots pine forests, with R^2 values close to 1, and a correlation of 0.97 for k = 15 trees (Figure 4.34 d).

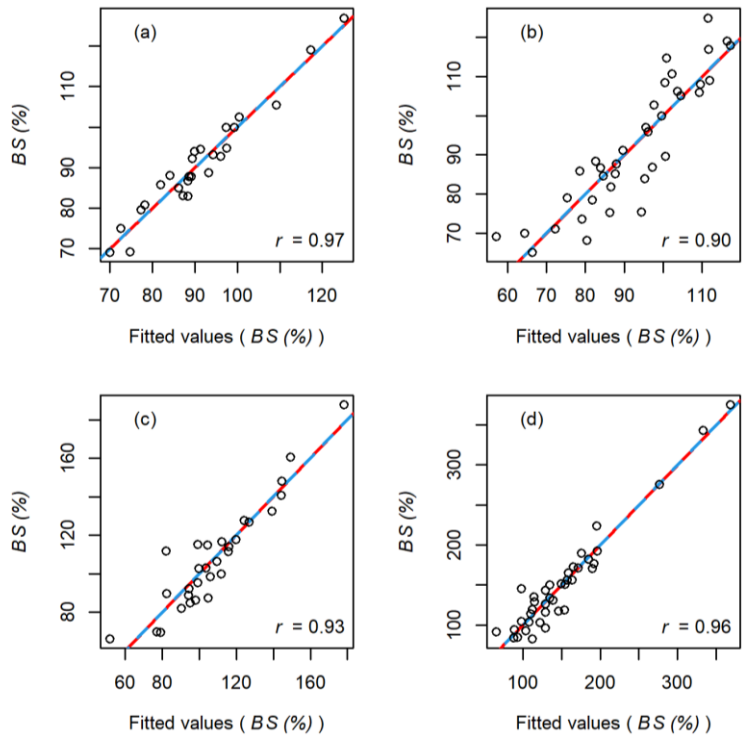

Figure 4.34. Scatter plots of relative biomass stock ($BS(\%)$) against $BS(\%)$ fitted values for (a) silver fir/beech-fir plots with MARS and k-tree plot design of k = 14, (b) beech plots with MARS and k-tree plot design of k = 16, (c) maritime pine plots with MARS model and angle-count plot design of BAF = 1.8, and (d) Scots pine plots with MARS and circular fixed area plot design of radius = 15 m. The red lines represent the linear model regressions, and the blue dashed lines represent the 1:1 relationship.

4.4.4 Exploring the potential of FORTLS metrics and variables for assessing maturity

According to the most important groups of explanatory variables for predicting maturity features (LTB, NS and $BS(\%)$), in all cases metrics (n, z, rho and r) played a more important role than variables (N, G, V, d, h) (Figure 4.35). Specifically, this applied to metrics related to descriptive statistics of z, ρ (rho) and r coordinates, with the latter being the less relevant in general, especially for LTB estimation. Metrics related to rho and z were mostly predominant in the fitted models. However, the fact that metrics based on z coordinate shown importance in LTB and $BS(\%)$ estimates, makes sense as tree heights are directly related to trees biomass and therefore with stand volume productivity (Burkhart and Tomé, 2012).

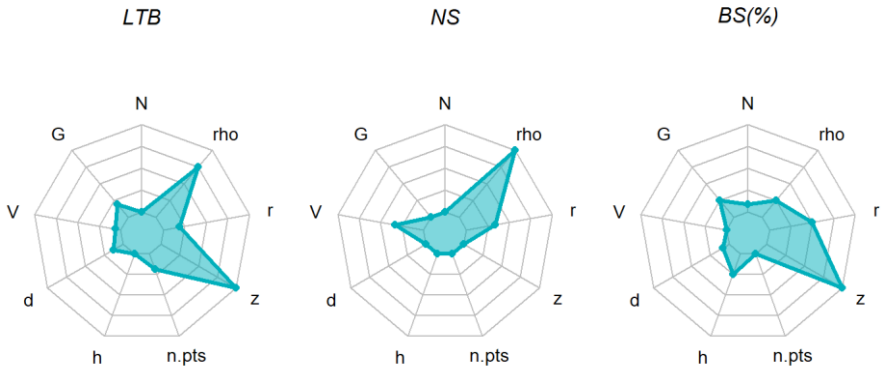

Figure 4.35. Star plot sowing the most influential group of explanatory variables to estimate live tree biomass (LTB) (left), naturalness score (NS) (middle), and relative biomass stock ($BS(\%)$) (right). The groups of variables included in the figure (G, V, d, h, n, z, rho and r) are explained in Table 3.17, pp. 100-101.

In the case of NS, the fact that the metrics related to the rho coordinate (i.e. horizontal heterogeneity) performed better was consistent with previous findings, by e.g. Seidel et al. (2016). These authors found that mean distance of the recorded hits in near-horizontal directions (±2º above/below horizon) performed better than other metrics for classifying forest of different degrees of naturalness

(including old-growth forest). In fact, the system performed well even when assessed by azimuthal sectors, unlike other metrics, which means that it is stable in all directions. Therefore, this is also consistent with the findings of previous studies in which old-growth stands forests were considered to have the highest variability in horizontal structural (Franklin and Van Pelt, 2004).

In summary, there is no optimum plot design for all forests and variables of interest, although angle-count plots generally performed better. Anyhow, some of the further research issues involving TLS single-scan approaches may be related to sampling design, in addition to improving the algorithm efficiency for detecting the maximum number of trees possible. In this sense, FORTLS offers the possibility of assessing three different plot designs as well as generating many metrics and variables capable of being related to important forest attributes by means of statistical models.

5. CONCLUSIONS

5 CONCLUSIONS

This section summarises the main achievements of the doctoral research. The following conclusions refer to the most relevant findings and hypotheses raised:

1. Site form (SF), the expected dominant height for a reference dominant diameter, is a potentially reliable estimator of site quality, performing similarly to site index (SI) for pure, even-aged stands of *Pinus radiata*. Unlike SI, SF works well in uneven-aged stands and is not based on stand age and could therefore be used in the absence of this variable or when it is costly to obtain in forest inventories. Furthermore, the possibility of estimating SF from conventional National Forest Inventory (NFI) data covering large scales makes this a valuable indicator for forest policy decision-making, where the scale of the predictions requires low-input indices. Nevertheless, further research using data on other species (especially those for which SI modelling has performed well) and that cover a wide range of management regimes and development stages, is advisable to consolidate SF as a useful site quality index for even-aged stands.

2. Live tree biomass (LTB) in mixed and pure silver-fir and beech forests peaked at intermediate levels of naturalness in mature forests and did not increase further at higher levels. Thus, the maximum value of LTB storage may be reached at earlier stages than the old-growth stage, although all biomass pools should be evaluated for a more complete understanding of biomass storage as a function of naturalness. These findings, applied to data sets such as NFIs in which the probabilistic design ensures representative sampling (i.e. of the degree of naturalness observed in the target population), enable estimation of the state of LTB stock relative to the maximum biomass stock (MBS) potential (i.e. expressed

relative to site quality by means of SF). This information has evident consequences for carbon accounting and management (as the main component of biomass) and may be useful in developing forest policies for carbon sequestration aimed at mitigating climate change. Although mature forests display the highest values of biomass accumulation, further research is required to address the changes in biomass and carbon dynamics in old-growth forests.

3. Mature forests display differences in structural characteristics according to biogeographical conditions and species composition. Tree species richness can be affected by forest type, as demonstrated by the low values obtained for beech forests, and also by the biogeographical region, with the Mediterranean region clearly yielding the lowest values in mature Scots pine forests. Regarding tree species mingling, the presence of shade tolerant species was found to be the main reason causing a high degree of this structural feature. Standing deadwood distribution was closely related to stand density (trees ha^{-1}), with the greatest values corresponding to high density and vice versa. Diameter differentiation, which can be influenced by many features (e.g. stand density, tree species mingling, etc.), followed an intraspecific gradient related to latitude shifting (Boreal > Atlantic > Mediterranean) and also an interspecific gradient (Beech-fir > silver fir > beech > pine forests), with similarities in both pine forests. Finally, in all cases (intra and interspecific gradients), horizontal tree arrangements were not significantly different, and the distribution was almost random. Regarding maturity, the degree of naturalness was directly related to diameter differentiation, indicating that this structural feature can be used to distinguish stages of maturity in the case study.

4. Despite the different types of forest considered in this doctoral research, the R package FORTLS proved useful for processing TLS single-scan data for forestry purposes. Estimates were obtained for conventional variables in mature forests similar to those measured by state-of-the-art techniques. Furthermore, more

accurate estimates can be provided by fitting predictive models with the set of metrics and variables generated by FORTLS. Thus, even more complex variables such as the relative biomass stock ($BS(\%)$) and the degree of naturalness (or maturity) can be predicted. In this regard, the MARS models performed best, followed by multiple linear models. In addition, these approaches have the advantage of being flexible enough to adapt to the best possible plot design for each variable by allowing the inclusion of different plot designs. Altogether these findings reveal the benefits of using TLS devices in forest inventories (especially NFIs), which may be important for many of the new European forest strategy objectives (e.g. protecting the EU's last remaining primary and old-growth forests). Further research considering larger and more complex case studies is necessary to consolidate FORTLS as an operational tool in forest inventories and also to develop new metrics and variables.

6. REFERENCES

6 REFERENCES

Adame, P., del Río, M., and Canellas, I. (2008). A mixed nonlinear height–diameter model for pyrenean oak (Quercus pyrenaica Willd.). *Forest Ecology and Management*, *256*(1-2), 88-98.

Adeyemi, A. A. (2016). Site quality assessment and allometric models for tree species in the Oban Forest, Nigeria. *Journal of Sustainable Forestry*, *35*(4), 280–298.

Adlard, P. G. (1980). Growing stock levels and productivity conclusions from thinning and spacing trials in young Pinus patula stands in Southern Tanzania. Commenwealth Forestry Institute, University of Oxford.

Aguirre, A., Moreno-Fernández, D., Alberdi, I., Hernández, L., Adame, P., Cañellas, I., and Montes, F. (2022). Mapping forest site quality at national level. *Forest Ecology and Management*, *508*, 120043.

Aguirre, O., Hui, G., von Gadow, K., and Jiménez, J. (2003). An analysis of spatial forest structure using neighbourhood-based variables. *Forest Ecology and Management*, *183*(1-3), 137-145.

Ahmadi K., Alavi S. J., and Kouchaksaraei, M. T. (2017). Constructing site quality curves and productivity assessment for uneven-aged and mixed stands of oriental beech (*Fagus oriental* Lipsky) in Hyrcanian forest, Iran. *Forest Science and Technology*, *13*(1),41–46.

Alberdi, I., Condés Ruiz, S., Martínez Millán, J., Martínez de Toda, S., Sánchez Peña, G., Pérez Martín, F., Villanueva Aranguren, J. A., and Vallejo Bombín, R. (2010). Spain. In E. Tomppo, T. Gschwantner, M. Lawrence, and R. E. McRoberts (Eds.), *National Forest Inventories* (pp. 527–540). Springer, Dordrecht.

Alberdi, I., Vallejo Bombín, R., Álvarez-González, J. G., Condés Ruiz, S., González-Ferreiro, E., Guerrero García, S., … and Cañellas, I. (2017). The multi-objective Spanish National Forest Inventory. *Forest Systems*, *26*(2), 1–17.

Alberdi, I., Nunes, L., Kovac, M., Bonheme, I., Cañellas, I., Rego, F. C., ... and Gasparini, P. (2019). The conservation status assessment of Natura 2000 forest habitats in Europe: capabilities, potentials and challenges of national forest inventories data. *Annals of Forest Science*, *76*(2), 1-15.

Angelsen, A., Brockhaus, M., Sunderlin, W. D., and Verchot, L. V. (Eds.) (2012). *Analysisg REDD+: Challenges and choices*. CIFOR.

Alía, R., Moro, J., and Denis, J. B. (1997). Performance of *Pinus pinaster* provenances in Spain: interpretation of the genotype by environment interaction. *Canadian Journal of Forest Research*, *27*(10), 1548–1559.

Alía, R., Martín Albertos, S., De Miguel Y Del Ángel, J., Galera Peral, R. M., Agúndez Leal, D., Gordo Alonso, J., Salvador Nemoz, L., Catalán Bachiller, G., Gil Sánchez, L. A. (1996). *Las regiones de procedencia de Pinus pinaster Aiton*. Organismo Autónomo Parques Nacionales

Altman, J., Fibich, P., Dolezal, J., and Aakala, T. (2014). TRADER: a package for tree ring analysis of disturbance events in R. *Dendrochronologia*, *32*(2), 107-112.

Aravind, H., (2020). olsrr: Tools for Building OLS Regression Models. R package version 0.5.3.

Arias-Rodil, M., Crecente-Campo, F., Barrio-Anta, M., and Diéguez-Aranda, U. (2015). Evaluation of age-independent methods of estimating site index and predicting height growth: a case study for maritime pine in Asturias (NW Spain). *European Journal of Forest Resarch, 134*(2), 223–233.

Assman, E. (1970). *The principles of forest yield study*. Pergamon Press.

Astrup, R., Ducey, M. J., Granhus, A., Ritter, T., and von Lüpke, N. (2014). Approaches for estimating stand-level volume using terrestrial laser scanning in a single-scan mode. *Canadian Journal of Forest Research*, *44*(6), 666-676.

Bailey, R. L., and Clutter, J. L. (1974). Base-age invariant polymorphic site curves. *Forest Science*, *20*(2), 155–159.

Bakuzis, E. V. (1969). The ecosystem concept in natural resource Management. *Forestry viewed in an ecosystem perspective* (pp. 189-258). Academic Press.

Barbati, A., Corona, P., and Marchetti, M. (2006). *European forest types. Categories and types for sustainable forest management and reporting*. EEA Technical report No. 9/2006. Office for Official Publications of the European Communities

Barbati, A., Corona, P., and Marchetti, M. (2010). *Annex to Enquiry: State of Forests and Sustainable Forest Management in Europe 2011. New European Forest Types*. Ministerial Conference of the Protection on Forests in Europe, Geneva, Italy.

Bates, D., and Eddelbuettel, D. (2013). Fast and Elegant Numerical Linear Algebra Using the RcppEigen Package. *Journal of Statistical Software*, *52*(5), 1-24.

Bauhus, J., Puettmann, K., and Messier, C. (2009). Silviculture for old-growth attributes. *Forest Ecology and Management*, *258*(4), 525-537.

Beltran, H. A., Chauchard, L., Velásquez, A., Sbrancia, R., and Pastur, G. M. (2016). Diametric site index: an alternative method to estimate site quality in Nothofagus obliqua and N. alpina forests. *Cerne*, *22*, 345–354.

Bergman, H. (2021). *Where are the forests with highest biomass in Sweden located?* [Bachelor´s degree thesis, Lund University]. Lund University Libraries

Bienert, A., Scheller, S., Keane, E., Mohan, F., and Nugent, C. (2007, September). Tree detection and diameter estimations by analysis of

forest terrestrial laser scanner point clouds. In *ISPRS workshop on laser scanning*, 36, 50-55. Espoo, Finland: IAPRS.

Bitterlich, W., 1948. *Die Winkelzählprobe. Allg. Forst-und Holzwirt. Zeitung Wien*, 59, 4–5

Bivand, R. S., Pebesma E., and Gómez-Rubio V. (2013). *Applied spatial data analysis with R, Second Edition*. Springer, NY.

Black, B. A., and Abrams, M. D. (2004). Development and application of boundary-line release criteria. *Dendrochronologia*, *22*(1), 31-42.

Bohn, U., Gollub, G., Hettwer, C., Neuhäuslová, Z., Raus, T., Schlüter, H., Weber, H., and Hennekens, S. (2000). *Map of the natural vegetation of Europe* [Map]. 1:2500000. Bonn: German Federal Agency for Nature conservation

Bonan, G. B. (2008). Forests and climate change: forcings, feedbacks, and the climate benefits of forests. *Science*, *320*(5882), 1444-1449.

Bončina, A., Trifković, V., and Bončina, Ž. (2021). Modeliranje višinske in debelinske rasti dominantnih dreves ter ocenjevanje indeksov produkcijske sposobnosti gozdnih rastišč. *Acta Silvae et Ligni*, *125*, 1-12.

Bormann, F. H., and Likens, G. E. (2012). *Pattern and process in a forested ecosystem*. Springer.

Bourquin-Mignot, C., and Girardclos, O. (2001). Construction d'une longue chronologie de hêtres au Pays-basque. La forêt d'Iraty et le Petit Âge Glaciaire. *Revue géographique des Pyrénées et du Sud-Ouest. Sud-Ouest Européen*, *11*(1), 59-71.

Bravo-Oviedo, A., Roig, S., Bravo, F., Montero, G., and del Río, M. (2011). Environmental variability and its relationship to site index in Mediterranean maritime pine. *Forest Systems*, *20*(1), 50–64.

Breiman, L., Friedman, J. H., Olshen, R. A., and Stone, C. J. (1984). *Classification and regression trees*. Routledge.

Brumelis, G., Jonsson, B. G., Kouki, J., Kuuluvainen, T., and Shorohova, E. (2011). Forest naturalness in northern Europe:

perspectives on processes, structures and species diversity. *Silva Fennica*, *45*(5), 807-821.

Brunner, A., and Gizachew, B. (2014). Rapid detection of stand density, tree positions, and tree diameter with a 2D terrestrial laser scanner. *European Journal of Forest Research*, *133*(5), 819-831.

Buchwald, E. (2005). A hierarchical terminology for more or less natural forests in relation to sustainable management and biodiversity conservation. In *Third expert meeting on harmonizing forest-related definitions for use by various stakeholders. Proceedings. Food and Agriculture Organization of the United Nations*, 111-127. Rome.

Buda, N. J., and Wang, J. R. (2006). Suitability of two methods of evaluating site quality for sugar maple in Central Ontario. *The Forestry Chronicle*, *82*(5), 733-744.

Bunn, A. G. (2008). A dendrochronology program library in R (dplR). *Dendrochronologia*, *26*(2), 115-124.

Buckland, S. T., Anderson, D. R., Burnham, K. P., Laake, J. L., Borchers, D. L., and Thomas, L. (2001). Introduction to distance sampling: estimating abundance of biological populations. Oxford University Press.

Bugmann, H., and Bigler, C. (2011). Will the CO_2 fertilization effect in forests be offset by reduced tree longevity? *Oecologia*, *165*(2), 533–544.

Büntgen, U., Krusic, P. J., Piermattei, A., Coomes, D. A., Esper, J., Myglan, V. S., Kirdyanov, A. V., Camarero, J. J., Crivellaro, A., Körner, C. (2019). Limited capacity of tree growth to mitigate the global greenhouse effect under predicted warming. *Nature communications*, *10*(1), 1-6.

Burkhart, H. E., and Tomé, M. (2012). Modeling Forest trees and stands. Springer.

Burrascano, S., Keeton, W. S., Sabatini, F. M., & Blasi, C. (2013). Commonality and variability in the structural attributes of moist

temperate old-growth forests: A global review. *Forest Ecology and Management*, *291*, 458-479.

Bušs, K. (1976). Fundamentals of forest classification in Latvia SSR. *Riga, Silava*.

Cabo, C., Ordóñez, C., López-Sánchez, C. A., and Armesto, J. (2018). Automatic dendrometry: Tree detection, tree height and diameter estimation using terrestrial laser scanning. *International Journal of Applied Earth Observation and Geoinformation*, *69*, 164-174.

Cabrera, M. (2001). Evolución de abetares del Pirineo aragonés. *Cuadernos de la Sociedad Española de Ciencias Forestales*, *11*, 43-52.

Calama, R., and Montero, G. (2004). Interregional nonlinear height diameter model with random coefficients for stone pine in Spain. *Canadian Journal of Forest Research*, *34*(1), 150-163.

Calders, K., Schenkels, T., Bartholomeus, H., Armston, J., Verbesselt, J., and Herold, M. (2015). Monitoring spring phenology with high temporal resolution terrestrial LiDAR measurements. *Agricultural and Forest Meteorology*, *203*, 158-168.

Calders, K., Adams, J., Armston, J., Bartholomeus, H., Bauwens, S., Bentley, L. P., ... and Verbeeck, H. (2020). Terrestrial laser scanning in forest ecology: Expanding the horizon. *Remote Sensing of Environment*, *251*, 112102.

Camarero, J. J. (2017). The multiple factors explaining decline in mountain forests: historical logging and warming-related drought stress is causing silver-fir dieback in the Aragón Pyrenees. In *High mountain conservation in a changing world* (pp. 131-154). Springer Nature.

Camarero, J. J., Bigler, C., Linares, J. C., and Gil-Pelegrín, E. (2011). Synergistic effects of past historical logging and drought on the decline of Pyrenean silver fir forests. *Forest Ecology and Management*, *262*(5), 759-769.

Campos, M. B., Litkey, P., Wang, Y., Chen, Y., Hyyti, H., Hyyppä, J., and Puttonen, E. (2021). A long-term terrestrial laser scanning

measurement station to continuously monitor structural and phenological dynamics of boreal forest canopy. *Frontiers in Plant Science*, *11*, 2132.

Carey, E. V., Sala, A., Keane, R., and Callaway, R. M. (2001). Are old forests underestimated as global carbon sinks? *Global Change Biology*, *7*(4), 339-344.

Castedo-Dorado, F., Dieguez-Aranda, U., and Álvarez-González, J. G. (2007). A growth model for Pinus radiata D. Don stands in North-Western Spain. *Annals of Forest Science*, *64*(4), 453–465.

Chiarucci, A., and Piovesan, G. (2020). Need for a global map of forest naturalness for a sustainable future. *Conservation Biology*, *34*(2), 368-372.

Chirici, G., Giannetti, F., McRoberts, R. E., Travaglini, D., Pecchi, M., Maselli, F., ... and Corona, P. (2020). Wall-to-wall spatial prediction of growing stock volume based on Italian National Forest Inventory plots and remotely sensed data. *International Journal of Applied Earth Observation and Geoinformation*, *84*, 101959.

Cieszewski, C. J., and Bailey, R. L. (2000). Generalized algebraic difference approach: theory based derivation of dynamic site equations with polymorphism and variable asymptotes. *Forest Science*, *46*(1), 116–126.

Cieszewski, C. J., Harrison, M., and Martin, S. W. (2000). Practical methods for estimating non-biased parameters in self-referencing growth and yield models. *University of Georgia PMRC-TR*, *7*(11).

Cieszewski, C. J. (2002). Comparing fixed- and variable-base-age site equations having single versus multiple asymptotes. *Forest Science*, *48*(1), 7-23.

Clark, R. G. (2016). Statistical efficiency in distance sampling. *PloS one*, *11*(3), e0149298.

Clutter, J. L., Fortson, J. C., Pienaar, L. V., Brister, G. H., and Bailey, R. L. (1983). *Timber management: a quantitative approach*. John Wiley & Sons

Connell, J. H. (1978). Diversity in tropical rain forests and coral reefs: high diversity of trees and corals is maintained only in a nonequilibrium state. *Science*, *199*(4335), 1302-1310.

Coops, N., Waring, R., and Landsberg, J. (1998). Assessing forest productivity in Australia and New Zealand using a physiologically-based model driven with averaged monthly weather data and satellite-derived estimates of canopy photosynthetic capacity. *Forest Ecology and Management*, *104*(1-3), 113-127.

COP21. (2015). The Paris Agreement. United Nations Framework Climate Change Conference (UNCCC). Paris

Copenheaver, C. A., Black, B. A., Stine, M. B., McManamay, R. H., and Bartens, J. (2009). Identifying dendroecological growth releases in American beech, jack pine, and white oak: within-tree sampling strategy. *Forest Ecology and Management*, *257*(11), 2235-2240.

Costa Tenorio, M., Morla Juaristi, C., and Sainz Ollero, H. (Eds.) (1997). *Los bosques ibéricos. Una interpretación geobotánica.* Editorial Planeta

Csárdi, G., and FitzJohn, R., (2019). progress: Terminal Progress Bars. R package version 1.2.2. https://CRAN.R-project.org/package=progress

Cuttelod, A., García, N., Malak, D. A., Temple, H. J., and Katariya, V. (2009). The Mediterranean: a biodiversity hotspot under threat. *Wildlife in a Changing World–an analysis of the 2008 IUCN Red List of Threatened Species*. IUCN

Dănescu, A., Albrecht, A. T., and Bauhus, J. (2016). Structural diversity promotes productivity of mixed, uneven-aged forests in southwestern Germany. *Oecologia*, *182*(2), 319-333.

Danson, F. M., Disney, M. I., Gaulton, R., Schaaf, C., and Strahler, A. (2018). The terrestrial laser scanning revolution in forest ecology. *Interface Focus*, *8*(2), 20180001.

Dassot, M., Constant, T., and Fournier, M. (2011). The use of terrestrial LiDAR technology in forest science: application fields, benefits and challenges. *Annals of Forest Science*, *68*(5), 959-974.

Dawkins, H. C. (1958). *The management of natural tropical high-forest with special reference to Uganda*. Oxford Imperial Forestry Institute

de Assis Barros, L., Venter, M., Elkin, C., and Venter, O. (2022). Managing forests for old-growth attributes better promotes the provision of ecosystem services than current age-based old-growth management. *Forest Ecology and Management*, *511*, 120130.

del Río, M., Pretzsch, H., Alberdi, I., Bielak, K., Bravo, F., Brunner, A., ... and Bravo-Oviedo, A. (2016). Characterization of the structure, dynamics, and productivity of mixed-species stands: review and perspectives. *European Journal of Forest Research*, *135*(1), 23-49.

Di Filippo, A., Biondi, F., Piovesan, G., and Ziaco, E. (2017). Tree ring-based metrics for assessing old-growth forest naturalness. *Journal of Applied Ecology*, *54*(3), 737-749.

Di Filippo, A., Pederson, N., Baliva, M., Brunetti, M., Dinella, A., Kitamura, K., ... and Piovesan, G. (2015). The longevity of broadleaf deciduous trees in Northern Hemisphere temperate forests: insights from tree-ring series. *Frontiers in Ecology and Evolution*, *3*, 46.

Diéguez-Aranda, U., Burkhart, H. E., and Rodríguez-Soalleiro, R. (2005). Modeling dominant height growth of radiata pine (Pinus radiata D. Don) plantations in North-Western Spain. *Forest Ecology and Management*, *215*, 271–284.

Diéguez, U., Rojo, A., Castedo, F., Álvarez, J., Barrio, M., Crecente, F., ... and Sánchez, F. (2009). *Herramientas selvícolas para la gestión forestal sostenible en Galici*a. Dirección Xeral de Montes, Consellería do Medio Rural, Xunta de Galicia.

Dieler, J., Uhl, E., Biber, P., Müller, J., Rötzer, T., and Pretzsch, H. (2017). Effect of forest stand management on species composition,

structural diversity, and productivity in the temperate zone of Europe. *European Journal of Forest Research, 136*(4), 739-766.

Disney, M. (2019). Terrestrial LiDAR: a three-dimensional revolution in how we look at trees. *New Phytologist, 222*(4), 1736-1741.

Dobbertin, M. (2002). Influence of stand structure and site factors on wind damage comparing the storms Vivian and Lothar. *Forest Snow and Landscape Research*, *77*(1/2), 187-205.

Drew, D. M. (2021). Exploring new frontiers in forecasting forest growth, yield and wood property variation. *Annals of Forest Science*, *78*(2), 1-2.

Duan, G., Gao, Z., Wang, Q. and Fu, L. (2018). Comparison of different height–diameter Modelling techniques for prediction of site productivity in natural uneven-aged pure stands. *Forests*, *9*(2), 63.

Dubayah, R. O., and Drake, J. B. (2000). Lidar remote sensing for forestry. *Journal of Forestry*, *98*(6), 44-46.

Ducey, M. J., and Astrup, R. (2013). Adjusting for nondetection in forest inventories derived from terrestrial laser scanning. *Canadian Journal of Remote Sensing*, *39*(5), 410-425.

Duncan, R. P. (1989). An evaluation of errors in tree age estimates based on increment cores in kahikatea (Dacrycarpus dacrydioides). *New Zealand Natural Sciences*, *16*, 31-37.

Dunn, O. J. (1961). Multiple comparisons among means. *Journal of the American statistical association*, *56*(293), 52-64.

Eddelbuettel, D. (2013). *Seamless R and C++ Integration with Rcpp*. Springer

Eddelbuettel, D., Balamuta, J. J. (2018). Extending R with C++: A Brief Introduction to Rcpp. *The American Statistician*, *72*(1), 28-36.

Eddelbuettel, D., and François, R. (2011). Rcpp: Seamless R and C++ Integration. Journal of Statistical Software, *40*(8), 1-18.

Ehbrecht, M., Schall, P., Ammer, C., and Seidel, D. (2017). Quantifying stand structural complexity and its relationship with forest

management, tree species diversity and microclimate. *Agricultural and Forest Meteorology*, *242*, 1-9.

Edminster, C. B., Mathiasen, R. L., Olsen, W. K. (1991). *A method for constructing site index curves from height-age measurements applied to Douglas-fir in the Southwest*. USDA Forest Service Research Note RM-510. Rocky Mountain Forest and Range Experiment Station, Ft. Collins, CO, 6 pp.

Ester, M., Kriegel, H. P., Sander, J., Xu, X. (1996). A density-based algorithm for discovering clusters in large spatial databases with noise. KDD'96: Proceedings of the Second International Conference on Knowledge Discovery and Data Mining, 226-231. Portland, Oregon

European Commission (2021). New EU Forest Strategy for 2030 [European Commission]. Brussels, 16.7.2021

European Environment Agency (2006). *Progress towards halting the loss of biodiversity by 2010* (Report No. 5/2006). Office for Official Publications of the European Communities

Fahey, T. J., Woodbury, P. B., Battles, J. J., Goodale, C. L., Hamburg, S. P., Ollinger, S. V., and Woodall, C. W. (2010). Forest carbon storage: ecology, management, and policy. *Frontiers in Ecology and the Environment*, *8*(5), 245-252.

FAO (2020). *Global Forest Resources Assessment 2020: Main report*. Food and Agriculture Organization of the United Nations.

Felipe-Lucia, M. R., Soliveres, S., Penone, C., Manning, P., van der Plas, F., Boch, S., ... and Allan, E. (2018). Multiple forest attributes underpin the supply of multiple ecosystem services. *Nature communications*, *9*(1), 1-11.

Felipe-Lucia, M. R., Soliveres, S., Penone, C., Fischer, M., Ammer, C., Boch, S., ... and Allan, E. (2020). Land-use intensity alters networks between biodiversity, ecosystem functions, and services. *Proceedings of the National Academy of Sciences*, *117*(45), 28140-28149.

Ferrara, R., Virdis, S. G., Ventura, A., Ghisu, T., Duce, P., and Pellizzaro, G. (2018). An automated approach for wood-leaf separation from terrestrial LIDAR point clouds using the density based clustering algorithm DBSCAN. *Agricultural and Forest Meteorology*, 262, 434-444.

Fisk, M. C., Zak, D. R., and Crow, T. R. (2002). Nitrogen storage and cycling in old-and second-growth northern hardwood forests. *Ecology*, *83*(1), 73-87.

Ford, S. E., and Keeton, W. S. (2017). Enhanced carbon storage through management for old-growth characteristics in northern hardwood-conifer forests. *Ecosphere*, *8*(4), e01721.

FORESCHANGE (2016). *Modelling the effects of intensity of perturbation on the structure of natural forests and their carbon stocks by using data from the National Forestry Inventory* (AGL2016-76769-C2-2-R) [National R&D&I Project]. State Research Agency cofunded by ERDF

Franco, J. D. A. (1997). *Pinus* L. In S. Castroviejo (Ed.), *Flora Ibérica* (Vol. 1, pp. 168-174). CSIC.

Franklin, J. F., and Van Pelt, R. (2004). Spatial aspects of structural complexity in old-growth forests. *Journal of Forestry*, *102*(3), 22-28.

Frelich, L. E., and Reich, P. B. (2003). Perspectives on development of definitions and values related to old-growth forests. *Environmental Reviews*, *11*(S1), S9-S22.

Friedlingstein, P., Jones, M. W., O'Sullivan, M., Andrew, R. M., Bakker, D. C., Hauck, J., ... and Zeng, J. (2022). Global carbon budget 2021. *Earth System Science Data*, *14*(4), 1917-2005.

Friedman, J. H. (1991). Multivariate adaptive regression splines. *The Annals of Statistics*, *19*(1), 1-67.

Friedman, J. H. (1993). Fast MARS Stanford University Department of *Technical Report*, 110.

Fu L, Lei X, Sharma RP, Li H, Zhu G, Hong L, You L, Duan G, Guo H, Lei Y, Li Y, and Tang, S. (2018a). Comparing height–age and height–diameter modelling approaches for estimating site productivity of natural uneven-aged forests. *Forestry: An International Journal of Forest Research*, 91, 419–433.

Fu, L., Sun, L., Hao, H., Jiang, L., Zhu, S., Ye, M., ... and Wu, R. (2018b). How trees allocate carbon for optimal growth: insight from a game-theoretic model. *Briefings in bioinformatics*, *19*(4), 593-602.

Gadow, K. (1999). Forest structure and diversity (Waldstruktur und diversität). *Allgemeine Forst-und Jagdzeitung*, *170*(7), 117-122.

Gadow, K. V., and Füldner, K. (1993). Zur bestandesbeschreibung in der forsteinrichtung. *Forst und Holz*, *48*(21), 602-606.

Gadow, K. V., and Hui, G. Y. (2002). Characterizing forest spatial structure and diversity. *Sustainable Forestry in Temperate Regions; Proc. of an international workshop organized at the University of Lund, Sweden*, 20-30.

Gazol, A., Sangüesa-Barreda, G., and Camarero, J. J. (2020). Forecasting forest vulnerability to drought in Pyrenean silver fir forests showing dieback. *Frontiers in Forests and Global Change*, *3*, 36.

Gil-Pelegrín, E., Villar Pérez, L., and López Unzu, F. (1989). Sobre la estructura de un hayedo-abetal virgen del Pirineo occidental: la selva de Aztaparreta (Alto Roncal, Navarra). *Acta Biológica Montana*, *9*, 225-236

Goelz, J. C. G., and Burk, T. E. (1992). Development of a well-behaved site index equation: jack pine in north Central Ontario. Canadian Journal of Forest Research, 22(6), 776–784.

Grassi, G., House, J., Kurz, W. A., Cescatti, A., Houghton, R. A., Peters, G. P., ... and Zaehle, S. (2018). Reconciling global-model estimates and country reporting of anthropogenic forest CO2 sinks. *Nature Climate Change*, *8*(10), 914-920.

Grassi, G., Stehfest, E., Rogelj, J., Van Vuuren, D., Cescatti, A., House, J., ... and Popp, A. (2021). Critical adjustment of land mitigation pathways for assessing countries' climate progress. *Nature Climate Change*, *11*(5), 425-434.

Grassi, G., Conchedda, G., Federici, S., Abad Viñas, R., Korosuo, A., Melo, J., ... and Tubiello, F. N. (2022). Carbon fluxes from land 2000–2020: bringing clarity on countries' reporting. *Earth System Science Data Discussions* [preprint], 1-49.

Hackenberg, J., Spiecker, H., Calders, K., Disney, M., and Raumonen, P. (2015). SimpleTree-an efficient open source tool to build tree models from TLS clouds. *Forests*, *6*(11), 4245-4294.

Hahsler, M., Piekenbrock, M., and Doran, D. (2019). dbscan: Fast density-based clustering with R. *Journal of Statistical Software*, *91*(1), 1-30.

Hardiman, B. S., Bohrer, G., Gough, C. M., Vogel, C. S., and Curtis, P. S. (2011). The role of canopy structural complexity in wood net primary production of a maturing northern deciduous forest. *Ecology*, *92*(9), 1818-1827.

Hardiman, B. S., Gough, C. M., Halperin, A., Hofmeister, K. L., Nave, L. E., Bohrer, G., and Curtis, P. S. (2013). Maintaining high rates of carbon storage in old forests: A mechanism linking canopy structure to forest function. *Forest Ecology and Management*, *298*, 111-119.

Herrera-Fernández, B., Campos, J. J., Kleinn, C. (2004). Site productivity estimation using height-diameter relationships in Costa Rican secondary forests. *Forest Systems*, *13*(2), 295–303.

Hester, J., Wickham, H., 2020. vroom: Read and Write Rectangular Text Data Quickly. R package version 1.3.2. https://CRAN.R-project.org/package=vroom

Hijmans, R. J., 2020. raster: Geographic Data Analysis and Modeling. R package version 3.4-5. https://CRAN.R-project.org/package=raster

Holmes, R. L. (1983). Computer-assisted quality control in tree-ring dating and measurement. *Tree-Ring Bulletin*, *43*, 69-78.

Holopainen, M., Vastaranta, M., and Hyyppä, J. (2014). Outlook for the next generation's precision forestry in Finland. *Forests*, *5*(7), 1682-1694.

Horn, J. L. (1965). A rationale and test for the number of factors in factor analysis. *Psychometrika*, *30*(2), 179-185.

Hoover, C. M., Leak, W. B., and Keel, B. G. (2012). Benchmark carbon stocks from old-growth forests in northern New England, USA. *Forest Ecology and Management*, *266*, 108-114.

Horvat, V., García De Vicuña, J., Biurrun, I., and García-Mijangos, I. (2018). Managed and unmanaged silver fir-beech forests show similar structural features in the western Pyrenees. *iForest-Biogeosciences and Forestry*, *11*(5), 698.

Hossfeld, J. W. (1882). *Mathematik für Forstmänner, Ökonomen und Cameralisten*. Gotha

Huang, S., Titus, S. J. (1993). An index of site productivity for uneven-aged or mixed-species stands. *Canadian Journal of Forest Research*, *23*(3), 558–562.

Hubau, W., Lewis, S. L., Phillips, O. L., … and Zemagho, L. (2020). Asynchronous carbon sink saturation in African and Amazonian tropical forests. *Nature*, *579*(7797), 80–87.

Idoate Lacasia, L., Stillhard, J., Portier, J., Brang, P., Zimmerman, S., Bugmann, H., and Hobi, M. (2022). *Factores impulsores del cambio a largo plazo de la biomasa en las reservas forestales Suizas*. 8º Congreso forestal Español. Sociedad Española de Ciencias Forestales, Lleida, Spain.

Intergovernmental Panel on Climate Change (IPCC). (2019). *2019 Refinement to the 2006 IPCC Guidelines for National Greenhouse Gas Inventories*.

Ishii, H. T., Tanabe, S. I., and Hiura, T. (2004). Exploring the relationships among canopy structure, stand productivity, and biodiversity of temperate forest ecosystems. *Forest Science*, *50*(3), 342-355.

Jaloviar, P., Saniga, M., Kucbel, S., Pittner, J., Vencurik, J., and Dovciak, M. (2017). Seven decades of change in a European old-growth forest following a stand-replacing wind disturbance: A long-term case study. *Forest Ecology and Management*, *399*, 197-205.

Jenkins, J. C., Chojnacky, D. C., Heath, L. S., and Birdsey, R. A. (2003). National-scale biomass estimators for United States tree species. *Forest Science*, *49*(1), 12-35.

Jiang, M., Medlyn, B. E., Drake, J. E., … and Ellsworth, D. S. (2020). The fate of carbon in a mature forest under carbon dioxide enrichment. *Nature*, *580*(7802), 227–231.

Jin, S., Tamura, M., and Susaki, J. (2016). A new approach to retrieve leaf normal distribution using terrestrial laser scanners. *Journal of Forestry Research*, *27*(3)**,** 631-638.

Juvinyà, C., LotfiParsa, H., Sauras-Yera, T., and Rovira, P. (2021). Carbon sequestration in Mediterranean soils following afforestation of abandoned crops: Biases due to changes in soil compaction and carbonate stocks. *Land Degradation & Development*, *32*(15), 4300-4312.

Keith, H., Vardon, M., Obst, C., Young, V., Houghton, R. A., and Mackey, B. (2021). Evaluating nature-based solutions for climate mitigation and conservation requires comprehensive carbon accounting. *Science of The Total Environment*, *769*, 144341.

Kenderes, K., Kral, K., Vrška, T., and Standovár, T. (2009). Natural gap dynamics in a Central European mixed beech-spruce-fir old-growth forest. *Ecoscience*, *16*(1), 39-47.

Ķēniņa, L., Jaunslaviete, I., Liepa, L., Zute, D., and Jansons, Ā. (2019). Carbon pools in old-growth Scots pine stands in hemiboreal Latvia. *Forests*, *10*(10), 911.

Kiviste, A., Hordo, M., Kangur, A., Kardakov, A., Laarmann, D., Lilleleht, A., ... and Korjus, H. (2015). Monitoring and modeling of forest ecosystems: the Estonian Network of Forest Research Plots. *Forestry Studies*, *62*, 26-38.

Kleinn, C., and Vilčko, F. (2006). A new empirical approach for estimation in k-tree sampling. *Forest Ecology and Management*, *237*(1), 522-533.

Koenker, R. W., and d'Orey, V. (1987). Algorithm AS 229: Computing regression quantiles. *Applied Statistics*, 383-393.

Koenker, R., and d'Orey, V. (1994). Remark AS R92: A remark on algorithm AS 229: Computing dual regression quantiles and regression rank scores. *Journal of the Royal Statistical Society. Series C (Applied Statistics)*, *43*(2), 410-414.

Koenker, R. (2021). quantreg: Quantile Regression. R package version 5.85. https://CRAN.R-project.org/package=quantreg

Kranabetter, J. M. (2009). Site carbon storage along productivity gradients of a late-seral southern boreal forest. *Canadian Journal of Forest Research*, *39*(5), 1053-1060.

Krieger, D. J. (2001). *Economic value of forest ecosystem services: a review*. The Wilderness Society.

Krok, G., Kraszewski, B., and Stereńczak, K. (2020). Application of terrestrial laser scanning in forest inventory–an overview of selected issues. *Forest Research Papers*, 81(4), 175-194.

Kruskal, W. H., and Wallis, W. A. (1952). Use of ranks in one-criterion variance analysis. *Journal of the American statistical Association*, *47*(260), 583-621.

Kucbel, S., Saniga, M., Jaloviar, P., and Vencurik, J. (2012). Stand structure and temporal variability in old-growth beech-dominated forests of the northwestern Carpathians: A 40-years perspective. *Forest Ecology and Management*, *264*, 125-133.

Laarmann, D., Korjus, H., Sims, A., Stanturf, J. A., Kiviste, A., and Köster, K. (2009). Analysis of forest naturalness and tree mortality

patterns in Estonia. *Forest Ecology and Management*, *258*, S187-S195.

Lamson, N. I. (1987). *Estimating northern red oak site-index class from total height and diameter of dominant and codominant trees in central Appalachian hardwood stands*. US Department of Agriculture, Forest Service, Northeastern Forest Experiment Station. 605

Larson, P. R. (1963). Stem form development of Forest trees. *Forest Science*, 9, 1–42.

Lau, A., Martius, C., Bartholomeus, H., Shenkin, A., Jackson, T., Malhi, Y., ... and Bentley, L. P. (2019). Estimating architecture-based metabolic scaling exponents of tropical trees using terrestrial LiDAR and 3D modelling. *Forest Ecology and Management*, *439*, 132-145.

Lewis, S. L., Lopez-Gonzalez, G., Sonké, B., Affum-Baffoe, K., Baker, T. R., Ojo, L. O., ... and Wöll, H. (2009). Increasing carbon storage in intact African tropical forests. *Nature*, *457*(7232), 1003-1006.

Ley 8 de 2018. De medidas frente al cambio climático y para la transición hacia un nuevo modelo energético en Andalucía. Artículo 37. 8 de octubre de 2018. BOJA No. 199.

Liang, X., Litkey, P., Hyyppa, J., Kaartinen, H., Vastaranta, M., and Holopainen, M. (2011). Automatic stem mapping using single-scan terrestrial laser scanning. *IEEE Transactions on Geoscience and Remote Sensing*, *50*(2), 661-670.

Liang, X., Kankare, V., Hyyppä, J., Wang, Y., Kukko, A., Haggrén, H., ... and Vastaranta, M. (2016). Terrestrial laser scanning in forest inventories. *ISPRS Journal of Photogrammetry and Remote Sensing*, *115*, 63-77.

Liang, X., Hyyppä, J., Kaartinen, H., Lehtomäki, M., Pyörälä, J., Pfeifer, N., ... and Wang, Y. (2018a). International benchmarking of terrestrial laser scanning approaches for forest inventories. *ISPRS journal of photogrammetry and remote sensing*, *144*, 137-179.

Liang, X., Kukko, A., Hyyppä, J., Lehtomäki, M., Pyörälä, J., Yu, X., ... and Wang, Y. (2018b). In-situ measurements from mobile platforms: An emerging approach to address the old challenges associated with forest inventories. *ISPRS Journal of Photogrammetry and Remote Sensing*, *143*, 97-107.

Lilleleht, A., Sims, A., and Pommerening, A. (2014). Spatial forest structure reconstruction as a strategy for mitigating edge-bias in circular monitoring plots. *Forest Ecology and Management*, *316*, 47-53.

Lindenmayer, D. B., Margules, C. R., and Botkin, D. B. (2000). Indicators of biodiversity for ecologically sustainable forest management. *Conservation Biology*, *14*(4), 941-950.

Lindenmayer, D. B., and Franklin, J. F. (2002). *Conserving forest biodiversity: a comprehensive multiscaled approach*. Island press.

Lindenmayer, D., and McCarthy, M. A. (2002). Congruence between natural and human forest disturbance: a case study from Australian montane ash forests. *Forest Ecology and Management*, *155*(1-3), 319-335.

Lingua, E., Garbarino, M., Mondino, E. B., and Motta, R. (2011). Natural disturbance dynamics in an old-growth forest: from tree to landscape. *Procedia Environmental Sciences*, *7*, 365-370.

Liu, J., Liang, X., Hyyppä, J., Yu, X., Lehtomäki, M., Pyörälä, J., ... and Chen, R. (2017). Automated matching of multiple terrestrial laser scans for stem mapping without the use of artificial references. *International Journal of Applied Earth Observation and Geoinformation*, *56*, 13-23.

López-Santalla, A., and López-Garcia, M. (2019). *Los Incendios Forestales en Españ*a*. Decenio 2006–2015*. Ministerio de Agricultura, Pesca y Alimentación

Lorimer, C. G. (1985). Methodological considerations in the analysis of forest disturbance history. *Canadian Journal of Forest Research*, *15*(1), 200-213.

Lorimer, C. G., and Frelich, L. E. (1989). A methodology for estimating canopy disturbance frequency and intensity in dense temperate forests. *Canadian Journal of Forest Research*, *19*(5), 651-663.

Lorimer, C. G., and Halpin, C. R. (2014). Classification and dynamics of developmental stages in late-successional temperate forests. *Forest ecology and management*, *334*, 344-357.

Lovell, J. L., Jupp, D. L. B., Newnham, G. J., and Culvenor, D. S. (2011). Measuring tree stem diameters using intensity profiles from ground-based scanning lidar from a fixed viewpoint. *ISPRS Journal of Photogrammetry and Remote Sensing*, *66*(1), 46-55.

Luguza, S., Snepsts, G., Donis, J., Desaine, I., Baders, E., Kitenberga, M., ... and Jansons, A. (2020). Advance regeneration of Norway spruce and Scots pine in hemiboreal forests in Latvia. *Forests*, *11*(2), 215.

Luyssaert, S., Schulze, E., Börner, A., Knohl, A., Hessenmöller, D., Law, B. E., ... and Grace, J. (2008). Old-growth forests as global carbon sinks. *Nature*, *455*(7210), 213-215.

Ma, L., Zheng, G., Eitel, J. U., Moskal, L. M., He, W., Huang, H. (2016). Improved salient feature-based approach for automatically separating photosynthetic and nonphotosynthetic components within terrestrial lidar point cloud data of forest canopies. *IEEE Transactions on geoscience and remote sensing*, *54*(2), 679-696.

Martin-Benito, D., Pederson, N., Lanter, C., Köse, N., Doğan, M., Bugmann, H., and Bigler, C. (2020). Disturbances and climate drive structure, stability, and growth in mixed temperate old-growth rainforests in the Caucasus. *Ecosystems*, *23*(6), 1170-1185.

McElhinny, C., Gibbons, P., Brack, C., and Bauhus, J. (2005). Forest and woodland stand structural complexity: its definition and measurement. *Forest Ecology and Management*, *218*(1-3), 1-24.

McGaughey, R. J. (2009). FUSION/LDV: Software for LIDAR data analysis and visualization. *US Department of Agriculture, Forest Service, Pacific Northwest Research Station: Seattle, WA, USA*.

Macias, M., Andreu, L., Bosch, O., Camarero, J. J., and Gutiérrez, E. (2006). Increasing aridity is enhancing silver fir Abies alba mill.) water stress in its south-western distribution limit. *Climatic Change*, *79*(3), 289-313.

Mackey, B., Kormos, C. F., Keith, H., Moomaw, W. R., Houghton, R. A., Mittermeier, R. A., ... and Hugh, S. (2020). Understanding the importance of primary tropical forest protection as a mitigation strategy. *Mitigation and adaptation strategies for global change*, *25*(5), 763-787.

MacLean, C. D. (1973). *Estimating productivity on sites with a low stocking capacity*. Pacific Northwest Forest and Range Experiment Station, US Department of Agriculture.

Malhi, Y., Jackson, T., Patrick Bentley, L., Lau, A., Shenkin, A., Herold, M., ... and Disney, M. I. (2018). New perspectives on the ecology of tree structure and tree communities through terrestrial laser scanning. *Interface Focus*, *8*(2), 20170052.

Mapa Forestal de España (MFE50) (2006). [Map]. 1:50000. Ministerio para la transición ecológica y el reto demográfico.

Marques, F. F., and Buckland, S. T. (2003). Incorporating covariates into standard line transect analyses. *Biometrics*, *59*(4), 924-935.

Matuszkiewicz, J. M., Affek, A. N., and Kowalska, A. (2021). Current and potential carbon stock in the forest communities of the Białowieża Biosphere Reserve. *Forest Ecology and Management*, *502*, 119702.

McLintock, T. F., and Bickford, C. A. (1957). *A proposed site index for red spruce in the northeast*. USDA Forest Service Northeastern Forest Experiment Station

McRoberts, R. E., Winter, S., Chirici, G., and LaPoint, E. (2012). Assessing forest naturalness. *Forest Science*, *58*(3), 294-309.

Messier, C., Puettmann, K. J., and Coates, K. D. (Eds.). (2013). *Managing forests as complex adaptive systems: building resilience to the challenge of global change*. Routledge.

Metslaid, M., Jogiste, K., Nikinmaa, E., Moser, W. K., and Porcar-Castell, A. (2007). Tree variables related to growth response and acclimation of advance regeneration of Norway spruce and other coniferous species after release. *Forest Ecology and Management*, *250*(1-2), 56-63.

Meyer, H. A. (1940). A mathematical expression for height curves. *Journal of Forestry*, *38*(5), 415–420.

Meyer, P., Aljes, M., Culmsee, H., Feldmann, E., Glatthorn, J., Leuschner, C., … and Schneider, H. (2021a). Quantifying old-growthness of lowland European beech forests by a multivariate indicator for forest structure. *Ecological Indicators*, *125*, 107575.

Meyer, P., Nagel, R., and Feldmann, E. (2021b). Limited sink but large storage: Biomass dynamics in naturally developing beech (Fagus sylvatica) and oak (Quercus robur, Quercus petraea) forests of north-western Germany. *Journal of Ecology*, *109*(10), 3602-3616.

Michalak, P. (2016). Ancient forest: keep the logging ban. *Nature*, *530*(7591), 419-419.

Milborrow, S. (2021). earth: Multivariate Adaptive Regression Splines. R package version 5.3.1. https://CRAN.R-project.org/package=earth

Miller, D. L., and Thomas, L., 2015. Mixture models for distance sampling detection functions. PLoS ONE, 10(3), e0118726.

Miller, D. L., Rexstad, E., Thomas, L., Marshall, L., and Laake, J. L. (2019). Distance Sampling in R. *Journal of Statistical Software*, *89*(1), 1-28.

Ministerio para la Transición Ecológica y el Reto Demográfico (MITERD) (Ed.) (2021). *Anuario de Estadística Forestal 2019*. MITERD.

Molina-Valero, J. A., Diéguez-Aranda, U., Álvarez-González, J. G., Castedo-Dorado, F., and Pérez-Cruzado, C. (2019a). Assessing site form as an indicator of site quality in even-aged Pinus radiata D. Don stands in north-western Spain. *Annals of Forest Science*, *76*(4), 1-10.

Molina Valero, J. A., Ginzo Villamayor, M. J., Novo Pérez, M. A., Álvarez-González, J. G., and Pérez-Cruzado, C. (2019b). Estimación del área basimétrica en masas maduras de *Pinus sylvestris* en base a una única medición del escáner láser terrestre (TLS). *Cuadernos de la Sociedad Española de Ciencias Foresstales*, *45*(3), 97-116.

Molina-Valero, J. A., Ginzo Villamayor, M. J., Novo Pérez, M. A., Álvarez-González, J. G., Montes, F., Martínez-Calvo, A., and Pérez-Cruzado, C. (2020). FORTLS: An R Package for Processing TLS Data and Estimating Stand Variables in Forest Inventories. *Environmental Sciences Proceedings*, 3(1), 38.

Molina-Valero, J. A., Camarero, J. J., Álvarez-González, J. G., Cerioni, M., Hevia, A., Sanchez-Salguero, R., Martin-Benito, D., and Perez-Cruzado, C. (2021). Mature forests hold maximum live biomass stocks. *Forest Ecology and Management*, *480*, 118635.

Molina-Valero, J. A., Martínez-Calvo, A., Villamayor, M. J. G., Pérez, M. A. N., Álvarez-González, J. G., Montes, F., and Pérez-Cruzado, C. (2022). Operationalizing the use of TLS in forest inventories: The R package FORTLS. *Environmental Modelling & Software*, 105337.

Montero, G., Ruiz-Peinado, R., and Muñoz, M. (2005). *Producción de biomasa y fijación de CO2 por los bosques españoles*. INIA-Instituto Nacional de Investigación y Tecnología Agraria y Alimentaria. Ministerio de Educación y Ciencia

Montes, F., Rubio-Cuadrado, Á., Sánchez-González, M., Aulló-Maestro, I., Cabrera, M., and Gómez, C. (2019). Occlusion probability in operational forest inventory field sampling with ForeStereo. *Photogrammetric Engineering & Remote Sensing*, *85*(7), 493-508.

Morales-Barquero, L., Skutsch, M., Jardel-Peláez, E. J., Ghilardi, A., Kleinn, C., and Healey, J. R. (2014). Operationalizing the definition of forest degradation for REDD+, with application to Mexico. *Forests*, *5*(7), 1653-1681.

Moreno-Fernández, D., Álvarez-González, J. G., Rodríguez-Soalleiro, R., Pasalodos-Tato, M., Cañellas, I., Montes, F., ... and Pérez-Cruzado, C. (2018). National-scale assessment of forest site productivity in Spain. *Forest Ecology and Management*, *417*, 197-207.

Mosseler, A., Lynds, J. A., and Major, J. E. (2003). Old-growth forests of the Acadian Forest Region. *Environmental Reviews*, *11*(S1), S47-S77.

Mund, M. (2004). *Carbon Pools of European Beech Forests (Fagus Sylvatica) Under Different Silvicultural Management* [Doctoral thesis]. University of Göttingen

Newnham, G. J., Armston, J. D., Calders, K., Disney, M. I., Lovell, J. L., Schaaf, C. B., ... and Danson, F. M. (2015). Terrestrial laser scanning for plot-scale forest measurement. *Current Forestry Reports*, *1*(4), 239-251.

Nagel, T. A., Levanic, T., and Diaci, J. (2007). A dendroecological reconstruction of disturbance in an old-growth Fagus-Abies forest in Slovenia. *Annals of Forest Science*, *64*(8), 891-897.

Nagel, T. A., Svoboda, M., and Kobal, M. (2014). Disturbance, life history traits, and dynamics in an old-growth forest landscape of southeastern Europe. *Ecological Applications*, *24*(4), 663-679.

Ngo, K. M., Turner, B. L., Muller-Landau, H. C., Davies, S. J., Larjavaara, M., bin Nik Hassan, N. F., and Lum, S. (2013). Carbon stocks in primary and secondary tropical forests in Singapore. *Forest Ecology and Management*, *296*, 81-89.

Nicholas, N. S., and Zedaker, S. M. (1992). Expected stand behavior: site quality estimation for southern Appalachian red spruce. *Forest Ecology and Management*, *47*(1-4), 39-50.

Nilsson, M., Nordkvist, K., Jonzén, J., Lindgren, N., Axensten, P., Wallerman, J., ... and Olsson, H. (2017). A nationwide forest attribute map of Sweden predicted using airborne laser scanning data and field data from the National Forest Inventory. *Remote Sensing of Environment*, *194*, 447-454.

Ninyerola, M., Pons, X., and Roure, J. M. (2005). Atlas Climático Digital de la Península Ibérica. Metodología y aplicaciones en bioclimatología y geobotánica. ISBN 932860-8-7. Universidad Autónoma de Barcelona, Bellaterra.

Nord-Larsen, T., and Schumacher, J. (2012). Estimation of forest resources from a country wide laser scanning survey and national forest inventory data. *Remote Sensing of Environment*, *119*, 148-157.

Nord-Larsen, T., Vesterdal, L., Bentsen, N. S., and Larsen, J. B. (2019). Ecosystem carbon stocks and their temporal resilience in a semi-natural beech-dominated forest. *Forest Ecology and Management*, *447*, 67-76.

Nowacki, G. J., and Abrams, M. D. (1997). Radial-growth averaging criteria for reconstructing disturbance histories from presettlement-origin oaks. *Ecological Monographs*, *67*(2), 225-249.

Odum, E. P. (1969). The Strategy of Ecosystem Development: An understanding of ecological succession provides a basis for resolving man's conflict with nature. *Science*, *164*(3877), 262-270.

Oliver, C. D., and Larson, B. C. (1996). *Forest stand dynamics*. John Wiley and Sons.

Olofsson, K., Holmgren, J., and Olsson, H. (2014). Tree stem and height measurements using terrestrial laser scanning and the RANSAC algorithm. *Remote Sensing*, *6*(5), 4323-4344.

Olofsson, K., and Holmgren, J. (2016). Single tree stem profile detection using terrestrial laser scanner data, flatness saliency features and curvature properties. *Forests*, *7*(9), 207.

Pan, Y., Birdsey, R. A., Fang, J., Houghton, R., Kauppi, P. E., Kurz, W. A., ... and Hayes, D. (2011). A large and persistent carbon sink in the world's forests. *Science*, *333*(6045), 988-993.

Pauly, M., Gross, M., and Kobbelt, L. P. (2002). Efficient simplification of point-sampled surfaces. *IEEE Visualization*, (pp. 163-170). Boston, USA.

Pebesma, E. J., Bivand, R. S. (2005). Classes and methods for spatial data in R. *R News*, *5*(2), 9–13.

Pebesma, E., 2018. Simple Features for R: Standardized Support for Spatial Vector Data. *The R Journal*, *10*(1), 439-446.

Peng, C. (2000). Growth and yield models for uneven-aged stands: past, present and future. *Forest Ecology and Management*, *132*(2-3), 259-279.

Penone, C., Allan, E., Soliveres, S., Felipe-Lucia, M. R., Gossner, M. M., Seibold, S., ... and Fischer, M. (2019). Specialisation and diversity of multiple trophic groups are promoted by different forest features. *Ecology Letters*, *22*(1), 170-180.

Pérez-Cruzado, C. (2011). *Models for estimating biomass and carbon in biomass and soils in Pinus radiata (D. Don), Eucalyptus globulus (Labill) and Eucalyptus nitens (Deane & Maiden) Maiden plantations established in former agricultural lands in northwestern Spain* [Doctoral thesis, University of Santiago de Compostela]. Minerva Institutional Repository - USC

Pérez-Cruzado, C., Merino, A., and Rodríguez-Soalleiro, R. (2011). A management tool for estimating bioenergy production and carbon sequestration in *Eucalyptus globulus* and *Eucalyptus nitens* grown as short rotation woody crops in north-west Spain. *Biomass and bioenergy*, *35*(7), 2839-2851.

Pérez-Cruzado, C., Mohren, G. M., Merino, A., and Rodríguez-Soalleiro, R. (2012). Carbon balance for different management practices for fast growing tree species planted on former pastureland in southern Europe: a case study using the CO2Fix model. *European Journal of Forest Research*, *131*(6), 1695-1716.

Pérez-Cruzado, C., Fehrmann, L., Magdon, P., Cañellas, I., Sixto, H., and Kleinn, C. (2015). On the site-level suitability of biomass models. *Environmental Modelling & Software*, *73*, 14-26.

Peterken, G. F. (1996). *Natural woodland: ecology and conservation in northern temperate regions*. Cambridge University Press.

Phillips, O. L., and Brienen, R. J. (2017). Carbon uptake by mature Amazon forests has mitigated Amazon nations' carbon emissions. *Carbon Balance and Management*, *12*(1), 1-9.

Pienaar, L. V., and Turnbull, K. J. (1973). The Chapman-Richards generalization of Von Bertalanffy's growth model for basal area growth and yield in even-aged stands. *Forest Science*, *19*(1), 2-22.

Piqué, M., Obon, B., Condés, S., and Saura, S. (2011). Comparison of relascope and fixed-radius plots for the estimation of forest stand variables in northeast Spain: an inventory simulation approach. *European Journal of Forest Research*, *130*(5), 851-859.

Põldveer, E., Korjus, H., Kiviste, A., Kangur, A., Paluots, T., and Laarmann, D. (2020). Assessment of spatial stand structure of hemiboreal conifer dominated forests according to different levels of naturalness. *Ecological Indicators*, *110*, 105944.

Põldveer, E., Potapov, A., Korjus, H., Kiviste, A., Stanturf, J. A., Arumäe, T., ... and Laarmann, D. (2021). The structural complexity index SCI is useful for quantifying structural diversity of Estonian hemiboreal forests. *Forest Ecology and Management*, *490*, 119093.

Pommerening, A. (2002). Approaches to quantifying forest structures. *Forestry: An International Journal of Forest Research*, *75*(3), 305-324.

Pommerening, A. (2006). Evaluating structural indices by reversing forest structural analysis. *Forest Ecology and Management*, *224*(3), 266-277.

Pommerening, A., and Stoyan, D. (2006). Edge-correction needs in estimating indices of spatial forest structure. *Canadian Journal of Forest Research*, *36*(7), 1723-1739.

Pommerening, A., and Särkkä, A. (2013). What mark variograms tell about spatial plant interactions. *Ecological Modelling*, *251*, 64-72.

Pregitzer, K. S., and Euskirchen, E. S. (2004). Carbon cycling and storage in world forests: biome patterns related to forest age. *Global Change Biology*, *10*(12), 2052-2077.

Pretzsch, H., Grote, R., Reineking, B., Rötzer, T. H., and Seifert, S. T. (2008). Models for forest ecosystem management: a European perspective. *Annals of Botany*, *101*(8), 1065-1087.

Pretzsch, H. (2009). Forest dynamics, growth, and yield. *Forest dynamics, growth and yield* (pp. 1-39). Springer

Puettmann, K. J., Coates, K. D., and Messier, C. C. (2012). *A critique of silviculture: managing for complexity*. Island Press.

Puettmann, K. J., Wilson, S. M., Baker, S. C., Donoso, P. J., Drössler, L., Amente, G., ... and Bauhus, J. (2015). Silvicultural alternatives to conventional even-aged forest management-what limits global adoption? *Forest Ecosystems*, *2*(1), 1-16.

R Core Team (2021). R: A language and environment for statistical computing. R Foundation for Statistical Computing. Vienna, Austria.

Real Decreto 163 de 2014. Por el que se crea el registro de huella de carbono, compensación y proyectos de absorción de dióxido de carbono. 29 de marzo de 2014. BOE No. 77.

Reineke, L. (1933). Perfecting a stand-density index for even-aged forests. *Journal of Agricultural Research*, *46*,627–638

Reinhardt, E. D. (1982). *Influence of site quality on the height-diameter relationship of western larch* [Master thesis]. University of Montana.

Reinhardt, E. D. (1983). *Using height/diameter curves to estimate site index in old-growth western larch stands*. University of Montana, Montana Forest and Conservation Experiment Station.

Ribe, R. G. (2009). In-stand scenic beauty of variable retention harvests and mature forests in the US Pacific Northwest: The effects of basal area, density, retention pattern and down wood. *Journal of Environmental Management*, *91*(1), 245-260.

Robador Moreno, A., Samsó Escolá, J.M., Ramajo Cordero, J., Barnolas Cortinas, A., Clariana García, P., Martín Alfageme, S.,

and Gil Peña, I. (2020). *Continuous digital geological map of Spain* (GEODE) [Map]. 1:50000. National Geographic Institute (IGN).

Roussel, J. R., Auty, D. (2020). Airborne LiDAR Data Manipulation and Visualization for Forestry Applications. R package version 3.0.4. https://cran.r-project.org/package=lidR

Roussel, J. R., Auty, D., Coops, N. C., Tompalski, P., Goodbody, T. R.H., Sanchez Meador, A., Bourdon, J.F., de Boissieu, F, Achim, A. (2020). lidR: An R package for analysis of Airborne Laser Scanning (ALS) data. *Remote Sensing of Environment*, *251*, 112061.

Ruiz-Peinado, R., del Río, M. and Montero, G. (2011). New models for estimating the carbon sink capacity of Spanish softwood species. *Forest Systems*, *20*(1), 176-188.

Ruiz-Peinado, R., Montero, G. and del Río, M. (2012). Biomass models to estimate carbon stocks for hardwood tree species. *Forest systems*, *21*(1), 42-52.

Ruíz Zorrilla, P. (1980). *Notas para una historia del pino en Galicia*. Ministerio de Cultura, Dirección General del Patrimonio Artístico, S.G. de Archivos. Madrid

Sabatini, F. M., Burrascano, S., Keeton, W. S., Levers, C., Lindner, M., Pötzschner, F., ... and Kuemmerle, T. (2018). Where are Europe's last primary forests? *Diversity and Distributions*, *24*(10), 1426-1439.

Sánchez-Salguero, R., Navarro-Cerrillo, R. M., Swetnam, T. W., and Zavala, M. A. (2012). Is drought the main decline factor at the rear edge of Europe? The case of southern Iberian pine plantations. *Forest Ecology and Management*, *271*, 158-169.

Sangüesa-Barreda, G., Camarero, J. J., Oliva, J., Montes, F., and Gazol, A. (2015). Past logging, drought and pathogens interact and contribute to forest dieback. *Agricultural and Forest Meteorology*, *208*, 85-94.

Santilli, M., Moutinho, P., Schwartzman, S., Nepstad, D., Curran, L., and Nobre, C. (2005). Tropical deforestation and the Kyoto Protocol. *Climatic Change*, *71*(3), 267-276.

Savage, V. M., Bentley, L. P., Enquist, B. J., Sperry, J. S., Smith, D. D., Reich, P. B., and Von Allmen, E. I. (2010). Hydraulic trade-offs and space filling enable better predictions of vascular structure and function in plants. *Proceedings of the National Academy of Sciences*, *107*(52), 22722-22727.

Schall, P., Schulze, E. D., Fischer, M., Ayasse, M., and Ammer, C. (2018). Relations between forest management, stand structure and productivity across different types of Central European forests. *Basic and Applied Ecology*, *32*, 39-52.

Schelhaas, M. J., Van Esch, P. W., Groen, T. A., De Jong, B. H. J., Kanninen, M., Liski, J., ... and Vilén, T. (2004). *CO2FIX V 3.1 A modelling framework for quantifying carbon sequestration in forest ecosystems* (No. 1068). Alterra-Centrum Ecosystemen.

Schultze, J., Gärtner, S., Bauhus, J., Meyer, P., and Reif, A. (2014). Criteria to evaluate the conservation value of strictly protected forest reserves in Central Europe. *Biodiversity and Conservation*, *23*(14), 3519-3542.

Seedre, M., Kopáček, J., Janda, P., Bače, R., and Svoboda, M. (2015). Carbon pools in a montane old-growth Norway spruce ecosystem in Bohemian Forest: Effects of stand age and elevation. *Forest Ecology and Management*, *346*, 106-113.

Seidel, D., Leuschner, C., Scherber, C., Beyer, F., Wommelsdorf, T., Cashman, M. J., and Fehrmann, L. (2013). The relationship between tree species richness, canopy space exploration and productivity in a temperate broad-leaf mixed forest. *Forest Ecology and Management*, *310*, 366-374.

Seidel, D., and Ammer, C. (2014). Efficient measurements of basal area in short rotation forests based on terrestrial laser scanning under special consideration of shadowing. *iForest-Biogeosciences and Forestry*, *7*(4), 227 -232.

Seidel, D., Ehbrecht, M., and Puettmann, K. (2016). Assessing different components of three-dimensional forest structure with single-scan terrestrial laser scanning: A case study. *Forest Ecology and Management*, *381*, 196-208.

Seidel, D., Ehbrecht, M., Annighöfer, P., and Ammer, C. (2019). From tree to stand-level structural complexity—Which properties make a forest stand complex? *Agricultural and Forest Meteorology*, *278*, 107699.

Seidl, R., Thom, D., Kautz, M., Martin-Benito, D., Peltoniemi, M., Vacchiano, G., Wild, J., Ascoli, D., Petr, M., and Honkaniemi, J. (2017). Forest disturbances under climate change. *Nature Climate Change*, 7, 395-402.

Serra-Maluquer, X., Gazol, A., Sangüesa-Barreda, G., Sánchez-Salguero, R., Rozas, V., Colangelo, M., ... and Camarero, J. J. (2019). Geographically structured growth decline of rear-edge Iberian Fagus sylvatica forests after the 1980s shift toward a warmer climate. *Ecosystems*, *22*(6), 1325-1337.

Shannon, C. E. (1949). *The mathematical theory of communication*. University of Illinois Press.

Shugart, H. H., Saatchi, S., and Hall, F. G. (2010). Importance of structure and its measurement in quantifying function of forest ecosystems. *Journal of Geophysical Research: Biogeosciences*, *115*(G2).

Sievert, C. (2020). *Interactive Web-Based Data Visualization with R, plotly, and shiny*. CRC Press.

Simons, N. K., Felipe-Lucia, M. R., Schall, P., Ammer, C., Bauhus, J., Blüthgen, N., ... and Weisser, W. W. (2021). National Forest Inventories capture the multifunctionality of managed forests in Germany. *Forest Ecosystems*, *8*(1), 1-19.

Simpson, E. H. (1949). Measurement of diversity. *Nature*, *163*(4148), 688-688.

Skovsgaard, J. P. and Vanclay, J. K. (2008). Forest site productivity: a review of the evolution of dendrometric concepts for even-aged

stands. *Forestry: An International Journal of Forest Research*, *81*, 13–31.

Smithwick, E. A., Harmon, M. E., Remillard, S. M., Acker, S. A., and Franklin, J. F. (2002). Potential upper bounds of carbon stores in forests of the Pacific Northwest. *Ecological Applications*, *12*(5), 1303-1317.

Snäll, T., Triviño, M., Mair, L., Bengtsson, J., and Moen, J. (2021). High rates of short-term dynamics of forest ecosystem services. *Nature Sustainability*, *4*(11), 951-957.

Soloway, A. D., Amiro, B. D., Dunn, A. L., and Wofsy, S. C. (2017). Carbon neutral or a sink? Uncertainty caused by gap-filling long-term flux measurements for an old-growth boreal black spruce forest. *Agricultural and Forest Meteorology*, *233*, 110-121.

Spies, T. A. (2004). Ecological concepts and diversity of old-growth forests. *Journal of Forestry*, *102*(3), 14-20.

Spies, T. A., Hemstrom, M. A., Youngblood, A., and Hummel, S. (2006). Conserving old-growth forest diversity in disturbance-prone landscapes. *Conservation Biology*, *20*(2), 351-362.

Stephenson, N. L., Das, A. J., Condit, R., Russo, S. E., Baker, P. J., Beckman, N. G., ... and Zavala, M. A. (2014). Rate of tree carbon accumulation increases continuously with tree size. *Nature*, *507*(7490), 90-93.

Stiers, M., Willim, K., Seidel, D., Ehbrecht, M., Kabal, M., Ammer, C., and Annighöfer, P. (2018). A quantitative comparison of the structural complexity of managed, lately unmanaged and primary European beech (Fagus sylvatica L.) forests. *Forest Ecology and Management*, *430*, 357-365.

Stout, B. B., Shumway, D. L. (1982). Site quality estimation using height and diameter. *Forest Science, 28*(3), 639–645

Strahler, A. H., Jupp, D. L. B., Woodcock, C. E., Schaaf, C. B., Yao, T., Zhao, F., and Boykin-Morris, W. (2008). Retrieval of forest structural parameters using a ground-based lidar instrument

(Echidna®). *Canadian Journal of Remote Sensing*, *34*(sup2), S426-S440.

Sundseth, K. (2009a). *Natura 2000 in the Atlantic Region.* European Commission. Environment Directorate General.

Sundseth, K. (2009b). *Natura 2000 in the Mediterranean Region*. European Commission. Environment Directorate General.

Sundseth, K. (2009c). *Natura 2000 in the Boreal Region.* European Commission. Environment Directorate General.

Therneau, T., and Atkinson, B. (2022). rpart: Recursive Partitioning and Regression Trees. R package version 4.1.16. https://CRAN.R-project.org/package=rpart

Thompson, I. D., Guariguata, M. R., Okabe, K., Bahamondez, C., Nasi, R., Heymell, V., and Sabogal, C. (2013). An operational framework for defining and monitoring forest degradation. *Ecology and Society*, *18*(2), 1-20.

Tomé, J., Tomé, M., Barreiro, S., and Paulo, J. A. (2006). Age-independent difference equations for modelling tree and stand growth. *Canadian Journal of Forest Research*, *36*(7), 1621-1630.

Tomppo, E., Gschwantner, T., Lawrence, M., and McRoberts, R. E. (Eds.). (2010). National forest inventories. Pathways for Common Reporting. Springer Dordrecht

Trochta, J., Krůček, M., Vrška, T., and Král, K. (2017). 3D Forest: An application for descriptions of three-dimensional forest structures using terrestrial LiDAR. *PloS one*, *12*(5), e0176871.

Trorey, L. G. (1932). A mathematical method for the construction of diameter height curves based on site. *The Forestry Chronicle*, 8, 121–132.

Trotsiuk, V., Svoboda, M., Weber, P., Pederson, N., Klesse, S., Janda, P., ... and Frank, D. (2016). The legacy of disturbance on individual tree and stand-level aboveground biomass accumulation and stocks in primary mountain *Picea abies* forests. *Forest Ecology and Management*, *373*, 108-115.

United Nations Conference on Environment and Development (UNCED). (1992). Forest principles: non-legally binding authoritative statement of principles for a global consensus on the management, conservation and sustainable development of all types of forests (A/CONF.151/26). Rio de Janeiro.

United Nations Framework Convention on Climate Change (UNFCCC). (1998). Kyoto protocol to the United Nations framework convention on climate change. Kyoto.

United Nations Framework Convention on Climate Change (UNFCCC). (2009). Copenhagen accord. Copenhagen.

Vaidyanathan, R., Xie, Y., Allaire, J.J., Cheng, J., Sievert, C., Russell, and K. (2020). htmlwidgets: HTML Widgets for R. R package version 1.5.3. https://CRAN.R-project.org/package=htmlwidgets

Vanclay, J. K. (1983). *Techniques for modelling timber yield from indigenous forests with special reference to Queenslan* [Doctoral thesis]. University of Oxford.

Vanclay, J. K., Henry, N. B. (1988). Assessing site productivity of indigenous cypress pine forest in southern Queensland. *The Commonwealth Forestry Review*, *67*(1), 53–64

Vanclay, J. K. (1992). Assessing site productivity in tropical moist forests: a review. *Forest Ecology and Management*, *54*(1-4), 257–287.

Vanclay, J. K. (1994). Modelling forest growth and yield. Applications to mixed tropical forests. CAB International.

Vanclay, J. K. (1995). Growth models for tropical forests: a synthesis of models and methods. *Forest Science*, *41*(1), 7–42

Villaescusa, R. Díaz (1998). Segundo inventario forestal nacional (1986–1996). Ministerio de Medio Ambiente, ICONA.

Villanueva, J. A. (2005). Tercer inventario forestal nacional (1997–2007). Ministerio de Medio Ambiente.

Wang, G. G. (1998). Is height of dominant trees at a reference diameter an adequate measure of site quality? *Forest Ecology and Management*, *112*(1-2), 49–54.

Wang, M., Borders, B., and Zhao, D. (2007). Parameter estimation of base-age invariant site index models: which data structure to use? *Forest Science*, *53*(5), 541–551.

Wang, Y., Ziv, G., Adami, M., Almeida, C. A. D., Antunes, J. F. G., Coutinho, A. C., ... and Galbraith, D. (2020). Upturn in secondary forest clearing buffers primary forest loss in the Brazilian Amazon. *Nature Sustainability*, *3*(4), 290-295.

Watson, J. E., Evans, T., Venter, O., Williams, B., Tulloch, A., Stewart, C., ... and Lindenmayer, D. (2018). The exceptional value of intact forest ecosystems. *Nature Ecology & Evolution*, *2*(4), 599-610.

Wei, X., Kimmins, J. P., and Zhou, G. (2003). Disturbances and the sustainability of long-term site productivity in lodgepole pine forests in the central interior of British Columbia—an ecosystem modeling approach. *Ecological Modelling*, *164*(2-3), 239-256.

Weiskittel, A. R., Hann, D. W., Kershaw, J. A., and Vanclay, J. K. (2011). *Forest growth and yield modeling*. John Wiley & Sons.

Wells, R. W., Lertzman, K. P., and Saunders, S. C. (1998). Old-growth definitions for the forests of British Columbia, Canada. *Natural Areas Journal*, *18*(4), 279-292.

West, G. B., Brown, J. H., and Enquist, B. J. (1997). A general model for the origin of allometric scaling laws in biology. *Science*, *276*(5309), 122-126.

West, G. B., Brown, J. H., and Enquist, B. J., (1999). The fourth dimension of life: fractal geometry and allometric scaling of organisms. *Science*, *284*(5420), 1677–1679.

White, J. C., Coops, N. C., Wulder, M. A., Vastaranta, M., Hilker, T., and Tompalski, P. (2016). Remote sensing technologies for enhancing forest inventories: A review. *Canadian Journal of Remote Sensing*, *42*(5), 619-641.

Wickham, H. (2021). tidyr: Tidy Messy Data. R package version 1.1.3. https://CRAN.R-project.org/package=tidyr

Wickham, H., Seidel, D. (2020). scales: Scale Functions for Visualization. R package version 1.1.1. https://CRAN.R-project.org/package=scales

Winter, S. (2012). Forest naturalness assessment as a component of biodiversity monitoring and conservation management. *Forestry*, *85*(2), 293-304.

Wirth, C., Gleixner, G., and Heimann, M. (Eds.) (2009). *Old-growth forests: function, fate and value - an overview*. Springer.

Wulder, M. A., White, J. C., Nelson, R. F., Næsset, E., Ørka, H. O., Coops, N. C., ... and Gobakken, T. (2012). Lidar sampling for large-area forest characterization: A review. *Remote Sensing of Environment*, *121*, 196-209.

Xia, S., Wang, C., Pan, F., Xi, X., Zeng, H., and Liu, H. (2015). Detecting stems in dense and homogeneous forest using single-scan TLS. *Forests*, *6*(11), 3923-3945.

Yao, T., Yang, X., Zhao, F., Wang, Z., Zhang, Q., Jupp, D., ... and Strahler, A. (2011). Measuring forest structure and biomass in New England forest stands using Echidna ground-based lidar. *Remote Sensing of Environment*, *115*(11), 2965-2974.

Yrttimaa, T., Luoma, V., Saarinen, N., Kankare, V., Junttila, S., Holopainen, M., ... and Vastaranta, M. (2022). Monitoring Tree Growth Allometry Using Two-Date Terrestrial Laser Scanning. *Forest Ecology and Management*, *518*, 120303.

Zenner, E. K. (1998). *A new index for describing the structural complexity of forests* [Doctoral thesis]. Oregon State University.

Zhang, W., Qi, J., Wan, P., Wang, H., Xie, D., Wang, X., and Yan, G. (2016). An Easy-to-Use Airborne LiDAR Data Filtering Method Based on Cloth Simulation. *Remote Sensing*, *8*(6), 501.

Zhang, W., Wan, P., Wang, T., Cai, S., Chen, Y., Jin, X., and Yan, G. (2019). A novel approach for the detection of standing tree stems

from plot-level terrestrial laser scanning data. *Remote Sensing*, *11*(2), 211.

Ziaco, E., Biondi, F., Di Filippo, A., and Piovesan, G. (2012). Biogeoclimatic influences on tree growth releases identified by the boundary line method in beech (Fagus sylvatica L.) populations of southern Europe. *Forest Ecology and Management*, *286*, 28-37.

GLOSSARY

GLOSSARY

ACRONYMS

FI	Forest inventory
GHG	Greenhouse gas
IPCC	Intergovernmental Panel on Climate Change
LULUCF	Land use, land-use change and forestry
NCD	Nationally determined contribution
NGHGI	National Greenhouse Gas Inventory
NFI	National Forest Inventory
REDD+	Reducing emissions from deforestation and forest degradation projects
SNFI	Spanish National Forest Inventory
TLS	Terrestrial laser scanning (or terrestrial LiDAR)
UNFCCC	United Nations Framework Convention on Climate Change

NOTATIONS

Symbol	Units	Description
BAI	cm^2	Basal area increment
BS	%	Relative Biomass Stock
dbh	cm	Diameter at breast height (1.3 m above ground level)
$\bar{d}$	cm	Arithmetic mean dbh
d_g	cm	Quadratic mean dbh
D_0	cm	Dominant dbh (independently of the definition)
G	m^2ha^{-1}	Stand basal area
h	m	Total tree height
$\bar{h}$	cm	Arithmetic mean tree total height
H_0	cm	Dominant h (independently of the definition)
LTB	Mg ha^{-1}	Live tree biomass (aboveground and belowground live trees).
MAI	m^3 year	Mean annual volume increment
MBS	Mg ha^{-1}	Stand level maximum biomass stock (referred to live tree -aboveground and belowground- biomass).
N	trees ha^{-1}	Stand density
NS	dimensionless	Naturalness score
ORA	year	Optimal rotation age. The age of the stand for the potential maximum MAI
SDI		Reineke's stand density index,
SI	m	Site index, define as dominant height for a specific base age

SF	m	Site form, defined as the dominant height at a reference dominant diameter
V	$m^3\ ha^{-1}$	Stand volume
W	$Mg\ ha^{-1}$	Stand biomass

Estimation of forest maturity linked to the biomass (or carbon) stock capacity is considered one of the most important issues regarding forest management and planning. This doctoral thesis explores such relationships and considers the use of stand level maximum biomass stock as a proxy for forest maturity through site quality gradient, as a measure that can feasibly be estimated from National Forest Inventory data. The research study was conducted in Spain for maritime pine (Pinus pinaster ssp. atlantica H. de Vill.), Scots pine (Pinus sylvestris L.), beech (Fagus sylvatica L.), beech-fir and silver fir (Abies alba Mill.) forests. Finally, the potential of terrestrial laser scanning (TLS) technology for estimating forest features in mature stands was also explored. For this purpose, the R package FORTLS was developed.